



UNIVERSIDAD DE CÓRDOBA

Programa de doctorado: Biociencias y ciencias agroalimentarias

**REDOX REGULATION OF PROTEOME, METABOLISM AND
SIGNALING IN HEPATOCARCINOMA TUMOR CELLS**

**REGULACIÓN REDOX DEL PROTEOMA, EL METABOLISMO Y
LA SEÑALIZACIÓN EN CÉLULAS TUMORALES DE
HEPATOCARCINOMA**

Directores:

Dra. C. Alicia Padilla Peña

Dr. José Antonio Bárcena Ruiz

Autora de la tesis:

María José López Grueso

Diciembre 2019

TITULO: *REDOX REGULATION OF PROTEOME, METABOLISM AND SIGNALING IN HEPATOCARCINOMA TUMOR CELLS*

AUTOR: *María José López Grueso*

© Edita: UCOPress. 2019
Campus de Rabanales
Ctra. Nacional IV, Km. 396 A
14071 Córdoba

<https://www.uco.es/ucopress/index.php/es/>
ucopress@uco.es

**REDOX REGULATION OF PROTEOME, METABOLISM AND
SIGNALING IN HEPATOCARCINOMA TUMOR CELLS**

María José López Grueso

PhD Thesis

Supervisors:

Dr.C. Alicia Padilla Peña

Dr. José Antonio Bárcena Ruiz

**Departamento de Bioquímica y Biología Molecular
Universidad de Córdoba**



TÍTULO DE LA TESIS: REDOX REGULATION OF PROTEOME, METABOLISM AND SIGNALING IN HEPATOCARCINOMA TUMOR CELLS

DOCTORANDA: M^a JOSÉ LÓPEZ GRUESO

INFORME RAZONADO DEL/DE LOS DIRECTOR/ES DE LA TESIS

(se hará mención a la evolución y desarrollo de la tesis, así como a trabajos y publicaciones derivados de la misma).

El trabajo que se presenta como tesis doctoral es fruto de una dedicación muy intensa de la doctoranda a lo largo de cuatro años, incluida una estancia de tres meses en la Universidad de Galway (Irlanda) y la participación en varios cursos y congresos nacionales e internacionales. Entre ellos se puede destacar la asistencia becada a un curso internacional de la FEBS en Grecia, la obtención del primer premio a la mejor comunicación oral en la XI reunión del GEIRLI y que fue seleccionada para una comunicación oral en un congreso internacional de la EMBO. La evolución del trabajo ha sido muy satisfactoria, a pesar de las dificultades encontradas en poner a punto diversas metodologías de gran complejidad. El objetivo principal de la tesis ha sido estudiar las funciones de las redoxinas en señalización celular y metabolismo en líneas celulares derivadas de hepatocarcinoma sometidas o no a altos niveles de óxido nítrico. La consecución de este objetivo se ha abordado utilizando técnicas complejas, algunas de ellas puestas a punto por primera vez en el grupo, como análisis del proteoma redox, estudios de metabolómica, silenciamiento génico, construcción de una línea celular humana knockout para Prdx6 o medida de flujos glucolítico y ruta de las pentosas fosfato con glucosa radioactiva, entre otras.

A lo largo del desarrollo de la tesis se han ido cumpliendo con creces los objetivos marcados, obteniéndose resultados de un buen nivel científico, como lo demuestran las siguientes publicaciones en revistas internacionales de alto índice de impacto (primer decil y cuartil) a las que han dado lugar:

Redox regulation of metabolic and signaling pathways by thioredoxin and glutaredoxin in NOS-3 overexpressing hepatoblastoma cells. *Raúl González, M. José López-Grueso, Jordi Muntané, J. Antonio Bárcena*, C. Alicia Padilla. Redox Biology* 6 (2015) 122–134. doi: 10.1016/j.redox.2015.07.007. IF: 6.337.

Thioredoxin and glutaredoxin regulate metabolism through different multiplex thiol switches. *MJ López-Grueso, R González-Ojeda, R Requejo-Aguilar, B McDonagh, CA Fuentes-Almagro, J. Muntané, J.A. Bárcena*, CA Padilla. Redox Biology*, 21(2019) 101049. doi:10.1016/j.redox.2018.11.007. 3. IF: 7.793.

Peroxiredoxin 6 Down-Regulation Induces Metabolic Remodelling and Cell Cycle Arrest in HepG2 Cells. *López-Grueso MJ, Tarradas RM, Carmona-Hidalgo B, Lagal DJ, Peinado J, McDonagh B, Requejo-Aguilar R, Bárcena JA*, Padilla CA. Antioxidants (accepted). IF: 4.52.*

Thioredoxin Downregulation enhances Sorafenib Effects in Hepatocarcinoma Cells. *M^o José López-Grueso, Raúl González, Jordi Muntané, J. Antonio Bárcena* and C. Alicia Padilla. Antioxidants (accepted). IF: 4.52.*

Además, hay que destacar que la doctoranda ha sido fundamental en el grupo de investigación, ya que con esta tesis doctoral se ha afianzado una nueva línea de investigación con líneas celulares humanas, que ha obtenido financiación pública. También ha colaborado en la formación de alumnos colaboradores y doctorandos de nueva incorporación e incluso ha codirigido un Trabajo fin de Grado de iniciación a la Investigación.

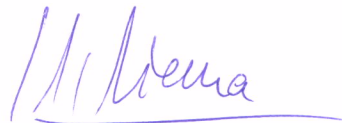
Por todo ello, se autoriza la presentación de la tesis doctoral.

Córdoba, 21 de OCTUBRE de 2019

Firma del/de los director/es



Fdo.: Carmen Alicia Padilla Peña



Fdo.: José Antonio Bárcena Ruíz



TÍTULO DE LA TESIS: REDOX REGULATION OF PROTEOME, METABOLISM AND SIGNALING IN HEPATOCARCINOMA TUMOR CELLS

DOCTORANDA: MARÍA JOSÉ LÓPEZ GRUESO

INFORME DEL FACTOR DE IMPACTO Y CUARTIL DEL JOURNAL CITATION REPORTS

A continuación se detalla el índice de impacto y cuartil de las publicaciones presentadas según la base de datos Web of Science (WOS):

- Título: Thioredoxin and glutaredoxin regulate metabolism through different multiplex thiol switches.
- Autores: **MJ López-Grueso**, R González-Ojeda, R Requejo-Aguilar, B McDonagh, CA Fuentes-Almagro, J. Muntané, J.A. Bárcena*, CA Padilla.
- Revista: Redox Biology 21 (2019) 101049

Área temática	Lugar que ocupa	Índice de impacto
Biochemistry & Molecular Biology	28/298 (D1;Q1)	7.793

- Título: Peroxiredoxin 6 Down-regulation Induces Metabolic Remodelling and Cell cycle Arrest in HepG2 Cells.
- Autores: **López-Grueso MJ**, Tarradas RM, Carmona-Hidalgo B, Lagal DJ, Peinado J, McDonagh B, Requejo-Aguilar R, Bárcena JA*, Padilla CA.
- Revista: Antioxidants (Accepted 18 October 2019)

Área temática	Lugar que ocupa	Índice de impacto
Biochemistry & Molecular Biology	63/298 (Q1)	4.52
Chemistry medical	6/61(D1;Q1)	

- Título: Thioredoxin downregulation enhances Sorafenib Effects in Hepatocarcinoma Cells.
- Autores: **M^a José López-Grueso**, Raúl González, Jordi Muntané, J. Antonio Bárcena* and C. Alicia Padilla.
- Revista: Antioxidants 8 (2019) 501

Área temática	Lugar que ocupa	Índice de impacto
Biochemistry & Molecular Biology	63/298 (Q1)	4.52
Chemistry medical	6/61(D1;Q1)	

A mis padres
A mis hermanos
A mi abuela

CONTENTS

Introduction	1
1.-Reactive oxygen and nitrogen species (ROS/RNS)	1
2.- Oxidative and nitrosative stress	4
2.1.- Sources of ROS/RNS	4
2.2.- Targets of ROS/RNS	6
3. Redox homeostasis and antioxidant systems	10
3.1.- Superoxide dismutase (SOD)	10
3.2.- Catalase	11
3.3.- Glutathione peroxidase (GPx)	11
3.4.-Peroxiredoxin (Prdx)	12
3.4.1.-Peroxiredoxin 6	16
3.5.-Thiol disulfide reductases	19
3.5.1.-Trx/TrxR system	19
3.5.2.- GSH/Grx/GR system	23
3.5.3.- Methionine sulfoxidereductase (Msr)	26
3.5.4.-Sulfiredoxin (Srx)	27
3.5.5.-S-nitrosoglutathionereductase (GSNOR)	27
4. Redox homeostasis, redox signaling and cancer	28
4.1.- Redox signaling pathways involved in carcinogenesis	29
4.2.- Impact of redox modulation of protein function on cell metabolism in HCC.....	31
4.3.- Redox involvement in HCC progression to invasiveness and metastasis	33
Hypothesis	35
Objectives	37
Conclusions	39
References	41

Summary	58
Resumen	60
Article 1: Thioredoxin and glutaredoxin regulate metabolism through different multiplex thiol switches. <i>MJ López-Gruoso, R González-Ojeda, R Requejo-Aguilar, B McDonagh, CA Fuentes-Almagro, J. Muntané, J.A Bárcena*, CA Padilla. Redox Biology</i> , 21 (2019) 101049	62
Article 2: Peroxiredoxin 6 down-regulation induces metabolic remodeling and cell cycle arrest in HepG2 cells. <i>López-Gruoso M.J., Tarradas R.M., Carmona-Hidalgo B., Lagal D.J., Peinado J., McDonagh B., Requejo-Aguilar R., Bárcena J.A.* , Padilla C.A. Antioxidants</i> (accepted 18 October 2019)	76
Article 3: Thioredoxin downregulation enhances Sorafenib effects in Hepatocarcinoma cells. <i>M^a José López-Gruoso, Raúl González, Jordi Muntané, J. Antonio Bárcena* and C. Alicia Padilla. Antioxidants</i> 8 (2019) 501.....	93
Other scientific contributions: Redox regulation of metabolic and signaling pathways by thioredoxin and glutaredoxin in NOS-3 Overexpressing hepatoblastoma cells. <i>Raúl González, M. José López-Gruoso, Jordi Muntané, J. Antonio Bárcena*, C. Alicia Padilla. Redox Biology</i> , 6 (2015) 122-134	111
Unpublished data	124

INTRODUCTION

1. Reactive oxygen and nitrogen species (ROS/RNS)

This Thesis has been developed in the field of Redox Biology and more precisely in the study of cellular mechanisms that maintain or disturb “Redox Homeostasis” and allow for redox regulation of protein function in signaling and metabolism in the context of cancer. I will begin the introduction to the subject with a brief description of the origin and characteristics of Reactive Oxygen and Nitrogen Species (ROS/RNS). Many reviews have been published on this subject of whom I highlight the following: ¹⁻⁶.

Reactive oxygen species (ROS) and reactive nitrogen species (RNS) are a family of molecules produced in all living organisms mainly as a consequence of aerobic life. Traditionally these reactive species have been considered responsible for the oxidative stress in the cells and for the damage to most biomolecules. However, emerging data show that ROS and RNS are necessary for life and play an important role in a wide variety of essential physiological processes. Aerobic organisms take molecular oxygen (O_2) from the air and is reduced to H_2O inside the cells in the reactions of the electron transport chain and oxidative phosphorylation. This process is called cellular respiration and it is where most of ROS are produced. In general, ROS can be classified into two groups, radical and non-radicals. The radical group is composed of superoxide anion ($O_2^{\cdot-}$), hydroxyl radical ($\cdot OH$), peroxy (ROO^{\cdot}) alkoxy radicals (RO^{\cdot}), nitric oxide radical (NO^{\cdot}), and nitrogen dioxide (NO_2^{\cdot}) which contain at least one unpaired electron in their external orbit capable of independent existence. On the other hand, the nonradical group is composed of a large variety of molecules, among which are hydrogen peroxide (H_2O_2), hypochlorous acid ($HOCl$), hypobromous acid ($HOBBr$), lipid peroxides ($ROOH$), aldehydes, ozone (O_3), singlet oxygen (1O_2), peroxyxynitrite ($ONOO^{\cdot}$) and peroxyxynitrous acid ($ONOOH$) (Figure 1).

Superoxide ion radical ($O_2^{\cdot-}$) is the most important widespread ROS resulting from the transfer of one electron to O_2 . $O_2^{\cdot-}$ is relatively stable and reacts poorly with biological components. Due to its pKa of 4.8, it can exist as either $O_2^{\cdot-}$ or hydroperoxyl radical (HO_2^{\cdot}) at low pH which can more easily penetrate biological membranes. Both $O_2^{\cdot-}$ and HO_2^{\cdot} can reduce ferric (Fe^{3+}) to ferrous (Fe^{2+}) ions. The superoxide anion radical also can act as a nucleophile and as oxidizing agent against ascorbate and tocopherol but the most important reaction is dismutation. In this reaction that can be

spontaneous or catalyzed by superoxide dismutase enzyme family (SOD), one superoxide radical reacts with another superoxide radical in which one radical is oxidized to oxygen and the other is reduced to H₂O₂.

Hydrogen peroxide (H₂O₂) is a stable molecule that can be also formed by the spontaneous transfer of two electrons to oxygen. It is not a radical but it can cause damage to the cell at low concentration (10 μM). Its harmful chemical effects can be direct or indirect by producing OH[·] in the presence of transition metal ions.

Hydroxyl radical (OH[·]) is the most aggressive radical species in biological systems. In contrast to the superoxide anion, OH[·] is a short-lived species which acts as a powerful oxidant for a wide range of both organic and inorganic molecules that are present in the cells. It is formed in a Fenton reaction, in which H₂O₂ reacts with metal ions (Fe²⁺ or Cu²⁺), or by the reaction between O₂^{·-} and H₂O₂ called Haber-Weiss reaction.

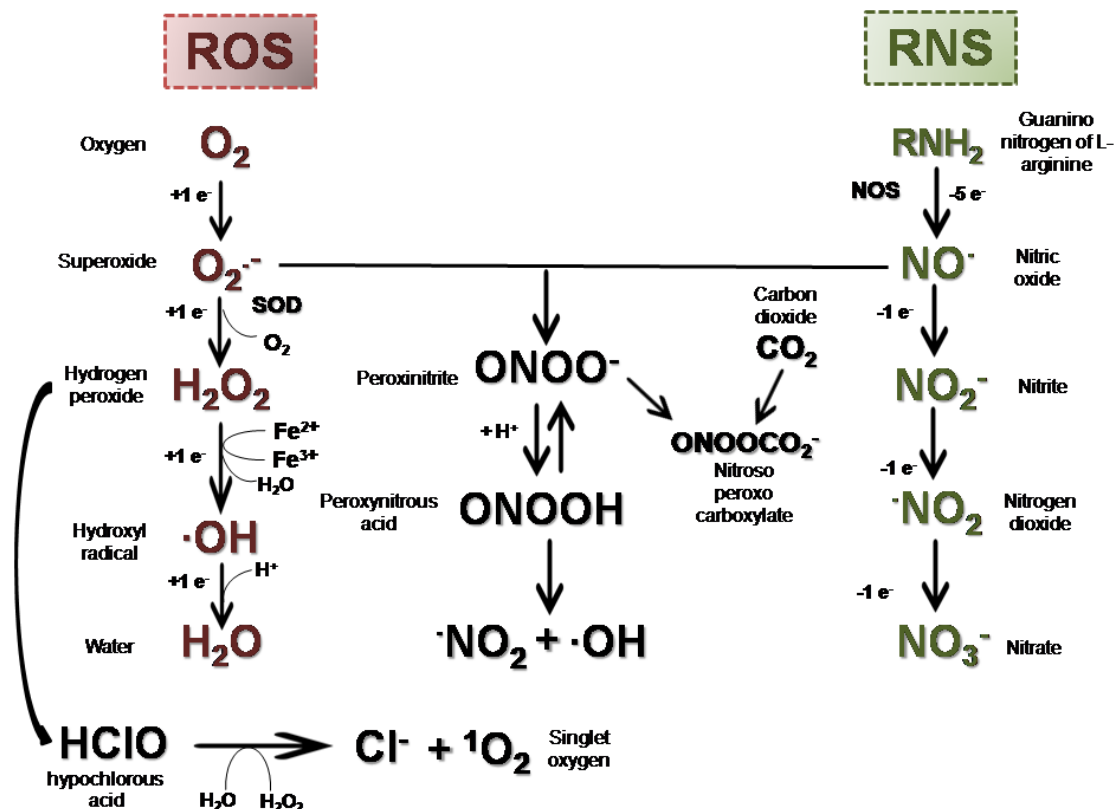


Figure 1. Reactive Oxygen Species (ROS) and Reactive Nitrogen Species (RNS). SOD, superoxide dismutase; NOS, nitric oxide synthase. Figure adapted from Nathan & Shiloh ⁷

Nitric oxide ($\cdot\text{NO}$) is a relatively stable and highly diffusible free-radical gas which reacts with oxygen to form nitrogen oxides. It can be included in both RNS family and ROS, and is synthesized by nitric oxide synthase (NOS) from L-arginine, oxygen and NADPH. Three isoforms of NOS have been described, neuronal (nNOS or NOS type I), inducible (iNOS or NOS type II) and endothelial (eNOS or NOS type III) which play different roles ⁸. Nitric oxide is both water- and lipid-soluble so it diffuses freely through the cytoplasm and plasma membrane and has a short half-life. It can react with a variety of radicals to form nitrite (NO_2^-), and nitrate (NO_3^-).

Peroxynitrite anion (ONOO^-).-Under physiological conditions, NO^\cdot is able to react with a superoxide anion producing peroxynitrite anion (ONOO^-). This reaction is important to maintain the balance of superoxide radicals and other ROS molecules. Peroxynitrite is a strong short-life oxidant that can diffuse across cell membranes and might provoke depletion of sulfhydry groups and oxidative damage on most biomolecules similar to OH^\cdot . It can directly react with CO_2 to form nitroso peroxy carboxylate (ONOOCO_2^-) or it can protonate to peroxynitrous acid (ONOOH). Peroxynitrite anion can also react fast with carbon dioxide to form carbonate (CO_3^{2-}) and nitrogen dioxide ($\cdot\text{NO}_2$) radicals that are responsible for component nitration. Alternatively, peroxynitrous acid can undergo homolytic fission to generate hydroxyl radicals and nitrogen dioxide.

Most ROS/RNS are short-lived species whose life span depend on the environmental conditions like pH or the presence of other species. For these reasons, the ROS/RNS selectivity for redox signaling is achieved by regulating the subcellular location and exposure time to promote kinetically competent redox reactions. Due to the instability of many types of ROS/RNS and the redox buffer capacity of the cell, it is very important that a colocalization exists between the source of ROS/RNS and targets as well as a modulation of the local redox buffer capacity ⁹.

2. Oxidative and nitrosative stress

The term "oxidative stress" was originally defined as a lack of balance between ROS/RNS and the antioxidant organism's capacity¹⁰, but the definition has been reviewed and the new version is *an imbalance between oxidants and antioxidants in favour of the oxidants, leading to a disruption of redox signalling and control and/or molecular damage*¹¹. Therefore, oxidative stress can be classified according to the amount of ROS/RNS, with levels ranging from physiological oxidative stress (eutress) to pathological oxidative stress (distress). At low or moderate cell levels, ROS act as signaling molecules that regulate critical physiological processes such as proliferation, apoptosis and inflammatory responses as well as activation of transcriptional factors¹²⁻¹⁴. ROS play an important role as regulatory mediators in signaling processes since organisms have developed specific mechanisms that allow them their use as signaling molecules¹⁵. However, at higher concentration, both ROS and RNS generate oxidative stress and nitrosative stress, respectively, that easily cause irreversible modifications in different biomolecules like proteins, lipids, or nucleic acids. Oxidative stress has been associated with different pathologies as neurodegenerative diseases (Parkinson, Alzheimer, Huntington's disease and amyotrophic lateral sclerosis), diabetes, rheumatoid diseases, cardiovascular disease, cataracts and cancer¹⁶⁻¹⁸. Besides, the progressive decline of antioxidant defence provokes the disability of physiological functions, promoting disease emergence and ageing^{14,19-21}.

2.1. Sources of ROS/RNS

Free radicals, both reactive oxygen species (ROS) and reactive nitrogen species (RNS), can have exogenous and endogenous origin. The totality of exogenous sources has been denominated as the "exposome"²² which includes tobacco smoke, pollution, ionizing or solar radiation and diet among others^{23,24}.

Although the risk of the organisms exposure to exogenous sources of ROS/RNS is high, the endogenous sources are more important since exposure to endogenously produced ROS/RNS in the cell is a continuous process throughout the life of each organism. The subcellular localization where ROS/RNS are generated as well as their temporal and spatial distribution is very important. The main organelles for ROS production under physiological conditions are mitochondria and cell membranes

but there are also other organelles, such as the endoplasmic reticulum (ER) and peroxisomes or even ROS/RNS producing enzymes (Figure 2).

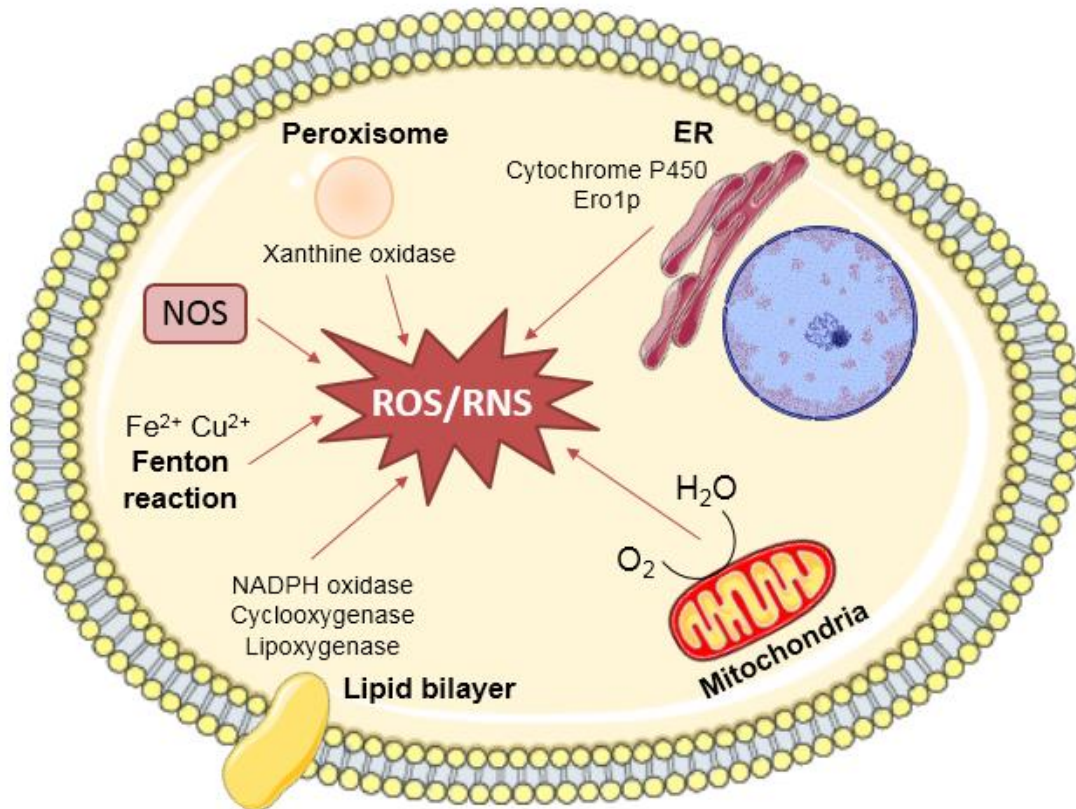


Figure 2. Cellular sources of ROS/RNS production. Figure adapted from Di Meo et al. ¹⁷

O_2^- is produced by one-electron reduction of molecular oxygen in the mitochondria when the flow of electrons through the electron transport chain (ETC) during the synthesis of ATP eventually fails ²⁵. The major sites of superoxide anion production are Complex I and Complex III of the ETC ²⁶ and then superoxide is converted to hydrogen peroxide by the action of mitochondrial superoxide dismutase (MnSOD). In addition, monoamino oxidase, α -ketoglutarate dehydrogenase, glycerol phosphate dehydrogenase and p66shc protein are other mitochondrial components that contribute to the generation of ROS ²⁷. Mitochondrial membrane potential has been proposed to influence ROS generation since an increase in the proton-motive force is associated with an increase in ROS production, as well as the opposite effect. However, the relationship between the proton-motive force and ROS production is not yet known ²⁸.

Another important intracellular source of ROS, mainly $O_2^{\cdot-}$ or H_2O_2 , is the NADPH oxidases (Nox) family of enzymes, and their dual oxidase relatives (Duox), which are localized to various cellular membranes. Nox family was first described in neutrophils as an important source of ROS for the phagocytic killing of pathogens during the immune response. This NADPH oxidase is composed of two membrane proteins, Nox2 and p22phox, three cytosolic proteins p67phox, p47phox, and p40phox, and a small GTP binding protein Rac. NADPH oxidase has also been involved in the production of ROS in non-phagocytic cells ²⁹. In human, there are seven Nox homologues (Nox1-5, Duox1 and 2 Duox2) that produce ROS for host defence and cell signaling ³⁰⁻³². It has also been reported that lipoxygenase ³³ and cyclooxygenase ³⁴ intermediaries stimulate the generation of ROS by Noxs.

The primary source of ROS from the ER is oxidative protein folding. The majority of protein disulfide formation reactions are initiated by the glycoprotein Ero1 which catalyses the two-electrons transfer from dithiols to O_2 resulting in the formation of H_2O_2 ³⁵. In addition, other enzymes of the ER such as cytochrome P450 reductase contribute to the formation of ROS ³⁶.

Peroxisomes are subcellular respiratory organelles that produce hydroxyl and superoxide radicals as well as hydrogen peroxide by xanthine oxidase and other enzymes ^{37,38}. In addition, peroxisomes contain the inducible form of nitric oxide synthase so that produces $\cdot NO$ ³⁹. Under some physiological or pathological conditions, peroxisomes may act as a H_2O_2 and $\cdot NO$ source ⁴⁰.

2.2. Targets of ROS/RNS

ROS and RNS could provoke reversible or irreversible redox modifications of biomolecules such as proteins, lipids, DNA and RNA, altering their structure and functionality.

Nucleic acids

Although DNA is a stable and well-protected molecule, both ROS and RNS can damage it by oxidation. Hydroxyl radicals are the main ROS that can directly react with purine and pyrimidine bases as well as deoxyribose sugar backbone and cause several types of damage, such as single and double DNA break and loss of purines ^{18,41}. The $\cdot OH$ can attack guanine at its C-8 position to produce 8-hydroxy deoxyguanosine (8-OHdG) which is considered the standard biomarker of oxidative damage in DNA ⁴². On

the other hand, peroxyxynitrite reacts with guanine causing nitrative and oxidative DNA lesions such as 8-nitroguanine and 8-oxodeoxyguanosine, respectively. 8-nitroguanine is unstable and can be spontaneously removed resulting in loss of purines (apurinic sites) and mutagenic DNA lesion ⁴³. In the case of RNA, it is more vulnerable to oxidative damage than DNA and 7,8-dihydro-8-oxoguanosine (8-oxoG) is the most study RNA damaged product ⁴⁴.

Lipids

Membrane lipids, especially polyunsaturated fatty acids, are the most susceptible to peroxidation by peroxyxynitrite-derived radicals which results in the compromise of the integrity and functionality of cell membranes. Malondialdehyde (MDA) and nitrito-, nitro-, nitrosoperoxo- and/or nitrated lipids are products of lipid peroxidation ^{45,46}. Peroxidation of polyunsaturated fatty acids yields lipid aldehydes represented by 4-hydroxynonenal (4HNE) ^{47,48}. Peroxyxynitrite also provokes the oxidation of arachidonic acid and the formation of F₂-isoprostanes which are considered as the marker of the oxidative lipid damage ⁴⁹.

Proteins

Proteins sustain most of the damage caused by ROS because they are the most abundant biomolecules in the cell. ROS/RNS provoke side-chain oxidation of amino acid residues, backbone fragmentation, unfolding and misfolding resulting in loss of protein function/enzymatic activity or their degradation by specific proteases ⁵⁰. All amino acids are sensitive towards oxidation but the sulfur atom of methionines and cysteines is more prone to oxidation than others. Oxidations of amino acids can be irreversible, like carbonylation or reversible by the activity of disulfide reductases on oxidized Cys or methionine sulfoxide reductase on Met-sulfoxide.

Irreversible

Lysine, arginine proline and histidine residues can be oxidated by ·OH giving rise to carbonyl derivates that serve as markers of ROS mediated protein oxidative damage. Aromatic amino acids like tyrosine, are also susceptible to be oxidized by ·OH or ONOO⁻ resulting in dityrosine (a marker for hydroxyl radical) and 3-nitrotyrosine (a marker for RNS), respectively ⁴⁸.

Reversible

Methionine (Met) and cysteine (Cys) residues are the amino acids most susceptible to oxidation by ROS. In organisms from bacteria to human, ROS are able

to reversibly regulate many important intracellular pathways through the redox modulation of specific Cys residues of target proteins which can function as redox-dependent switches. Similar to the phosphorylation/dephosphorylation of Ser and Thr residues, the post-translational modification of specific Cys and their reversion provide a mechanism for the regulation of the protein function⁵¹. The first evidence that supported the role of ROS as signal transduction was the increases of ROS generation after growth factor stimulation such as PDGF and EGF^{52,53}. The Cys residues that are targets for reversible oxidation at physiological pH by ROS include those with a low-pK_a (4-5) thiol group that are in the thiolate form (S⁻)⁵⁴. These reactive Cys are easily oxidized by H₂O₂ to a sulfenic form (-SOH) which is unstable and can be oxidized successively to sulfinic acid (-SO₂H) and sulphonic acid (-SO₃H). The reversible oxidation of thiolate anion to sulphenic acid leads many effects on protein stability, activity, subcellular localization or protein-protein interaction⁵¹. Other post-translational modifications of Cys include nitrosation (-SNO), glutathionylation (-SSG), or the formation of an inter- or intramolecular disulfide bond (-SS-) (Figure 3)^{13,14,48,55}.

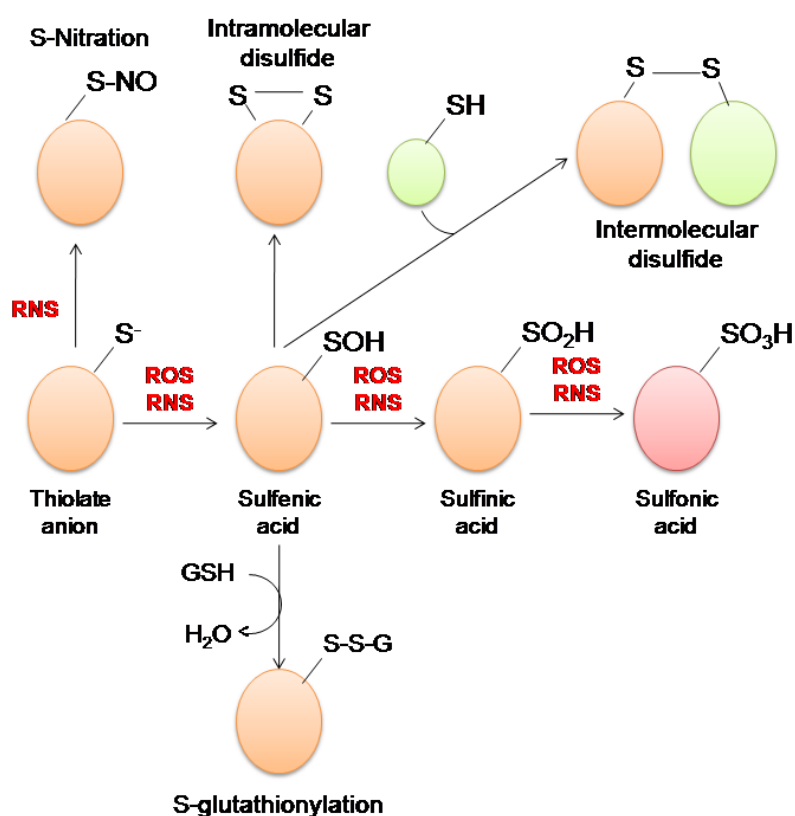


Figure 3. Schematic overview of reversible modifications of reactive cysteines.

Due to the importance of reversible modifications in cysteine residues, several proteomic approaches by mass spectrometry have been developed that allow us to identify the specific post-translational modification (PTM), the modified amino acid and the percentage of modified protein by that PTM. Most of the redox proteomics approaches initially block all free thiols with an alkylating reagent, such as iodoacetamide or N-ethylmaleimide, followed by the specific reduction of the PTM, such as dithiothreitol, and subsequent labeling with either the heavy isotope of the initial blocking reagent or another different ⁵⁶⁻⁵⁸. Thus, the Thiol Redox Proteome refers to the set of mapped protein cysteines showing reversible redox changes under given conditions or in response to stimuli ⁵⁹. Its detailed description may provide an insightful snapshot of the set of thiol redox switches in a cell under given conditions ^{59,60}. The identification and modulation by reversible redox PTMs of key proteins that can control metabolic flow, would offer promising therapeutic candidates for a number of disease states such as cancer ⁶¹.

On the other hand, methionine is easily and reversibly oxidized to methionine sulfoxide derivatives by a wide range of ROS and might provide an analogous redox-dependent system. Recent studies indicate that both actin polymerization and the activity of the Ca²⁺/Calmodulin-dependent kinase II (CaMKII) can be regulated by reversible oxidation of specific Met residue ⁶²⁻⁶⁴.

This doctoral thesis has focused on the study of reversible PTMs in cysteine residues since its reversible nature allows them to play a critical role in function/enzymatic activity as redox switches involved in cell signaling. The relevance of these reversible modifications and their reversal by disulfide reductases will be described in detail later.

3. Redox homeostasis and antioxidant systems

The regulation of intracellular ROS levels is crucial to maintain cellular homeostasis since different ROS levels can induce different biological responses. Redox homeostasis is achieved thanks to antioxidant systems responsible for maintaining the balance between generation and elimination of ROS/RNS. The concept of biological antioxidant can be defined as any compound that is able, at low concentrations, to compete with another oxidizable substrate so that delays or prevents its oxidation. Under physiological conditions, the cell temporarily disrupts that balance, either by slightly increasing the concentration of ROS or decreasing the activity of one or more antioxidant systems, to allow redox signaling ⁶⁵. Therefore, moderate levels of ROS promote cell proliferation and differentiation and activate stress-sensitive survival pathways ⁶⁶.

As a consequence of the exposure of living beings to radical species all organisms have developed antioxidant systems to protect them against these reactive species. The antioxidant defense systems are either enzymatic or non-enzymatic. The enzymatic antioxidant can be divided into those that directly detoxify the radicals such as SOD, catalase, glutathione peroxidase (GPx), and peroxiredoxin (Prx), and those that react with reversibly oxidized thiol groups of proteins such as thioredoxin/thioredoxin reductase system (Trx/TrxR), glutathione/glutaredoxin/glutathion reductase system (GSH/Grx/GR), sulfiredoxin and methionine sulfoxide reductase. The non-enzymatic systems include numerous small compounds that are able to prevent oxidative damage by direct or indirect interaction with ROS such as lipoic acid ⁶⁷, ascorbic acid ⁶⁸ and glutathione ⁶⁹.

Antioxidant enzyme systems are briefly described below and more in detail those that have been studied in this Thesis: Trx/TrxR (articles 1 and 3), GSH/Grx/GR (article 1) and peroxiredoxins (article 2).

3.1. Superoxide dismutase (SOD)

SOD was the first well-characterized antioxidant enzyme able to catalyze the dismutation of O_2^- to H_2O_2 ⁷⁰. Three different types of SOD exist in mammals: copper-zinc SOD (SOD1), manganese SOD (SOD2) and SOD3, present in the cytoplasm, mitochondrial matrix and extracellular medium, respectively. SODs play a critical role in

endothelial and mitochondrial function by preventing ONOO⁻ and OH⁻ formation and participate in compartmentalized redox signaling to regulate many vascular functions⁷¹.

3.2. Catalase

Catalase is a heme enzyme responsible for the detoxification of various phenols, alcohols, and hydrogen peroxide through the depletion of H₂O₂ to H₂O and O₂ without consumption of endogenous reducing equivalents. Catalases are classified into three groups based on their structure and function: the first and the second group are formed by heme-containing enzymes whereas the third group contains manganese catalases. The human catalase belongs to the first group and is characterized by a small subunit (62 kDa), with heme *b* as its prosthetic group and NADPH as cofactor. Catalase is mainly located in peroxisomes but also in cytosol. Changes in its activity or expression are related to pathological processes as Zellweger syndrome, acatalasemia or WAGR syndrome ⁷².

3.3 Glutathione peroxidase (GPx)

Glutathione peroxidase is a selenium-containing enzyme that catalyses both the reduction of H₂O₂ and organic hydroperoxides to water or corresponding alcohols using GSH as electron donor. Eight isoforms of GPx exist in humans, five of them (GPx1, GPx2, GPx3, GPx4, and GPx6) contain a selenocysteine residue in their active sites and three employ an active-site cysteine. GPx enzymes play an important role in H₂O₂ and cell signaling ⁷³.

The tripeptide L-γ-glutamyl-L-cysteinyl-glycine, or GSH, is the major low-molecular-weight antioxidant in mammalian cells involved in the control of the thiol/disulfide redox potential of the cell. Due to the sulfhydryl group (-SH) of cysteine, GSH is not only used as scavenger of a wide range of ROS/RNS, but is also utilized as antioxidant defense by three members of glutathione peroxidase (GPx) and by 1-Cys peroxirredoxins. H₂O₂ is reduced by GSH to H₂O and glutathione disulfide (GSSG) and then, GSSG is reduced to GSH by glutathione reductase (GR) which uses NADPH as electron donor. Therefore, intracellular GSH can exist as a reduced monomer or as oxidized disulfide dimer (GSH/GSSG) and although is mainly freely distributed in the cytosol (about 85-95% of concentration) can also be located in the mitochondria, peroxisomes, the nuclear matrix and ER. The concentration of GSH in the cytosol is in the range 1-2 mM whereas in hepatocytes the concentration can reach up 10 mM.

However, in plasma, the concentration of GSH decreases to μM because of its rapid catabolism. GSH is a ubiquitous molecule that not only acts as an antioxidant defense molecule and an important reservoir of the amino acid cysteine but also participates in many different physiological processes as detoxification of xenobiotics and cell cycle regulation, proliferation and apoptosis^{69,74,75}.

3.4. Peroxiredoxins (Prdx)

As a member of this family, human peroxiredoxin 6, has been studied in the second article of this Thesis so this antioxidant family will be described in more detail.

Peroxiredoxins (Prdx), together with CAT, SOD and GPx, are one of the most important enzymes involved in defense against oxidative stress, constituting a ubiquitous family of thiol-dependent peroxidases. Prdx family enzymes have a molecular weight of 20-30 kDa and are present in all the studied organisms. Their function consists in the reduction of H_2O_2 , peroxynitrite and alkyl hydroperoxides to water, nitrite and the corresponding alcohol, respectively^{76,77}. For a long time, the role of Prdx has been studied as defense against oxidative stress and has been considered as the major cellular defense system against peroxides. However, in recent years, it has been suggested that Prxs are involved in other processes such as cell signaling or membrane remodelling, in addition to antioxidant defense.

All Prdx isoforms contain a crucially conserved active-site cysteine, known as the peroxidatic cysteine (C_p), which is located in a universally conserved Pxxx(T/S)xxC motif in the amino-terminal portion of the protein⁷⁸. Six isoforms of Prdx exist in humans, classified into three subgroups depending on the number and localization of the cysteine residues involved in their catalytic activities^{76,79,80}:

Typical 2-Cys Prdx subgroup (Prdx1-4)

They contain another additional conserved Cys, referred to as resolving cysteine (C_r) in the carboxyl-terminal region. Both conserved Cys residues are necessary for their catalytic activity. The $\text{C}_p\text{-SH}$ is selectively oxidized by H_2O_2 to the $\text{C}_p\text{-SOH}$ intermediate, and then an intermolecular disulfide is formed with $\text{C}_r\text{-SH}$. Finally, a dithiol, usually Trx, attacks the intersubunit disulfide bridge using electrons from NADPH and the catalytic cycle can be repeated. Prdx can react with a second H_2O_2 molecule before it is able to react with $\text{C}_r\text{-SH}$ and originate the hyperoxidized

form (C_p -SO₂H). The C_p -SO₂H residue can be reduced by an ATP-dependent reaction catalyzed by sulfiredoxin (Srx) (Figure 4).

Typical 2-Cys Prdx in the reduced or hyperoxidized state forms homodimers containing two identical active sites, except Prdx2 which has been demonstrated that exists also in decameric forms⁸¹. Prdx1 and Prdx2 are mainly localized in the cytosol, Prdx3 in mitochondria, and Prdx4 predominantly in the ER⁸².

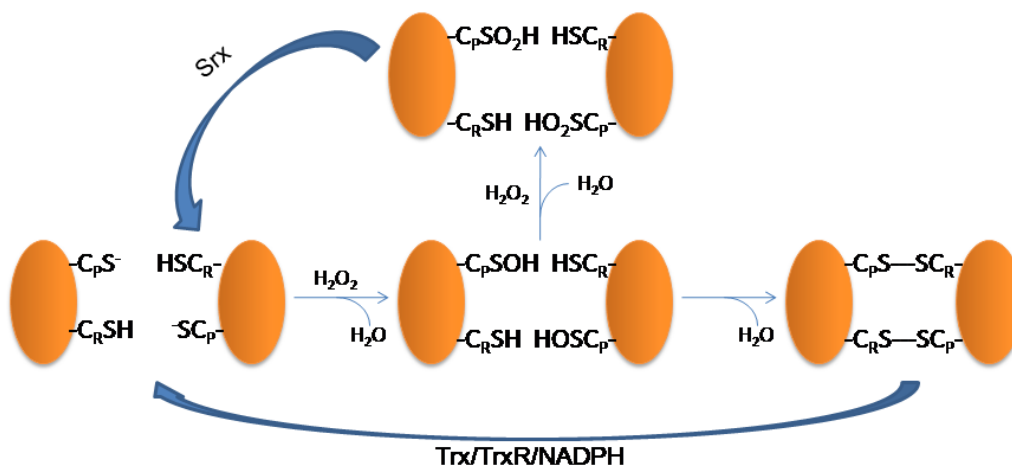


Figure 4. Reaction mechanism of human Prdx1-4. Figure adapted from Seo et al.⁸⁰ Srx, Sulfiredoxin; Trx, Thioredoxin; TrxR, Trx reductase.

Atypical 2-Cys Prdx subgroup (Prx5)

The carboxyl-terminal region of this Prdx is smaller than the 2-Cys Prdx described above so that the C_r (Cys-152) is closer to C_p (Cys-47). The C_p residue of the active site is oxidized and forms an intramolecular disulfide intermediate with the C_p within the same subunit. The intramolecular disulfide formed is reduced by Trx system (Figure 5). Prdx5 is localized in the cytosol, mitochondria and peroxisomes, and it does not form dimers⁸³.

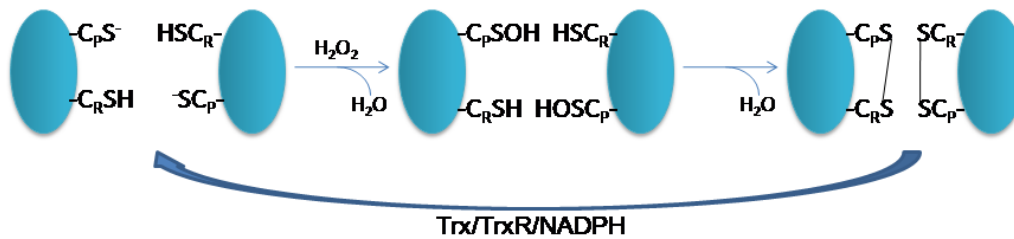


Figure 5. Reaction mechanism of human Prdx5. Figure adapted from Seo et al.⁸⁰. Trx, Thioredoxin; TrxR, Trx reductase.

1-Cys Prdx subgroup (Prdx6)

This Prdx has only the C_p and it does not have C_r . In human, Prx6, in addition to the C_p , contains other Cys residue at position 91. However, the function of this cysteine has not been solved yet. The catalytic mechanism of these peroxidase upon exposure to H_2O_2 is that C_p residue is oxidized and does not form a disulfide because of unavailability of another reduced Cys-SH nearby (Figure 6). Prdx6 uses GSH as a primary physiological reductant in the presence of GST- π instead of thioredoxin for peroxidase activity⁸⁴. However, Prx1 from *Saccharomyces cerevisiae* can use glutaredoxin (Grx2)⁸⁵. Yeast mitochondrial Prx1 can also use GSH as resolving thiol in a very peculiar manner without being consumed during the catalytic cycle and the reducing equivalents of a NADPH provided by the mitochondrial Trx system⁸⁶. Prdx6 is not able to form decamers⁸⁷ and it is localized predominantly in the cytosol but also in other organelles such as lysosomes^{88,89}.

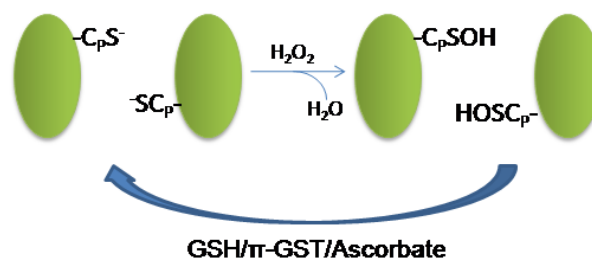


Figure 6. Reaction mechanism of human Prdx6. Figure adapted from Seo et al.⁸⁰

In recent years, Prdx have been considered not only as antioxidant defense but also as sensors and transducers of signaling by H_2O_2 . Because the thiol groups of the effectors proteins have less affinity for H_2O_2 compared with the C_p of Prdxs, there are

several mechanisms that could be involved in peroxide signaling. In addition, there are other enzymes that react with H_2O_2 faster than the target protein, such as catalase and glutathione peroxidase. The reversible inactivation of 2-Cys Prdx by hyperoxidation and the local production of H_2O_2 around lipid rafts are achieved by the closeness of the target protein to the local activation of Noxs⁹⁰. This reversible inactivation seems to be important for peroxide-mediated signaling and it has been labelled the 'floodgate mode'⁹¹. Indeed, both the local concentration of H_2O_2 and the inactivation of local H_2O_2 -eliminating enzymes are important to oxidize a target protein. Some of those target proteins that are directly oxidized by H_2O_2 are protein tyrosine phosphatases (PTPs) such as PTEN, protein tyrosine kinases (PTKs) such as Src family members, AGC protein kinases such as Akt, or transcription factors such as Activator Protein 1 (AP1) and Nuclear Factor- κ B (NF- κ B)^{90,92}.

Hyperoxidation triggers the formation of high molecular weight forms of 2-Cys Prdx which acquire a new function as chaperone⁹³. On the other hand, hyperoxidation allows for the accumulation of H_2O_2 for signaling purposes such as MAPK signaling pathway which has been involved in cellular outcomes as diverse as proliferation, survival, differentiation and death⁹². An example of the inactivation of the signaling by inactivation of Prdx is the hyperoxidized form of Prdx3 resulting from leaky cytochrome p450 during the conversion of cholesterol to corticosterone that has a role in the regulation of steroidogenesis. The inactivation of Prdx3 activates p38 mitogen-activated protein kinase (MAPK) which leads to the inhibition of steroidogenesis⁹⁴. Moreover, the Prdx3-SO₂H and Srx in the mitochondria of adrenal gland have a circadian oscillation as a conserved mechanism which is important to control the circadian oscillation of corticosterone⁹⁵.

Another H_2O_2 signaling mechanism consists in Prdx-mediated oxidation instead of directly by H_2O_2 . Oxidized Prdx forms an intermolecular disulfide with a bound effector protein that then through reshuffling of Prdx would transmit the oxidized state to the effector protein. In mammals, Prdx1 physically interact with apoptosis signaling kinase 1 (ASK1) resulting in ASK1-ASK1 oligomers and then ASK1 activation. Prdx1 also catalyzed the oxidation of the multifunctional protein APE1/Ref-1. The same happens with Prdx2 and the transcriptional factor STAT3 or the redox sensitive chaperone DJ-1^{90,92,96}. Oxidized Prdx4 forms an intramolecular disulfide with protein disulfide isomerase (PDI) which then allows PDI to transfer the disulfide bond to a target protein in the ER for the correct folding of the protein⁹².

Last but not least, Prdx are involved in H₂O₂ signaling by modulating the redox state of thioredoxin which is responsible for the reduction of the Prdx disulfide. It has been proposed that it is the oxidation of Trx that allows the target protein to be oxidized. Recent studies carried out in *Saccharomyces cerevisiae* suggest that in some cases the main role of Prdx may be regulating the redox state of Trx, rather than eliminating H₂O₂ ⁹⁰.

Prdx could regulate the redox state of signalling pathways proteins involved in redox homeostasis and in the control of cellular physiological functions such as growth, apoptosis, differentiation, embryonic development, lipid metabolism, and immune response. Recently, Prdx have been linked to different pathologies as the development of cancer and neurodegenerative and inflammatory diseases ^{77,97}.

3.4.1. Peroxiredoxin 6

Prdx6, the 'non-selenium glutathione peroxidase', is the unique member of the Prdx family that belongs to the 1-Cys that not only has general peroxidase activity. This enzyme also presents three lipid-related enzymatic activities associated with phospholipids such as a) hydrolysis of the *sn*-2 fatty acyl bond of glycerophospholipids to produce free fatty acids and a lysophospholipids, i.e., phospholipase A₂ activity (PLA₂) ^{88,98}; b) reduction of phospholipids hydroperoxides to the corresponding alcohol, i.e., phospholipid hydroperoxide glutathione peroxidase activity (PHGPx) ⁹⁹; and the more recently discovered c) transfer of a fatty acyl CoA to the *sn*-2 position of lysophosphatidylcholine (LPC), i.e., LPC acyl transferase (LPCAT) activity ¹⁰⁰. Hence, Prdx6 is a true "moonlighting" protein. Its expression is mediated by Nrf2 via an antioxidant response element-driven mechanism ¹⁰¹.

It is worth to note that Prdx6 is the only member of the peroxiredoxins family to be able to reduce peroxidized phospholipids in the cell membrane ^{99,102}. Ser32 and His26 residues of Prdx6 are essential for oxidized phospholipid binding ¹⁰². Both the peroxidase and PLA₂ activities of Prdx6 can play an important role in the repair of peroxidized phospholipids in cell membranes giving to Prdx6 the ability to protect cells against oxidant stress ¹⁰³.

The catalytic center for PLA₂ activity of Prdx6 is formed by Ser32-His26-Asp140, a triad of amino acids commonly expressed in proteases and proteins with PLA₂ activity ¹⁰⁴. The triad Ser32-His26-Asp140 is at the protein surface while Cys47 of peroxidase activity is located at the base of a shallow pocket (Figure 7). The distance between Ser32 and Cys47 is ~ 28 Å and there are few positively charged amino acids

forming a groove between the two active sites ¹⁰⁵. PLA₂ activity is greater with phosphatidylcholine (PC) as substrate than phosphatidylethanolamine and phosphatidylglycerol and Prdx6 shows no preference for the *sn*-2 acyl group ⁸⁹.

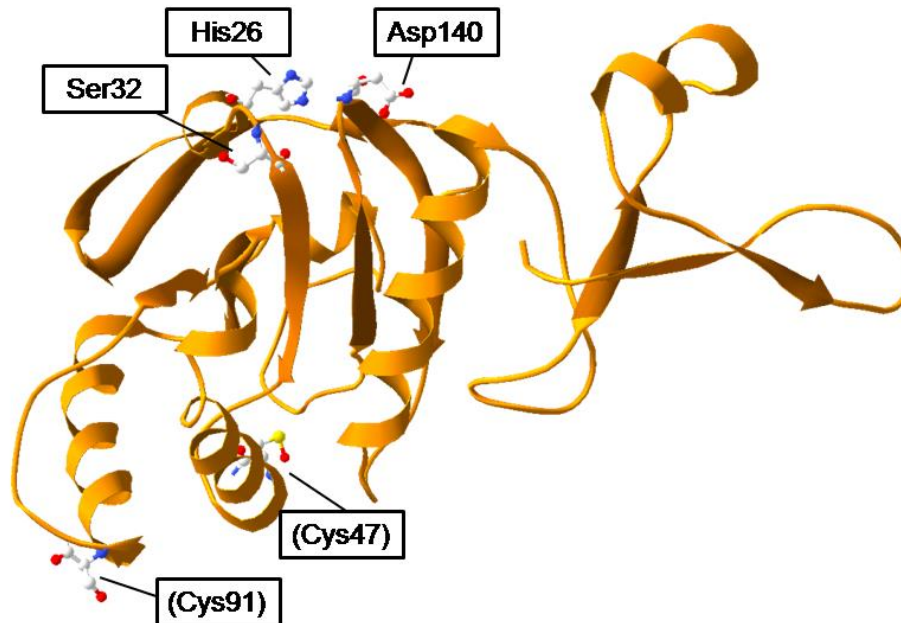


Figure 7. Ribbon of the model of Prdx6 3D structure with highlighted cysteine residues.
PDB:1prx

The subcellular localization of Prdx6 is important because PLA₂ activity is optimal at pH 4 and peroxidase activity at pH 7-8 ⁹⁸ and also at pH 4 the peroxidase activity of Prdx6 is likely 2 orders of magnitude greater than the PLA₂ activity ¹⁰⁶. This pH specificity for both enzymatic activities can be explained by the differential binding kinetics of the Prdx6 ^{102,104}. Prdx6 can be phosphorylated at Thr177 by mitogen-activated protein kinase (MAPK; ERK or p38) activity increasing the PLA₂ activity both at pH 4 and 7 without affecting its peroxidase activity. Thus, this suggests a physiologically regulated system which allows Prdx6 to act either as peroxidase or PLA₂ at neutral pH under oxidative stress conditions ¹⁰⁷. Furthermore, Prdx6 is targeted to acidic organelles after binding to the 14-4-3ε protein at a peptide (31-40 aa) previously phosphorylated by MAPK; Ser32 is essential for this binding ^{108,109}.

Phosphorylation of Prdx6 also has a critical role in the activation of Nox2, a protein of the Noxs family. Nox2 is the canonical Nox responsible for O₂⁻ generation in neutrophils to kill bacteria as well as playing an important role in normal cell signaling during cell proliferation and cell migration among other processes ⁵¹. Phosphorylated Prdx6 through PLA₂ activity is essential for translocation of Nox2 cytoplasmic

components and activation of the enzyme complex in response to angiotensin II (Ang II) or phorbol 12-myristate 13 -acetate in pulmonary microvascular endothelial cells (PMVEC). However, it is unknown which product of PLA₂ activity is responsible for Nox2 activation¹¹⁰. The PLA₂ activity is also regulated by p67^{phox}, a component of the Nox2 activation cascade that binds to phosphorylated Prdx6 and inhibits its PLA₂ activity¹¹¹. In addition to Nox2, Prdx6 has been shown to bind to the SH3 domains of Nox activator 1 (Noxa1), a Nox1-supportive components, and co-stabilize it, activating Nox1 oxidase activity. Both peroxidase and PLA₂ activities support the Nox1-mediated migration of colon epithelial cells. However, it seems that the mechanism that regulates Nox1 and Nox2 are different¹¹². The role of Prdx6 in the activation of Noxs denotes that Prdx6 acts at the same time as pro-oxidant, activating Nox1 and Nox2 that play an essential role in cell signaling, or anti-oxidant by peroxidase activity preventing the damage caused by oxidative stress.

Phospholipids are the major constituents of cell membranes and hydroperoxids phospholipids generated in response to oxidative stress alter the physicochemical properties of membranes, resulting in cellular dysfunction¹¹³. A study carried out in Prdx6^{-/-} mice indicated that PLA₂ activity plays an important role in the synthesis via deacylation/recyclation pathway and in the degradation of internalized dipalmitoyl phosphatidylcholine (DPPC), the major phospholipid component of lung surfactant, involving Prdx6 in both the degradation and the remodelling of lung surfactant phospholipids¹¹⁴⁻¹¹⁶.

The peroxidase activity is not the main mechanism for Prdx6 antioxidant function, the PLA₂ activity also plays an important role in protecting cells against oxidative stress as well as cell membrane repair. Peroxidation of cell membrane phospholipids is one of the major indicators of oxidative stress that can result in cell death. This damage can be reversed through peroxidase activity or hydrolysis of the phospholipid fatty acyl bond (PLA₂ activity) followed by reacylation with a reduced fatty acyl CoA (LPCAT activity) but both activities are necessary for the maximal rate of recovery. Therefore, both peroxidase activity and PLA₂ and LPCAT activities of Prdx6 are responsible for repairing peroxidized membrane phospholipids, a process essential for cell survival^{103,117,118}.

Prdx6 not only has physiological functions in normal cells but also its overexpression has been demonstrated to be involved in some pathologies such as

CNS neurodegenerative diseases (Parkinson's disease^{119,120} and Alzheimer's disease¹²¹), diabetes¹²², male infertility^{123,124}, and cancer¹²⁵.

3.5. Thiol disulfide reductases

This enzymatic antioxidant family covers those systems that react with reversibly oxidized thiol groups of proteins. They are thioredoxin/thioredoxin reductase system (Trx/TrxR system), glutathione/glutaredoxin/glutathion reductase system (GSH/Grx/GR system), sulfiredoxin, methionine sulfoxide reductase and S-nitrosoglutathione reductase.

3.5.1 Trx/TrxR system

The thioredoxin system consists of redox-active thioredoxin (Trx), thioredoxin reductase (TrxR) and NADPH and was discovered as the electron/hydrogen donor for ribonucleotide reductase (RNR)¹²⁶. Trx (~12 kDa) is a small thiol-disulfide oxidoreductase expressed ubiquitously in all organisms and it is essential for embryonic development¹²⁷⁻¹²⁹. Two distinct Trx systems exist in mammals: Trx1/TrxR1 which constitutes the cytosolic system but also can be translocated into the nucleus or can be exported and acts as cytokine or chemokine, and Trx2/TrxR2 system located in the mitochondria. In addition, a third testis-specific TrxR3 exists that is expressed in germ cells and is known as thioredoxin glutathione reductase (TGR)^{130,131}. The expression of Trx1 is regulated both by nuclear factor E2-related factor 2 (Nrf2)¹³².

All members of Trx of all organisms share the same overall 3D structure called "Trx-fold" which consists of three α -helices surrounding a central core of a four-stranded β -sheet. The conserved motif Cys-X-X-Cys of the active site, located on the exterior, promotes the electron and disulfide exchange between Trx and their substrates. In mammals, the active site of Trx contains the motif Cys-Gly-Pro-Cys which is highly conserved¹³³. The first step of the catalytic mechanism consists of a nucleophilic attack on a target disulfide by the N-terminal active site thiol, which has a low pK_a, resulting in the formation of a transient covalently bound mixed disulfide. In the second step, the mixed disulfide is reduced by the C-terminal active site thiol yielding the reduced target and oxidized Trx. Lastly, the disulfide in the active site of Trx is reduced by TrxR using the electrons provided by NADPH (Figure 8). Because of the low redox potential of its active site dithiol, catalysis of the reaction by Trx is

thermodynamically more favourable than that catalyzed by GSH. For this reason, Trx becomes the major disulfide reductant in the cytosol^{130,131,134–136}.

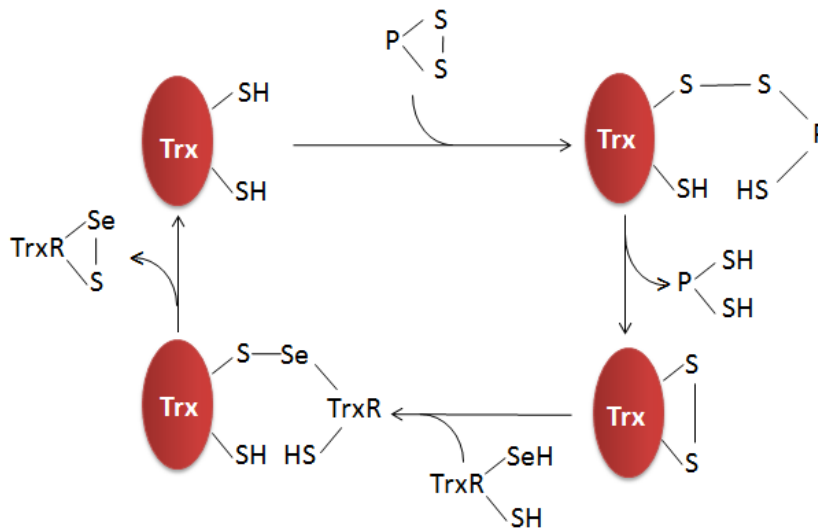


Figure 8. Reaction mechanism of human thioredoxin. Figured adapted from Arnér & Holmgren¹³¹. Trx, Thioredoxin; TrxR, Thioredoxin reductase.

Unlike the rest of organisms, the three mammalian TrxR are selenoproteins with flavin adenine dinucleotide (FAD) and NADPH binding domains. Mammalian TrxR has the conserved Gly-Cys-SelenoCys-Gly motif at C-terminal as a catalytic active site that is essential to reduce Trx and other substrates. TrxR is a homodimeric protein and both subunits are essential to build the electron transfer pathway from NADPH to Trx during a single catalytic cycle. Due to TrxR enzymes ability to reduce a wide range of substrates, these could be divided into two groups: i) substrates that may be reduced by the easily accessible active site of the enzyme such as Grx2 and protein disulfide isomerase (PDI), and ii) some low molecular weight antioxidants (LMWA) that can be reduced directly by the FAD motif at the N-terminal domain of the enzyme such as dehydroascorbate. TrxR are not only important as antioxidant defense systems but also as regulators of redox-sensitive cell signaling pathways. TrxR are related with some pathologies as male infertility, cataract, Alzheimer's disease and cancer^{137,138}. TrxR1 is overexpressed in multiple types of cancer so specifically inhibiting TrxR1 could be a good anticancer therapy^{139,140}.

The reductase activity of Trx1 is inhibited by the Trx interacting protein (TXNIP), also called Trx-binding protein-2 (TBP-2), which interacts with the active center of Trx1 through the formation of a disulfide bond between the Cys32 in Trx1 and Cys247 in TXNIP^{141–143}. TXNIP, together with importin α 1, mediates the nuclear import of Trx1

^{144,145}. In addition to inhibiting Trx1, TXNIP is a multifunctional protein that regulates lipids and glucose metabolism, inflammation and tumorigenesis ¹⁴⁶.

Nitric oxide participates in cellular signal transduction through reversible S-nitrosation of the thiol group of Cys, forming S-nitroso-proteins (SNO-proteins). S-nitrosation results from three different reactions: nitric oxide-derived species, such as N_2O_3 , by oxidation of SNO radical anion ($RSNO^{\cdot-}$) or by the transfer of the NO group from an S-nitrosothiol (SNO) to an acceptor Cys thiol known as S-transnitrosation. The selectivity of S-nitrosation is achieved in part by a high degree of spacetime accuracy and by the existence of a hydrophobic motif characterized by aromatic residues. Transnitrosases are SNO-proteins that transfer its NO group to an acceptor protein ¹⁴⁷.

The two enzymatic systems that denitrosate in physiological contexts are the Trx/Trx system and GSH/GSNO reductase. S-nitrosoglutathione (GSNO) represents the principal low-molecular-weight SNO in cells. Its levels are regulated by GSNO reductase (GSNOR) and it reacts with reduced Cys thiol to form SNO-proteins and GSH. GSNO reductase does not directly denitrosate SNO proteins, but as the GSNO pool is in equilibrium with protein thiols, reduction of GSNO by GSNOR indirectly results in protein denitrosation ^{148,149}.

The Trx/TrxR system catalyzes both transnitrosation and denitrosation of Cys thiol ¹⁴⁷. In addition to the catalytic cysteines, Trx1 contains three extra Cys residues (Cys62, Cys69, and Cys73) (Figure 9). Cys73 is physiologically S-nitrosated and it is able to transnitrosate the caspase-3 protein forming SNO-caspase-3, which leads to inhibition of its activity ¹⁵⁰. A number of studies report on targets of Trx1-mediated transnitrosation or denitrosation, including Prx1 ^{151,152}. Nitrosation of Cys73 of Trx is favoured after the formation of a disulfide between Cys32-Cys35 that is responsible to attenuate the Trx1 disulfide reductase and denitrosase activities ¹⁵¹. On the other hand, Trx/TrxR system is the major SNO-protein denitrosase of a wide spectrum of nitrosated proteins that is present in all living organisms ^{153,154}. Trx1 catalyzes the direct desnitrosation of SNO-protein through the formation of a mixed disulfide intermediate between Cys32 and Cys35 of Trx and the target protein ^{148,155}. Trx1 catalyzes desnitrosation of Caspase-3 ¹⁴⁸. NOS3 (or eNOS) itself is also a target of Trx1 leading to activation of the enzyme as part of a regulatory mechanism of NOS3 by reversible auto-S-nitrosation ^{155,156}. Thus, as the principal regulator of redox signaling, under physiological conditions, Trx1 protects against oxidative damage via reductase activity, but under oxidative stress, the oxidized Cys32-Cys35 accumulates and Cys73 becomes S-nitrosated. In this way, Trx1 offers an alternative modality of protein

regulation via transnitrosation ¹⁵¹. So depending on the redox state of the cell, Trx1 catalyzes either trans-S-nitrositation or S-denitrositation.

Due to the variety of substrates, Trx1 is involved in signaling pathways such as cell growth, proliferation and apoptosis, transcriptional regulation and the most widely studied, disulfide reduction of oxidized proteins to maintain the redox balance and facilitating the reduction of H₂O₂ by supporting peroxidase actions of peroxiredoxins. Trx1 supports the peroxiredoxin family in the reduction of hydrogen and lipid peroxides through the reduction of oxidized Prdxs ^{136,152}.

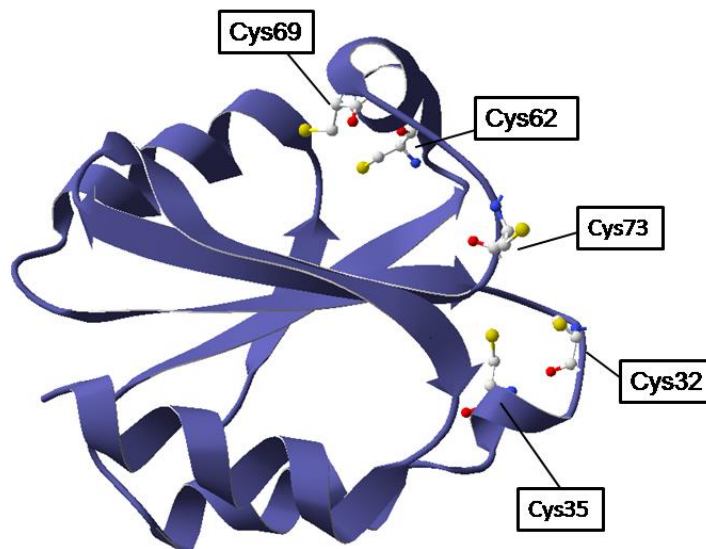


Figure 9. Ribbon of the model of Trx1 3D structure with highlighted cysteine residues.
PDB:4rqf

The phosphatase PTEN is the terminator of the Akt signaling pathway that is important for cell proliferation, growth, and survival. Cys32 of Trx1 directly interacts with Cys212 of the C2 domain of PTEN and inhibits its phosphatase activity leading to activation of the Akt pathway and eventually resulting in cell proliferation ¹⁵⁷. Another process regulated by Trx1 is apoptosis. Under physiological conditions, reduced Trx is binding to ASK1, inhibiting apoptosis. However, when ROS levels increase, Trx1 is oxidized leading the dissociation of the complex and activation of apoptosis signal cascade ^{158,159}. Apoptosis is also redox-regulated through modulation of caspases whose activity depends on modifications in the thiol state of their active site such as S-nitrosation. As described above, Trx1 catalyzes the denitrosation by means of its canonical active site dithiol ¹⁴⁸ or trans-nitrosation from Cys73-SNO ¹⁵⁰.

The DNA-binding activity of several transcription factors has been shown to be modulated post-translationally by redox changes in cysteine residues^{160–162}. Trx1 regulates the activity of the tumor suppressor protein p53, NF- κ B, and AP-1. NF- κ B controls many biological processes including cell survival, proliferation, immunity, and inflammation¹⁶³. In the cytosol, NF- κ B activation is inhibited by reduced Trx1 but under oxidative conditions, Trx1 is translocated to the nucleus and enhances the DNA-binding activity of NF- κ B through the reduction of the essential Cys62^{164,165}. As with the activation of NF- κ B, AP-1 is redox-regulated by Trx1 and the Redox Effector Factor 1 (Ref-1). AP-1 is a complex formed by c-FOS, c-Jun and ATF sub-families which is involved in a wide range of cellular processes as cellular proliferation, death, survival and differentiation¹⁶⁶. After exposure to IR, reduced Trx1 interacts with Ref-1 in the nucleus and enhancing the AP-1 DNA binding activity^{167–169}. The same happens with p53, Trx1 and Ref-1 enhanced p53 expression¹⁷⁰.

3.5.2. GSH/Grx/GR system

The glutaredoxin system consists of glutathione (GSH), glutaredoxin (Grx) and NADPH-dependent glutathione reductase (GR). The Grx was discovered by Arne Holmgren in 1976 as an alternative electron donor for RNR in *E.coli*. Grx was then characterized as GSH-dependent oxidoreductase^{171–173}.

Structurally, Grxs belong to the Trx-fold family of proteins. Trx and Grx share a common structural motif which consists of a four-stranded β -sheet surrounded by three α -helices and a similar active site motif located on the loop connecting β -sheet 1 and α -helix 1 and a *cis*-Pro residue¹⁷⁴. Human Grx contains two additional α -helices¹⁷⁵. However, Grx displays two unique structural features: an active site environment that gives the advantage to be attacked by GSH and a hydrophobic surface area that allows it to interact with protein substrates (Figure 10)^{176,177}. Grx are, depending on the number of active site Cys residues, classified into dithiol (Cys-Pro-Tyr-Cys) and monothiol (Cys-Gly-Phe-Ser) enzymes which are able to bind and use GSH as substrate despite its lack of the second active site cysteine. Grx are versatile oxidoreductase able to reduce a variety of substrates as protein disulfides, mixed disulfides as in protein deglutathionylation and at least one compound devoid of thiol groups such as ascorbate.

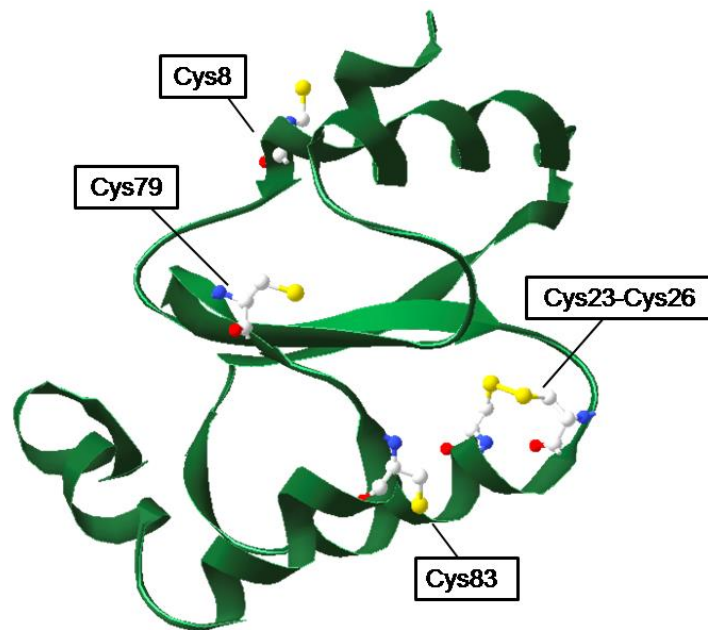


Figure 10. Ribbon of the model of Grx1 3D structure with highlighted cysteine residues.
PDB:1ert

Similar to Trx, Grx catalyze the reversible reduction of protein disulfides through the dithiol mechanism which utilizes both cysteine residues in their active site and then the oxidized Grx is reduced by GSH and glutathione reductase (GR) using NADPH as electron donor. In the first step, the target disulfide is nucleophilically attacked by the more N-terminal Cys residue and then the disulfide intermediate formed between the two proteins is attacked by the second active site thiolate. The resulting disulfide in the active site is reduced by one molecule of GSH and the mixed disulfide form is subsequently reduced by a second GSH. Grx catalyze deglutathionylation of proteins (Proteins-SSG) usually through a monothiol mechanism in which the second Cys of the active site, if present, does not participate. Regardless the mechanism, the resulting glutathione disulfide (GSSG) is regenerated by glutathione reductase (GR) using NADPH (Figure 11) ^{130,131,174,178}. Both NADPH-dependent thioredoxin reductase and glutathione reductase, besides providing reducing power for production of DNA precursors by RNR, are responsible for recycling the Trx and Grx systems in a way that maintains redox homeostasis, preventing and repairing oxidative stress as well as regulating cell signaling ¹⁷⁹.

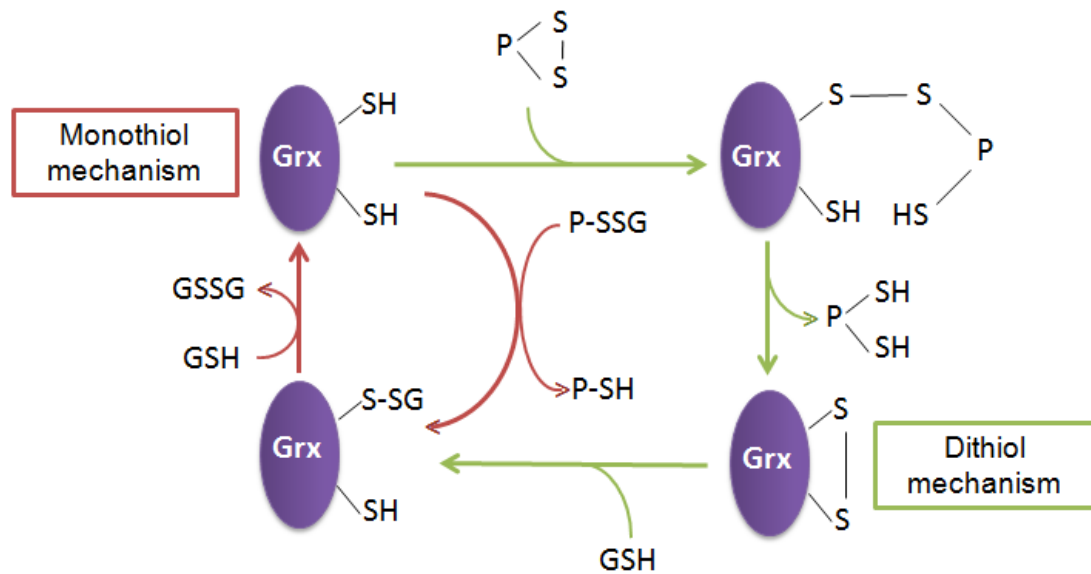


Figure 11. Reaction mechanism of human Grx1. Figured adapted from Arnér & Holmgren ¹³¹. GSH, reduced glutathione; GSSG, oxidized glutathione.

A plethora of Grx are coded for in plant genomes ¹⁸⁰, but in mammals, four Grxs have been described: Grx1 and Grx2 as dithiol, and Grx3 (also known as protein interacting cousin of Trx, PICOT) and Grx5 as monothiol ¹³¹. Grx1 is mainly localized in the cytosol, but it can be translocated to the nucleus, exported from the cell and in the intermembrane space of mitochondria ^{174,181}. Grx2 is located in the mitochondria and in the cytoplasm and nucleus of testes and in a number of tumor cells ¹⁸². Grx3 is present in the nucleus and cytoplasm while Grx5 is found in mitochondria ¹³¹.

Grx1 is involved in multicellular processes as protein disulfide reduction such as ribonucleotide reductase ¹⁸³ and post-translational modification of proteins by S-glutathionylation with a role mainly as a deglutathionylase ^{184,185}. Protein S-glutathionylation is a post-translational modification of specific Cys residues regulating the normal function of proteins with an important role in redox signaling. S-glutathionylation may be enzymatic catalyzed by glutathione transferases such as glutathione s-transferase π ¹⁸⁶, but it is mainly a spontaneous consisting of the reversible formation of a protein mixed disulfide with GSH (Protein-SSG). It exists several mechanisms of protein-SSG formation: i) the thiol-disulfide exchange with GSSG but it is an unlikely mechanism of protein S-glutathionylation since the required very low GSH/GSSG ratio is unlikely under physiological conditions; ii) the sulfenic acid (-SOH) formed at sensitive protein Cys after oxidation by ROS/RNS reacts quickly with GSH to form protein-SGG; and iii) by consumption of glutathione thiyl radicals (GS \cdot); and iv) by reaction with GSNO. S-glutathionylation modifies key proteins that belong to

several functional categories such as redox homeostasis, protein folding and degradation, Glycolysis, energy sensing, insulin signaling, calcium homeostasis, the cytoskeleton, apoptosis and transcriptional regulation ^{184,187–189}.

The GSH/Grx/GR system catalyzes reversible deglutathionylation of protein-SSG both through dithiol and monothiol mechanisms; however, the monothiol mechanism is prevalent. The N-terminal active site cysteinyl residue of Grx forms a GSH-mixed disulfide intermediate. Thus, the target protein is reduced and the Grx-SSG formed is reduced by GSH to produce GSSG as a product ¹⁹⁰.

Grx1 regulates apoptosis *via* MAPK, ASK1 and caspase-3 just like Trx1. Reduced Grx1 binds to ASK1 inhibiting its kinase activity but oxidation of Grx1 results in dissociation of the complex and therefore in the activation of ASK1 protein kinase activating JNK1- and p38-dependent signal pathways ¹⁹¹. There is a crosstalk between protein S-glutathionylation and S-nitrosation. Caspase-3 is also susceptible to inhibition by glutathionylation, and this is regulated by Grx1 ¹⁹². The same happens with NOS3, Grx1 regulates its activity by deglutathionylation ¹⁹³. Glyceraldehyde-3-phosphate dehydrogenase (GAPDH) ¹⁹⁴ and protein tyrosine phosphatase 1B (PTP1B) ¹⁹⁵ also targets proteins of Grx1 deglutathionylase activity. Recently, other targets of the Grx1 deglutathionylase activity have been found, such as IL-1 β ¹⁹⁶, DJ-1 and HSP60 ¹⁹⁷.

3.5.3. Methionine sulfoxide reductase (Msr)

The amino acid methionine, like cysteine, is also a target ROS can be oxidized to methionine sulfoxide (MetO) forming two enantiomers: S-MetO and R-MetO. This oxidation is reversed by the methionine sulfoxide reductases (Msr) and Trx/TrxR system that can catalyze the reduction of free and protein-bound MetO ¹⁹⁸. The Msr system consists of two major proteins, MsrA and MsrB, that can reduce both enantiomers. In human, MsrA enzyme can be found in two isoforms: one form that can be transported to the mitochondria and another form that is located in the cytosol. MsrB proteins (selenoprotein (MsrB1) and the other two non-selenoproteins (MsrB2 and MsrB3), could be targeted to different subcellular compartments. Due to their action, Msr enzymes are involved in regulation of protein function, in signal-transduction pathways, and preventing cellular accumulation of faulty proteins. Msr system failures can promote oxidative damage and neurodegenerative diseases as well as shorter life span ¹⁹⁹.

3.5.4. Sulfiredoxin (Srx)

Sulfiredoxin (Srx) is a recently discovered member of the oxidoreductases family that catalyzes the reduction of the cysteine sulfinic acid (hyperoxidation) of the 2-Cys peroxiredoxins enzymes back to their stable thiol state using ATP and magnesium²⁰⁰. Therefore, the inactivation of Prdx caused by the increased in hydrogen peroxide as an intracellular cell signaling agent is reversed by Srx²⁰¹. Another important possible function of Srx is the deglutathiolylation of proteins such as peroxiredoxin, actin and protein tyrosine phosphatase 1B²⁰². Srx is mainly located in the cytosol but it gets translocated to the mitochondria during an oxidative stress²⁰³.

3.5.5 S-nitrosoglutathione reductase (GSNOR)

Human S-nitrosoglutathione reductase (GSNOR) or ADH5, belongs to alcohol dehydrogenase (ADH) family. It is the unique member of the family that not only use short-chain alcohols as the main substrate but also GSNO and S-hydroxymethylglutathione. GSNOR regulates the levels of intracellular NO• available by catalyzing the breakdown of GSNO so indirectly regulates protein-S-nitration. It is located to the nucleus and cytoplasm and functions as a homodimer²⁰⁴. It has been demonstrated that GSNOR deficiency together with defective DNA repair promote hepatocarcinoma carcinogenesis²⁰⁵.

4. Redox homeostasis, redox signaling and cancer

Redox homeostasis, that is, the correct balance between the levels of ROS/RNS and antioxidant systems is essential for the proper functioning of cells. A wide variety of stimuli by different signal molecules (growth factors, cytokines and G-protein-coupled receptors) have been described which generate H₂O₂, which can have a dual role, either in signaling or in oxidative stress²⁰⁶. In addition, a large number of kinases, phosphatases or transcription factors involved in signaling are regulated by their redox state. This will affect key cellular processes such as proliferation, differentiation or death.

In humans, oxidative stress has been linked to a wide variety of serious diseases, such as neurodegenerative disorders, atherosclerosis, hypertension, inflammatory disease, immune system dysfunctions, type 2 diabetes, aging and cancer^{16,65,207,208}. The central nervous system (CNS) is particularly susceptible to oxidation due to the high lipid content and consumption of oxygen, and low levels of antioxidant enzymes. The hippocampus, substantia nigra and striatum are region of the brain that may attack by free radicals. So the oxidative stress is involved in neurodegenerative diseases as Alzheimer's and Parkinson's⁶. Type 2 diabetes is characterized by an altered production of ROS. The main source of ROS seems to be the mitochondria, whose morphology is altered resulting in mitochondrial dysfunction. The relationship between insulin resistance and constitutive ROS production is attributed to alterations in signaling pathways such as JNK pathway¹⁴.

This doctoral thesis has focused on cancer, oxidative/nitrosative stress and the role of redoxins. Specifically, a model of human hepatocarcinoma, HepG2 cell line has been studied. Hepatocarcinoma (HCC) is the most common liver malignancy and is one of the leading causes of cancer death in the world. It represents 80% of the primary hepatic neoplasm that appears mainly in a context of chronic liver cirrhosis. It is the sixth most frequent neoplasm, the third cause of cancer death, and 7% of registered malignancies²⁰⁹. Gene mutations that encode signaling proteins that regulate cell division and cell death are those that transform a normal cell into tumor cells. Although in patients with hepatocarcinoma, the main prevalent genetic mutations are related to telomerase signaling, Wnt-B-catenin, PI3/Akt/mTOR, p53 and MAPK, alterations in redox regulatory mechanisms are also observed²¹⁰.

Cancer cells are characterized by the production of high levels of ROS due to hypoxia-inducible factor 1 (HIF-1), enhanced metabolic activity, mitochondrial dysfunction, oncogene and tumor suppressor activities, activation of Nox, etc. Moreover, the tendency of cancer cells to undergo major changes in their own metabolism (Warburg metabolic reprogramming), such as increased activity in aerobic glycolysis and deregulation of lipid metabolism is also partly modulated by oxidative stress. It has been shown that there is a relationship between oncogenes signaling and oxidative stress (eg., activation of Ras increases ROS levels produced by oxidative phosphorylation that is essential for proliferation) ^{211–214}. However, cancer cells proliferate despite the elevated ROS production thanks to the induction of antioxidant defenses ²¹⁵.

Hanahan and Weinberg originally described six mutation-driven acquired competencies that a tumor cell needs ²¹⁶. Ten years later, they have updated the list of hallmarks, and each of them is related to alterations in signaling transduction ²¹³. Many signaling pathways that are involved in tumor development, progression and malignancy such as cellular proliferation, evasion of apoptosis or anoikis, tissue invasion and metastasis and angiogenesis are redox-sensitive ²¹⁷. A number of signaling proteins that undergo redox changes are targets of redoxins, including Trx1 and Grx1. In addition, it has been shown that Trx1 and TrxR1 are often overexpressed in tumor cells and that high Trx1 could be linked to drug resistance during cancer treatment ²¹⁸.

4.1. Redox signaling pathways involved in carcinogenesis

In cancer cells, high rate of proliferation and evasion of apoptosis depends on the constitutive activation of redox-sensitive signal-transduction at the level of kinases such as MAPK family and PI3K/Akt, phosphatases as PTPB1, PPA2 and PTEN or some redox-sensitive transcription factor as NF- κ B, Nrf2 and STAT. ROS activates the members of **MAPK** family including ERK1/2, JNK, and p38 promoting proliferation, migration, and invasion in HCC ²¹⁹. Hepatocyte growth factor (HGF) induced H₂O₂ generation and JNK phosphorylation in HCC ²²⁰. This MAPK activation requires the oxidation and inactivation of several PTPs that dephosphorylate MAPKs including oxidation in the active site Cys215 of **PTPB1** ²²¹ which is reduced by Trx1 ²²². Moreover, Grx1 also regulates Cys215 of PTPB1 via glutathionylation ¹⁹⁵. On the other hand, activities of JNK and p38 are regulated by the upstream ASK1. ASK1 plays

important role in tumorigenesis by regulating apoptosis and inflammation ^{223,224} and the association with Trx1 ^{159,225} and Grx1 ¹⁹¹ regulates its activity.

ROS induce also **PI3K/Akt signaling** which contributes to tumorigenesis and facilitates the invasion and metastasis by promoting matrix metalloproteinase-9 (MMP-9) secretion ²²⁶. Akt, also called protein kinase B (PKB) can be inactivated by protein phosphatase 2 (PP2A) dephosphorylation when Akt is in its oxidized form which suggests that Akt is a redox-regulated protein. It has been shown that Grx1 prevented Akt from forming a specific disulfide bond between Cys297 and Cys311 and suppressed its association with **PP2A** under oxidative stress ²²⁷. ROS-Akt signaling is activated by inactivation of PTEN through sulfenylation at Cys124 followed by Cys71-Cys124 disulfide bonding that is reverted by Trx1 ²²⁸. Therefore, ROS mediate hyperactivation of PI3K/Akt signaling that results in promotion of tumor cell survival, apoptosis inhibition and resistance to chemotherapy ²²⁹. Regarding apoptosis, there is a relationship with the level of redoxins. As described before, Trx/TrxR system catalyzes the denitrosation of caspase-3 thus showing an anti-apoptotic action. Some experimental data suggested that Trx/TrxR system also participates in the denitrosation of SNO-caspase-9 and the reductive reactivation of caspase-8 ²³⁰. NO[•] production has an important role in the regulation of the carcinogenic process. For instance, S-nitrosation of some proteins, such as CD95, stimulates apoptosis whereas S-nitrosation of other proteins, such as caspases and Bcl-2, inhibits apoptosis ²³¹. In addition, NO[•] stimulates the proliferation of tumor cells through PI3K/Akt signaling activation by nitrosation of Ras Cys118 ²³². In HepG2 cells, overexpression of NOS3 has antiproliferative effect ²³³. NF-κB is a redox-sensitive transcription factor that plays an important role in regulating gene expression involved in cell survival, proliferation, immunity, and inflammation ¹⁶³. ROS can regulate NF-κB activity. As described above, DNA-binding activity of NF-κB is regulated by Trx1 ^{164,165}. In cancer cells, NF-κB activates the expression of many genes involved in cell transformation, proliferation, and angiogenesis ²³⁴. It has been described that ROS production and NF-κB activation promote hepatocellular carcinoma progression ²³⁵.

Despite the high production of ROS, cancer cells proliferate thanks to the induction of antioxidant defense expression such as Trx and proteins that regulate GSH levels through the activation of the transcription factor **Nrf2** ²¹⁵, the major driver of redox-sensitive gene expression. In the cytoplasm, Kelch-like ECH-associated protein 1 (Keap1) interacts with Nrf2 inhibiting its activity. Under oxidative conditions, Keap1 is oxidized and dissociates from Nrf2 allowing its activation ⁶⁶. The redox state

of Cys273 and Cys 288 of Keap1 seem to be critical for the ubiquitination-promoting activity²³⁶.

STAT3 is a transcription factor that promotes cell survival and proliferation and is constitutively activated in human cancer cell lines. STAT3 is activated by tyrosine phosphorylation and then dimerized and translocated into the nucleus, where together with other transcription factors activates the expression of latent genes. Constitutive phosphorylation of STAT3 causes important changes in apoptosis, angiogenesis, invasion, migration and proliferation resulting in malignant transformation in cancer cells²³⁷. Tyrosine phosphorylation of STAT3 is regulated by ROS and itself also influences ROS production. It has been described that STAT3 transcriptional activity depends on its thiol state, which is influenced by H₂O₂ and Prx2 levels and by the thioredoxin system activity²³⁸. These authors have found that inhibition of TrxR increased STAT3 oxidation and as a consequence decreased its activity. In this oxidation state of STAT3 they have observed the formation of Trx1-STAT3 disulfide exchange intermediates, suggesting that Trx1 may be a direct mediator of STAT3 disulfide reduction. Prdx6 also promoted growth of lung tumors in mice through activation of JAK2/STAT3 signaling²³⁹. The role of Prdx6 in cancer is controversial and it has not been much related to cell signaling. Both, peroxidase and PLA₂ activities of Prdx6 were required for tumor development in xenografted mice lung in a process dependent on arachidonic acid (AA) release²⁴⁰. AA production and Nox2 activation was also involved in stimulation of metastasis by Prdx6 PLA₂ activity in several cancer models^{240,241}, although in another study Nox2 activation was shown to proceed by Prdx6 mediated lysophosphatidic acid (LPA) receptor activation²⁴².

4.2. Impact of redox modulation of protein function on cell metabolism in HCC

The activation of oncogenes and the inactivation of tumor suppressors cause a reprogramming in the metabolism of a tumor cell²⁴³. Cancer cells are characterized by having a high rate of aerobic glycolysis that they use to generate ATP in the presence of oxygen, which is known as the Warburg effect. Tumor cells redirect glucose to the pentose phosphate pathway (PPP) to generate NADPH, and macromolecules such as non-essential amino acids, nucleotides and fatty acids that are necessary to cope with the high proliferation rate^{244,245}. Glucose can also be used to produce ATP and lactate thus maintaining the NAD/NADH ratio, which contributes to tumor progression²⁴⁶. The

tricarboxylic acid cycle (TCA) is still active in tumor cells but depends primarily on glutamine metabolism, which replenishes the TCA intermediates. Cancer cells, instead of using TCA for the synthesis of ATP, prefer the intermediates for the production of NADPH and to support fatty acid synthesis in hypoxia or under downregulation of oxidative phosphorylation ²⁴⁷.

The increase in the metabolism of a tumor cell is usually related to an increase in ROS. However, tumor cells adapt to acquire resistance to oxidative stress so that they can increase their metabolism and proliferation rate without suffering oxidative damage ²⁰⁷. The tumor cell uses, in addition to the PPP ²⁴⁸, the folate ²⁴⁹ and malic enzyme pathways ²⁰⁷ to generate NADPH, a cofactor that is necessary in the biosynthetic pathways and to maintain reduced levels of GSH ²⁵⁰. The diversion of glucose to PPPs, glycerol and serine pathways is determined in part by the activity of pyruvate kinase 2 (PKM2) and glyceraldehyde-3-phosphate dehydrogenase (GAPDH) which are redox-regulated enzymes. PKM2 is an isoform of pyruvate kinase expressed in tumor cells, whose Cys358 can be reversibly oxidized when ROS levels are elevated, inactivating the enzyme and lowering the production of the end product pyruvate. This closing of the exit of glycolytic flux induces the accumulation of intermediates upstream stimulating its diversion at 3-phosphoglycerate (3PGA) towards Serine, glycine, the folate cycle, which is another source of NADPH, and eventually towards glutathione biosynthesis ²⁵¹. As with PKM2, reversible oxidation of Cys152 of GAPDH results in enzyme inactivation allowing for diversion of dihydroxyacetone-phosphate (DHAP) towards glycerol for phospholipid biosynthesis, and diversion of triose phosphate and hexose phosphate via PPP towards NADPH and ribose for nucleotide biosynthesis. Moreover, GAPDH can be S-glutathionylated and reduced by Grx1 ¹⁹⁴. NO[•] also regulates the activity of several metabolic enzymes by S-nitrosation such as aconitase (ACO) ²⁵², isocitrate dehydrogenase (IDH) and α -ketoglutarate dehydrogenase (α -KGDH) ²⁵³ that are reversibly denitrosated by Trx1. In addition, S-nitrosation of Cys247 of GAPDH and its reversion by Trx1 stimulates apoptosis ²³¹.

Redox modulation of these two enzymes, GAPDH and PKM2, and the consequences in the glycolytic and lateral fluxes are well documented, but the responsibility of flux control does not rely exclusively on them. Other glycolytic enzymes are also sensitive to redox changes at specific cysteines with effects on their activity and also contribute to connect redox status with flux control like phosphoglycerate mutase (PGAM) ²⁵⁴ and Triose phosphate isomerase ^{255,256}. Changes in the activity of one single enzyme cannot be extrapolated to equivalent changes in metabolic flux through the whole pathway.

4.3. Redox involvement in HCC progression to invasiveness and metastasis

Epithelial-mesenchymal transition (EMT) is an important process that happens in normal development in which epithelial cells lose many of their properties to become mesenchymal cells, which means important changes in architecture and behavior ²⁵⁷. This de-differentiation process also takes place in tumor cells and constitutes the first step towards metastasis as the disease progresses.

There are several ROS-associated signaling pathways involved in EMT. Among these pathways, there are ROS-dependent activation proteins such as Smad, Snail, E-Cadherin, β -catenin and matrix metalloproteinases (MMPs). Transforming Growth Factor- β (TGFB) provokes an increase in the production of ROS that results in the phosphorylation of Smad2, p38MAPK and ERK 1/2 ²⁵⁸. In addition, ROS may regulate EMT through a mechanism that involves NF- κ B in closed collaboration with HIF-1 and cyclooxygenase-2 (COX-2). A critical molecular event of EMT is down-regulation of the cell adhesion molecule E-cadherin and its replacement by N-cadherin. E-cadherin is present in the plasma membrane of normal epithelial cells but not in mesenchymal cells ²⁵⁹, it acts as a suppressor factor of invasion and metastasis in tumor cells and it is usually degraded during transformation or malignancy ²⁶⁰. It has been described by several authors that the activation of Akt leads to a significant reduction in E-cadherin expression and nuclear localization of Snail, suggesting a role for the PI3K/Akt signaling pathway in the transient shift from E-cadherin to N-cadherin, and EMT progression in cancer ^{260,261}. The hyperactivation of PI3K/Akt signaling by mediated by ROS has been described previously and its relationship with tumor cell survival, apoptosis inhibition and resistance to chemotherapy ²²⁹. In fact, the activation of Akt is thought to be responsible for mediating the acquired resistance to sorafenib via mTOR but independent of protein phosphatase 2A in hepatocarcinoma cells ²⁶². Sorafenib simultaneously targets tyrosine kinase receptors such as vascular endothelial growth factor receptor (VEGFR) 2 and 3, platelet-derived growth factor receptor- β (PDGFR- β), Flt3 and c-Kit, as well as molecular components of the MAPK signaling pathway ²⁶³. Several studies have reported Sorafenib downregulates cell survival pathways and increase apoptosis in hepatoma cells and these effects have been associated with the induction of oxidative stress in hepatocarcinoma cells ²⁶⁴. Sorafenib is the recommended therapy for the patients with locally advanced/metastatic disease but the effectiveness is not high and tumor cells become resistant as its invasive capacity and malignancy progresses. It is important to consider the adaptations that occur in this process similar to EMT. JAK/STAT3 has also been related to EMT and cancer progression ²³⁷. It has

been observed that STAT3 activation is involved in EMT, invasion and generation of metastasis in hepatocellular carcinoma (HCC) ²⁶⁵. Trx1 expression in cancer cells is associated with aggressive tumor growth, which makes Trx1 an attractive target for cancer therapy. Although Trx1 has been suggested as potential prognostic marker of HCC, the mechanism of Trx in the pathogenesis and treatment of HCC is still not well known ²⁶⁶.

HYPOTHESIS

Hypothesis

Redox signaling and oxidative damage are balanced in the cell. Oxidative/nitrosative stress is critical for the accumulation of intracellular altered proteins, induction of autophagy, and further cellular apoptosis in unsolved physiopathological intracellular outcome while redox signaling through the transient oxidation/reduction of key Cys residues in regulatory proteins plays a role in all hallmarks of cancer.

Nitric oxide (NO) is a signaling molecule that is produced in cells by the action of nitric oxide synthases in response to various stimuli and that generates nitrosative and oxidative stress with consequences on cell proliferation and death. Most of the effects of NO are produced by reversible S-nitrosation and other types of oxidations of sensitive cysteines in key proteins of metabolic and cell signaling pathways, with consequences on the function of these target proteins. The reversal of these oxidations is carried out by the "Redoxin" family of proteins, that play a role in antioxidant defense and redox signaling. There are several studies that link ROS/RNS with the redoxins, thioredoxin, glutaredoxin and peroxiredoxin, and the process of regulated cell death and cell proliferation.

This project aims to demonstrate that redoxins exert their role acting on metabolic fluxes by controlling the redox state of metabolic enzymes and on proteins involved in signaling pathways.

The hypothesis will be tested in various models of cellular cytotoxicity and experimental hepatocarcinogenesis and in a model of apoptosis induction in hepatocarcinoma cells (HepG2) with elevated levels of NO due to overexpression of NOS3, as well as with reduced levels of the different redoxins by gene silencing. Determination of proliferation and cell death parameters; measurement of the activation status of various signaling pathways (AKT, mTOR, etc.); analysis of the Redox Proteome, the metabolome and the main metabolic fluxes of these cells will be also carried out.

The data obtained are intended to demonstrate the potential beneficial effect of NO as a pro-apoptotic or anti-tumor agent, and the role of redoxins in the resistance of tumor cells against this effect. The obtained results will contribute to the knowledge of redox posttranslational modification (PTM) mechanisms that participate in an

integrated manner with other PTMs in the regulation of cell metabolism, proliferation and death. The effect of Trx on the resistance of cells to treatment with Sorafenib (a drug that is administered to patients with hepatocarcinoma) as a function of the invasiveness and malignancy potential will be tested using a set of cell lines with different degrees of differentiation (HepG2, SNU423 and SNU475) treated with the drug and with interfering RNA of Trx1.

The results are reported in three articles and are expected to provide new insights for the design of antitumor therapies.

OBJECTIVES

Objectives

The aim of this PhD Thesis project is to study the functions of redoxins (Trx1, Grx1 and Prdx6) in the regulation of signaling pathway and metabolism in hepatocarcinoma cell lines subjected or not to oxidative/nitrosative stress. To achieve the main objective, the following partial objectives have been carried out:

1. Determination of the differential "thiolic redox proteome" of HepG2 cells that express different levels of nitric oxide by ESI-LC-MS/MS when the levels of Trx1, Grx1 and Prdx6 are down-regulated by specific interfering RNAs. This objective was addressed in **Articles 1 and 2**. It included optimization of the methodology in the case of Prdx6 redox proteome. **(Article 2)**.

2. Description of the in vivo physiological significance of Trx1, Grx1 and Prdx6 induced redox changes in the proteome. This objective was dealt with in **Article 1** measuring the metabolic flux of glycolysis and pentose phosphate with radioactively labelled glucose and the activity of glycolytic enzymes. In addition, the functions of the three redoxins in the context of proliferation and cell death by apoptosis were studied. **(Article 1 and 2)**.

3. Extension of the study of the metabolic functions of the three redoxins to the greatest possible number of metabolic pathways. This objective was addressed by a comprehensive analysis of the metabolome of HepG2 cells with silenced levels of each of the 3 redoxins (Trx1, Grx1 and Prdx6). **(Articles 1 and 2)**.

4. Quantification of the activity and expression levels of Trx1, Grx1 and Prdx6 in HepG2 cells subject or not to high levels of NO as well as low levels of Prdx6. **(Unpublished data)**.

5. Correlation and integration of the results obtained in the previous sections with the degree of cell death due to apoptosis and their metabolic state in these tumor cells. **(Articles 1 and 2)**.

6. Comparing the effects of Trx1 in HepG2 cells with its effect in other hepatoblastoma cell lines with different degree of differentiation, malignancy and invasiveness potential. This objective was addressed in **Article 3** by quantifying the Global Proteome in samples of HepG2, SNU423 and SNU475 cells treated with Sorafenib, a drug that is administered to patients with hepatocarcinoma, and/or interfering RNA of Trx1.

7. Obtaining the HepG2 Knockout line for Prdx6 through CRISPR/Cas9 technology. **(Unpublished data).**

CONCLUSIONS

Conclusions

1. The data presented here in show that Trx and/or Grx are involved in redox modifications of targeted cysteines of several glycolytic enzymes affecting their activity, but importantly, changes in the activity of one single enzyme cannot be extrapolated to equivalent changes in metabolic flux through the whole pathway. These changes are part of a widespread adaptive mechanism aimed at redistributing metabolic fluxes between Glycolysis and its off-shooting pathways to respond to subtle changes in the cellular redox environment. Trx and Grx share a number of protein Cys redox targets but down regulation of either redoxin has markedly different metabolic outcomes: silencing of Trx1 stimulates glycolytic flux while silencing of Grx1 decelerates it. **(Article 1)**

2. Besides its canonical antioxidant action, Trx1 also contributes to oxidative modification of some protein thiols, likely by activation of NOS3 and unbalancing ROS/RNS levels, reflecting the delicate sensitivity of redox equilibrium to changes in any of the elements involved and the difficulty of forecasting metabolic responses to redox environmental changes. **(Article 1)**

3. A correlation can be put forward between the reversible oxidation of Cys91 of Prdx6 upon Grx1 silencing that is accompanied by a significative increase in *sn*-2-arachidonyl containing phospholipids and Cys91 sensitivity to glutathionylation, considering the well-known deglutathionylase activity of Grx1. **(Article 1)**

4. The complex wide effects of moderate Prdx6 down-regulation should be a reflection of its moonlighting properties acting as peroxidase, phospholipase and LPC-acyltransferase. The response of HepG2 cells to Prdx6 silencing spans from metabolic and signaling pathways remodeling to alterations in the redox proteome and membrane turnover with effects in cell cycle progression and proliferation. The role of Prdx6 in cancer cells has been studied previously with conflicting outcomes. Most reports point to a pro-proliferating and antiapoptotic action of Prdx6, but some studies have found the opposite effect, depending on the stage of tumor development. Moreover, these effects have not always been assigned to a particular activity of

Prdx6, either peroxidase, PLA2 or LPCAT, neither a common mechanism has been provided. In the study reported in Article 2 Prdx6 silencing down to $\approx 40\%$ would represent a situation mimicking a cellular response to endogenous or exogenous stimuli under normal or oxidative stress conditions. It appears that the cell responds to Prdx6 down-regulation by initiating a biosynthetic program leading to membrane and vesicle trafficking rearrangement with signs of entering cell cycle G1 phase but inability to proceed on to S phase. The mechanisms behind these phenomena involve reversible thiol oxidative changes in key proteins. HK2-Cys³⁶⁸ and Prdx6 “extra” Cys⁹¹ stand out as relevant thiol switches. The former could affect association with the mitochondrial membrane with consequences on the rate of glucose catabolism and mitochondrial permeability; the latter is not conserved among the 1-Cys type Peroxiredoxin and has been given little attention so far but could turn out to bear relevant functions in human cells. **(Article 2)**

5. Based on the results obtained in Article 2 and the contrasting reports on the roles and mechanisms of multifunctional Prdx6 in several pathologies, obtaining a knockout cell line of the human peroxiredoxin 6 can be a first step to determine the implications of this protein into a cellular level. With this objective and using the CRISPR-Cas9 technique, a human hepatocarcinoma cell line HepG2~~prdx6~~/~~prdx6~~ has been constructed and characterized demonstrating that both alleles of the Prdx6 gene were mutated by deletion. **(Unpublished data)**

6. The study presented in **Article 3** shows that Sorafenib treatment had a limited effect on Trx1/TrxR1- rich and poorly-differentiated HCC cells expected to be present at high proportion in the advanced stage of the disease. However, when the application of Sorafenib is combined with Trx1 knock-down, which implies a thiol oxidative redox change of STAT3, it affects very significantly the signaling pathways involved in metastatic and invasive potential of mesenchymal cells. It is suggested that combination of Sorafenib with thioredoxin inhibitors should be taken into account in the design of anticancer therapies. **(Article 3)**

REFERENCES

References

1. Gutteridge, J. M. C. Biological origin of free radicals, and mechanisms of antioxidant protection. *Chem. Biol. Interact.* **91**, 133–140 (1994).
2. Nordberg, J. & Arnér, E. S. J. Reactive oxygen species, antioxidants, and the mammalian thioredoxin system. *Free Radic. Biol. Med.* **31**, 1287–1312 (2001).
3. Kohen, R. & Nyska, A. Invited Review: Oxidation of Biological Systems: Oxidative Stress Phenomena, Antioxidants, Redox Reactions, and Methods for Their Quantification. *Toxicol. Pathol.* **30**, 620–650 (2002).
4. Szabó, C., Ischiropoulos, H. & Radi, R. Peroxynitrite: biochemistry, pathophysiology and development of therapeutics. *Nat. Rev. Drug Discov.* **6**, 662–680 (2007).
5. Ozcan, A. & Ogun, M. Biochemistry of Reactive Oxygen and Nitrogen Species. in *Basic Principles and Clinical Significance of Oxidative Stress* (InTech, 2015). doi:10.5772/61193
6. Phaniendra, A., Jestadi, D. B. & Periyasamy, L. Free Radicals: Properties, Sources, Targets, and Their Implication in Various Diseases. *Indian J. Clin. Biochem.* **30**, 11–26 (2015).
7. Nathan, C. & Shiloh, M. U. Reactive oxygen and nitrogen intermediates in the relationship between mammalian hosts and microbial pathogens. *Proc. Natl. Acad. Sci.* **97**, 8841–8848 (2000).
8. Alderton, W. K., Cooper, C. E. & Knowles, R. G. Nitric oxide synthases: structure, function and inhibition. *Biochem. J.* **357**, 593 (2001).
9. Dickinson, B. C. & Chang, C. J. Chemistry and biology of reactive oxygen species in signaling or stress responses. *Nat. Chem. Biol.* **7**, 504–511 (2011).
10. Sies, H. Oxidative Stress: Introductory Remarks. in *Oxidative Stress* 1–8 (Elsevier, 1985). doi:10.1016/B978-0-12-642760-8.50005-3
11. Sies, H. On the history of oxidative stress: Concept and some aspects of current development. *Curr. Opin. Toxicol.* **7**, 122–126 (2018).
12. Sies, H., Berndt, C. & Jones, D. P. Oxidative Stress. *Annu. Rev. Biochem.* **86**, 715–748 (2017).
13. Janssen-Heininger, Y. M. W. *et al.* Redox-based regulation of signal transduction: Principles, pitfalls, and promises. *Free Radic. Biol. Med.* **45**, 1–17 (2008).
14. Finkel, T. Signal transduction by reactive oxygen species. *J. Cell Biol.* **194**, 7–15 (2011).
15. D’Autréaux, B. & Toledano, M. B. ROS as signalling molecules: Mechanisms that generate specificity in ROS homeostasis. *Nat. Rev. Mol. Cell Biol.* **8**, 813–824 (2007).
16. Valko, M. *et al.* Free radicals and antioxidants in normal physiological functions and human disease. *Int. J. Biochem. Cell Biol.* **39**, 44–84 (2007).

17. Di Meo, S., Reed, T. T., Venditti, P. & Victor, V. M. Role of ROS and RNS Sources in Physiological and Pathological Conditions. *Oxid. Med. Cell. Longev.* **2016**, 1–44 (2016).
18. Halliwell, B. & Gutteridge, J. M. C. *Free Radicals in Biology and Medicine*. (Oxford University Press, 2015). doi:10.1093/acprof:oso/9780198717478.001.0001
19. Krause, K.-H. Aging: A revisited theory based on free radicals generated by NOX family NADPH oxidases. *Exp. Gerontol.* **42**, 256–262 (2007).
20. Schieber, M. & Chandel, N. S. ROS Function in Redox Signaling and Oxidative Stress. *Curr. Biol.* **24**, R453–R462 (2014).
21. Liguori, I. *et al.* Oxidative stress, aging, and diseases. *Clin. Interv. Aging* **13**, 757–772 (2018).
22. Wild, C. P. The exposome: from concept to utility. *Int. J. Epidemiol.* **41**, 24–32 (2012).
23. Go, Y. M. & Jones, D. P. Redox biology: Interface of the exposome with the proteome, epigenome and genome. *Redox Biol.* **2**, 358–360 (2014).
24. Jones, D. P., Park, Y. & Ziegler, T. R. Nutritional Metabolomics: Progress in Addressing Complexity in Diet and Health. *Annu. Rev. Nutr.* **32**, 183–202 (2012).
25. Murphy, M. P. How mitochondria produce reactive oxygen species. *Biochem. J.* **417**, 1–13 (2009).
26. Quinlan, C. L., Perevoshchikova, I. V., Hey-Mogensen, M., Orr, A. L. & Brand, M. D. Sites of reactive oxygen species generation by mitochondria oxidizing different substrates. *Redox Biol.* **1**, 304–312 (2013).
27. Starkov, A. A. The Role of Mitochondria in Reactive Oxygen Species Metabolism and Signaling. *Ann. N. Y. Acad. Sci.* **1147**, 37–52 (2008).
28. Mailloux, R. J. & Harper, M.-E. Mitochondrial proticity and ROS signaling: lessons from the uncoupling proteins. *Trends Endocrinol. Metab.* **23**, 451–458 (2012).
29. Takeya, R., Ueno, N. & Sumimoto, H. Regulation of Superoxide- Producing NADPH Oxidases in Nonphagocytic Cells. in *Methods in Enzymology* **406**, 456–468 (2006).
30. Lambeth, J. D. Nox/Duox family of nicotinamide adenine dinucleotide (phosphate) oxidases. *Curr. Opin. Hematol.* **9**, 11–17 (2002).
31. Bedard, K. & Krause, K.-H. The NOX Family of ROS-Generating NADPH Oxidases: Physiology and Pathophysiology. *Physiol. Rev.* **87**, 245–313 (2007).
32. Schröder, K., Weissmann, N. & Brandes, R. P. Organizers and activators: Cytosolic Nox proteins impacting on vascular function. *Free Radic. Biol. Med.* **109**, 22–32 (2017).
33. Cho, K.-J., Seo, J.-M. & Kim, J.-H. Bioactive lipoyxygenase metabolites stimulation of NADPH oxidases and reactive oxygen species. *Mol. Cells* **32**, 1–5 (2011).

34. Hong, H.-Y., Jeon, W.-K. & Kim, B.-C. Up-regulation of heme oxygenase-1 expression through the Rac1/NADPH oxidase/ROS/p38 signaling cascade mediates the anti-inflammatory effect of 15-deoxy- Δ 12,14 -prostaglandin J 2 in murine macrophages. *FEBS Lett.* **582**, 861–868 (2008).
35. Gross, E. *et al.* Generating disulfides enzymatically: Reaction products and electron acceptors of the endoplasmic reticulum thiol oxidase Ero1p. *Proc. Natl. Acad. Sci.* **103**, 299–304 (2006).
36. Hrycay, E. G. & Bandiera, S. M. Involvement of Cytochrome P450 in Reactive Oxygen Species Formation and Cancer. in *Advances in Pharmacology* **74**, 35–84 (Elsevier Inc., 2015).
37. del Río, L. A., Sandalio, L. M., Palma, J., Bueno, P. & Corpas, F. J. Metabolism of oxygen radicals in peroxisomes and cellular implications. *Free Radic. Biol. Med.* **13**, 557–580 (1992).
38. Schrader, M. & Fahimi, H. D. Peroxisomes and oxidative stress. *Biochim. Biophys. Acta - Mol. Cell Res.* **1763**, 1755–1766 (2006).
39. Stolz, D. Peroxisomal localization of inducible nitric oxide synthase in hepatocytes. *Hepatology* **36**, 81–93 (2002).
40. Fritz, R. *et al.* Compartment-dependent management of H₂O₂ by peroxisomes. *Free Radic. Biol. Med.* **42**, 1119–1129 (2007).
41. Dizdaroglu, M., Jaruga, P., Birincioglu, M. & Rodriguez, H. Free radical-induced damage to DNA: mechanisms and measurement. *Free Radic. Biol. Med.* **32**, 1102–1115 (2002).
42. Helbock, H. J., Beckman, K. B. & Ames, B. N. 8-Hydroxydeoxyguanosine and 8-hydroxyguanine as biomarkers of oxidative DNA damage. in *Methods in Enzymology* **300**, 156–166 (1999).
43. Hiraku, Y., Kawanishi, S., Ichinose, T. & Murata, M. The role of iNOS-mediated DNA damage in infection- and asbestos-induced carcinogenesis. *Ann. N. Y. Acad. Sci.* **1203**, 15–22 (2010).
44. Hofer, T. *et al.* Hydrogen peroxide causes greater oxidation in cellular RNA than in DNA. *Biol. Chem.* **386**, 333–337 (2005).
45. Rubbo, H. *et al.* Nitric oxide regulation of superoxide and peroxynitrite-dependent lipid peroxidation. Formation of novel nitrogen-containing oxidized lipid derivatives. *J. Biol. Chem.* **269**, 26066–26075 (1994).
46. Marnett, L. J. Lipid peroxidation - DNA damage by malondialdehyde. *Mutat. Res. - Fundam. Mol. Mech. Mutagen.* **424**, 83–95 (1999).
47. Doorn, J. A. & Petersen, D. R. Covalent adduction of nucleophilic amino acids by 4-hydroxynonenal and 4-oxononenal. *Chem. Biol. Interact.* **143–144**, 93–100 (2003).
48. Kelly, F. J. & Mudway, I. S. Protein oxidation at the air-lung interface. *Amino Acids* **25**, 375–396 (2003).
49. Milne, G. L., Musiek, E. S. & Morrow, J. D. F₂ -Isoprostanes as markers of oxidative stress in vivo : An overview. *Biomarkers* **10**, 10–23 (2005).

50. Davies, K. J. & Delsignore, M. E. Protein damage and degradation by oxygen radicals. *J. Biol. Chem.* **262**, 9895–9901 (1987).
51. Holmström, K. M. & Finkel, T. Cellular mechanisms and physiological consequences of redox-dependent signalling. *Nat. Rev. Mol. Cell Biol.* **15**, 411–421 (2014).
52. Sundaresan, M., Yu, Z.-X., Ferrans, V. J., Irani, K. & Finkel, T. Requirement for Generation of H₂O₂ for Platelet-Derived Growth Factor Signal Transduction. *Science (80-.)*. **270**, 296–299 (1995).
53. Bae, Y. S. *et al.* Epidermal Growth Factor (EGF)-induced Generation of Hydrogen Peroxide. *J. Biol. Chem.* **272**, 217–221 (1997).
54. Meng, T., Fukada, T. & Tonks, N. K. Reversible Oxidation and Inactivation of Protein Tyrosine Phosphatases In Vivo. *Mol. Cell* **9**, 387–399 (2002).
55. Ghezzi, P. Oxidoreduction of protein thiols in redox regulation. *Biochem. Soc. Trans.* **33**, 1378–1381 (2005).
56. McDonagh, B., Ogueta, S., Lasarte, G., Padilla, C. A. & Bárcena, J. A. Shotgun redox proteomics identifies specifically modified cysteines in key metabolic enzymes under oxidative stress in *Saccharomyces cerevisiae*. *J. Proteomics* **72**, 677–89 (2009).
57. McDonagh, B. Detection of ROS Induced Proteomic Signatures by Mass Spectrometry. *Front. Physiol.* **8**, 1–7 (2017).
58. McDonagh, B., Sakellariou, G. K., Smith, N. T., Brownridge, P. & Jackson, M. J. Differential cysteine labeling and global label-free proteomics reveals an altered metabolic state in skeletal muscle aging. *J. Proteome Res.* **13**, 5008–5021 (2014).
59. Go, Y.-M. & Jones, D. P. Thiol/disulfide redox states in signaling and sensing. *Crit. Rev. Biochem. Mol. Biol.* **48**, 173–181 (2013).
60. Klomsiri, C., Karplus, P. A. & Poole, L. B. Cysteine-based redox switches in enzymes. *Antioxidants Redox Signal.* **14**, 1065–1077 (2011).
61. Tennant, D. A., Durán, R. V. & Gottlieb, E. Targeting metabolic transformation for cancer therapy. *Nat. Rev. Cancer* **10**, 267–277 (2010).
62. Erickson, J. R. *et al.* A Dynamic Pathway for Calcium-Independent Activation of CaMKII by Methionine Oxidation. *Cell* **133**, 462–474 (2008).
63. Hung, R.-J., Spaeth, C. S., Yesilyurt, H. G. & Terman, J. R. SelR reverses Mical-mediated oxidation of actin to regulate F-actin dynamics. *Nat. Cell Biol.* **15**, 1445–1454 (2013).
64. Lee, B. C. *et al.* MsrB1 and MICALs Regulate Actin Assembly and Macrophage Function via Reversible Stereoselective Methionine Oxidation. *Mol. Cell* **51**, 397–404 (2013).
65. Dröge, W. Free Radicals in the Physiological Control of Cell Function. *Physiol. Rev.* **82**, 47–95 (2002).
66. Trachootham, D., Lu, W., Ogasawara, M. A., Valle, N. R. & Huang, P. Redox Regulation of Cell Survival. *Antioxid. Redox Signal.* **10**, (2008).

67. Shay, K. P., Moreau, R. F., Smith, E. J., Smith, A. R. & Hagen, T. M. Alpha-lipoic acid as a dietary supplement: Molecular mechanisms and therapeutic potential. *Biochim. Biophys. Acta - Gen. Subj.* **1790**, 1149–1160 (2009).
68. Beyer, R. E. The role of ascorbate in antioxidant protection of biomembranes: Interaction with vitamin E and coenzyme Q. *J. Bioenerg. Biomembr.* **26**, 349–358 (1994).
69. Helmut, S. Glutathione and its role in cellular functions. *Free Radic. Biol. Med.* **27**, 916–921 (1999).
70. McCord, JM and Fridovich, I. Superoxide dismutase. An enzymic function for erythrocyte (hemocuprein). *J. Biol. Chem.* **244**, 6049–6055 (1969).
71. Fukai, T. & Ushio-Fukai, M. Superoxide Dismutases: Role in Redox Signaling, Vascular Function, and Diseases. *Antioxid. Redox Signal.* **15**, 1583–1606 (2011).
72. Glorieux, C. & Calderon, P. B. Catalase, a remarkable enzyme: targeting the oldest antioxidant enzyme to find a new cancer treatment approach. *Biol. Chem.* **398**, 1095–1108 (2017).
73. Labunskyy, V. M., Hatfield, D. L. & Gladyshev, V. N. Selenoproteins: Molecular Pathways and Physiological Roles. *Physiol. Rev.* **94**, 739–777 (2014).
74. Forman, H. J., Zhang, H. & Rinna, A. Glutathione: Overview of its protective roles, measurement, and biosynthesis. *Mol. Aspects Med.* **30**, 1–12 (2009).
75. Franco, R. & Cidlowski, J. A. Apoptosis and glutathione : beyond an antioxidant. *Cell Death Differ.* **16**, 1303–1314 (2009).
76. Rhee, S. G., Kang, S. W., Chang, T. S., Jeong, W. & Kim, K. Peroxiredoxin, a novel family of peroxidases. *IUBMB Life* **52**, 35–41 (2001).
77. Nicolussi, A., D'inzeo, S., Capalbo, C., Giannini, G. & Coppa, A. The role of peroxiredoxins in cancer (Review). *Mol. Clin. Oncol.* 139–153 (2017). doi:10.3892/mco.2017.1129
78. Nelson, K. J. *et al.* Analysis of the peroxiredoxin family: Using active-site structure and sequence information for global classification and residue analysis. *Proteins Struct. Funct. Bioinforma.* **79**, 947–964 (2011).
79. Hofmann, B., Hecht, H. & Flohé, L. Peroxiredoxins. *Biol. Chem.* **383**, 347–364 (2002).
80. Rhee, S. G., Woo, H. A., Kil, I. S. & Bae, S. H. Peroxiredoxin functions as a peroxidase and a regulator and sensor of local peroxides. *J. Biol. Chem.* **287**, 4403–4410 (2012).
81. Wood, Z. A., Poole, L. B., Hantgan, R. R. & Karplus, P. A. Dimers to doughnuts: Redox-sensitive oligomerization of 2-cysteine peroxiredoxins. *Biochemistry* **41**, 5493–5504 (2002).
82. Sue, G. R., Ho, Z. C. & Kim, K. Peroxiredoxins: A historical overview and speculative preview of novel mechanisms and emerging concepts in cell signaling. *Free Radic. Biol. Med.* **38**, 1543–1552 (2005).
83. Seo, M. S. *et al.* Identification of a new type of mammalian peroxiredoxin that

- forms an intramolecular disulfide as a reaction intermediate. *J. Biol. Chem.* **275**, 20346–20354 (2000).
84. Manevich, Y., Feinstein, S. I. & Fisher, A. B. Activation of the antioxidant enzyme 1-CYS peroxiredoxin requires glutathionylation mediated by heterodimerization with GST. *Proc. Natl. Acad. Sci.* **101**, 3780–3785 (2004).
 85. Pedrajas, J. R., Padilla, C. A., McDonagh, B. & Bárcena, J. A. Glutaredoxin participates in the reduction of peroxides by the mitochondrial 1-CYS peroxiredoxin in *saccharomyces cerevisiae*. *Antioxidants Redox Signal.* **13**, 249–258 (2010).
 86. Pedrajas, J. R. *et al.* Glutathione Is the Resolving Thiol for Thioredoxin Peroxidase Activity of 1-Cys Peroxiredoxin Without Being Consumed During the Catalytic Cycle. *Antioxid. Redox Signal.* **24**, 115–128 (2016).
 87. Barranco-Medina, S., Lázaro, J. J. & Dietz, K. J. The oligomeric conformation of peroxiredoxins links redox state to function. *FEBS Lett.* **583**, 1809–1816 (2009).
 88. Kim, T. S. *et al.* Identification of a human cDNA clone for lysosomal type Ca²⁺-independent phospholipase A2 and properties of the expressed protein. *J. Biol. Chem.* **272**, 2542–2550 (1997).
 89. Akiba S, Docia C, Chen X, F. A. Characterization of acidic Ca(2+)-independent phospholipase A2 of bovine lung. *Comp Biochem Physiol B Biochem Mol Biol* **120**, 393–404 (1998).
 90. Netto, L. E. S. & Antunes, F. The Roles of Peroxiredoxin and Thioredoxin in Hydrogen Peroxide Sensing and in Signal Transduction. *Mol. Cells* **39**, 65–71 (2016).
 91. Wood, Z. A., Poole, L. B. & Karplus, P. A. Peroxiredoxin Evolution and the Regulation of Hydrogen Peroxide Signaling. *Science (80-.)*. **300**, 650–653 (2003).
 92. Rhee, S. G., Woo, H. A. & Kang, D. The Role of Peroxiredoxins in the Transduction of H₂O₂ signals. **28**, 537–557 (2018).
 93. Toledano, M. B. & Huang, B. Microbial 2-Cys Peroxiredoxins : Insights into Their Complex Physiological Roles. **39**, 31–39 (2016).
 94. Kil, I. S. *et al.* Feedback Control of Adrenal Steroidogenesis via H₂O₂ - Dependent , Reversible Inactivation. *Mol. Cell* **46**, 584–594 (2012).
 95. Rhee, S. G. Overview on Peroxiredoxin. *Mol. Cells* **39**, 1–5 (2016).
 96. Latimer, H. R. & Veal, E. A. Peroxiredoxins in Regulation of MAPK Signalling Pathways ; Sensors and Barriers to Signal Transduction. *Mol. Cells* **39**, 40–45 (2016).
 97. Park, M. H., Jo, M., Kim, Y. R., Lee, C. K. & Hong, J. T. Roles of peroxiredoxins in cancer, neurodegenerative diseases and inflammatory diseases. *Pharmacol. Ther.* **163**, 1–23 (2016).
 98. Chen, J. W., Dodia, C., Feinstein, S. I., Jain, M. K. & Fisher, A. B. 1-Cys peroxiredoxin, a bifunctional enzyme with glutathione peroxidase and phospholipase A2 activities. *J. Biol. Chem.* **275**, 28421–28427 (2000).

99. Fisher, A. B., Dodia, C., Manevich, Y., Chen, J. W. & Feinstein, S. I. Phospholipid hydroperoxides are substrates for non-selenium glutathione peroxidase. *J. Biol. Chem.* **274**, 21326–21334 (1999).
100. Fisher, A. B. *et al.* A novel lysophosphatidylcholine acyl transferase activity is expressed by peroxiredoxin 6. *J. Lipid Res.* **57**, 587–596 (2016).
101. Chowdhury, I. *et al.* Oxidant stress stimulates expression of the human peroxiredoxin 6 gene by a transcriptional mechanism involving an antioxidant response element. *Free Radic. Biol. Med.* **46**, 146–153 (2009).
102. Manevich, Y. *et al.* Binding of peroxiredoxin 6 to substrate determines differential phospholipid hydroperoxide peroxidase and phospholipase A2 activities. *Arch. Biochem. Biophys.* **485**, 139–149 (2009).
103. Li, Haitao; Benipal, Bavneet, Zhou, Suiping; Dodia, Chandra; Chatterjee, Shampa, Tao, Jian-Qin; Sorokina, Elena M; Raabe, Tobias; Feinstein, Sheldon I and Fisher, A. B. Critical Role of Peroxiredoxin 6 in the Repair of Peroxidized Cell Membranes. *Free Radic. Biol. Med.* **87**, 356–365 (2015).
104. Manevich, Y., Reddy, K. S., Shuvaeva, T., Feinstein, S. I. & Fisher, A. B. Structure and phospholipase function of peroxiredoxin 6: identification of the catalytic triad and its role in phospholipid substrate binding. *J. Lipid Res.* **48**, 2306–2318 (2007).
105. Kim, K. H., Lee, W. & Kim, E. E. K. Crystal structures of human peroxiredoxin 6 in different oxidation states. *Biochem. Biophys. Res. Commun.* **477**, 717–722 (2016).
106. Kang, S. W., Baines, I. C. & Rhee, S. G. Characterization of a mammalian peroxiredoxin that contains one conserved cysteine. *J. Biol. Chem.* **273**, 6303–6311 (1998).
107. Wu, Y. *et al.* Mitogen-activated protein kinase-mediated phosphorylation of peroxiredoxin 6 regulates its phospholipase A 2 activity. *Biochem. J* **679**, 669–679 (2009).
108. Sorokina, E. M. *et al.* Mutation of serine 32 to threonine in peroxiredoxin 6 preserves its structure and enzymatic function but abolishes its trafficking to lamellar bodies. *J. Biol. Chem.* **291**, 9268–9280 (2016).
109. Sorokina, E. M., Feinstein, S. I., Zhou, S. & Fisher, A. B. Intracellular targeting of peroxiredoxin 6 to lysosomal organelles requires MAPK activity and binding to 14-3-3 ϵ . *Am. J. Physiol. Cell Physiol.* **300**, C1430–C1441 (2011).
110. Chatterjee, S. *et al.* Peroxiredoxin 6 phosphorylation and subsequent phospholipase A2 activity are required for agonist-mediated activation of NADPH oxidase in mouse pulmonary microvascular endothelium and alveolar macrophages. *J. Biol. Chem.* **286**, 11696–11706 (2011).
111. Krishnaiah, S. Y., Dodia, C., Feinstein, S. I. & Fisher, A. B. p67phox terminates the phospholipase A2-derived signal for activation of NADPH oxidase (NOX2). *FASEB J.* **27**, 2066–2073 (2013).
112. Kwon, J. *et al.* Peroxiredoxin 6 (Prdx6) supports NADPH oxidase1 (Nox1)-based superoxide generation and cell migration. *Free Radic. Biol. Med.* **96**, 99–115 (2016).

113. Catalá, A. Lipid peroxidation of membrane phospholipids generates hydroxy-alkenals and oxidized phospholipids active in physiological and/or pathological conditions. *Chem. Phys. Lipids* **157**, 1–11 (2009).
114. Fisher, A. B., Dodia, C., Yu, K., Manevich, Y. & Feinstein, S. I. Lung phospholipid metabolism in transgenic mice overexpressing peroxiredoxin 6. *Biochim. Biophys. Acta - Mol. Cell Biol. Lipids* **1761**, 785–792 (2006).
115. Fisher, A. B., Dodia, C., Feinstein, S. I. & Ho, Y.-S. Altered lung phospholipid metabolism in mice with targeted deletion of lysosomal-type phospholipase A 2. *J. Lipid Res.* **46**, 1248–1256 (2005).
116. Fisher, A. B. & Dodia, C. Lysosomal-type PLA2 and turnover of alveolar DPPC. *Am. J. Physiol. Lung Cell. Mol. Physiol.* **280**, L748-54 (2001).
117. Lien, Y.-C., Feinstein, S. I., Dodia, C. & Fisher, A. B. The Roles of Peroxidase and Phospholipase A2 Activities of Peroxiredoxin 6 in Protecting Pulmonary Microvascular Endothelial Cells Against Peroxidative Stress. *Antioxid. Redox Signal.* **16**, 440–451 (2011).
118. Fisher, A. B. *et al.* Peroxiredoxin 6 phospholipid hydroperoxidase activity in the repair of peroxidized cell membranes. *Redox Biol.* **14**, 41–46 (2018).
119. Power, J. H. T., Shannon, J. M., Blumbergs, P. C. & Gai, W. P. Nonselenium glutathione peroxidase in human brain: Elevated levels in Parkinson's disease and dementia with Lewy bodies. *Am. J. Pathol.* **161**, 885–894 (2002).
120. Yun, H., Choi, D. Y., Oh, K. W. & Hong, J. T. PRDX6 Exacerbates Dopaminergic Neurodegeneration in a MPTP Mouse Model of Parkinson's Disease. *Mol. Neurobiol.* **52**, 422–431 (2015).
121. Power, J. H. T. *et al.* Peroxiredoxin 6 in human brain: Molecular forms, cellular distribution and association with Alzheimer's disease pathology. *Acta Neuropathol.* **115**, 611–622 (2008).
122. Pacifici, F. *et al.* Peroxiredoxin 6, a novel player in the pathogenesis of diabetes. *Diabetes* **63**, 3210–3220 (2014).
123. Ozkosem, B., Feinstein, S. I., Fisher, A. B. & O'Flaherty, C. Advancing age increases sperm chromatin damage and impairs fertility in peroxiredoxin 6 null mice. *Redox Biol.* **5**, 15–23 (2015).
124. Ozkosem, B., Feinstein, S. I., Fisher, A. B. & O'Flaherty, C. Absence of Peroxiredoxin 6 Amplifies the Effect of Oxidant Stress on Mobility and SCSA/CMA3 Defined Chromatin Quality and Impairs Fertilizing Ability of Mouse Spermatozoa1. *Biol. Reprod.* **94**, 1–10 (2016).
125. Fisher, A. B. The phospholipase A2 activity of peroxiredoxin 6. *J. Lipid Res.* **59**, 1132–1147 (2018).
126. Laurent, T. C., Mooren, E. C. & Reichard, P. Enzymatic synthesis of deoxyribonucleotides. iv. isolation and characterization of thioredoxin, the hydrogen donor from Escherichia coli B. *J. Biol. Chem.* **239**, 3436–3444 (1964).
127. Matsui, M. *et al.* Early Embryonic Lethality Caused by Targeted Disruption of the Mouse Thioredoxin Gene. *Dev. Biol.* **178**, 179–185 (1996).
128. Conrad, M. *et al.* Essential Role for Mitochondrial Thioredoxin Reductase in

- Hematopoiesis, Heart Development, and Heart Function. *Mol. Cell. Biol.* **24**, 9414–9423 (2004).
129. Jakupoglu, C. *et al.* Cytoplasmic Thioredoxin Reductase Is Essential for Embryogenesis but Dispensable for Cardiac Development. *Mol. Cell. Biol.* **25**, 1980–1988 (2005).
 130. Holmgren, A. *et al.* Thiol redox control via thioredoxin and glutaredoxin systems. *Biochem. Soc. Trans.* **33**, 1375 (2005).
 131. Hanschmann, A. U. E., Godoy, R., Berndt, C., Hudemann, C. & Lillig, C. H. Thioredoxins, Glutaredoxins, and Peroxiredoxins-Molecular Mechanisms and Health Significance: From Cofactor to Antioxidants to Redox Signaling. **19**, 1539–1605 (2013).
 132. Kim, Y.-C. *et al.* Hemin-induced Activation of the Thioredoxin Gene by Nrf2. *J. Biol. Chem.* **276**, 18399–18406 (2001).
 133. Eklund, H., Gleason, F. K. & Holmgren, A. Structural and functional relations among thioredoxins of different species. *Proteins Struct. Funct. Genet.* **11**, 13–28 (1991).
 134. Arnér, E. S. J. & Holmgren, A. Physiological functions of thioredoxin and thioredoxin reductase. *Eur. J. Biochem.* **267**, 6102–6109 (2000).
 135. Holmgren, A. & Bjornstedt, M. Thioredoxin and thioredoxin reductase. in *Methods in Enzymology* **252**, 199–208 (1995).
 136. Matsuzawa, A. Thioredoxin and redox signaling: Roles of the thioredoxin system in control of cell fate. *Arch. Biochem. Biophys.* **617**, 101–105 (2017).
 137. Mustacich, D. & Powis, G. Thioredoxin reductase. *Biochem. J* **346**, 1–8 (2000).
 138. Arnér, E. S. J. Focus on mammalian thioredoxin reductases — Important selenoproteins with versatile functions. *Biochim. Biophys. Acta - Gen. Subj.* **1790**, 495–526 (2009).
 139. Arnér, E. S. J. Targeting the Selenoprotein Thioredoxin Reductase 1 for Anticancer Therapy. in *Advances in Cancer Research* **136**, 139–151 (2017).
 140. Stafford, W. C. *et al.* Irreversible inhibition of cytosolic thioredoxin reductase 1 as a mechanistic basis for anticancer therapy. *Sci. Transl. Med.* **10**, eaaf7444 (2018).
 141. Chen, K.-S. & DeLuca, H. F. Isolation and characterization of a novel cDNA from HL-60 cells treated with 1,25-dihydroxyvitamin D-3. *Biochim. Biophys. Acta - Gene Struct. Expr.* **1219**, 26–32 (1994).
 142. Junn, E. *et al.* Vitamin D 3 Up-Regulated Protein 1 Mediates Oxidative Stress Via Suppressing the Thioredoxin Function. *J. Immunol.* **164**, 6287–6295 (2000).
 143. Patwari, P., Higgins, L. J., Chutkow, W. A., Yoshioka, J. & Lee, R. T. The Interaction of Thioredoxin with Txnip. *J. Biol. Chem.* **281**, 21884–21891 (2006).
 144. Ago, T. *et al.* A Redox-Dependent Pathway for Regulating Class II HDACs and Cardiac Hypertrophy. *Cell* **133**, 978–993 (2008).
 145. Nishinaka, Y. *et al.* Importin α 1 (Rch1) Mediates Nuclear Translocation of

- Thioredoxin-binding Protein-2/Vitamin D 3 -up-regulated Protein 1. *J. Biol. Chem.* **279**, 37559–37565 (2004).
146. Spindel, O. N., World, C. & Berk, B. C. Thioredoxin Interacting Protein: Redox Dependent and Independent Regulatory Mechanisms. *Antioxid. Redox Signal.* **16**, 587–596 (2012).
147. Anand, P. & Stamler, J. S. Enzymatic mechanisms regulating protein S-nitrosylation: implications in health and disease. *J. Mol. Med.* **90**, 233–244 (2012).
148. Benhar, M., Forrester, M. T., Hess, D. T. & Stamler, J. S. Regulated Protein Denitrosylation by Cytosolic and Mitochondrial Thioredoxins. *Science (80-.)*. **320**, 1050–1054 (2008).
149. Benhar, M., Forrester, M. T. & Stamler, J. S. Protein denitrosylation: enzymatic mechanisms and cellular functions. *Nat. Rev. Mol. Cell Biol.* **10**, 721–732 (2009).
150. Mitchell, D. A. & Marletta, M. A. Thioredoxin catalyzes the S-nitrosation of the caspase-3 active site cysteine. *Nat. Chem. Biol.* **1**, 154–158 (2005).
151. Wu, C. *et al.* Redox Regulatory Mechanism of Transnitrosylation by Thioredoxin. *Mol. Cell. Proteomics* **9**, 2262–2275 (2010).
152. Wu, C. *et al.* Thioredoxin 1-Mediated Post-Translational Modifications: Reduction, Transnitrosylation, Denitrosylation, and Related Proteomics Methodologies. *Antioxid. Redox Signal.* **15**, 2565–2604 (2011).
153. Benhar, M., Thompson, J. W., Moseley, M. A. & Stamler, J. S. Identification of S-Nitrosylated Targets of Thioredoxin Using a Quantitative Proteomic Approach. *Biochemistry* **49**, 6963–6969 (2010).
154. Forrester, M. T. *et al.* Proteomic analysis of S-nitrosylation and denitrosylation by resin-assisted capture. *Nat. Biotechnol.* **27**, 557–559 (2009).
155. Benhar, M. Nitric oxide and the thioredoxin system: a complex interplay in redox regulation. *Biochim. Biophys. Acta - Gen. Subj.* **1850**, 2476–2484 (2015).
156. Ravi, K., Brennan, L. A., Levic, S., Ross, P. A. & Black, S. M. S-nitrosylation of endothelial nitric oxide synthase is associated with monomerization and decreased enzyme activity. *Proc. Natl. Acad. Sci.* **101**, 2619–2624 (2004).
157. Meuillet, E. J., Mahadevan, D., Berggren, M., Coon, A. & Powis, G. Thioredoxin-1 binds to the C2 domain of PTEN inhibiting PTEN's lipid phosphatase activity and membrane binding: a mechanism for the functional loss of PTEN's tumor suppressor activity. *Arch. Biochem. Biophys.* **429**, 123–133 (2004).
158. Saitoh, M., Nishitoh, H., Fujii, M., Takeda, K., Tobiume, K., Sawada, Y., Kawabata, M., Miyazono, K., and Ichijo, H. Mammalian thioredoxin is a direct inhibitor of apoptosis signal-regulating kinase (ASK) 1. *EMBO J.* **17**, 2596–2606 (1998).
159. Matsuzawa, A. & Ichijo, H. Redox control of cell fate by MAP kinase: physiological roles of ASK1-MAP kinase pathway in stress signaling. *Biochim. Biophys. Acta - Gen. Subj.* **1780**, 1325–1336 (2008).
160. Morel, Y. & Barouki, R. Repression of gene expression by oxidative stress. *Biochem. J.* **342**, 481 (1999).

161. Dalton, T. P., Shertzer, H. G. & Puga, A. Regulation of gene expression by reactive oxygen. *Annu. Rev. Pharmacol. Toxicol.* **39**, 67–101 (1999).
162. Arrigo, A.-P. Gene expression and the thiol redox state. *Free Radic. Biol. Med.* **27**, 936–944 (1999).
163. Chen, Z. J. Ubiquitin signalling in the NF- κ B pathway. *Nat. Cell Biol.* **7**, 758–765 (2005).
164. Matthews, J. R., Wakasugi, N., Virelizier, J.-L., Yodoi, J. & Hay, R. T. Thioredoxin regulates the DNA binding activity of NF- χ B by reduction of a disulphid bond involving cysteine 62. *Nucleic Acids Res.* **20**, 3821–3830 (1992).
165. Hirota, K. *et al.* Distinct Roles of Thioredoxin in the Cytoplasm and in the Nucleus. *J. Biol. Chem.* **274**, 27891–27897 (1999).
166. Shaulian, E. & Karin, M. AP-1 as a regulator of cell life and death. *Nat. Cell Biol.* **4**, E131–E136 (2002).
167. Galter, D., Mlihm, S. & Dröge, W. Distinct effects of glutathione disulphide on the nuclear transcription factors kappaB and the activator protein-1. *Eur. J. Biochem.* **221**, 639–648 (1994).
168. Hirota, K. *et al.* AP-1 transcriptional activity is regulated by a direct association between thioredoxin and Ref-1. *Proc. Natl. Acad. Sci.* **94**, 3633–3638 (1997).
169. Wei, S. J. *et al.* Thioredoxin nuclear translocation and interaction with redox factor-1 activates the activator protein-1 transcription factor in response to ionizing radiation. *Cancer Res.* **60**, 6688–6695 (2000).
170. Ueno, M. *et al.* Thioredoxin-dependent redox regulation of p53-mediated p21 activation. *J. Biol. Chem.* **274**, 35809–35815 (1999).
171. Holmgren, A. Hydrogen donor system for Escherichia coli ribonucleoside-diphosphate reductase dependent upon glutathione. *Proc. Natl. Acad. Sci.* **73**, 2275–2279 (1976).
172. Holmgren, A. Glutathione-dependent synthesis of deoxyribonucleotides. *J. Biol. Chem.* **254**, 3664–3671 (1979).
173. Holmgren, A. Glutathione-dependent synthesis of deoxyribonucleotides. Characterization of the enzymatic mechanism of Escherichia coli glutaredoxin. *J. Biol. Chem.* **254**, 3672–3678 (1979).
174. Lillig, C. H., Berndt, C. & Holmgren, A. Glutaredoxin systems. *Biochim. Biophys. Acta - Gen. Subj.* **1780**, 1304–1317 (2008).
175. Sun, C., Berardi, M. J. & Bushweller, J. H. The NMR solution structure of human glutaredoxin in the fully reduced form. *J. Mol. Biol.* **280**, 687–701 (1998).
176. Xia, T.-H. *et al.* NMR structure of oxidized Escherichia coli glutaredoxin: Comparison with reduced E. coli glutaredoxin and functionally related proteins. *Protein Sci.* **1**, 310–321 (2008).
177. Bushweller, J. H., Aaslund, F., Wuethrich, K. & Holmgren, A. Structural and functional characterization of the mutant Escherichia coli glutaredoxin (C14.fwdarw.S) and its mixed disulfide with glutathione. *Biochemistry* **31**, 9288–9293 (1992).

178. Berndt, C. & Lillig, C. H. Glutathione, Glutaredoxins, and Iron. *Antioxid. Redox Signal.* **27**, 1235–1251 (2017).
179. Miller, C. G., Holmgren, A., Arnér, E. S. J. & Schmidt, E. E. NADPH-dependent and -independent disulfide reductase systems. *Free Radic. Biol. Med.* **127**, 248–261 (2018).
180. Meyer, Y., Belin, C., Delorme-Hinoux, V., Reichheld, J. P. & Riondet, C. Thioredoxin and glutaredoxin systems in plants: Molecular mechanisms, crosstalks, and functional significance. *Antioxidants Redox Signal.* **17**, 1124–1160 (2012).
181. Padilla, C. A., Martinez-Galisteo, E., Barcena, J. A., Spyrou, G. & Holmgren, A. Purification from Placenta, Amino Acid Sequence, Structure Comparisons and cDNA Cloning of Human Glutaredoxin. *Eur. J. Biochem.* **227**, 27–34 (1995).
182. Lönn, M. E. *et al.* Expression Pattern of Human Glutaredoxin 2 Isoforms: Identification and Characterization of Two Testis/Cancer Cell-Specific Isoforms. *Antioxid. Redox Signal.* **10**, 547–558 (2008).
183. Holmgren, A. Thioredoxin and glutaredoxin systems. *J. Biol. Chem.* **264**, 13963–13966 (1989).
184. Mieyal, J. J., Gallogly, M. M., Qanungo, S., Sabens, E. A. & Shelton, M. D. Molecular Mechanisms and Clinical Implications of Reversible Protein S - Glutathionylation. *Antioxid. Redox Signal.* **10**, 1941–1988 (2008).
185. Shelton, M. D., Chock, P. B. & Mieyal, J. J. Glutaredoxin: Role in Reversible Protein S -Glutathionylation and Regulation of Redox Signal Transduction and Protein Translocation. *Antioxid. Redox Signal.* **7**, 348–366 (2005).
186. Townsend, D. M. *et al.* Novel Role for Glutathione S -Transferase π . *J. Biol. Chem.* **284**, 436–445 (2009).
187. Grek, C. L., Zhang, J., Manevich, Y., Townsend, D. M. & Tew, K. D. Causes and Consequences of Cysteine S -Glutathionylation. *J. Biol. Chem.* **288**, 26497–26504 (2013).
188. Popov, D. Protein S -glutathionylation: from current basics to targeted modifications. *Arch. Physiol. Biochem.* **120**, 123–130 (2014).
189. Dominko, K. & Đikić, D. Glutathionylation: a regulatory role of glutathione in physiological processes. *Arch. Ind. Hyg. Toxicol.* **69**, 1–24 (2018).
190. Gravina, S. A. & Mieyal, J. J. Thioltransferase is a specific glutathionyl mixed-disulfide oxidoreductase. *Biochemistry* **32**, 3368–3376 (1993).
191. SONG, J. J. & LEE, Y. J. Differential role of glutaredoxin and thioredoxin in metabolic oxidative stress-induced activation of apoptosis signal-regulating kinase 1. *Biochem. J.* **373**, 845–853 (2003).
192. Pan, S. & Berk, B. C. Glutathiolation Regulates Tumor Necrosis Factor- α -Induced Caspase-3 Cleavage and Apoptosis. *Circ. Res.* **100**, 213–219 (2007).
193. Chen, C.-A., De Pascali, F., Basye, A., Hemann, C. & Zweier, J. L. Redox Modulation of Endothelial Nitric Oxide Synthase by Glutaredoxin-1 through Reversible Oxidative Post-Translational Modification. *Biochemistry* **52**, 6712–6723 (2013).

194. Lind, C., Gerdes, R., Schuppe-Koistinen, I. & Cotgreave, I. A. Studies on the mechanism of oxidative modification of human glyceraldehyde-3-phosphate dehydrogenase by glutathione: Catalysis by glutaredoxin. *Biochem. Biophys. Res. Commun.* **247**, 481–486 (1998).
195. Barrett, W. C. *et al.* Regulation of PTP1B via glutathionylation of the active site cysteine 215. *Biochemistry* **38**, 6699–6705 (1999).
196. Zhang, X. *et al.* Positive Regulation of Interleukin-1 β Bioactivity by Physiological ROS-Mediated Cysteine S-Glutathionylation. *Cell Rep.* **20**, 224–235 (2017).
197. Yang, F. *et al.* Glutaredoxin-1 Silencing Induces Cell Senescence via p53/p21/p16 Signaling Axis. *J. Proteome Res.* **17**, 1091–1100 (2018).
198. Moskovitz, J. *et al.* Identification and characterization of a putative active site for peptide methionine sulfoxide reductase (MsrA) and its substrate stereospecificity. *J. Biol. Chem.* **275**, 14167–14172 (2000).
199. Moskovitz, J. Methionine sulfoxide reductases: ubiquitous enzymes involved in antioxidant defense, protein regulation, and prevention of aging-associated diseases. *Biochim. Biophys. Acta - Proteins Proteomics* **1703**, 213–219 (2005).
200. Rhee, S. G., Jeong, W., Chang, T.-S. & Woo, H. A. Sulfiredoxin, the cysteine sulfinic acid reductase specific to 2-Cys peroxiredoxin: its discovery, mechanism of action, and biological significance. *Kidney Int.* **72**, S3–S8 (2007).
201. Ramesh, A., Varghese, S. S., Doraiswamy, J. & Malaiappan, S. Role of sulfiredoxin in systemic diseases influenced by oxidative stress. *Redox Biol.* **2**, 1023–1028 (2014).
202. Findlay, V. J. *et al.* A Novel Role for Human Sulfiredoxin in the Reversal of Glutathionylation. *Cancer Res.* **66**, 6800–6806 (2006).
203. Noh, Y. H., Baek, J. Y., Jeong, W., Rhee, S. G. & Chang, T.-S. Sulfiredoxin Translocation into Mitochondria Plays a Crucial Role in Reducing Hyperoxidized Peroxiredoxin III. *J. Biol. Chem.* **284**, 8470–8477 (2009).
204. Barnett, S. D. & Buxton, I. L. O. The role of S-nitrosoglutathione reductase (GSNOR) in human disease and therapy. *Crit. Rev. Biochem. Mol. Biol.* **52**, 340–354 (2017).
205. Tang, C.-H., Wei, W., Hanes, M. A. & Liu, L. Hepatocarcinogenesis Driven by GSNOR Deficiency Is Prevented by iNOS Inhibition. *Cancer Res.* **73**, 2897–2904 (2013).
206. Rhee, S. G., Bae, Y. S., Lee, S.-R. & Kwon, J. Hydrogen Peroxide: A Key Messenger That Modulates Protein Phosphorylation Through Cysteine Oxidation. *Sci. Signal.* **2000**, pe1–pe1 (2000).
207. Sosa, V. *et al.* Oxidative stress and cancer: An overview. *Ageing Res. Rev.* **12**, 376–390 (2013).
208. Duracková, Z. Some current insights into oxidative stress. *Physiol. Rev.* **59**, 459–469 (2010).
209. Galle, P. R. *et al.* EASL Clinical Practice Guidelines: Management of hepatocellular carcinoma. *J. Hepatol.* **69**, 182–236 (2018).

210. Schulze, K. *et al.* Exome sequencing of hepatocellular carcinomas identifies new mutational signatures and potential therapeutic targets. *Nat. Genet.* **47**, 505–511 (2015).
211. Weinberg, F. & Chandel, N. S. Reactive oxygen species-dependent signaling regulates cancer. *Cell. Mol. Life Sci.* **66**, 3663–3673 (2009).
212. Weinberg, F. *et al.* Mitochondrial metabolism and ROS generation are essential for Kras-mediated tumorigenicity. *Proc. Natl. Acad. Sci.* **107**, 8788–8793 (2010).
213. Hanahan, Douglas and Weinberg, R. A. Hallmarks of Cancer: The Next Generation. *Cell* **144**, 646–674 (2011).
214. Cairns, R. A., Harris, I. S. & Mak, T. W. Regulation of cancer cell metabolism. *Nat. Rev. Cancer* **11**, 85–95 (2011).
215. DeNicola, G. M. *et al.* Oncogene-induced Nrf2 transcription promotes ROS detoxification and tumorigenesis. *Nature* **475**, 106–109 (2011).
216. Hanahan, D. & Weinberg, R. A. The Hallmarks of Cancer. *Cell* **100**, 57–70 (2000).
217. Hornsveld, M. & Dansen, T. B. The Hallmarks of Cancer from a Redox Perspective. *Antioxid. Redox Signal.* **25**, 300–325 (2016).
218. Du, Y., Zhang, H., Lu, J. & Holmgren, A. Glutathione and Glutaredoxin Act as a Backup of Human Thioredoxin Reductase 1 to Reduce Thioredoxin 1 Preventing Cell Death by Aurothioglucose. *J. Biol. Chem.* **287**, 38210–38219 (2012).
219. Du, J. *et al.* Lysophosphatidic Acid Induces MDA-MB-231 Breast Cancer Cells Migration through Activation of PI3K/PAK1/ERK Signaling. *PLoS One* **5**, e15940 (2010).
220. Wu, J.-R. *et al.* Hydrogen peroxide inducible clone-5 mediates reactive oxygen species signaling for hepatocellular carcinoma progression. *Oncotarget* **6**, 32526–32544 (2015).
221. Lou, Y.-W. *et al.* Redox regulation of the protein tyrosine phosphatase PTP1B in cancer cells. *FEBS J.* **275**, 69–88 (2008).
222. Schwertassek, U. *et al.* Reactivation of oxidized PTP1B and PTEN by thioredoxin 1. *FEBS J.* **281**, 3545–3558 (2014).
223. Iriyama, T. *et al.* ASK1 and ASK2 differentially regulate the counteracting roles of apoptosis and inflammation in tumorigenesis. *EMBO J.* **28**, 843–853 (2009).
224. Kamiyama, M., Naguro, I. & Ichijo, H. In vivo gene manipulation reveals the impact of stress-responsive MAPK pathways on tumor progression. *Cancer Sci.* **106**, 785–796 (2015).
225. Saitoh, M. Mammalian thioredoxin is a direct inhibitor of apoptosis signal-regulating kinase (ASK) 1. *EMBO J.* **17**, 2596–2606 (1998).
226. Ruhul Amin, A. R. M., Senga, T., Oo, M. L., Thant, A. A. & Hamaguchi, M. Secretion of matrix metalloproteinase-9 by the proinflammatory cytokine, IL-1beta: a role for the dual signalling pathways, Akt and Erk. *Genes to Cells* **8**, 515–523 (2003).

227. Murata, H. *et al.* Glutaredoxin Exerts an Antiapoptotic Effect by Regulating the Redox State of Akt. *J. Biol. Chem.* **278**, 50226–50233 (2003).
228. Kwon, J. *et al.* Reversible oxidation and inactivation of the tumor suppressor PTEN in cells stimulated with peptide growth factors. *Proc. Natl. Acad. Sci.* **101**, 16419–16424 (2004).
229. Helfinger, V. & Schröder, K. Redox control in cancer development and progression. *Mol. Aspects Med.* **63**, 88–98 (2018).
230. Sengupta, R., Billiar, T. R., Kagan, V. E. & Stoyanovsky, D. A. Nitric oxide and thioredoxin type 1 modulate the activity of caspase 8 in HepG2 cells. *Biochem. Biophys. Res. Commun.* **391**, 1127–1130 (2010).
231. Li, H., Wan, A., Xu, G. & Ye, D. Small changes huge impact: the role of thioredoxin 1 in the regulation of apoptosis by S-nitrosylation. *Acta Biochim. Biophys. Sin. (Shanghai)*. **45**, 153–161 (2013).
232. Lim, K.-H., Ancrile, B. B., Kashatus, D. F. & Counter, C. M. Tumour maintenance is mediated by eNOS. *Nature* **452**, 646–649 (2008).
233. González, R., López-Grueso, M. J., Muntané, J., Bárcena, J. A. & Padilla, C. A. Redox regulation of metabolic and signaling pathways by thioredoxin and glutaredoxin in NOS-3 overexpressing hepatoblastoma cells. *Redox Biol.* **6**, 122–134 (2015).
234. Antunes, F. & Han, D. Redox Regulation of NF-κB: From Basic to Clinical Research. *Antioxid. Redox Signal.* **11**, 2055–2056 (2009).
235. Wang, F. *et al.* Activation of the NF-κB pathway as a mechanism of alcohol enhanced progression and metastasis of human hepatocellular carcinoma. *Mol. Cancer* **14**, 10 (2015).
236. Kobayashi, M. & Yamamoto, M. Molecular Mechanisms Activating the Nrf2-Keap1 Pathway of Antioxidant Gene Regulation. *Antioxid. Redox Signal.* **7**, 385–394 (2005).
237. Linher-Melville, K. & Singh, G. The complex roles of STAT3 and STAT5 in maintaining redox balance: Lessons from STAT-mediated xCT expression in cancer cells. *Mol. Cell. Endocrinol.* **451**, 40–52 (2017).
238. Sobotta, M. C. *et al.* Peroxiredoxin-2 and STAT3 form a redox relay for H₂O₂ signaling. *Nat. Chem. Biol.* **11**, 64–70 (2015).
239. Yun, H.-M. *et al.* PRDX6 promotes tumor development via the JAK2/STAT3 pathway in a urethane-induced lung tumor model. *Free Radic. Biol. Med.* **80**, 136–144 (2015).
240. Ho, J. N. *et al.* Phospholipase A2 Activity of Peroxiredoxin 6 Promotes Invasion and Metastasis of Lung Cancer Cells. *Mol. Cancer Ther.* **9**, 825–832 (2010).
241. Schmitt, A., Schmitz, W., Hufnagel, A., Scharl, M. & Meierjohann, S. Peroxiredoxin 6 triggers melanoma cell growth by increasing arachidonic acid-dependent lipid signalling. 267–279 (2015). doi:10.1042/BJ20141204
242. Vázquez-Medina, J. P. *et al.* The phospholipase A 2 activity of peroxiredoxin 6 modulates NADPH oxidase 2 activation via lysophosphatidic acid receptor signaling in the pulmonary endothelium and alveolar macrophages. *FASEB J.*

- 30**, 2885–2898 (2016).
243. Levine, A. J. & Puzio-Kuter, A. M. The Control of the Metabolic Switch in Cancers by Oncogenes and Tumor Suppressor Genes. *Science (80-.)*. **330**, 1340–1344 (2010).
 244. Gatenby, R. A. & Gillies, R. J. Why do cancers have high aerobic glycolysis? *Nat. Rev. Cancer* **4**, 891–899 (2004).
 245. Ward, P. S. & Thompson, C. B. Metabolic Reprogramming: A Cancer Hallmark Even Warburg Did Not Anticipate. *Cancer Cell* **21**, 297–308 (2012).
 246. Dhup, S., Kumar Dadhich, R., Ettore Porporato, P. & Sonveaux, P. Multiple Biological Activities of Lactic Acid in Cancer: Influences on Tumor Growth, Angiogenesis and Metastasis. *Curr. Pharm. Des.* **18**, 1319–1330 (2012).
 247. DeBerardinis, R. J. *et al.* Beyond aerobic glycolysis: Transformed cells can engage in glutamine metabolism that exceeds the requirement for protein and nucleotide synthesis. *Proc. Natl. Acad. Sci.* **104**, 19345–19350 (2007).
 248. Patra, K. C. & Hay, N. The pentose phosphate pathway and cancer. *Trends Biochem. Sci.* **39**, 347–354 (2014).
 249. Fan, J. *et al.* Quantitative flux analysis reveals folate-dependent NADPH production. *Nature* **510**, 298–302 (2014).
 250. Gill, J. G., Piskounova, E. & Morrison, S. J. Cancer, Oxidative Stress, and Metastasis. *Cold Spring Harb. Symp. Quant. Biol.* **81**, 163–175 (2016).
 251. Anastasiou, D. *et al.* Inhibition of Pyruvate Kinase M2 by Reactive Oxygen Species Contributes to Cellular Antioxidant Responses. *Science (80-.)*. **334**, 1278–1283 (2011).
 252. Tórtora, V., Quijano, C., Freeman, B., Radi, R. & Castro, L. Mitochondrial aconitase reaction with nitric oxide, S-nitrosoglutathione, and peroxynitrite: Mechanisms and relative contributions to aconitase inactivation. *Free Radic. Biol. Med.* **42**, 1075–1088 (2007).
 253. Shi, Q. *et al.* Inactivation and Reactivation of the Mitochondrial α -Ketoglutarate Dehydrogenase Complex. *J. Biol. Chem.* **286**, 17640–17648 (2011).
 254. Prehu, M.-O., Prehu, C., Calvin, M. & Rosa, R. Rabbit M type phosphoglycermutase: comparative effects of two thiol reagents, antibody reaction and hybridization studies. *Comp. Biochem. Physiol. Part B Comp. Biochem.* **89**, 257–262 (1988).
 255. Hameed M. S., S. & Sarma, S. P. The Structure of the Thioredoxin–Triosephosphate Isomerase Complex Provides Insights into the Reversible Glutathione-Mediated Regulation of Triosephosphate Isomerase. *Biochemistry* **51**, 533–544 (2012).
 256. Dumont, S., Bykova, N. V., Pelletier, G., Dorion, S. & Rivoal, J. Cytosolic triosephosphate isomerase from *Arabidopsis thaliana* is reversibly modified by glutathione on cysteines 127 and 218. *Front. Plant Sci.* **7**, 1–16 (2016).
 257. Lamouille, S., Xu, J. & Derynck, R. Molecular mechanisms of epithelial–mesenchymal transition. *Nat. Rev. Mol. Cell Biol.* **15**, 178–196 (2014).

258. Rhyu, D. Y. *et al.* Role of reactive oxygen species in TGF- β 1-induced mitogen-activated protein kinase activation and epithelial-mesenchymal transition in renal tubular epithelial cells. *J. Am. Soc. Nephrol.* **16**, 667–675 (2005).
259. Thiery, J. P. & Sleeman, J. P. Complex networks orchestrate epithelial-mesenchymal transitions. *Nat. Rev. Mol. Cell Biol.* **7**, 131–142 (2006).
260. Larue, L. & Bellacosa, A. Epithelial-mesenchymal transition in development and cancer: Role of phosphatidylinositol 3' kinase/AKT pathways. *Oncogene* **24**, 7443–7454 (2005).
261. Barber, A. G. *et al.* PI3K/AKT pathway regulates E-cadherin and Desmoglein 2 in aggressive prostate cancer. *Cancer Med.* **4**, 1258–1271 (2015).
262. Dong, J. *et al.* Activation of phosphatidylinositol 3-kinase/AKT/snail signaling pathway contributes to epithelial-mesenchymal transition-induced multi-drug resistance to sorafenib in hepatocellular carcinoma cells. *PLoS One* **12**, 1–16 (2017).
263. Cervello, M. *et al.* Molecular mechanisms of sorafenib action in liver cancer cells. *Cell Cycle* **11**, 2843–2855 (2012).
264. Coriat, R. *et al.* Sorafenib-induced hepatocellular carcinoma cell death depends on reactive oxygen species production in vitro and in vivo. *Mol. Cancer Ther.* **11**, 2284–2293 (2012).
265. Zhang, C., Guo, F., Jia, W. & Ge, Y. STAT3 activation mediates epithelial-to-mesenchymal transition in human hepatocellular carcinoma cells. *Hepatology* **61**, 1082–1089 (2014).
266. Reichl, P. & Mikulits, W. Accuracy of novel diagnostic biomarkers for hepatocellular carcinoma: An update for clinicians (Review). *Oncol. Rep.* **36**, 613–625 (2016).

ABSTRACT

Abstract

The redoxins Thioredoxin (Trx), Glutaredoxin (Grx) and Peroxiredoxins (Prdx) play a very important role both in the maintenance of redox homeostasis and in signaling through reversible oxidation/reduction reactions in cysteine residues key to the regulation of protein function. The main objective of this project is to demonstrate that redoxins exert a role in the control of metabolic flux of tumor cells by regulating the redox state of metabolic enzymes and proteins involved in cell signaling.

To study the functions of human Trx1 and Grx1, we have used the hepatocarcinoma-derived HepG2 cell line as an experimental model under both normal and oxidative/nitrosative conditions. We have shown that silencing of Trx1 or Grx1 causes major changes in the redox proteome reflected in significant changes in the reduced/oxidized ratio of enzyme cysteines such as glyceraldehyde-3-phosphate dehydrogenase (GAPDH) Cys247 and triosephosphate isomerase (TPI) Cys255 that affect their activity. Trx1 silencing increases glycolytic flux and induces membrane remodelling as indicated by the increase in sphingomyelins and ceramides. On the other hand, Grx1 silencing decreases the glycolytic flux and increases the synthesis of fatty acids and phospholipids stimulating lipogenesis. These results indicate that, although both redoxins have some common target cysteines, their down-regulation causes different metabolic changes. Among the redox targets of Grx1 is the “extra” non-peroxidatic Cys91, of Prdx6, the only member of the 1-Cys peroxiredoxin family in humans, which in addition to having characteristic peroxidase activity is the only one that also has phospholipase A2 activity calcium independent (iPLA₂).

Prdx6 silencing in HepG2 cells decreases proliferation and increases cell volume without changing the number of cells; decreases the rate of glucose entry and nucleotide biosynthesis while the levels of amino acids, polyamines, phospholipids and most glycolipids increase. Changes in the global proteome reflect an increase in vesicle traffic while the redox proteome shows changes in various enzymes among which are hexokinase 2 (HK2) Cys368, phosphoenolpyruvate carboxykinase 2 (PCK2) Cys55-63, and 3-phosphoglycerate dehydrogenase (PHGDH) Cys18-19 and Cys281. These results indicate that Prdx6 silencing induces both a predominant metabolic remodelling towards a glyconeogenic flow from amino acids with diversion at the synthesis of serine and other biosynthetic pathways, as well as cell cycle arrest at G1/S transition. It remains to be determined which Prdx6 activity is responsible for these effects, whether its peroxidase or PLA2 or both and what are the detailed mechanisms that lead to these effects.

The next step has been to verify whether these actions of the studied redoxins also take place in advanced states of hepatocarcinoma in which resistance to the standard treatment with Sorafenib is frequent. In line with this, a study has been carried out in three hepatocarcinoma cell lines with different degrees of epithelial-mesenchymal transition and therefore with increasing invasive potential and malignancy (HepG2, SNU423 and SNU475), treated with Sorafenib and/or silenced for Trx1. This drug is known as a tyrosine kinase inhibitor and we have observed that treatment with Sorafenib induces reductive changes in key tumor signaling proteins, such as STAT3, MAPK and Akt, in the three cell lines but large changes in the global proteome have only been seen in cells of intermediate dedifferentiation state (SNU423). Silencing of Trx1 does not have a great effect on the overall proteome of the three cell lines but it does counteract the reducing effect of Sorafenib on a thiol group at STAT3 and sensitizes the more mesenchymal hepatocarcinoma cell line (SNU475) against Sorafenib, inactivating TGF β 1 pathway and stimulating HIPPO signaling. Therefore, these results support the idea that the combined treatment of Sorafenib with Trx1 inhibitors could help to design more effective therapies against advanced hepatocarcinoma resistant to Sorafenib.

RESUMEN

Resumen

Las redoxinas Tiorredoxina (Trx), Glutarredoxina (Grx) y Peroxirredoxina (Prdx) juegan un papel muy importante tanto en el mantenimiento de la homeostasis redox como en señalización a través de reacciones de oxidación/reducción reversibles en residuos de cisteína claves para la regulación de la función de la proteína. El objetivo principal de este proyecto es estudiar las funciones de las redoxinas en señalización celular y metabolismo en líneas celulares derivadas de hepatocarcinoma sometidas o no a altos niveles de óxido nítrico.

Para el estudio de las funciones de la Trx1 y Grx1 hemos empleado como modelo experimental la línea celular derivada de hepatoblastoma (HepG2) bajo condiciones normales y de estrés oxidativo/nitrosativo. Hemos demostrado que el silenciamiento de Trx1 o Grx1 provoca grandes cambios en el proteoma redox tiólico reflejado en cambios significativos en la ratio reducido/oxidado de cisteínas de enzimas como la Cys247 de la gliceraldehido-3-fosfato deshidrogenasa (GAPDH) y Cys255 de la triosafosfato isomerasa (TPI) los cuales afectan a la actividad de dichas enzimas. El silenciamiento de Trx1 aumenta el flujo glucolítico e induce remodelamiento de la membrana lipídica como indica el incremento de esfingomielinas y ceramidas. Por otro lado, el silenciamiento de Grx1 disminuye el flujo glucolítico y aumenta la síntesis de ácidos grasos y fosfolípidos estimulando lipogénesis. Los resultados indican que, a pesar de que ambas redoxinas tengan algunas cisteínas diana comunes, su silenciamiento provoca cambios metabólicos diferentes. Entre las dianas redox de la Grx1 se encuentra la Cys91, no peroxidática, de la Prdx6, el único miembro de la familia de las peroxirredoxinas de 1-Cys en humanos, que además de poseer la actividad peroxidasa característica, es la única que presenta actividad actividad fosfolipasa A2 independiente de calcio (iPLA₂).

El silenciamiento de Prdx6 en HepG2 disminuye la proliferación y el número de células mientras que el volumen celular aumenta. Además la entrada de glucosa y la biosíntesis de nucleótidos disminuyen mientras que los niveles de amino ácidos, poliaminas, fosfolípidos y la mayoría de glicolípidos aumentan. El efecto del silenciamiento de Prdx6 sobre el proteoma global muestra un aumento en el tráfico de vesículas mientras que el proteoma redox muestra cambios en diversas enzimas de rutas metabólicas entre las que se encuentran la Cys368 de la hexoquinasa 2 (HK2), la Cys55-63 de la fosfoenolpiruvato carboxiquinasa 2 (PCK2), y las Cys18-19 y Cys281 de la 3-fosfoglicerato deshidrogenasa (PHGDH). Los resultados indican que el silenciamiento de Prdx6 induce tanto un remodelamiento metabólico predominante

hacia gluconeogénesis desde amino ácidos con desviación hacia la síntesis de serina y otras vías biosintéticas, así como detención del ciclo celular en la transición G1/S. Está por determinar qué actividad de la Prdx6 es responsable de estos efectos, si su peroxidasa o la PLA₂ o ambas y cuáles son los mecanismos detallados que conducen a esos efectos.

El siguiente paso ha sido comprobar si estas acciones de las redoxinas estudiadas tienen lugar igualmente en estados avanzados de hepatocarcinoma en los que se suele dar una resistencia al tratamiento estándar con Sorafenib. En línea con esto, se ha llevado a cabo un estudio en tres líneas celulares de hepatocarcinoma con distinto grado de transición epitelio-mesenquimal y por tanto, con mayor potencial de invasividad y malignidad (HepG2, SNU423 y SNU475), tratadas con Sorafenib y/o silenciando la Trx1. El Sorafenib es un medicamento conocido por su actividad como un inhibidor de tirosinas quinasas y nosotros hemos observado que el tratamiento con Sorafenib induce cambios reductores en proteínas clave de señalización tumoral, tales como STAT3, MAPK y Akt, en las tres líneas celulares pero los grandes cambios en el proteoma global se han visto únicamente en células en estado intermedio de dediferenciación (SNU423). El silenciamiento de Trx1 no tiene un gran efecto en el proteoma global de las tres líneas pero sí contrarresta el efecto reductor del Sorafenib sobre un grupo tiol de STAT3 y sensibiliza a las células de hepatocarcinoma más mesenquimales (SNU475) frente al Sorafenib, inactivando la vía de TGFβ1 y estimulando la vía de señalización HIPPO. Por lo tanto, los resultados apoyan la idea de que el tratamiento combinado de Sorafenib con inhibidores de la Trx1 podría ayudar al diseño de terapias más efectivas contra el hepatocarcinoma en estado avanzado resistente a Sorafenib.

ARTICLE 1

Thioredoxin and glutaredoxin regulate metabolism through different multiplex thiol switches. **MJ López-Grueso**, R González-Ojeda, R Requejo-Aguilar, B McDonagh, CA Fuentes-Almagro, J. Muntané, J.A. Bárcena*, CA Padilla.

Redox Biology 21 (2019) 101049

DOI: 10.1016/j.redox.2018.11.007



Research Paper

Thioredoxin and glutaredoxin regulate metabolism through different multiplex thiol switches

MJ López-Grueso^{a,e}, R González-Ojeda^b, R Requejo-Aguilar^{a,e}, B McDonagh^c,
CA Fuentes-Almagro^d, J. Muntané^c, J.A. Bárcena^{a,e,*}, CA Padilla^{a,e}

^a Dept. Biochemistry and Molecular Biology, University of Córdoba, Córdoba, Spain

^b Institute of Biomedicine of Seville (IBIS), IBIS/“Virgen del Rocío” University Hospital/CSIC/University of Seville, Seville, Spain

^c Dept. of Physiology, School of Medicine, NUI Galway, Ireland

^d SCAI, University of Córdoba, Córdoba, Spain

^e Maimónides Biomedical Research Institute of Córdoba (IMIBIC), Córdoba, Spain



ARTICLE INFO

Keywords:

Redox proteome
Thiol redox regulation
Glycolysis
S-nitrosation
NO synthase
Redoxins

ABSTRACT

The aim of the present study was to define the role of Trx and Grx on metabolic thiol redox regulation and identify their protein and metabolite targets. The hepatocarcinoma-derived HepG2 cell line under both normal and oxidative/nitrosative conditions by overexpression of NO synthase (NOS3) was used as experimental model. Grx1 or Trx1 silencing caused conspicuous changes in the redox proteome reflected by significant changes in the reduced/oxidized ratios of specific Cys's including several glycolytic enzymes. Cys⁹¹ of peroxiredoxin-6 (PRDX6) and Cys¹⁵³ of phosphoglycerate mutase-1 (PGAM1), that are known to be involved in progression of tumor growth, are reported here for the first time as specific targets of Grx1. A group of proteins increased their Cys_{RED}/Cys_{OX} ratio upon Trx1 and/or Grx1 silencing, including caspase-3 Cys¹⁶³, glyceraldehyde-3-phosphate dehydrogenase (GAPDH) Cys²⁴⁷ and triose-phosphate isomerase (TPI) Cys²⁵⁵ likely by enhancement of NOS3 auto-oxidation. The activities of several glycolytic enzymes were also significantly affected. Glycolysis metabolic flux increased upon Trx1 silencing, whereas silencing of Grx1 had the opposite effect. Diversion of metabolic fluxes toward synthesis of fatty acids and phospholipids was observed in siRNA-Grx1 treated cells, while siRNA-Trx1 treated cells showed elevated levels of various sphingomyelins and ceramides and signs of increased protein degradation. Glutathione synthesis was stimulated by both treatments. These data indicate that Trx and Grx have both, common and specific protein Cys redox targets and that down regulation of either redoxin has markedly different metabolic outcomes. They reflect the delicate sensitivity of redox equilibrium to changes in any of the elements involved and the difficulty of forecasting metabolic responses to redox environmental changes.

1. Introduction

The importance of redox homeostasis for cancer cell survival in the context of energy metabolism is well established [2,57,83]. Sensitive cysteine residues on target proteins are at the center of regulatory mechanisms, whose redox state are controlled by two major cellular systems, the Thioredoxin (Trx)/Trx reductase (TrxR) and the Glutaredoxin (Grx)/glutathione (GSH) systems [30,8].

Nitric oxide (NO) plays important roles in signal transduction [52]. It is synthesized in cells by NO synthase (NOS) isoenzymes whose expression may be regulated as part of cellular responses to several stimuli [1]. NO has contradictory effects on tumor cells, either pro-apoptotic or anti-apoptotic according to cell type, intracellular

concentration range and subcellular site of its generation [23,44]. Post-translational redox modifications (redox PTM) of target sensitive proteins and more specifically, S-nitrosation of sensitive cysteine residues in those proteins, is the basis of NO activity in signaling pathways, although other reversible oxidative modifications of cysteines are also to be expected since high levels of NO are accompanied by increased levels of reactive oxygen species (ROS) [85]. Reversible regulation of redox PTMs is necessary for this process to have regulatory and biological meaning. Intracellular levels of GSNO and S-nitrosated proteins are controlled by GSNO reductase, alcohol dehydrogenase class-3 (ADH III), which is a NADH-dependent enzyme that is conserved from bacteria to human and metabolizes GSNO to oxidized glutathione and NH₃ [47]. GSNO reductase does not directly denitrosate SNO proteins, but as

* Correspondence to: Dep. of Biochemistry and Molecular Biology, Campus de Rabanales, Ed. Severo Ochoa, 1^a Pl. University of Córdoba, 14071 Córdoba, Spain.
E-mail address: ja.barcena@uco.es (J.A. Bárcena).

<https://doi.org/10.1016/j.redox.2018.11.007>

Received 5 October 2018; Received in revised form 8 November 2018; Accepted 11 November 2018

Available online 16 November 2018

2213-2317/ © 2018 The Authors. Published by Elsevier B.V. This is an open access article under the CC BY-NC-ND license (<http://creativecommons.org/licenses/by-nc-nd/4.0/>).

the GSNO pool is in equilibrium with protein thiols, reduction of GSNO by the GSNO reductase indirectly results in protein denitrosation [47].

Trx has been shown to catalyze denitrosation *in vitro* and to affect levels of cellular protein nitrosothiols. It has been shown to also catalyze the direct denitrosation of proteins *in vivo* through the action of its conserved active site dithiol, which in human Trx1 is Cys32 and Cys35 [4,5]. NOS3 (or eNOS) itself is a target of Trx leading to activation of the enzyme as part of a regulatory mechanism of NOS3 by reversible auto-S-nitrosation [15,4,64,67].

Mammalian Trx1 contains additional conserved Cys at positions 62, 69 and 73. Cys73 is particularly prone to S-nitrosation [26] and is implicated in the specific and reversible transfer of a nitrosothiol between Trx1 and caspase 3 with the resulting inhibition of apoptosis [60]. It has been shown that S-nitrosation of Cys73 is favored after formation of a disulfide between Cys32-Cys35, that attenuates Trx1 disulfide reductase and denitrosase activities [86]. Depending on the redox state of the cell, Trx1 catalyzes either trans-S-nitrosation or S-denitrosation so that upon inhibition of disulfide reduction or S-denitrosation activity, Cys⁷³-SNO-Trx1 could catalyze trans-S-nitrosation of target proteins [26,86]. Thus, as a master regulator of redox signaling, Trx1 would protect proteins via its reductase activity, but under highly oxidative environments, the Cys32/Cys35 oxidized disulfide form accumulates, Cys73 becomes S-nitrosated and Trx1 offers an alternative modality of protein regulation via transnitrosation [86].

Glutaredoxin is involved in post-translational modification of proteins by S-glutathionylation with a role mainly as a deglutathionylase [39,54,75]. Grx1 catalyzes reversible S-glutathionylation of protein targets involved in Glycolysis, energy sensing, calcium homeostasis, apoptosis and transcriptional regulation [59]. Grx1 has also been shown to counteract the proapoptotic action of NO in tumor cell lines [22,35] and to regulate NOS3 activity by glutathionylation [9], an activity shared with Trx [78]. However, no direct evidence of Grx1 as denitrosase has been reported so far.

The thiol-based mechanism of NO multiple actions and the roles of Trx and Grx in the context of protein function regulation by reversible redox changes at target cysteines justify the study of cells under nitrosative stress. Exogenous addition of NO donors is a widely used experimental approach to this end, but endogenously produced RNS would better mimic a physiological situation. The levels of ROS and NO increase to 140% in NOS3 overexpressing HepG2 cells relative to control cells [21], which makes them a good experimental model to study the significance of Trx and Grx roles in the regulation of cellular physiology under nitrosative and oxidative conditions.

The Thiol Redox Proteome refers to the set of mapped protein cysteines showing reversible redox changes under given conditions or in response to stimuli [20]. Its detailed description may provide an insightful snapshot of the set of thiol redox switches [19,38] in a cell under given conditions. Several qualitative and quantitative proteomic approaches have been devised to study the redox proteome [24,27,32,43,46,50,53,55] and to define Trx target proteins either as reductase or transnitrosase [46,6,87] or target proteins of Grx as deglutathionylase [54]. The identification and modulation by reversible redox PTMs of key proteins that can control metabolic flow, would offer promising therapeutic candidates for a number of disease states such as cancer [80]. Moreover, redox signals work in tandem with other signals to control different cellular processes.

One common characteristic to all types of cancers is reprogramming of energy metabolism to generate ATP through intense glycolytic flux from glucose to lactate even when oxygen is present, a phenomenon known as “the Warburg effect”. Mitochondria remain functional and part of the glucose consumed is diverted into biosynthetic pathways upstream of pyruvate. Altered cell metabolism is a characteristic feature of many cancers resulting in changes to metabolite concentrations and eventually affecting cell signaling pathways and metabolic fluxes [79,83]. There is a complex connection between metabolism and proliferation with many checkpoints still to be discovered.

We have previously assessed the role of NOS-3 overexpression on several metabolic checkpoints in HepG2 cells showing the prominence of the oxidative branch of the Pentose Phosphate Pathway (oxPPP) to direct the metabolic flux towards NADPH and the increase in Trx and Grx, but at the same time a decrease in nucleotide biosynthesis and proliferation [23]. Downregulation of Trx and Grx reduced cell proliferation and increased caspase-8 and caspase-3.

Here we have applied a quantitative proteomic and metabolomic approach to evaluate HepG2 cells under high levels of endogenous NO and ROS by NOS3 overexpression and \approx 80% down-regulation of Grx1 or Trx1 with specific siRNA. Proteins undergoing significant redox changes have been identified, their sensitive cysteines have been mapped and their “reduced Cys/oxidized Cys” ratios have been determined. Known targets of redox PTMs have been confirmed and new targets have been discovered, mostly metabolic enzymes. Glycolytic metabolic flux, complex lipids and glutathione metabolism and protein degradation, among other pathways, were affected by Trx1 or Grx1 silencing, concomitant with redox changes at specific cysteines in glycolytic enzymes.

2. Material and methods

2.1. Materials and reagents

All reagents were of analytical grade and were purchased from Sigma, unless otherwise stated. HepG2 cell line used in this work was obtained from ATCC LGC Standards Company (Teddington, UK). Cell culture dishes and flasks were from TPP (Switzerland). Anti-Trx1 and anti-Grx1 were obtained from rabbit in our laboratory. Antibodies against PKM2, caspase-3, NOS-3 and β -actin were from Santa Cruz Biotechnology, (Dallas, TX, USA). Antibodies against PRDX6 were from Abcam (Cambridge, UK). ECL was from GE Healthcare (Wauwatosa, Wisconsin, USA). siRNA for Grx1 and Trx1 were from GE Healthcare Dharmacon (Wauwatosa, Wisconsin, USA). [¹⁴C-1]-Glucose, [¹⁴C-6]-Glucose and [³H-3]-Glucose were from Perkin Elmer (USA).

2.2. Cell growth conditions

Cells were transfected with the pcDNA/4TO (5100 bp; Invitrogen, Molecular Probes, Inc.) resulting in 4TO control cell line, as well as with the same expression vector containing NOS3 cDNA sequence (3462 bp; NCBI, ImaGenes, full length cDNA clone sequence BC063294) under the control of the cytomegalovirus promoter resulting in 4TO-NOS cell line. Cell lineages 4TO and 4TO-NOS were selected with zeocin (15 mg/L; Invitrogen) as was described by González et al. [21]. Cells were maintained in EMEM Medium (Eagle Minimum Essential Medium), pH 7.4, supplemented with 10% fetal bovine serum, 2.2 g/L NaHCO₃, 1 mM sodium pyruvate, 100 U/L penicillin, 100 μ g/mL streptomycin, 0.25 μ g/mL amphotericin, and the corresponding selective zeocin antibiotic in 5% CO₂ atmosphere at 37 °C.

2.3. Silencing of Trx1 and Grx1

Human Grx1 and Trx1 were down-regulated in non-transfected HepG2 cells (WT), 4TO and 4TO-NOS cells using specific siRNA in 6-well plates (20,000 cells/cm²) according to the manufacturer's recommendations (Dharmacon, GE Healthcare Life Sciences). Grx and Trx siRNA (25 nmol) were mixed with the transfection reagent DharmaFECT 1, previously pre-incubated with culture medium (antibiotic/antimycotic and serum free), and incubated for 20 min at room temperature. Afterwards, the interference solutions were added to cultured cells for 72 h in 2% culture medium in the absence of antibiotic/antimycotic solution [89]. Silencing of Trx 1 and Grx1 was always checked by Western blot and activity assay to confirm that their levels were reduced by \approx 80% [22].

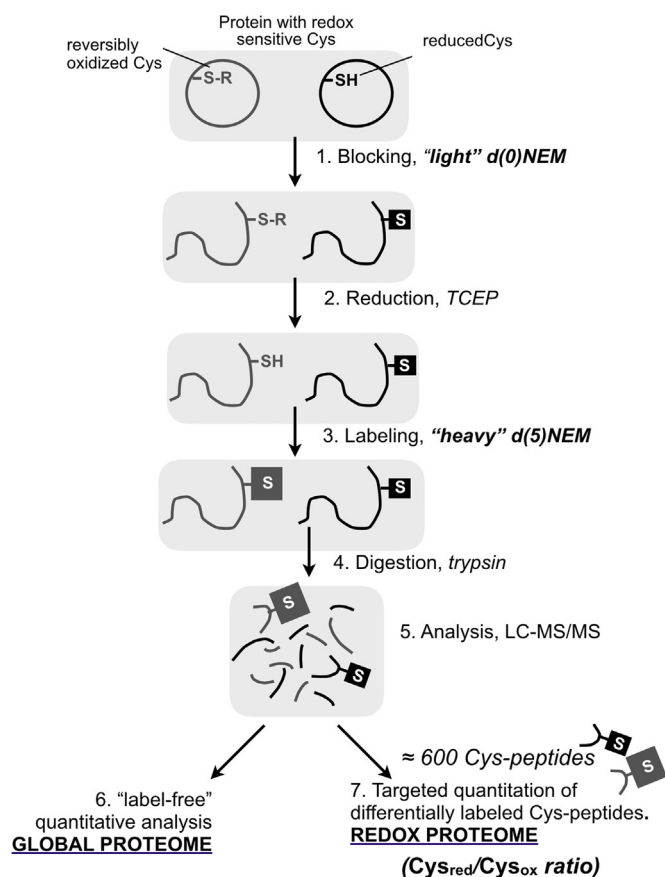


Fig. 1. Proteomics experimental strategy. The procedure follows the already classical three-step approach. In this case, the thiol blocking agent was NEM, the cysteine reductant was TCEP and the newly formed thiols were labeled with "heavy" d(5)-NEM in which 5 hydrogen atoms had been substituted by deuterium atoms. LC-MS/MS data were analyzed for global protein changes with MaxQuant software for "label-free" quantitation [12]. Redox protein changes were analyzed from the set of Cys-peptides identified by targeted quantification using Skyline [48] and calculating the "light"(reduced)/"heavy"(oxidized) Cys ratio. See M&M section for a detailed description.

2.4. Sample preparation for redox proteomics

The experiments were routinely carried out at 100,000 cells/cm² and the cells were washed with PBS. The methodological strategy is summarized in Fig. 1 as described before [55]. Reversibly oxidized Cys were labeled with "heavy" NEM in which 5 hydrogen atoms had been substituted by deuterium atoms here named "d(5)NEM" and reduced cysteines were blocked with "light" NEM, here named "d(0)NEM". Cell extracts were obtained with lysis solution (50 mM ammonium bicarbonate, 50 mM d(0)NEM, 0.5% CHAPS, 1 mM PMSF); samples were centrifuged at 15,000g for 5 min at 4 °C, excess d(0)NEM was removed using Zeba spin desalting columns (Thermo Scientific). 100 µg of protein were diluted up to 160 µl with 25 mM ammonium bicarbonate, incubated with denaturing reagent by addition of 10 µl of 1% w/v RapiGest (Waters) in 25 mM ammonium bicarbonate, incubated at 80 °C for 10 min and vortexed. 10 µl of a 100 mM solution of TCEP was added followed by incubation at 60 °C for 10 min to reduce the reversibly oxidized cysteines that were subsequently alkylated by adding 10 µl of 200 mM d(5)NEM and incubated at room temperature for 30 min. An aliquot was taken at this point to check the procedure by SDS-PAGE.

Proteolytic digestion was performed by addition of 10 µl 12.5 ng/µl of trypsin (Promega) in 25 mM ammonium bicarbonate and incubated at 37 °C temperature overnight. Protein digestion was stopped by

addition of 3 µl trifluoroacetic acid (1.5% final concentration). Digested samples were dialyzed through detergent removal column (Pierce) to eliminate any possible rest of CHAPS and dried in speedvac.

2.5. LC-MS/MS

Protein analyses were performed at the Proteomics Facility (SCAI) at the University of Córdoba. Peptides were scanned and fragmented with the LTQ Orbitrap XL mass spectrometer (Thermo Fisher Scientific) equipped with a nano-UHPLC Ultimate 3000 (Dionex-Thermo Scientific). Chromatography conditions were: mobile phase solution A: 0.1% formic acid in ultrapure water; mobile phase solution B: 80% acetonitrile, 0.1% formic acid. A chromatography gradient was performed in C18 nano-capillary column (Acclaim PepMap C18, 75 µm internal diameter, 3 µm particle size, Dionex-Thermo Scientific) as follows: 5 min, 4% solution B; 60 min, 4–35% solution B; 10 min, 35–80% B; 10 min, 80% B; 10 min 4% B. The nano-electrospray voltage was set to 1300 V and the capillary voltage to 50 V at 190 °C. The LTQ Orbitrap XL was operated in parallel mode, allowing for the accurate measurement of the precursor survey scan (400–1500 *m/z*) in the Orbitrap selection, a 30,000 full-width at half-maximum (FWHM) resolution at *m/z* 400 concurrent with the acquisition of top five CID Data-Dependent MS/MS scans in the LIT for peptide sequence. Singly charged ions were excluded. The normalized collision energies used were 35% for CID. The maximum injection times for MS and MS/MS were set to 500 ms and 50 ms, respectively. The precursor isolation width was 3 amu and the exclusion mass width was set to 5 ppm. Monoisotopic precursor selection was allowed and singly charged species were excluded. The minimum intensity threshold for MS/MS was 500 counts for the linear ion trap and 1000 counts for the Orbitrap. MS2 spectra were searched with SEQUEST engine against a database of Uniprot_Human_Nov2014 (www.uniprot.org). Peptides were generated from a tryptic digestion with up to one missed cleavage, including NEM and (d5)NEM modification in Cys and methionine oxidation as dynamic modifications. Statistical data were calculated with percolator tool against decoy database using 1% FDR as threshold for significance.

2.6. Label-free MS protein quantification

The analysis of MS raw data of the two studies was performed using the MaxQuant (v1.5.7.0) [12] and Perseus (v1.5.6.0) [82] software. Three RAW data files per sample from 3 separate experiments were analyzed. Proteins were identified by searching raw data against the human UniprotKB/Swiss-Prot protein database (February 2018 version). The modifications NEM and d(5)NEM and methionine oxidation was set as variable modifications for the second study. Cleavage specificity was by trypsin, allowing for a maximum of two missed cleavages, a mass tolerance of 10 ppm for precursors and 0.01 Da for fragment ions. The false discovery (FDR) cut-off for protein identification was 1%. Enabling the "match between runs" option allowed for identification transfer between samples. Similar proteins were grouped, and only unique peptides were used for quantification. Identified from reverse database or contaminants hits proteins were removed prior to further analysis. Finally, the resultant list was analyzed according to the instructions of the software developers [82]. The criteria for considering a differentially expressed protein were that it was identified and quantified using at least two unique peptides; has a fold change of at least 1.5 and had a *P* ≤ 0.05 value.

2.7. Targeted analysis of differentially labeled Cys residues

The method devised has been described before [55]. Briefly, Cys-containing peptides detected with identical amino acid sequences and both d(0) and d(5) NEM modifications independently with a confident individual peptide ion score were considered redox peptides. Redox peptides detected from Proteome Discoverer analyses of RAW files were

selected for targeted analysis using m/z data and retention times with the open software Skyline [48]. Targeted analysis applying m/z , retention times, and fragmentation spectra for peptide selection allowed the calculation of the reduced/oxidized ratio (or d(0)/d(5) NEM) of the Cys residues using the individual parent ion intensities. The individual reduced/oxidized ratio for redox Cys peptides in each sample was used to calculate an average ratio of reduced/oxidized calculated for the specific Cys residues.

2.8. Metabolomic analysis

Metabolomic analyses were performed at Metabolon, NC USA and the samples were prepared following the specific guidelines. Global biochemical profiles were determined in 2×10^6 HepG2 cells collected from different treatment groups (wild type, 4TO and 4TO-NOS cells treated with specific siRNA for Trx and Grx or with non-target siRNA). Each experiment was done four times and the dry cell pellets were immediately frozen in liquid nitrogen and stored at -80°C until shipment. Samples were prepared using the automated MicroLab STAR[®] system from Hamilton Company. To remove protein, dissociate small molecules bound to protein or trapped in the precipitated protein matrix, and to recover chemically diverse metabolites, proteins were precipitated with methanol under vigorous shaking for 2 min (Glen Mills GenoGrinder 2000) followed by centrifugation. The resulting extract was divided into five fractions: two for analysis by two separate reverse phase (RP)/UPLC-MS/MS methods with positive ion mode electrospray ionization (ESI), one for analysis by RP/UPLC-MS/MS with negative ion mode ESI, one for analysis by HILIC/UPLC-MS/MS with negative ion mode ESI, and one sample was reserved for backup. Raw data was extracted, peak-identified and QC processed using Metabolon's hardware and software. Peaks were quantified using area-under-the-curve and normalized.

2.9. Biotin switch technique

All operations were performed in darkness and following the protocol described by Martínez-Ruiz et al. [51] with some modifications. Treated cells were resuspended in lysis buffer (50 mM Tris-HCl, pH 7.4, 300 mM NaCl, 5 mM EDTA, 0.1 mM neocuproine, 1% Triton X-100, 1 mM PMSF, 1 $\mu\text{g}/\text{mL}$ aprotinin and 2 $\mu\text{g}/\text{mL}$ leupeptin) and incubated on ice for 15 min. Samples were centrifuged at 10,000g, 4°C for 15 min and supernatants were collected. Extracts were adjusted to 1.0 mg/mL of protein and were blocked with 4 volumes of blocking buffer (225 mM HEPES, pH 7.2, 0.9 mM EDTA, 90 μM neocuproine, 2.5% SDS and 50 mM NEM) at 37°C for 30 min with stirring. After blocking, samples were precipitated with cold acetone and pellets were resuspended in HENS buffer (250 mM HEPES, pH 7.2, 1 mM EDTA, 0.1 mM neocuproine, 1% SDS) with 100 mM ascorbate and 1 mM biotin-HPDP and incubated for 1 h at room temperature. Finally, samples were passed through Zeba spin desalting columns (Thermo Scientific Pierce) to eliminate ascorbate and biotinylated proteins were detected by western blot with "anti-biotin". In addition, the biotinylated proteins were captured with neutravidin-agarose (Pierce) and recovered using 100 mM β -mercaptoethanol for subsequent Western blot analysis of specific target proteins.

2.10. Rate of glycolysis and Pentose Phosphate Pathway (PPP)

These were measured following the protocol described by Requejo-Aguilar et al. [68] with some modifications. The resuspended cells (1.5×10^5 cells) were incubated in "Elliot" buffer (122 mM NaCl, 11 mM Na_2HPO_4 , 0.4 mM KH_2PO_4 , 1.2 mM SO_4Mg , 3.1 mM KCl, 1.3 mM CaCl_2 , pH7.4) in the presence of 5 μCi of D-[3- ^3H]glucose, (0.5 $\mu\text{Ci mL}^{-1}$ of D-[1- ^{14}C]glucose or 1 $\mu\text{Ci mL}^{-1}$ of [6- ^{14}C]glucose and 5 mM D-glucose in sealed vials. The glycolytic flux was measured by assaying the rate of $^3\text{H}_2\text{O}$ production from [3- ^3H]glucose, and the PPP

flux as the difference between [1- ^{14}C]glucose and [6- ^{14}C]glucose incorporated into $^{14}\text{CO}_2$. Glucose concentrations in Elliot buffer were measured by enzymatic analysis spectrophotometrically.

2.11. Measurement of enzymatic activities, lactate and protein

All glycolytic enzymatic activities were measured in fresh cell lysates obtained in the absence of reducing agents. Cell lysates were prepared with lysis buffer containing 50 mM HEPES pH 7.2, 2 mM EDTA, 100 mM NaCl, 1% Triton X-100, 1 mM PMSF. Commercial preparations of pure enzymes were used to calibrate the assays and to determine the linear dependence activity range. Pyruvate kinase (PK) and triose phosphate isomerase (TPI) activities were measured according to the method described by Fielek and Mohrenweiser [16] without DTT in the assay mixture. Glyceraldehyde-3-phosphate dehydrogenase (G3PDH) activity was measured as an increase in absorption at 340 nm resulting from reduction of NAD^+ at 25°C . The reaction mixture contained 130 mM Tris-HCl, pH 8.0, 0.25 mM NAD^+ , and 5 mM DL-glyceraldehyde-3-phosphate. Three technical replicates were routinely done for each independent experiment. Lactate concentration in the culture medium after 72 h of treatment with the siRNA Grx1 or siRNA Trx1 was determined by an enzymatic colorimetric assay (505 nm) using the kit Labkit (Chemelex, S.A). Protein concentration was determined by the Bradford method (Bio-Rad) using BSA as standard.

2.12. SDS-PAGE and Western blotting

SDS-PAGE was performed with homogeneous 10% non-reducing gels for detection of biotinylated proteins and 12% Criterion XT Precast Gel (Bio-Rad) for detection of specific proteins (Trx1, PRDX6, PKM2, caspase-3, NOS3). After electrophoresis, proteins were transferred to a nitrocellulose membrane with a semi-dry electrophoretic transfer system (Bio-Rad). The membranes were incubated overnight at 4°C with the corresponding dilutions of primary antibodies: 1:4000 against biotin, 1:1000 against PRDX6, 1:500 against PKM2, caspase-3 and NOS3, 1:500 against Trx1 and Grx1. Then washed and incubated with the corresponding secondary antibodies conjugated to peroxidase (anti-rabbit, anti-goat or anti-mouse) used at 1:8000 dilution and the chemiluminescent signal was induced by ECL reagent (Thermo-Fisher). Ponceau staining was used as cell protein-loading control and actin was used as reference for quantitative densitometric normalization.

2.13. Statistics

Where appropriate, results are expressed as mean \pm SEM of at least three independent experiments. Data were compared using ANOVA with the least significant difference test *post hoc* multiple comparison analysis. The threshold for statistically significant differences was set at $p \leq 0.05$. In the case of Global and Redox Proteome, data were analyzed using Student's T-test comparing control vs siRNA treatment. The threshold for this statistically significant differences was set at $q \leq 0.05$ according to the method of Storey [77] using the R-package. In the case of the metabolomic analysis following normalization to Bradford protein concentration and log transformation a mixed model ANOVA was used to identify biochemicals that differed significantly between experimental groups; statistical significance was set at $p \leq 0.05$.

3. Results and discussion

Overexpression of NOS3 in HepG2 cells caused a $\approx 25\%$ increase in ROS, NO and NOS activity compared with the same cells transformed with the empty vector [21] and constituted a physiological model for endogenously oxidative/nitrosative stressed cells to study the role of Trx1 and Grx1. Treatment with Trx1 or Grx1 specific siRNA down-regulated the levels and activities of either redoxin by $\approx 80\%$ (Ref.

Fig. 5 in [22]). These cells were collected and lysed under conditions that allowed blocking of reduced protein thiols with “light” d(0)NEM followed by reduction of reversibly oxidized Cys and labelling with “heavy” d(5)NEM (Fig. 1). Samples were prepared and analyzed by a proteomics LC-MS/MS approach allowing for global “label-free” quantitation and for targeted analysis of differentially labeled Cys-peptides [55,71].

3.1. Global proteome

Quantitative differences between the proteomes of WT, 4TO and 4TO-NOS, treated or not with siRNA-Trx1 and siRNA-Grx1, were determined by “label-free” analysis. The significant differential proteomes were determined from roughly 600 unique proteins identified in each study. Only 14 proteins varied significantly between 4TO-NOS and 4TO HepG2 cells and a smaller number changed upon either siRNA treatment in 4TO or 4TO-NOS cells, as shown in Suppl. File 1.

Overexpression of NOS3 and down-regulation of Trx1 or Grx1 in HepG2 cells has marked phenotypical consequences like slow-down of proliferation and apoptosis exacerbation as previously reported [22]. To investigate whether these phenotypical changes might have been triggered by redox postranslational modification of key proteins, we analyzed the redox proteome.

3.2. Redox proteome

Trx1 and Grx1 main action is to reverse oxidative changes in protein thiols, not only those involved in regulatory postranslational modifications of metabolic and signaling proteins, but also those associated with thiol-dependent ROS scavenging enzymes, like peroxiredoxins. Any change in the levels of either redoxin should have consequences on the redox state of sensitive proteins which could reveal detailed knowledge on their functions. Silencing with specific siRNA provides a gentler experimental approach to mimic physiological down-regulation events compared to a full knockout, although detection of the expected subtle changes in molecular indicators requires precise analytical methods to study the redox proteome.

3.2.1. NOS3 overexpression alters the Redox Proteome

The levels of ROS and NO had been measured in 4TO-NOS cells by standard general methods (DCFH₂-DA fluorescence and colorimetric nitrite determination, respectively) showing an increase of 40% in the cells overexpressing NOS3 [21]. Now, the Cys_{red}/Cys_{ox} ratio was determined for every Cys peptide identified/quantified in WT (234/168 peptides), 4TO (411/328 peptides) and 4TO-NOS (366/289 peptides) HepG2 cells. Overlapping of Cys-peptides between samples was 65–68% for identified peptides and 71–77% for quantified peptides (Suppl. Fig. 2). The majority of quantified peptides were in the Cys-SH state with Cys_{red}/Cys_{ox} ratios ranging from nearly 40 to around 2. Ninety-four Cys-peptides underwent significant changes in their Cys_{red}/Cys_{ox} ratios when the cells overexpressed NOS3 compared to cells transfected with empty vector (Fig. 2; Suppl. File 2). Changes were predominantly oxidative, but 13 proteins were ≥ 1.5 fold reduced in the oxidative/nitrosative environment of NOS3 overexpressing cells. Their reductive change could be direct or indirect consequence of the observed marked induction of Trx1 and Grx1 [22], but other perturbations in metabolic and signaling pathways induced by NOS3 overexpression could also be responsible.

The presence of acidic residues around the modified cysteine in these redox target proteins is particularly apparent (Fig. 2B). 77% (10/13) of the proteins showing an increase in their reduced/oxidized Cys ratio had at least one Glu or Asp between positions +2 and -2, centered on the target cysteine, whereas this percentage was lower (46%; 16/35) for the proteins undergoing an oxidative change. The accumulated content of Asp and Glu in the average protein from the UniProtKB TrEMBL is 11.65%, therefore, the frequency of at least one acidic

residue at these positions is markedly higher than expected at random and could be related to the sensitivity of these Cys residues to nitrosative stress induced redox changes.

Taken together, these changes show that NOS3 overexpression exerts oxidative pressure on a number of protein cysteine residues with potential regulatory effects mainly at the level of Glycolysis/gluconeogenesis, protein synthesis and folding, endoplasmic reticulum processes, and cell death and survival (Fig. 2C). To check whether Trx1 or Grx1 are involved in this redox disturbance, both redoxins were down-regulated with specific siRNA and the redox state of individual Cys residues was measured again.

3.2.2. Specific protein cysteines underwent oxidative and reductive changes upon Trx1 or Grx1 silencing depending on NOS3 overexpression

Silencing of Trx1 or Grx1 to $\approx 20\%$ their normal levels in WT and NOS3-overexpressing HepG2 cells did result in significant redox changes of specific protein cysteines, compared with their respective controls. We had previously reported that the activities of both redoxins decreased to the same extent as Trx1 and Grx1 protein levels in their respective siRNA treated cells, excluding the induction of other active isoforms [22]. Moreover, analysis of the differential proteome of these cells in the present study did not show compensatory induction of isoforms.

A selection of target proteins with ≥ 1.5 or ≤ 0.67 fold redox changes is presented in Fig. 3A. Three groups can be distinguished in this table. i) Proteins in the upper part of the table showed sensitive cysteines which underwent an oxidative shift in WT cells, but a reductive shift in NOS3 overexpressing cells, upon silencing of either redoxin. ii) A second group in the middle part of the table shows cysteines that were more oxidized only in 4TO-NOS cells upon either redoxin silencing. iii) Finally, a third group was only sensitive towards Trx1 silencing almost exclusively in NOS3-overexpressing cells. Six proteins: Cofilin-1, 40S ribosomal protein S5 and isoforms Gamma, Theta/delta and Beta/alpha of the 14-3-3 family of proteins, showed high sensitivity to both redoxins but their redox changes, though conspicuous, did not display clear trends and have been omitted.

These changes could be the consequence of direct interaction of either redoxin with the target proteins or could be due to indirect effects. They were almost exclusively oxidative in WT cells as one would expect from the canonical antioxidant functions of Grx1 and Trx1. However, in NOS3 overexpressing cells, the effect of silencing the redoxins, especially Trx1, also resulted in reductive changes in several protein cysteines. The reason for this apparently contradictory result could rely on the fact that NOS3 itself is sensitive to redox modification and can be activated by Trx1 and Grx1 through denitrosation and de-glutathionylation [4,78]. Hence, decreasing the levels of these redoxins by specific siRNA should result in higher levels of redox modified NOS3, lower NOS3 activity and lower protein S-nitrosation levels followed by higher reduced/oxidized ratio of sensitive cysteines in target proteins. We had previously determined the level of Tyr nitration, a good indication of the degree of nitrosative/oxidative stress, in siRNA-Trx1 and siRNA-Grx1 treated WT and NOS3 overexpressing HepG2 cells [22]. Nitro-tyrosine levels were markedly higher in WT HepG2 cells but decreased to 50% in NOS3 overexpressing HepG2 cells which is a further evidence of NOS3 inactivation upon Trx1 and Grx1 down-regulation.

3.2.3. Redoxins-sensitive cysteines show specific sequence motifs

Defining sequence signatures around redox sensitive cysteines would help predict and find redox regulated target proteins. A search for short linear motifs in the sequences around the redox modified Cys's shown in Fig. 3A using the *motif-x* algorithm [10] produced three motifs with high enrichment score among the input set of proteins compared with the background occurrence in the whole human proteome (Fig. 3B). There is a Lys at position +1 or +4 in motifs 1 and 2 respectively and a threonine at +4 in motif 3. It is well known that nucleophilic reactivity of Cys's is dependent on ionization to thiolate

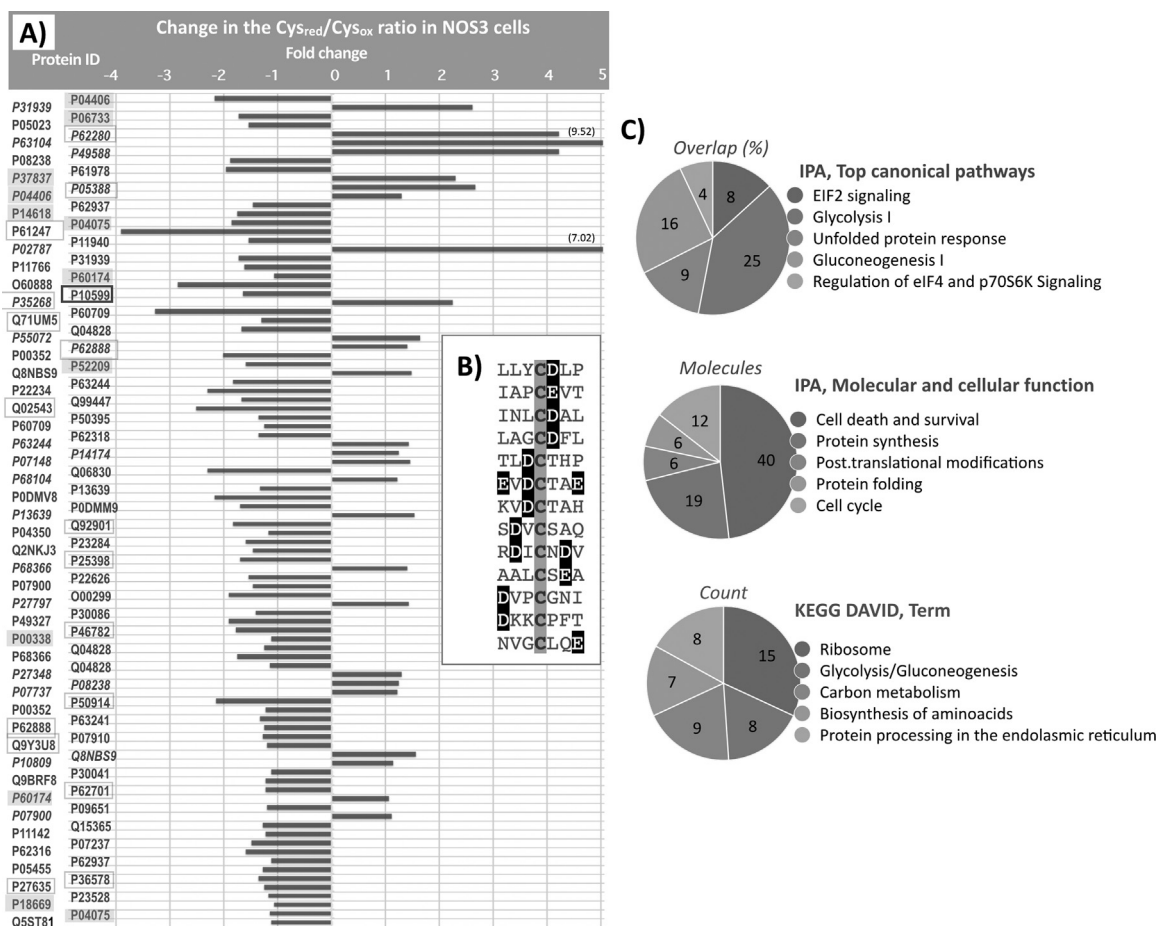


Fig. 2. NOS3 over expression alters the Reduced/Oxidized ratio of specific Cys on target proteins. **A)** The UniProt ID of the protein is shown in the vertical axis and the relative change in the Cys_{red}/Cys_{ox} ratio in 4TO_NOS cells is indicated in the horizontal axis as fold change relative to the ratio in control 4TO cells transformed with the empty vector. Proteins are ordered according to their statistical q score (Storey & Tibshirani) from 0.0000516 (top) to 0.0497383 (bottom). Proteins with negative values were more oxidized after NOS3 overexpression; those with positive values (IDs in *italic*) were more reduced. Two proteins showed reductive changes higher than fivefold as indicated. P10599, square boxed with thick line, is Trx1(C⁷³); ID of enzymes of Glycolysis and its branching pathways are highlighted with grey squares and ribosomal proteins are square boxed with thin line. **B)** sequence context around the cysteine residue of 13 peptides whose reduced/oxidized ratio increased ≥ 1.5 on NOS3 overexpression, showing the presence of acidic residues (white letters highlighted in black) close to the affected cysteine (grey shadowed). Protein names and Cys mapping are detailed in sheet “NOS3 Vo” of the Excel file shown in [Suppl Fig. 2](#). **C)** Systems Biology analysis of the whole set of redox modified proteins using Ingenuity Pathway Analysis (Qiagen) and DAVID [Huang et al. *Nature Protoc.* 2009;4(1):44–57]. The five most significant terms from each analysis are shown with p values ranging from 9.18E–19 to 9.75E–04.

avored by low pKa. Computational and experimental results indicate that the surrounding charged side chains can contribute, but do not primarily control, the thiolate pKa in the Trx superfamily and other proteins with reactive Cys [69,70]. However, a search for denitrosation sites in proteins found two potential motifs with lysine at + 6 and + 7 [87] and a structural analysis of cysteine S-nitrosation sites found lysine at position + 3 and threonine at + 5 with moderate frequency [49]. The presence of a lysine residue near the target Cys is also common to human proteins S-nitrosation motifs [42]. A study that combined sequence, structure, and electrostatic approaches predicted that Thr, its hydroxyl group, and hydrogen-bonding capabilities play an important role in Cys deprotonation and reactivity [70]. Hence, our results with Lys or Thr upstream of Cys fit in with the current structural landscape of redox sensitive Cys's, where some signatures have been put forward but evidences for a strong consensus sequence motif has not yet been achieved.

Two proteins were specifically sensitive to Grx1 silencing, PGAM1(Cys¹⁵³) and PRDX6(Cys⁹¹). Alignment of both Cys-peptides showed a striking conservation score around the affected Cys stressing their assignment as Grx1 targets (Fig. 3C). These Cys's are positioned in a coil in the protein structure with 3.78% and 4.00% solvent accessibility, respectively, and are enriched in acidic residues around the central

cysteine. They fit in the *Homo sapiens* HC05 group glutathionylation motif as catalogued at dbGSH (<http://csb.cse.yzu.edu.tw/dbGSH>). PRDX6 is 1-Cys peroxiredoxin with prominent features as it depends on GSH and GST-Pi for peroxidase activity and also has phospholipase A2 (PLA2) activity, which plays a role for activation of NADPH oxidase 1 and 2 (NOX1, NOX2) [17,41]. The Grx-dependent redox modified Cys at position 91 is not the canonical catalytic (“peroxidatic”) cysteine that lies at position 47 of PRDX6. Cys⁹¹ has not been given attention so far and has been routinely substituted by Ser in the recombinant protein, supposedly to avoid unwanted thiol oxidation and “shuffling” and to facilitate handling. Further experiments have been undertaken to find out whether the Grx-specific redox sensitivity of PRDX6 Cys⁹¹ plays a role on any of the protein functions.

3.2.4. Part of the observed cysteine redox changes were due to direct S-nitrosation

As determined previously [21], NOS3 overexpression not only increases the levels of NO but those of other ROS as well, so reversible oxidation of Cys residues could be due to S-nitrosation or other types of oxidative modifications induced by ROS. To ascertain whether S-nitrosation was actually taking place, we have carried out the Biotin Switch Technique (BST). We have limited this analysis to siRNA-Trx1

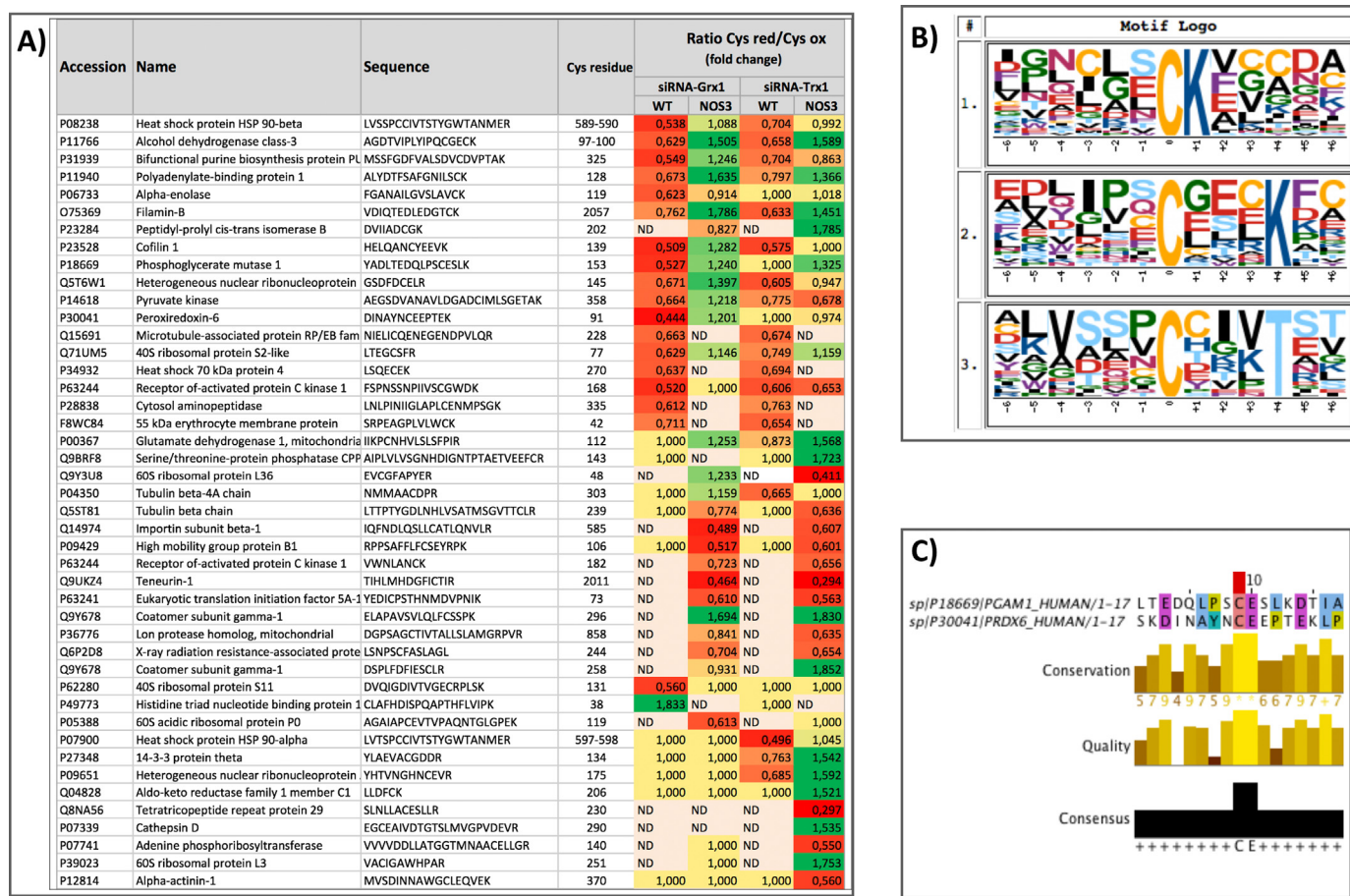


Fig. 3. Changes in the reduced/oxidized ratio of specific Cys on target proteins upon Trx1 and Grx1 silencing. **A)** The UniProt ID and name of the protein, the sequence of the Cys-peptide and the position of the Cys residue affected are shown together with the redox change observed expressed as fold change of the Cys_{red}/Cys_{ox} ratio relative to the non-silenced cells. Oxidative changes are colored red and reductive changes are green. Only proteins showing fold changes ≥ 1.5 or ≤ 0.66 are included. All the values are statistically significant according to their q value (Storey & Tibshirani). Cells colored yellow with a value of 1.00 represent non-significant changes; ND, peptide not detected. **B)** Putative consensus sequences of Trx1 and Grx1 related sensitive Cys-peptides; the sequences of the peptides showing significant redox changes upon Trx1 or Grx1 silencing in WT and NOS3-overexpressing HepG2 cells were subjected to Motif-X ([10]; <http://motif-x.med.harvard.edu>) with the following parameters: central character “C”, width “13”, occurrences “20”, significance “0.0001”, background “ipi. HUMAN.fasta”; motif scores for logos 1, 2 and 3 were 8.57, 6.30 and 4.86, respectively. **C)** Two Cys peptides specifically sensitive towards Grx1 but not Trx1 belonging to Phosphoglyceromutase-1(Cys153) and Peroxisome oxidin-6(Cys91) were highly conserved as shown by pairwise alignment with a 17 residue window around the sensitive Cys, matrix EBLOSUM62, gap penalty 2; a very high conservation score was found with 2 identities (11.8%) and 6 similarities (35.3%).

treated cells, since Trx1 is well-known to display denitrosase activity.

Analysis of total biotinylated proteins by Western blotting showed clear differences between control and NOS3 overexpressing HepG2 cells as expected. When we compared Trx1 silenced cells with their control, no significant differences were detected at the level of total protein, but interestingly clear differences were found in band patterns indicating changes in S-nitrosated Cys's at the level of individual proteins: some proteins increased while others decreased upon Trx1 silencing (Fig. 4A). These results are in agreement with the finding that several proteins underwent a significant reductive shift on their key Cys's (Fig. 3).

To test individual proteins, PRDX6, PKM2, caspase-3, NOS3 and Trx1 were chosen to analyze their nitrosation state on Trx1 silencing by the BST as shown in Fig. 4B and C. All five proteins were captured with the BST, indicating that they are targets of S-nitrosation. Despite the high variability of the technique, a clear trend was observed in 4TONOS cells showing higher amounts of S-nitrosated PRDX6 and PKM in Trx1-silenced cells than in control cells. This trend was also observed in 4TO and in normal HepG2 cells (not shown). PRDX6 and PKM are likely substrates of Trx1 denitrosase activity, although the involved cysteines cannot be mapped with this technique and we cannot tell whether the S-nitrosated Cys are Cys⁹¹ or Cys⁴⁷ in PRDX6 and Cys³⁵⁸ or another Cys

in PKM. The peptide containing peroxidic Cys⁴⁷ of PRDX6 was not detected in any of our samples. We have previous experience on the difficulty of detecting this tryptic peptide [65], but it was detected using different technical tools in another study where Cys⁴⁷ was actually more oxidized in sciatic nerve of old compared to young mice [56]. Since we have found that the “extra” Cys⁹¹ of PRDX6 is not sensitive to Trx1 but to Grx1 silencing (Fig. 3), which has no denitrosase activity, it is tempting to conclude that Cys⁴⁷ might be target of S-nitrosation in a Trx1-dependent manner while Cys⁹¹ might be a Grx1-dependent target of glutathionylation. A preliminary mass spectrometric analysis of recombinant PRDX6 showed that both Cys⁴⁷ and Cys⁹¹ are liable to spontaneous reversible glutathionylation (Suppl. Fig. 1). These data open the door to interesting insights into PRDX6 molecular properties and functions.

Redox sensitivity of PKM2 Cys³⁵⁸ has been reported before [2,53], however the identity of its redox reversible modification was not determined. Our data show higher S-nitrosation levels of PKM2 in Trx1 silenced cells in parallel with reversible oxidative modification of Cys³⁵⁸ suggesting PKM2 as target of Trx1 denitrosase activity. On the other hand, caspase-3, Trx1 and NOS3 itself, were S-nitrosated in NOS3 overexpressing cells, apparently to a lesser extent when Trx1 was silenced (Fig. 3C).

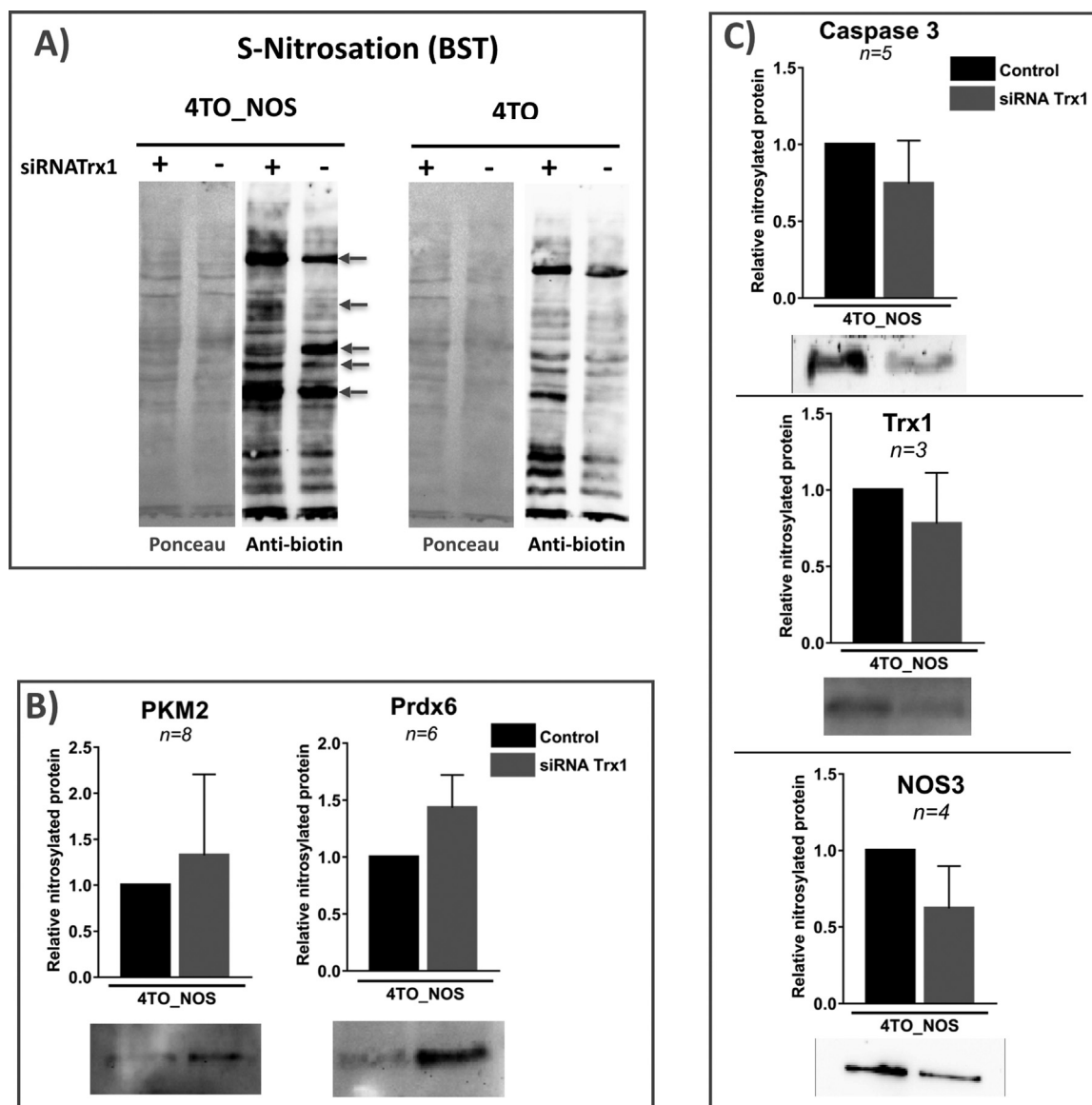


Fig. 4. Protein S-nitrosation in HepG2 cells over expressing NOS3 and treated with specific siRNA-Trx1. A) NOS3 over expressing HepG2 cells, 4TO-NOS, and control 4TO cells transformed with empty vector were silenced or not, for Trx1 and subject to BST; biotinylated proteins constituting the “S-nitrosome” were separated on SDS-PAGE, transferred to Nitrocellulose membrane and revealed with avidin-peroxidase conjugate. Membranes stained with Ponceau reagent before transfer are presented in the left panels to show the protein load. Arrows point to bands with increased or diminished intensity upon Trx1 silencing. B) and C) biotinylated proteins from 4TO-NOS HepG2 cells were captured on avidin-agarose, eluted with β -ME, subjected to Western blot and revealed with specific antibodies to 5 selected proteins as indicated. The intensity of the bands was quantified by image analysis as described in M&M; relative abundances of each protein in the fraction of biotinylated proteins compared to non-silenced control cells are shown, together with the number of replicas and the bars showing standard deviation; trimmed images from membranes showing representative band patterns are included below each graph.

These results confirm that S-nitrosation contributes to redox changes taking place on target Cys's in HepG2 cells depending on the overexpression of NOS3 and affected by the prevailing levels of Trx1.

3.2.5. Proteins with redoxin-sensitive cysteines are abundant in Glycolysis

Clustering of redox sensitive proteins with DAVID [33,34] revealed a significant enrichment in Glycolysis in either normal or NOS3 overexpressing HepG2 cells for both redoxins, but with higher score for Grx1 silencing. Enzymes belonging to Glycolysis or its branching pathways affected by thiol redox changes upon Tx1 or Grx1 silencing or upon overexpression of NOS3 are listed in Fig. 5A and are shown in context schematically in Fig. 5B.

3.2.5.1. Glyceraldehyde-3-phosphate dehydrogenase. The peptide containing Cys¹⁵²/Cys¹⁵⁶ of GAPDH was markedly more oxidized in

NOS3 overexpressing cells. Cys¹⁵² is part of the active site and its oxidation renders the enzyme inactive [25,61]. We confirmed that GAPDH activity decreased in NOS3 overexpressing HepG2 cells (Fig. 5C). Silencing of Trx1 or Grx1 in normal HepG2 cells did result in diminished levels of GAPDH activity as expected, but this loss correlated with oxidation of another Cys residue, Cys²⁴⁷, and not with the redox state of Cys^{152/156}, that did not change (Fig. 5A). GAPDH Cys²⁴⁷ was indeed more oxidized in Trx1 and Grx1 down-regulated WT cells, but more reduced in NOS3 overexpressing cells when Trx1 was silenced. Reversible S-thiolation of GAPDH was earlier reported [73] and since then Cys²⁴⁷ or its equivalent has been mapped and found to be S-glutathionylated, S-nitrosated and S-acetylated [24] even in plants [3], as well as a predicted target of Trx trans-nitrosation [86].

It would seem that GAPDH-C²⁴⁷ is prone to oxidative modification by nitrosation or glutathionylation under the prevailing redox cellular

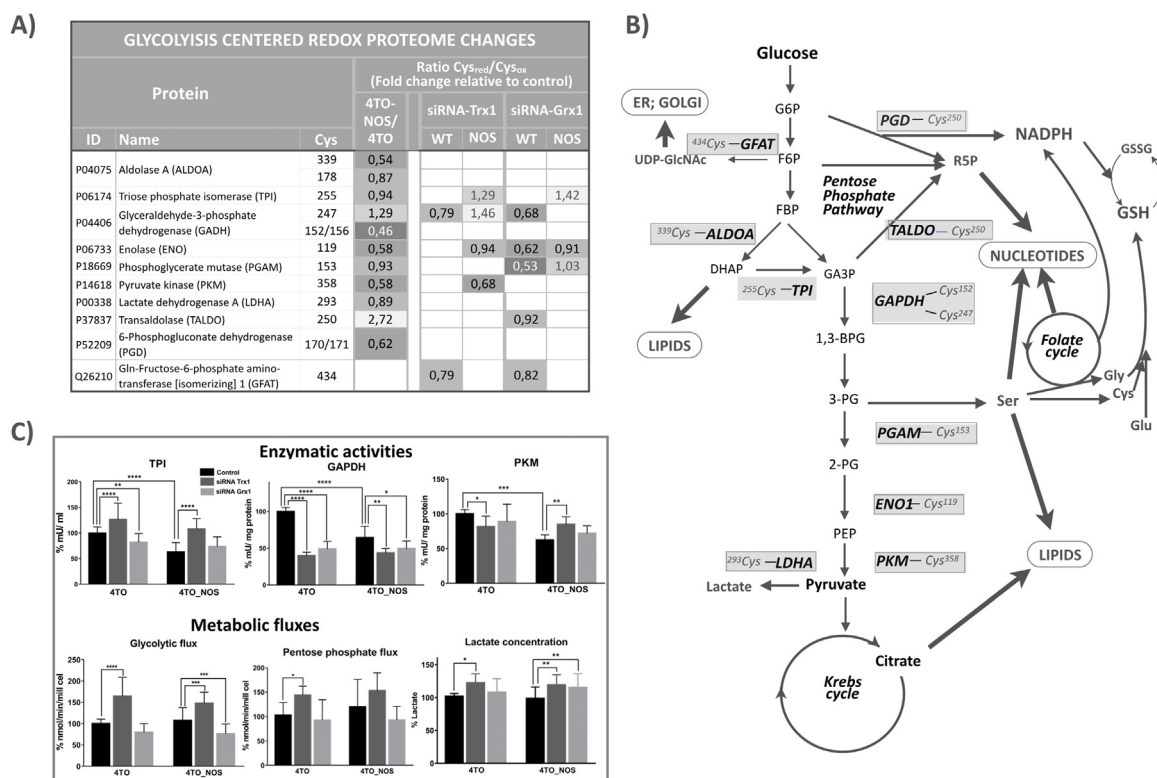


Fig. 5. Silencing Trx1 or Grx1 affects glycolytic enzymes redox state and activities and glycolytic flux. A) Enzymes of Glycolysis and related pathways undergoing significant ($q \leq 0.1$) cysteine redox changes on NOS3 overexpression and upon Trx1 or Grx1 down-regulation have been selected. The precise cysteine residues affected and the changes in the values of their reduced/oxidized cysteine ratios relative to the control (4TO-NOS vs 4TO; siRNA treated vs untreated) are shown. The values for siRNA treated 4TO-NOS cells have been weighted by subtracting the changes observed in siRNA treated 4TO control cells; B) Glycolysis centered metabolic network showing the main glycolytic stream and off-shooting pathways; the final destinations of metabolic fluxes are indicated with thick arrows; the enzymes with redox altered cysteines and their residue position are highlighted. C) Enzymatic activities of triosephosphate isomerase, glyceraldehyde-3-phosphate dehydrogenase and pyruvate kinase, Glycolysis and Pentose Phosphate Pathway fluxes and lactate concentration in siRNA Trx1 and siRNAGrx1 treated 4TO_NOS and 4TO cells are shown relative to untreated 4TO control cells. Between 4 and 9 independent experiments were done for each parameter and a Student *t*-test was calculated for statistical significance with values $p \leq 0.001$, $0.001 > p \leq 0.01$ and $0.01 > p \leq 0.05$ marked with ***, ** and *, respectively.

environment in normal HepG2 cells and to its reversal by either Trx or Grx, respectively. When this fragile equilibrium is displaced by down regulation of either redoxin, the oxidative state of Cys247 increases. However, as discussed in Section 2b, decreasing the levels of Trx1 by specific siRNA in NOS3 overexpressing cells should result in higher levels of redox modified NOS3, lower NOS3 activity and lower GAPDH-C²⁴⁷ nitrosation levels. The levels of nitro-Tyr, an indication of ROS and RNS, did actually decrease down to 50% on either redoxin silencing [22]. This would explain the reductive shift in GAPDH-C²⁴⁷.

Besides its conventional metabolic role, a number of studies have identified the participation of GAPDH in diverse cellular functions and these oxidative changes not only affect its glycolytic function but also stimulate the participation of GAPDH in cell death [11,25]. Our findings point to Cys²⁴⁷ as a sensitive target of the antioxidant activity of Trx1 and Grx1 in WT cells with consequences on its enzymatic activity.

The rationale to explain the decrease in activity of GAPDH would be that it is rewarding for the cells to slow down the glycolytic flux at this point to facilitate upstream diversion of glucose catabolism toward the Pentose Phosphate Pathway (PPP) and to increase NADPH production in this prevalent oxidative environment. However, it has yet to be demonstrated whether inactivation of GAPDH is reflected directly in slowing down of glycolytic flux. Actually, we have observed that inactivation of GAPDH in siRNA-Trx1 treated cells is paralleled by an increase in glycolytic flux (Fig. 5C). Alterations in glycolytic enzymes can regulate autophagy e.g. the moonlighting behaviour of GAPDH enables its direct interaction with mTOR [58] or translocate to the nucleus and upregulate Atg12 [11], both mechanisms being related to the activation of autophagic process. siTrx1 and siGrx1 increased

caspase-3 and TUNEL in 4TO and 4TO-NOS3 cells [22] and increased the oxidative status of the heat shock 70 kDa protein 4 (HspA4) Cys²⁷⁰ (Fig. 3A), an interactor with HspA8 (heat shock cognate 71 protein), which drives chaperone-mediated autophagy [13]. Redox changes at target cysteines in GAPDH and HspA4 suggest that Trx1 and Grx1 signaling promoted a shift from autophagic survival to apoptotic pathway.

3.2.5.2. Phosphoglyceromutase-1. (PGAM1) Cys¹⁵³ was more oxidized in WT cells when Grx1 was down-regulated. PGAM1 is commonly upregulated in human cancers and regulates anabolic biosynthesis by controlling intracellular levels of 3-phosphoglycerate (3-PG) and 2-phosphoglycerate (2-PG) to promote tumor growth [28]. Both 3-PG and 2-PG are allosteric regulators of glycolytic branching pathways: 3-PG inhibits 6-phosphogluconate dehydrogenase (6PGD) of PPP, whereas 2-PG activates phosphoglycerate dehydrogenase (PHGDH) of glycine and serine synthesis pathway. It is worth noting that activation of PGAM1 by phosphorylation at Tyr²⁶, common in human cancer cells, promotes cell proliferation and tumor growth [29]. Cys¹⁵³ is not close to the active site but it has been noted that proteomes of Cys PTMs have localized these modifications primarily in non-catalytic regions [24]. Moreover, Cys¹⁵³ is in the same region of the protein as Tyr²⁶ and Lys¹⁰⁰. It has been demonstrated that increased levels of ROS stimulate PGAM Lys¹⁰⁰ deacetylation and activity by promoting its interaction with SIRT2 [88]; its modification by oxidation could equally affect its activity or even the phosphorylation and acetylation state of Tyr²⁶ and Lys¹⁰⁰ located nearby.

Cellular response to oxidative stress are mediated by the HIF-1 α , which is required for the upregulation of mRNAs encoding glucose

transporters and glycolytic enzymes, with the notable exception of PGAM [37], indicating a possible posttranscriptional regulatory mechanism. Sensitivity of PGAM1 activity to thiol specific reagents was initially reported for the rabbit enzyme [66], but to our knowledge, this is the first time that a Grx1-dependent redox change is observed and mapped to Cys¹⁵³ suggesting a novel form of regulation that could contribute to modulation of glycolytic flux for biosynthetic and antioxidant purposes in response to the redox environment.

3.2.5.3. Pyruvate Kinase. PKM2 (P14618-1) behaves similarly: its Cys³⁵⁸ is close to the allosteric activator fructose-1,6-bisphosphate (FBP) binding site and is sensitive to oxidative stress [2,53]. It has been shown that ROS-dependent inhibition of PKM2 is needed to maintain the availability of glucose-6-phosphate (G-6-P) for flux into the PPP and to sustain cell survival when endogenous ROS accumulate. Regulation of PKM2 via oxidation of Cys³⁵⁸ is critical under these conditions for optimal tumor growth [2]. Coherent with this, we show here that NOS3 overexpression oxidizes Cys³⁵⁸ accompanied by a significant decrease in activity (Fig. 5C). Cys³⁵⁸ is further oxidized when Trx1 is down-regulated, but surprisingly, PKM activity is significantly recovered to the same level as in siRNA-Trx1 treated control cells (Fig. 5C). An increase in the PKM1/PKM2 isoenzyme ratio induced by redox regulation of splicing events as reported in hepatoma cells [84] would explain this result. These data demonstrate the complexity of Trx1 involvement in maintaining the redox state of this Cys³⁵⁸ and the activity of this critical enzyme.

3.2.5.4. Enolase. Cys¹¹⁹ of Alpha-enolase is sensitive to oxidative conditions in NOS3 cells and is a target of Grx1 antioxidant activity in WT cells (Fig. 5A). This cysteine was found to be reactive toward mercury resin specific for Cys-SNO [24] and its glutathionylation in SH-SY5Y neuroblastoma cells resulted in loss of enzymatic activity [36]. Further studies will confirm the regulatory role of this Grx1 dependent redox change of α -Enolase Cys¹¹⁹.

3.2.5.5. Triose phosphate isomerase. TPI Cys²⁵⁵ was more reduced when either Trx1 or Grx1 were silenced in NOS3 cells (Fig. 5A). TPI from several organisms has been shown to be regulated by redox changes involving glutathione at a cysteine equivalent to human Cys²⁵⁵. The equivalent Cys in *P. falciparum* TPI, Cys²¹⁷, is located at the interphase of a complex formed between TPI and Trx [74], whereas *A. thaliana* TPI is inactivated by glutathionylation at Cys²¹⁸ in a manner reverted by Grx [14]. Our results agree with these showing a significant decrease in TPI activity when Grx1 is silenced in control cells. However, silencing of either Trx1 or Grx1 in NOS3 overexpressing cells increased the activity of TPI in parallel with reduction of Cys²⁵⁵, a likely consequence of NOS3 inactivation, as already discussed above. It is tempting to speculate that TPI Cys²⁵⁵ could act as a thiol redox switch to help divert the glycolytic flow from DHAP towards lipid synthesis as part of a metabolic response to changes in the redox environment [45].

Several enzymes from Glycolysis off-shooting pathways showed significant redox changes: Lactate dehydrogenase A (LDHA) Cys²⁹³ and 6-phosphogluconate dehydrogenase (PGD) Cys^{170/171} were slightly more oxidized in NOS3 cells; Glutamine-Fructose-6-phosphate aminotransferase [isomerizing] 1 (GFAT) Cys⁴³⁴ was sensitive to both Trx1 and Grx1 down-regulation; and Transaldolase (TALDO) Cys²⁵⁰ was markedly more reduced in NOS3 cells

Altogether, these data show widespread redox sensitivity of key cysteines in glycolytic enzymes eventually affecting their activities. The prominent role played by Trx1 and Grx1 on these thiol redox switches could be meaningful as part of a pleiotropic redoxin reductive action as a kind of “redox regulon” [20] to coordinate an integrated response to ROS that would balance pyruvate and NADPH production and biosynthetic flux diversion (Fig. 5B). However, the precise consequences of these redoxin-dependent redox changes on metabolic fluxes cannot be predicted from the changes of individual enzymatic activities [81].

Knowledge of *Flux Control Coefficients* of each enzyme would be necessary and the fluxes through glycolysis branched pathways should also be taken into account. As a first approach we have measured glycolytic metabolic flux and metabolites levels, as described below.

3.3. Glycolytic flux and metabolite profiles were differentially affected by Trx1 and Grx1 silencing

Glycolytic and Pentose Phosphate Pathway fluxes were determined using radiolabelled glucose and measuring the formation of [³H]H₂O from [³-³H]glucose during the reaction catalysed by enolase and that of [¹⁴C]CO₂ from [¹-¹⁴C]glucose by 6-phosphogluconate dehydrogenase, respectively. A metabolomic analysis was also undertaken. As shown in Fig. 5C, Trx1 silencing had a stimulating effect on both pathways in either NOS3 overexpressing cells and control cells, whereas Grx1 silencing had the opposite effect in all cases. These effects could be a reflection of the differential action of both redoxins on the redox state of glycolytic enzymes (see Fig. 5A).

3.3.1. Grx1 silencing slows down Glycolysis and stimulates lipogenesis

The relationships between cysteine redox state, enzymatic activities and metabolic fluxes are not straightforward, the metabolic profiles in siRNA-Grx1 treated cells were coherent with lower glycolytic flux showing increased levels of extracellular and intracellular glucose (Fig. 6A). Sedoheptulose-7-phosphate (Su7P) accumulated in WT and NOS3 overexpressing HepG2 cells treated with siRNA-Grx1 (Fig. 6B). This was accompanied by increased levels of several polyols including arabitol, xylitol, ribitol, mannitol and sorbitol, indicative of transaldolase (TALDO) malfunctioning [76], and decreased levels of ribose. These metabolic changes indicate slowing down of glucose processing through the non-oxidative part of PPP as a consequence of Grx1 silencing. Redox changes detected in TALDO-Cys²⁵⁰, 6-phosphogluconate dehydrogenase (PGD) Cys^{170/171} and TPI-Cys²⁵⁵ could be involved in the underlying regulatory mechanisms.

Another effect of Grx1 silencing was an increase in 3-phosphoglycerate (3PG) and lower levels of pyruvate (Fig. 6C) coincident with PGAM-Cys¹⁵³ oxidation and likely deviation of 3PG toward serine pathway. Moreover, unchanged or increased levels of citrate and lower levels of α -ketoglutarate and fumarate (Fig. 6D), might indicate slowing down of Krebs cycle but deviation of citrate to fatty acid biosynthesis. Accordingly, elevated levels of acyl-carnitine (Fig. 6H) and *de novo* synthesis of phospholipids, was evidenced in siRNA-Grx1 treated cells, represented by high levels of phosphatidylcholine and the family of 2-arachidonoyl phospholipids with the exception of phosphatidylserine (Figs. 6L and 6N). The increase in 2-arachidonoyl phospholipids runs parallel with oxidation of PRDX6 Cys⁹¹ and it is worth noting the specificity of cytosolic Ca²⁺-independent PLA2 activity for *sn*-2-arachidonic acid glycerophospholipids [63], a precursor of eicosanoids, which represent a class of lipid mediators. Moreover, arachidonic acid has been shown to mediate the known proliferative action of PRDX6 [72]. These changes speak of active membrane remodeling and/or lipid signaling events in Grx1 down-regulated cells.

Levels of several intermediary metabolites of purine pathway were markedly elevated in Grx1 silenced cells with the exception of IMP but including S-adenosylmethionine (SAM) (Fig. 6G). Elevated levels of SAM should indicate intensification of the methionine/folate pathway connected to glutathione synthesis and supplier of NADPH as an alternative to PPP (Fig. 5B). The synthesis of glutathione was actually exacerbated as indicated by increased levels of gamma-glutamylcysteine and cysteinylglycine (Fig. 6F).

3.3.2. Trx1 silencing induces membrane remodeling

There were similarities and differences between the effects of Grx1 and Trx1 silencing in metabolites' levels. Increased glutathione metabolism (Fig. 6F) and a marked decrease in 3-hydroxy-3-methylglutarate (Fig. 6M) of mevalonate pathway are among the coincidences, but the

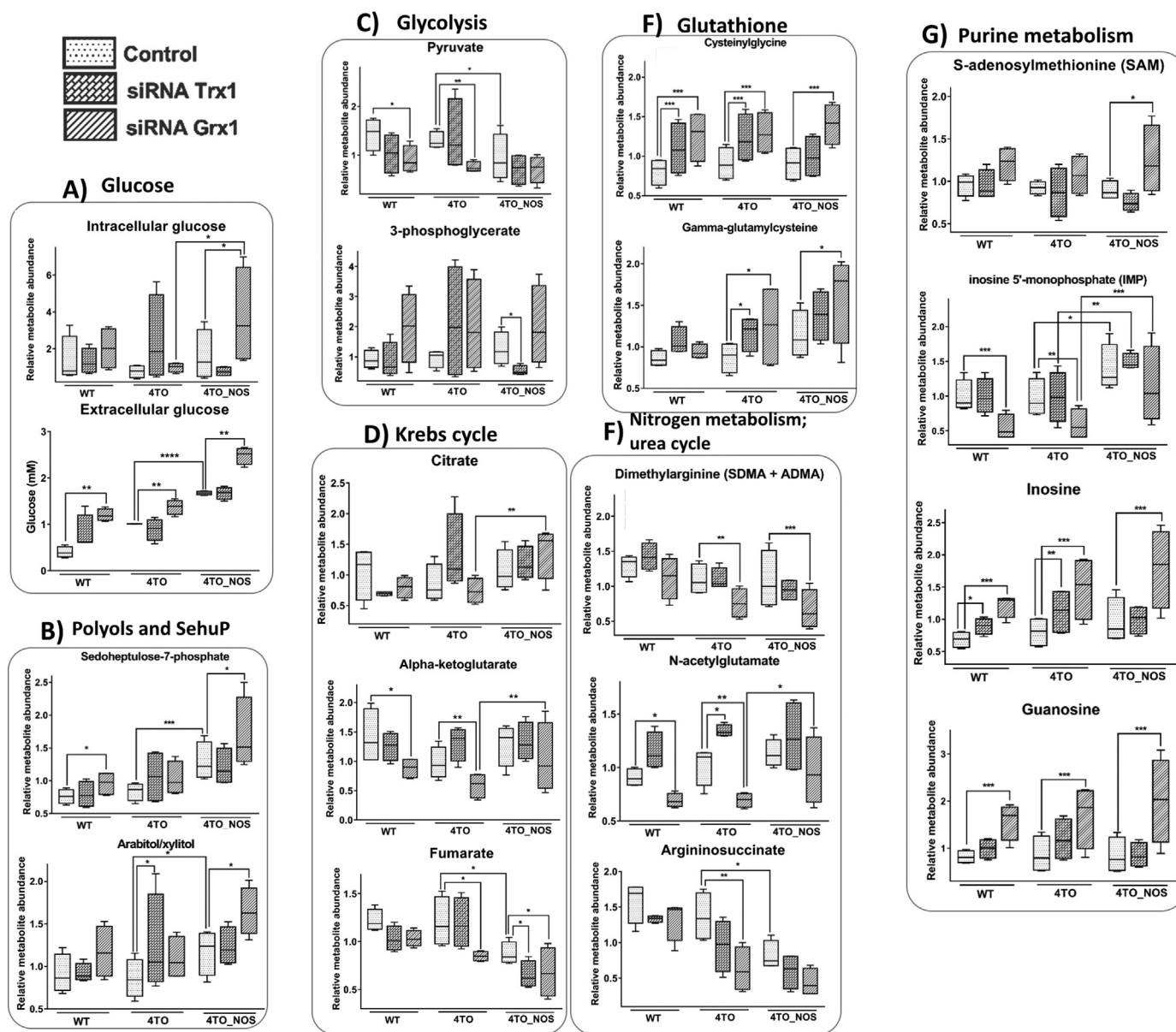


Fig. 6. Metabolites concentrations in normal and NOS3 overexpressing HepG2 under Trx1 and Grx1 down-regulation. A metabolomics analysis was performed in normal (WT), 4TO and 4TO_NOS cells treated with siRNA-Trx1, siRNA-Grx1 or control siRNA-nonTarget as described in Materials & Methods. A selection of metabolites representing the most conspicuous changing trends when cells are treated with siRNA-Trx1 or siRNA-Grx1 is shown. The results presented in this figure are part of a larger metabolic study. Extracellular glucose concentration was determined in culture media by a standard method independently of the metabolomic analysis.

levels of gamma-glutamylaminoacids is higher in siRNA-Grx1 (see [Suppl. File 3](#)) and siRNA-Trx1 did not affect Su7P and glucose levels ([Fig. 6B](#)). Trx silencing elicited trending and significant increases in dipeptides (see [Suppl. File 3](#)) that may reflect increased proteasome-mediated elimination of oxidized proteins in the setting of oxidative stress. Increases in protein degradation could suggest Keap1-Nrf2 signaling and increased autophagy. Notably, many of these changes were not observed in NOS3 overexpressing 4TO_NOS cells.

Trx1 silencing also showed signs of lipid remodeling but differed from Grx1 in promoting a trend of increasing sphingomyelins and ceramides ([Figs. 6I and 6J](#)). Ceramide is involved in apoptotic processes and in the formation of membrane raft redox signaling platforms (MRRSP) that participate in the assembly and activation of NOX complexes [62]. These changes are consistent with the pro-apoptotic effect of Trx and Grx silencing in these cells as we had already reported [22]. The sensitivity of sphingomyelins to redox changes is a key to the

cross-talk between sphingolipids and redox signaling through the regulation of NADPH oxidase, mitochondrial integrity, NOS, and antioxidant enzymes [7]. The trend of sphingomyelins' pool increase on Trx1 silencing could have an influence on mitochondrial lipid composition and integrity. However, cardiolipin, a typical and prominently functional mitochondrial phospholipid, was not detected. Hence, involvement of mitochondria cannot be excluded and is worth of further attention.

4. Conclusions

In the cell there is a delicate balance between effective redox signaling mechanisms and potentially damaging oxidative damage. Oxidative/nitrosative induced PTMs are critical for the accumulation of redox modified proteins, induction of autophagy, and further cellular apoptosis in unsolved pathophysiological intracellular responses while

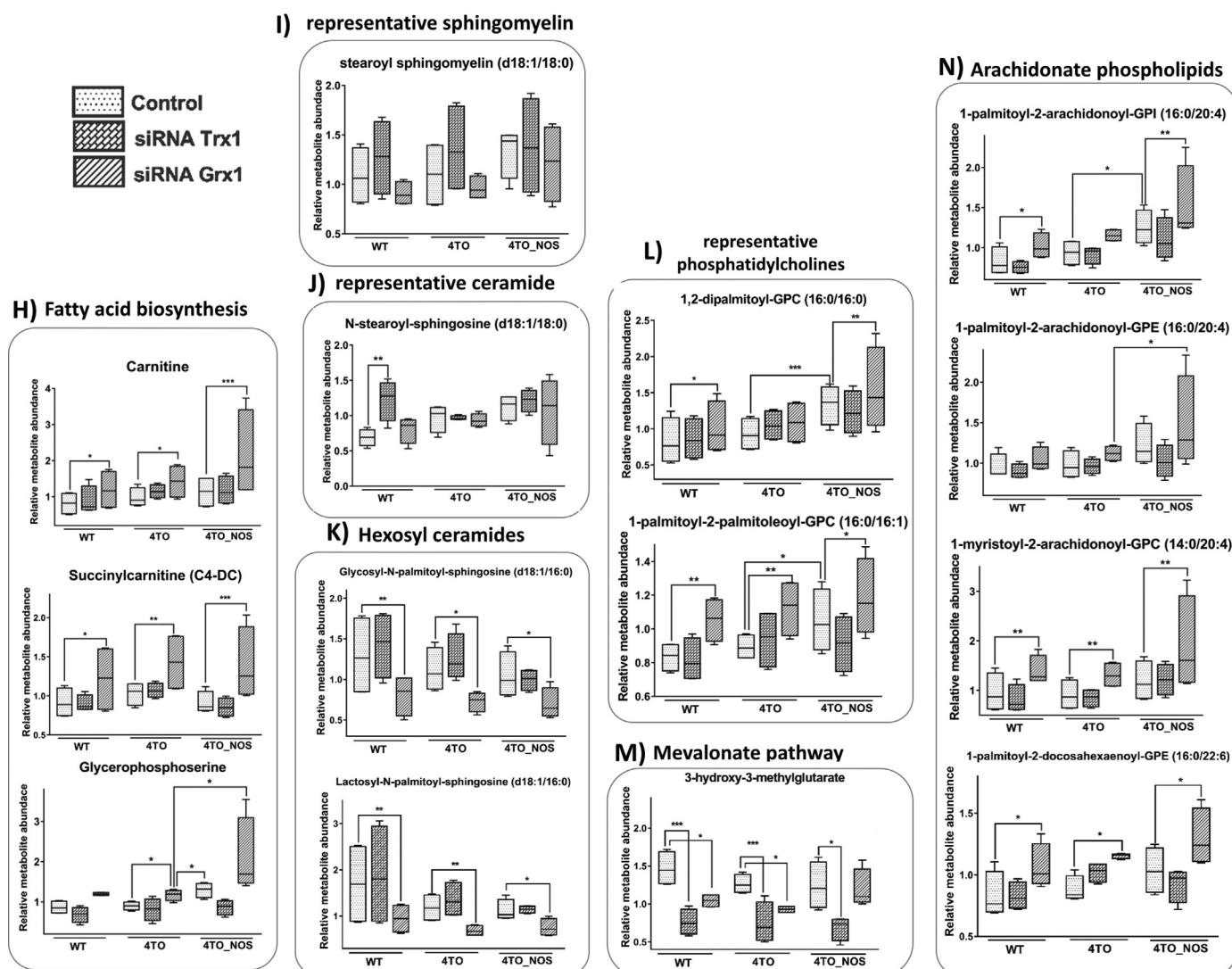


Fig. 6. (continued)

redox signaling through the transient oxidation/reduction of key Cys residues in regulatory proteins plays a role in many of the hallmarks of cancer [31].

The data presented herein show that Trx and/or Grx are involved in redox modifications of targeted cysteines of several glycolytic enzymes affecting their activity, although changes in the activity of one single enzyme cannot be extrapolated to equivalent changes in overall metabolic flux. These changes are part of a widespread adaptive mechanism aimed at redistributing metabolic fluxes between Glycolysis and its off-shooting pathways to respond to subtle changes in the cellular redox environment. Trx and Grx share a number of protein Cys redox targets but down regulation of either redoxin has markedly different metabolic outcomes: silencing of Trx1 stimulates glycolytic flux while silencing of Grx1 decelerates it.

Besides its canonical antioxidant action, Trx1 also contributes to oxidative modifications of protein thiols, likely by activation of NOS3, reflecting the delicate sensitivity of redox equilibrium to changes in any of the elements involved and the difficulty of forecasting metabolic responses to redox environmental changes.

A correlation can be put forward between the reversible oxidation of Cys91 of PRDX6 upon Grx1 silencing that is accompanied by a significant increase of *sn*-2-arachidonoyl containing phospholipids and Cys91 sensitivity to glutathionylation, considering the well-known de-glutathionylase activity of Grx.

To our knowledge, this is the first demonstration of a role for Grx1 and Trx1 in the crosstalk between lipids metabolism and redox signaling. Further and deeper insights into the underlying mechanisms, *i.e.* possible involvement of PRDX6 and Nrf2 signaling [40], CD95 ligand or TNF α induced activation of sphingomyelinases and ceramide induced MRRSP activation of NOX [18], etc., are expected to be discovered with ongoing focused experiments.

Acknowledgements

This research has been financed by grants from the Spanish Ministry of Economy and Competitiveness (BFU2016-80006-P), the Andalusian Government (Consejería de Economía, Innovación, Ciencia y Empleo, BIO-0216 and CTS-6264 and Consejería de Igualdad, Salud y Políticas Sociales, PI-00025-2013 and PI-0198-2016), Institute of Health Carlos III, Spain (PI13/00021, PI16/00090, CIBEREHD and CIBERNED) co-financed by European Development Regional Fund, Europe. We are indebted to Beatriz Carmona (EJ17-BIO216, Programa de Empleo Joven, FEDER/Junta de Andalucía) for her excellent technical assistance in the Biochemistry and Molecular Biology lab.

Appendix A. Supplementary material

Supplementary data associated with this article can be found in the

online version at doi:10.1016/j.redox.2018.11.007.

References

- [1] W.K. Alderton, C.E. Cooper, R.G. Knowles, Nitric oxide synthases: structure, function and inhibition, *Biochem J* 357 (2001) 593–615.
- [2] D. Anastasiou, G. Pouligiannis, J.M. Asara, M.B. Boxer, J.-K. Jiang, M. Shen, G. Bellinger, A.T. Sasaki, J.W. Locasale, D.S. Auld, C.J. Thomas, M.G. Vander Heiden, L.C. Cantley, Inhibition of pyruvate kinase M2 by reactive oxygen species contributes to cellular antioxidant responses, *Science* 334 (2011) 1278–1283.
- [3] M. Bedhomme, M. Adamo, C.H. Marchand, J. Couturier, N. Rouhier, S.D. Lemaire, M. Zaffagnini, P. Trost, Glutathionylation of cytosolic glyceraldehyde-3-phosphate dehydrogenase from the model plant *Arabidopsis thaliana* is reversed by both glutaredoxins and thioredoxins in vitro, *Biochem J* 445 (2012) 337–347.
- [4] M. Benhar, Nitric oxide and the thioredoxin system: a complex interplay in redox regulation, *Biochim. Biophys. Acta* 1850 (2015) 2476–2484.
- [5] M. Benhar, M.T. Forrester, D.T. Hess, J.S. Stamler, Regulated Protein Denitrosylation by Cytosolic and Mitochondrial Thioredoxins, *Science* 320 (2008) 1050–1054.
- [6] M. Benhar, J.W. Thompson, M.A. Moseley, J.S. Stamler, Identification of S-nitrosylated targets of thioredoxin using a quantitative proteomic approach, *Biochemistry* 49 (2010) 6963–6969.
- [7] O.M. Bhat, X. Yuan, G. Li, R. Lee, P.-L. Li, Sphingolipids and Redox Signaling in Renal Regulation and Chronic Kidney Diseases, *Antioxid Redox Signal*, arS 2017 (2018) 7129–7154.
- [8] B.B. Buchanan, Y. Balmer, Redox regulation: a broadening horizon, *Annu Rev Plant Biol* 56 (2005) 187–220.
- [9] C.-A. Chen, F. De Pascali, A. Basye, C. Hemann, J.L. Zweier, Redox modulation of endothelial nitric oxide synthase by glutaredoxin-1 through reversible oxidative post-translational modification, *Biochemistry* 52 (2013) 6712–6723.
- [10] M.F. Chou, D. Schwartz, Biological sequence motif discovery using motif-x, *Curr Protoc Bioinformatics* (2011) 15–24 Chapter 13, Unit13.
- [11] A. Colell, D.R. Green, J.-E. Ricci, Novel roles for GAPDH in cell death and carcinogenesis, *Cell Death Differ.* 16 (2009) 1573–1581.
- [12] J. Cox, M. Mann, MaxQuant enables high peptide identification rates, individualized p.p.b.-range mass accuracies and proteome-wide protein quantification, *Nat Biotechnol* 26 (2008) 1367–1372.
- [13] M. Dodson, V. Darley-Usmar, J. Zhang, Cellular metabolic and autophagic pathways: traffic control by redox signaling, *Free Radic Biol Med* 63 (2013) 207–221.
- [14] S. Dumont, N.V. Bykova, G. Pelletier, S. Dorion, J. Rivoal, Cytosolic Triosephosphate Isomerase from *Arabidopsis thaliana* Is Reversibly Modified by Glutathione on Cysteines 127 and 218, *Front Plant Sci* 7 (2016) 1942.
- [15] P.A. Erwin, A.J. Lin, D.E. Golan, T. Michel, Receptor-regulated dynamic S-nitrosylation of endothelial nitric-oxide synthase in vascular endothelial cells, *J Biol Chem* 280 (2005) 19888–19894.
- [16] S. Fielek, H.W. Mohrenweiser, Erythrocyte Enzyme Deficiencies Assessed with a Miniature Centrifugal Analyzer, *Clin. Chem.* 25 (1979) 384–388.
- [17] A.B. Fisher, Peroxiredoxin 6 in the repair of peroxidized cell membranes and cell signaling, *Arch Biochem Biophys* 617 (2017) 68–83.
- [18] C.R. Gault, L.M. Obeid, Y.A. Hannun, An Overview of Sphingolipid Metabolism: From Synthesis to Breakdown, *Adv. Exp. Med. Biol.* 688 (2010) 1–23.
- [19] Y.-M. Go, D.P. Jones, Thiol/disulfide redox states in signaling and sensing, *Critical Reviews in Biochemistry and Molecular Biology* (2013) 1–19.
- [20] Y.M. Go, D.P. Jones, The Redox Proteome, *Journal of Biological Chemistry* (2013).
- [21] R. González, G. Ferrín, P. Aguilar-Melero, I. Ranchal, C.I. Linares, R.I. Bello, M. la Mata de, V. Gogvadze, J.A. Bárcena, J.M. Alamo, S. Orrenius, F.J. Padillo, B. Zhivotovskiy, J. Muntané, Targeting hepatoma using nitric oxide donor strategies, *Antioxid Redox Signal* 18 (2013) 491–506.
- [22] R. González, M.J. López-Grueso, J. Muntané, J.A. Bárcena, C.A. Padilla, Redox regulation of metabolic and signaling pathways by thioredoxin and glutaredoxin in NOS-3 overexpressing hepatoblastoma cells, *Redox Biology* 6 (2015) 122–134.
- [23] R. González, F.J. Molina-Ruiz, J.A. Bárcena, C.A. Padilla, J. Muntané, Regulation of Cell Survival, Apoptosis, and Epithelial-to-Mesenchymal Transition by Nitric Oxide-Dependent Post-Translational Modifications, *Antioxid Redox Signal* 29 (2018) 1312–1332.
- [24] N.S. Gould, P. Evans, P. Martínez-Acedo, S.M. Marino, V.N. Gladyshev, K.S. Carroll, H. Ischiropoulos, Site-Specific Proteomic Mapping Identifies Selectively Modified Regulatory Cysteine Residues in Functionally Distinct Protein Networks, *Chemistry & Biology* 22 (2015) 965–975.
- [25] M.R. Hara, N. Agrawal, S.F. Kim, M.B. Cascio, M. Fujimuro, Y. Ozeki, M. Takahashi, J.H. Cheah, S.K. Tankou, L.D. Hester, C.D. Ferris, S.D. Hayward, S.H. Snyder, A. Sawa, S-nitrosylated GAPDH initiates apoptotic cell death by nuclear translocation following Siah1 binding, *Nat. Cell Biol.* 7 (2005) 665–674.
- [26] S.I. Hashemy, A. Holmgren, Regulation of the catalytic activity and structure of human thioredoxin 1 via oxidation and S-nitrosylation of cysteine residues, *J Biol Chem* 283 (2008) 21890–21898.
- [27] J.M. Held, S.R. Danielson, J.B. Behring, C. Atsriku, D.J. Britton, R.L. Puckett, B. Schilling, J. Campisi, C.C. Benz, B.W. Gibson, Targeted quantitation of site-specific cysteine oxidation in endogenous proteins using a differential alkylation and multiple reaction monitoring mass spectrometry approach, *Molecular & Cellular Proteomics* 9 (2010) 1400–1410.
- [28] T. Hitosugi, L. Zhou, S. Elf, J. Fan, H.-B. Kang, J.H. Seo, C. Shan, Q. Dai, L. Zhang, J. Xie, T.-L. Gu, P. Jin, M. Alečković, G. LeRoy, Y. Kang, J.A. Sudderth, R.J. DeBerardinis, C.-H. Luan, G.Z. Chen, S. Muller, D.M. Shin, T.K. Owonikoko, S. Lonial, M.L. Arellano, H.J. Khoury, F.R. Khuri, B.H. Lee, K. Ye, T.J. Boggon, S. Kang, C. He, J. Chen, Phosphoglycerate mutase 1 coordinates glycolysis and biosynthesis to promote tumor growth, *Cancer Cell* 22 (2012) 585–600.
- [29] T. Hitosugi, L. Zhou, J. Fan, S. Elf, L. Zhang, J. Xie, Y. Wang, T.-L. Gu, M. Alečković, G. LeRoy, Y. Kang, H.-B. Kang, J.H. Seo, C. Shan, P. Jin, W. Gong, S. Lonial, M.L. Arellano, H.J. Khoury, G.Z. Chen, D.M. Shin, F.R. Khuri, T.J. Boggon, S. Kang, C. He, J. Chen, Tyr26 phosphorylation of PGAM1 provides a metabolic advantage to tumours by stabilizing the active conformation, *Nat Commun* 4 (2013) 1790.
- [30] A. Holmgren, C. Johansson, C. Berndt, M.E. Lönn, C. Hudemann, C.H. Lillig, Thiol redox control via thioredoxin and glutaredoxin systems, *Biochem Soc Trans* 33 (2005) 1375–1377.
- [31] M. Hornsveid, T.B. Dansen, The Hallmarks of Cancer from a Redox Perspective, *Antioxid Redox Signal* 25 (2016) 300–325.
- [32] W. Hu, S. Tedesco, B. McDonagh, J.A. Bárcena, C. Keane, D. Sheehan, Selection of thiol- and disulfide-containing proteins of *Escherichia coli* on activated thiol-Sepharose, *Analytical Biochemistry* 398 (2010) 245–253.
- [33] D.W. Huang, B.T. Sherman, R.A. Lempicki, Bioinformatics enrichment tools: paths toward the comprehensive functional analysis of large gene lists, *Nucleic Acids Res* 37 (2009) 1–13.
- [34] D.W. Huang, B.T. Sherman, R.A. Lempicki, Systematic and integrative analysis of large gene lists using DAVID bioinformatics resources, *Nat Protoc* 4 (2009) 44–57.
- [35] C. Inadomi, H. Murata, Y. Ihara, S. Goto, Y. Urata, J. Yodoi, T. Kondo, K. Sumikawa, Overexpression of glutaredoxin protects cardiomyocytes against nitric oxide-induced apoptosis with suppressing the S-nitrosylation of proteins and nuclear translocation of GAPDH, *Biochemical and Biophysical Research Communications* (2012) 1–6.
- [36] T. Ishii, K. Uchida, Induction of reversible cysteine-targeted protein oxidation by an endogenous electrophile 15-deoxy-delta12,14-prostaglandin J2, *Chem Res Toxicol* 17 (2004) 1313–1322.
- [37] N.V. Iyer, L.E. Kotch, F. Agani, S.W. Leung, E. Laughner, R.H. Wenger, M. Gassmann, J.D. Gearhart, A.M. Lawler, A.Y. Yu, G.L. Semenza, Cellular and developmental control of O2 homeostasis by hypoxia-inducible factor 1 alpha, *Genes Dev.* 12 (1998) 149–162.
- [38] P.A. Karplus, L.B. Poole, Cysteine-based redox switches in enzymes, *Antioxid Redox Signal* 14 (2011) 1065–1077.
- [39] P. Klatt, S. Lamas, Regulation of protein function by S-glutathiolation in response to oxidative and nitrosative stress, *FEBS J* 267 (2000) 4928–4944.
- [40] O. Kuda, M. Brezinova, J. Silhavy, V. Landa, V. Zidek, C. Dodia, F. Kreuchwig, M. Vrbacky, L. Balas, T. Durand, N. Hübnér, A.B. Fisher, J. Kopecky, M. Pravenec, Nrf2-mediated Antioxidant Defense and Peroxiredoxin 6 are Linked to Biosynthesis of Palmitic Acid Ester of 9-Hydroxystearic Acid, *Diabetes*. (2018).
- [41] J. Kwon, A. Wang, D.J. Burke, H.E. Boudreau, K.J. Lektrom, A. Korzeniowska, R. Sugamata, Y.-S. Kim, L. Yi, I. Ersoy, S. Jaeger, K. Palaniappan, D.R. Ambruso, S.H. Jackson, T.L. Leto, Peroxiredoxin 6 (Prdx6) supports NADPH oxidase1 (Nox1)-based superoxide generation and cell migration, *Free Radic Biol Med*. (2016).
- [42] T.-Y. Lee, Y.-J. Chen, T.-C. Lu, H.-D. Huang, Y.-J. Chen, SNOsite: exploiting maximal dependence decomposition to identify cysteine S-nitrosylation with substrate site specificity, *PLoS ONE* 6 (2011) e21849.
- [43] L.I. Leichert, U. Jakob, Quantifying changes in the thiol redox proteome upon oxidative stress in vivo, *Proc Natl Acad Sci USA* 105 (2008) 8197–8202.
- [44] C.-Q. Li, G.N. Wogan, Nitric oxide as a modulator of apoptosis, *Cancer Lett* 226 (2005) 1–15.
- [45] P.-L. Li, E. Gulbins, Bioactive Lipids and Redox Signaling: Molecular Mechanism and Disease Pathogenesis, *Antioxid Redox Signal*. (2018).
- [46] M. Lindahl, A. Mata-Cabana, T. Kieselbach, The disulfide proteome and other reactive cysteine proteomes: analysis and functional significance, *Antioxid Redox Signal* 14 (2011) 2581–2642.
- [47] L. Liu, A. Hausladen, M. Zeng, L. Que, J. Heitman, J.S. Stamler, A metabolic enzyme for S-nitrosothiol conserved from bacteria to humans, *Nature* 410 (2001) 490–494.
- [48] B. MacLean, D.M. Tomazela, N. Shulman, M. Chambers, G.L. Finney, B. Frewen, R. Kern, D.L. Tabb, D.C. Liebler, M.J. MacCoss, Skyline: an open source document editor for creating and analyzing targeted proteomics experiments, *Bioinformatics* 26 (2010) 966–968.
- [49] S.M. Marino, V.N. Gladyshev, Structural analysis of cysteine S-nitrosylation: a modified acid-based motif and the emerging role of trans-nitrosylation, *J Mol Biol* 395 (2010) 844–859.
- [50] P. Martínez-Acedo, E. Núñez, F.J.S. Gómez, M. Moreno, E. Ramos, A. Izquierdo-Álvarez, E. Miro-Casas, R. Mesa, P. Rodríguez, A. Martínez-Ruiz, D.G. Dorado, S. Lamas, J. Vázquez, A novel strategy for global analysis of the dynamic thiol redox proteome, *Mol Cell Proteomics* 11 (2012) 800–813.
- [51] A. Martínez-Ruiz, S. Lamas, Detection and proteomic identification of S-nitrosylated proteins in endothelial cells, *Arch Biochem Biophys* 423 (2004) 192–199.
- [52] A. Martínez-Ruiz, I.M. Araújo, A. Izquierdo-Álvarez, P. Hernansanz-Agustín, S. Lamas, J.M. Serrador, Specificity in S-nitrosylation: a short-range mechanism for NO signaling? *Antioxid Redox Signal* 19 (2013) 1220–1235.
- [53] B. McDonagh, S. Ogueta, G. Lasarte, C.A. Padilla, J.A. Bárcena, Shotgun redox proteomics identifies specifically modified cysteines in key metabolic enzymes under oxidative stress in *Saccharomyces cerevisiae*, *J Proteomics* 72 (2009) 677–689.
- [54] B. McDonagh, J.R. Pedrajas, C.A. Padilla, J.A. Bárcena, Thiol redox sensitivity of two key enzymes of heme biosynthesis and pentose phosphate pathways: uroporphyrinogen decarboxylase and transketolase, *Oxid Med Cell Longev* 2013 (2013) 932472–13.
- [55] B. McDonagh, G.K. Sakellariou, N.T. Smith, P. Brownridge, M.J. Jackson, Differential cysteine labeling and global label-free proteomics reveals an altered metabolic state in skeletal muscle aging, *J Proteome Res* 13 (2014) 5008–5021.
- [56] B. McDonagh, S.M. Scullion, A. Vasilaki, N. Pollock, A. McArdle, M.J. Jackson,

- Ageing-induced changes in the redox status of peripheral motor nerves imply an effect on redox signalling rather than oxidative damage, *Free Radic Biol Med* 94 (2016) 27–35.
- [57] C.M. Metallo, M.G. Vander Heiden, Understanding metabolic regulation and its influence on cell physiology, *Molecular Cell* 49 (2013) 388–398.
- [58] N.L. Mi, H.H. Sang, J. Kim, A. Koh, S.L. Chang, H.K. Jung, H. Jeon, D.-H. Kim, P.-G. Suh, H.R. Sung, Glycolytic flux signals to mTOR through glyceraldehyde-3-phosphate dehydrogenase-mediated regulation of Rheb, *Mol Cell Biol* 29 (2009) 3991–4001.
- [59] J.J. Mieyal, M.M. Gallogly, S. Qanungo, E.A. Sabens, M.D. Shelton, Molecular mechanisms and clinical implications of reversible protein S-glutathionylation, *Antioxid Redox Signal* 10 (2008) 1941–1988.
- [60] D.A. Mitchell, M.A. Marletta, Thioredoxin catalyzes the S-nitrosation of the caspase-3 active site cysteine, *Nature Chemical Biology* 1 (2005) 154–158.
- [61] S. Mohr, J.S. Stamler, B. Brüne, Posttranslational modification of glyceraldehyde-3-phosphate dehydrogenase by S-nitrosylation and subsequent NADH attachment, *J Biol Chem* 271 (1996) 4209–4214.
- [62] M.J. Morgan, Y.-S. Kim, Z. Liu, Lipid rafts and oxidative stress-induced cell death, *Antioxid Redox Signal* 9 (2007) 1471–1483.
- [63] M. Murakami, I. Kudo, Phospholipase A2, *J. Biochem.* 131 (2002) 285–292.
- [64] J.M. Patel, J. Zhang, E.R. Block, Nitric oxide-induced inhibition of lung endothelial cell nitric oxide synthase via interaction with allosteric thiols: role of thioredoxin in regulation of catalytic activity, *Am. J. Respir. Cell Mol. Biol.* 15 (1996) 410–419.
- [65] J.R. Pedrajas, B. McDonagh, F. Hernández-Torres, A. Miranda-Vizuete, R. González-Ojeda, E. Martínez-Galisteo, C.A. Padilla, J.A. Bárcena, Glutathione Is the Resolving Thiol for Thioredoxin Peroxidase Activity of 1-Cys Peroxiredoxin Without Being Consumed During the Catalytic Cycle, *Antioxid Redox Signal* 24 (2016) 115–128.
- [66] M.O. Prehu, C. Prehu, M.C. Calvin, R. Rosa, Rabbit M type phosphoglyceromutase: comparative effects of two thiol reagents antibody reaction and hybridization studies, *Comp. Biochem. Physiol., B* 89 (1988) 257–262.
- [67] K. Ravi, L.A. Brennan, S. Levic, P.A. Ross, S.M. Black, S-nitrosylation of endothelial nitric oxide synthase is associated with monomerization and decreased enzyme activity, *Proc Natl Acad Sci USA* 101 (2004) 2619–2624.
- [68] R. Requejo-Aguilar, I. Lopez-Fabuel, D. Jimenez-Blasco, E. Fernandez, A. Almeida, J.P. Bolaños, DJ1 represses glycolysis and cell proliferation by transcriptionally up-regulating Pink1, *Biochem J* 467 (2015) 303–310.
- [69] G. Roos, N. Foloppe, J. Messens, Understanding the pK(a) of redox cysteines: the key role of hydrogen bonding, *Antioxid Redox Signal* 18 (2013) 94–127.
- [70] F.R. Salsbury, S.T. Knutson, L.B. Poole, J.S. Fetrow, Functional site profiling and electrostatic analysis of cysteines modifiable to cysteine sulfenic acid, *Protein Sci* 17 (2008) 299–312.
- [71] B. Schilling, M.J. Rardin, B.X. MacLean, A.M. Zawadzka, B.E. Frewen, M.P. Cusack, D.J. Sorensen, M.S. Bereman, E. Jing, C.C. Wu, E. Verdin, C.R. Kahn, M.J. MacCoss, B.W. Gibson, Platform-independent and Label-free Quantitation of Proteomic Data Using MS1 Extracted Ion Chromatograms in Skyline: APPLICATION TO PROTEIN ACETYLATION AND PHOSPHORYLATION, *Molecular & Cellular Proteomics* 11 (2012) 202–214.
- [72] A. Schmitt, W. Schmitz, A. Hufnagel, M. Schartl, S. Meierjohann, Peroxiredoxin 6 triggers melanoma cell growth by increasing arachidonic acid-dependent lipid signalling, *Biochem J* 471 (2015) 267–279.
- [73] I. Schuppe-Koistinen, P. Moldéus, T. Bergman, I.A. Cotgreave, S-thiolation of human endothelial cell glyceraldehyde-3-phosphate dehydrogenase after hydrogen peroxide treatment, *Eur J Biochem* 221 (1994) 1033–1037.
- [74] H.M.S. Shahul, S.P. Sarma, The structure of the thioredoxin-triosephosphate isomerase complex provides insights into the reversible glutathione-mediated regulation of triosephosphate isomerase, *Biochemistry* 51 (2012) 533–544.
- [75] M.D. Shelton, P.B. Chock, J.J. Mieyal, Glutaredoxin: role in reversible protein S-glutathionylation and regulation of redox signal transduction and protein translocation, *Antioxid Redox Signal* 7 (2005) 348–366.
- [76] A. Stincone, A. Prigione, T. Cramer, M.M.C. Wamelink, K. Campbell, E. Cheung, V. Olin-Sandoval, N.-M. Grüning, A. Krüger, M. Tauqeer Alam, M.A. Keller, M. Breitenbach, K.M. Brindle, J.D. Rabinowitz, M. Ralser, The return of metabolism: biochemistry and physiology of the pentose phosphate pathway, *Biol Rev* 90 (2014) 927–963.
- [77] J.D. Storey, R. Tibshirani, Statistical significance for genomewide studies, *Proceedings of the National Academy of Sciences* 100 (2003) 9440–9445.
- [78] J. Subramani, V. Kundumani-Sridharan, R.H.P. Hilgers, C. Owens, K.C. Das, Thioredoxin Uses a GSH-independent Route to Deglutathionylate Endothelial Nitric-oxide Synthase and Protect against Myocardial Infarction, *J Biol Chem* 291 (2016) 23374–23389.
- [79] L.B. Sullivan, D.Y. Gui, M.G.V. Heiden, Altered metabolite levels in cancer: implications for tumour biology and cancer therapy, *Nat. Rev. Cancer* 16 (2016) 680–693.
- [80] D.A. Tennant, R.V. Durán, E. Gottlieb, Targeting metabolic transformation for cancer therapy, *Nat. Rev. Cancer* 10 (2010) 267–277.
- [81] B. Teusink, J. Passarge, C.A. Reijenga, E. Esgalhado, C.C. van der Weijden, M. Schepper, M.C. Walsh, B.M. Bakker, K. van Dam, H.V. Westerhoff, J.L. Snoep, Can yeast glycolysis be understood in terms of in vitro kinetics of the constituent enzymes? Testing biochemistry, *Eur J Biochem* 267 (2000) 5313–5329.
- [82] S. Tyanova, T. Temu, J. Cox, The MaxQuant computational platform for mass spectrometry-based shotgun proteomics, *Nat Protoc* 11 (2016) 2301–2319.
- [83] M.G. Vander Heiden, L.C. Cantley, C.B. Thompson, Understanding the Warburg effect: the metabolic requirements of cell proliferation, *Science* 324 (2009) 1029–1033.
- [84] L. Wei, Y. Dai, Y. Zhou, Z. He, J. Yao, L. Zhao, Q. Guo, L. Yang, Oroxilin A activates PKM1/HNF4 alpha to induce hepatoma differentiation and block cancer progression, *Cell Death and Disease* 8 (2017) e2944.
- [85] T. Wei, C. Chen, J. Hou, W. Xin, A. Mori, Nitric oxide induces oxidative stress and apoptosis in neuronal cells, *Biochim. Biophys. Acta* 1498 (2000) 72–79.
- [86] C. Wu, T. Liu, W. Chen, S.-I. Oka, C. Fu, M.R. Jain, A.M. Parrott, A.T. Baykal, J. Sadoshima, H. Li, Redox regulatory mechanism of transnitrosylation by thioredoxin, *Molecular & Cellular Proteomics* 9 (2010) 2262–2275.
- [87] C. Wu, A.M. Parrott, C. Fu, T. Liu, S.M. Marino, V.N. Gladyshev, M.R. Jain, A.T. Baykal, Q. Li, S. Oka, J. Sadoshima, A. Beuve, W.J. Simmons, H. Li, Thioredoxin 1-mediated post-translational modifications: reduction, transnitrosylation, denitrosylation, and related proteomics methodologies, *Antioxid Redox Signal* 15 (2011) 2565–2604.
- [88] Y. Xu, F. Li, L. Lv, T. Li, X. Zhou, C.-X. Deng, K.-L. Guan, Q.-Y. Lei, Y. Xiong, Oxidative stress activates SIRT2 to deacetylate and stimulate phosphoglycerate mutase, *Cancer Res.* 74 (2014) 3630–3642.
- [89] L. Yang, D. Wu, X. Wang, A.I. Cederbaum, Depletion of cytosolic or mitochondrial thioredoxin increases CYP2E1-induced oxidative stress via an ASK-1-JNK1 pathway in HepG2 cells, *Free Radic Biol Med* 51 (2011) 185–196.

ARTICLE 2

Peroxiredoxin 6 down-regulation induces metabolic remodeling and cell cycle arrest in HepG2 cells. **López-Grueso M.J.**, Tarradas R.M., Carmona-Hidalgo B., Lagal D.J., Peinado J., McDonagh B., Requejo-Aguilar R., Bárcena J.A. and Padilla C.A. **Antioxidants** (Accepted 18 October 2019)



Article

Peroxiredoxin 6 Down-Regulation Induces Metabolic Remodeling and Cell Cycle Arrest in HepG2 Cells

López-Grueso M.J.¹, Tarradas R.M.¹, Carmona-Hidalgo B.¹, Lagal D.J.¹, Peinado J.^{1,2}, McDonagh B.³, Requejo-Aguilar R.^{1,2}, Bárcena J.A.^{1,2,*} and Padilla C.A.^{1,2}

¹ Dept. of Biochemistry and Molecular Biology, University of Córdoba, 14074 Córdoba, Spain; q02logrm@uco.es (L.-G.M.J.); rosa.tarradas.valero@gmail.com (T.R.M.); cahibeatriz@gmail.com (C.-H.B.); b32larud@uco.es (L.D.J.); bb1pepej@uco.es (P.J.); bb2reagr@uco.es (R.-A.R.); bb1papec@uco.es (P.C.A.)

² Maimónides Biomedical Research Institute of Córdoba (IMIBIC), 14004 Córdoba, Spain

³ Department of Physiology, School of Medicine, NUI Galway, H91 TK33 Galway, Ireland; BRIAN.MCDONAGH@nuigalway.ie

* Correspondence: ja.barcena@uco.es

Received: 27 September 2019; Accepted: 18 October 2019; Published: date

Abstract: Peroxiredoxin 6 (Prdx6) is the only member of 1-Cys subfamily of peroxiredoxins in human cells. It is the only Prdx acting on phospholipid hydroperoxides possessing two additional sites with phospholipase A2 (PLA2) and lysophosphatidylcholine-acyl transferase (LPCAT) activities. There are contrasting reports on the roles and mechanisms of multifunctional Prdx6 in several pathologies and on its sensitivity to, and influence on, the redox environment. We have down-regulated Prdx6 with specific siRNA in hepatoblastoma HepG2 cells to study its role in cell proliferation, redox homeostasis, and metabolic programming. Cell proliferation and cell number decreased while cell volume increased; import of glucose and nucleotide biosynthesis also diminished while polyamines, phospholipids, and most glycolipids increased. A proteomic quantitative analysis suggested changes in membrane arrangement and vesicle trafficking as well as redox changes in enzymes of carbon and glutathione metabolism, pentose-phosphate pathway, citrate cycle, fatty acid metabolism, biosynthesis of aminoacids, and Glycolysis/Gluconeogenesis. Specific redox changes in Hexokinase-2 (HK2), Prdx6, intracellular chloride ion channel-1 (CLIC1), PEP-carboxykinase-2 (PCK2), and 3-phosphoglycerate dehydrogenase (PHGDH) are compatible with the metabolic remodeling toward a predominant gluconeogenic flow from aminoacids with diversion at 3-phosphoglycerate toward serine and other biosynthetic pathways thereon and with cell cycle arrest at G1/S transition.

Keywords: Peroxiredoxin; thiol redox regulation; redox proteome; redox homeostasis; lipid metabolism; cell cycle

1. Introduction

Peroxiredoxins (Prdx) are ubiquitous, abundant, and highly conserved enzymes whose main function is to catalyze the reduction of peroxides, taking part in the antioxidant battle of cells against ROS. They all possess a catalytic or “peroxidatic” Cys residue that acts as a hydrogen donor to the peroxide substrate and have been classified in six subfamilies, of which three are present in mammalian cells [1]. Human Prdx1 to Prdx4 belong to the “typical 2-Cys type” and Prdx5 belongs to the “atypical 2-Cys” subfamily. They have a second “resolving” Cys that plays a critical role in the catalytic cycle and is then reduced by thioredoxin (Trx). Human Prdx6 belongs to the “1-Cys” subfamily, which, unlike the other members of the Prdx family, does not possess a “resolving Cys” and may substitute Trx by glutathione in the final step of the catalytic cycle [2–5]. Mouse and human

Prdx6 have an additional non-conserved Cys residue (Cys91 in human) with a so far unknown function.

Several members of the Prdx family are moonlighting proteins that have acquired additional functions during evolution. For instance, some Prdx of the 2-Cys subfamily can form oligomers with chaperone activity when overoxidized [6] or can act as sensors and transmitters of H₂O₂ signaling [7]. Prdx6 is peculiar and stands out from the rest of Prdx for its multiple functions. It is the only Prdx acting on phospholipid hydroperoxides and has two additional catalytic sites: one is responsible for acidic calcium-independent phospholipase A2 activity (PLA2) [8] and the other displays lysophosphatidylcholine acyl transferase (LPCAT) activity [9]. It has been proposed that these outstanding properties confer on Prdx6 the capacity to fulfill important functions associated with phospholipid turnover and membrane repair [10]. Posttranslational modifications and changes in subcellular localization regulate the actions of Prdx6. Phosphorylation of Thr177 by MAPK [11] and overoxidation of peroxidatic Cys47 [12,13] stimulate the PLA2 activity. Prdx6 is present in the cytoplasm but can translocate to the plasma and mitochondrial membranes and can also associate with lysosomal-type organelles [14,15]. Association of Prdx6 with plasma membrane contributes to NADPH (reduced nicotinamide adenine dinucleotide phosphate) oxidase (NOX1, NOX2) activity [16] and translocation to the mitochondria takes part in the initiation of mitophagy [15].

Its multiple functionality makes Prdx6 an important player in cell physiology and pathology [17,18] and both peroxidase and PLA2 activities have been associated with tumor progression [19] and dopaminergic neuron degeneration [20]. However, contrasting findings have been reported concerning its roles in cancer. Down-regulation of Prdx6 with specific siRNA decreased proliferation and induced apoptosis in canine haemangiosarcoma cells [21], whereas overexpression of Prdx6 attenuated apoptosis in ovarian cancer cells [22] and promoted growth of lung tumors in mice through activation of JAK2/STAT3 signaling [23]. It has also been reported that Prdx6 either enhance tumor multiplicity or reduce tumor number in mice skin cells, depending on the stage of tumor development [24]. Both peroxidase and PLA2 activities of Prdx6 were required for tumor development in xenografted mice lung in a process dependent on arachidonic acid (AA) release [25]. AA production and NOX2 activation was also involved in stimulation of metastasis by Prdx6 PLA2 activity in several cancer models [25,26], although in another study, NOX2 activation was shown to proceed through Prdx6 mediated lysophosphatidic acid (LPA) receptor activation [27]. Prdx6 has also been related to pathogenesis of cardiometabolic diseases [17] and inflammatory diseases with contrasting roles of peroxidase and PLA2 activities [18].

In a recent study, we have found that weakening the cell's antioxidant potential by experimental down-regulation of glutaredoxin 1 (Grx1) in HepG2 cells affects the phospholipid metabolism and the redox state of Prdx6 "extra residue" Cys91 [28]. In view of the above-outlined background of contrasting reports on the roles and mechanisms of multifunctional Prdx6 in several pathologies and its sensitivity to the redox environment, we have undertaken a project based on down-regulating Prdx6 with specific siRNA in hepatoblastoma HepG2 cells to study the role of Prdx6 in cell proliferation, redox homeostasis and metabolic programming. Silencing with specific siRNA provides a good experimental approach to mimic physiological down-regulation events that may occur as part of a cell response to various stimuli. We have found that the cells respond to Prdx6 silencing by adapting carbon and lipid metabolism and by modulating signaling pathways to stop cell cycle progression at the G1/S phase transition.

2. Materials and Methods

2.1. Materials and Reagents

All reagents were of analytical grade and were purchased from Sigma (St. Louis, Missouri, USA) unless otherwise specified. HepG2 cell line used in this work was obtained from the ATCC LGC Standards Company (Teddington, UK). Cell culture dishes and flasks were from TPP (Switzerland). The specific small interfering RNA for PRDX6 (siRNA_{Prdx6}) and non-target (NT) were from Dharmacon (Lafayette, CO, USA) and ECL was from GE Healthcare (Wauwatosa,

Wisconsin, USA). Antibodies against PRDX6 were from Abcam (Cambridge, UK). Antibodies against CD95 were from Santa Cruz Biotechnology, (Dallas, TX, USA). Antibodies against Actin were from Sigma.

2.2. Cell Growth Conditions, Proliferation and Cell Viability

Cells were grown in EMEM Medium (Eagle Minimum Essential Medium), pH 7.4, supplemented with 10% fetal bovine serum, 2.2 g/L NaHCO₃, 1 mM sodium pyruvate, 100 U/L penicillin, 100 µg/mL streptomycin, and 0.25 µg/mL amphotericin in 5% CO₂ atmosphere at 37 °C. Cell proliferation was analyzed using a colorimetric ELISA (Roche Applied Science, Penzberg, Germany). 20,000 cells/cm² were cultured in 96-well multiplates at 37 °C and 5% CO₂. 72h after siRNAPrx6 addition HepG2 cells were incubated with 10 µM BrdU labeling solution for 6h at 37 °C. Then cells were fixed with 200 µl of FixDenat solution for 30 min at room temperature. From this point, the incubations were done at room temperature. After this time, fixed cells were incubated with 100 µl of anti-BrdU-POD solution with a previous dilution of 1: 100 for 90 min, and washed with PBS. Finally, fixed cells were incubated with 100 µl of substrate solution for 30 min. Total number of cells and cell viability in a HepG2 cell suspension were quantified using the trypan blue dye exclusion method in 90 mm dishes.

2.3. Silencing of Prdx6

Human Prdx6 was down-regulated in HepG2 cells using a specific pool of four small interfering RNA (Ref. L-019173-00-0005) according to the manufacturer's recommendations (Dharmacon, GE Healthcare, Life Science). 20,000 cells/cm² were cultured in dishes and treated with 25 nmol of siRNA mixed with the transfection reagent DharmaFECT-1 preincubated with culture medium (antibiotic and serum free) for 20 min at RT, in a 1:2 proportion and the interference solution was kept for 72 h to obtain the maximum inhibition of ≈60%. Non-targeting (NT) negative controls were run in parallel. Silencing of Prdx6 was always checked by Western blot.

2.4. Measurement of Cell Death and Area of Cell Nuclei

Apoptosis in HepG2 cells was analyzed through Annexin V-FITC (Canvax, Córdoba, Spain). Annexin-V binds to phosphatidylserine (PS) residues which are on the outer plasma membrane of apoptotic cells. Annexin-V is labeled with the fluorophore FITC to visualize apoptotic cells by fluorescent microscopy. 20,000 cells/cm² were cultured on a coverslip introduced in each well of a 24-well plate at 37 °C and 5% CO₂. 2.5 µl of Annexin-V-FITC was added after siRNAPrx6 following the instructions of the manufacturer. Then, cells were fixed in methanol and permeabilized with 0.2% Triton-X100 solution in PBS. Cells nuclei were stained using DAPI. Fluorescence was measured with a fluorescence microscope (Olympus BX43) using standard fluorescein filter set to view Annexin-V-FITC fluorescence at 520 nm and view blue DAPI at 460 nm. The area of cell nuclei was measured on the DAPI pictures using the open source software "ImageJ" [29].

2.5. Measurement of Enzymatic Activities, Glucose and Protein

HepG2 PLA2 activity was assayed using the Red/Green BODIPY based EnzChek Phospholipase A2 Assay (Invitrogen) (pH 7.0, in the absence of calcium) in 96-well plates [30]. Cells were sonicated (4 × 5 s) in PLA2 buffer (50 mM Tris-HCl, 1 mM EGTA, pH 7.0) supplemented with protease and phosphatase inhibitors, and the supernatant collected by centrifugation at 15,000 ×g for 15 min was adjusted to ≈ 50 µg protein and preincubated for 10 min at 37 °C in the absence or presence of MJ33 (10 µM) [31]. At 60 min, samples were analyzed in a Microplate reader (Varioskan, Thermo Scientific) at an excitation of 460 nm and emissions of 515 nm. Background was subtracted and the ±MJ33 differential 515 nm emission were recorded. Caspase-3, caspase-8, and caspase-9 associated activities were determined using the corresponding fluorescence peptide-based substrates (100 µM) in the reaction mixture (50 mM HEPES pH7.5, 100 mM NaCl, 10% sucrose, 0.1% Chaps, 1 mM EDTA and 5 mM DTT). The substrates used were Ac-DEVD-AFC, Ac-LETD-AFC, and

Ac-LEHD- AFC for caspase-3, -8, and -9, respectively. The fluorescence due to the reaction product was recorded with a GENios Microplate Reader (TECAN) set at 400 nm excitation and 505 nm emission. Glucose concentration in the culture medium was determined by a standard enzymatic colorimetric assay at 505 nm (LabKit, Chemelex, S.A.). Protein concentration in the samples was determined by the Bradford method (Bio-Rad) using BSA as the standard.

2.6. Proteomics

2.6.1. Sample Preparation and Mass Spectrometry

The experiments were routinely carried out at 20,000 cells/cm² and a modification of the methodological strategy described previously [28] was used. Reduced cysteines were blocked with “light” Iodoacetamide (IAM) while reversibly oxidized Cys were labeled with “heavy” IAM (Iodoacetamide-13C₂, 2d₂) incorporating Δ mass of 4 Da. Cell extracts were obtained with a lysis solution (50 mM Tris-HCl pH 8.5, 5 mM IAM light, 0.5% CHAPS, 1 mM PMSF); samples were centrifuged at 15,000g for 5 min at 4 °C. 100 μ g of protein were diluted up to 80 μ l with 50 mM Tris-HCl pH 8.5 and incubated with 4 μ l of 160 mM DTT at 37 °C for 30 min to reduce the reversibly oxidized cysteines. Subsequently, cysteines were alkylated adding 6 μ l of 240 mM IAM heavy and incubated at room temperature for 30 min in darkness. Finally, the excess of IAM and CHAPS was removed using Zeba spin desalting columns (Thermo Scientific) equilibrated with 25 mM ammonium bicarbonate pH 7.0. The level of silencing was checked at this point by SDS-PAGE.

Proteolytic digestion and proteomic analyses were performed as described previously [28]. The spectrometer used was the Thermo Orbitrap Fusion (Q-OT-qIT, Thermo Scientific) equipped with a nano-UHLC Ultimate 3000 (Dionex-Thermo Scientific).

2.6.2. Label-Free MS Protein and Redox Quantification

The “label-free” quantification was performed using the MaxQuant (v1.5.7.0) free software [32] configuring “light” IAM and “heavy” IAM and methionine oxidation as variable modifications. No imputation of missing values was implemented. Finally, only the conditions with three or more values per identification were considered and analyzed using a Student’s T-test. The criteria for considering a differentially expressed protein were that it was identified and quantified using at least two unique peptides and it showed a fold change of at least 1.5 and a $p \leq 0.05$ value. MS² spectra were searched with SEQUEST engine against a database of Uniprot_Human_Nov2014 (www.uniprot.org). The Cys-containing peptides labeled with light and heavy IAM modifications independently were quantified using the open software Skyline [33]. The individual reduced/oxidized ratio for specific Cys residues was calculated in each sample in order to obtain the redox proteome. The intensities of missed cleaved peptides were taken into account for the calculations.

2.7. Metabolomics

The metabolomic study is part of a larger study and the analyses were performed at Metabolon, NC USA (www.metabolon.com). The samples from four different experiments were prepared following the company specific guidelines as described before [28]. Briefly, dry cell pellets were immediately frozen in liquid nitrogen and stored at -80 °C until shipment. Samples were prepared using the automated MicroLab STAR[®] system from Hamilton Company. To remove protein, dissociate small molecules bound to protein or trapped in the precipitated protein matrix, and to recover chemically diverse metabolites, proteins were precipitated with methanol under vigorous shaking for 2 min (Glen Mills GenoGrinder 2000) followed by centrifugation. The resulting extract was divided into five fractions: two for analysis by two separate reverse phase (RP)/UPLC-MS/MS methods with positive ion mode electrospray ionization (ESI), one for analysis by RP/UPLC-MS/MS with negative ion mode ESI, one for analysis by HILIC/UPLC-MS/MS with negative ion mode ESI, and one sample was reserved for backup. Extraction of raw data, peak identification and quantification, and QC were performed using Metabolon’s hardware and software.

2.8. SDS-PAGE and Western Blotting

SDS-PAGE was performed in 12% Criterion XT Precast Gels (Bio-Rad) for detection of specific proteins (Prdx6, CD95, Actin). After electrophoresis, proteins were transferred to a nitrocellulose membrane in a semi-dry electrophoretic transfer system (Bio-Rad) for 40 min at 400 mA constant. Transfer and protein load were checked by staining with Ponceau reagent. The membranes were incubated overnight at 4 °C with the corresponding dilutions of primary antibodies: 1:500 CD95, 1:2000 Prdx6, and 1:4000 Actin. They were then washed with TBS-T and incubated with the corresponding secondary antibodies conjugated to peroxidase (anti-rabbit, anti-goat, or anti-mouse) used at 1:8000 dilution. The chemiluminescent signal induced by ECL reagent (GE Healthcare) was detected in a ChemiDoc image analyzer (Bio-Rad) and quantified by densitometry with Quantity-One 1-D analysis software (Bio-Rad) using Actin as reference for loading normalization.

2.9. Statistics

Where appropriate, results are expressed as mean \pm SD of at least three independent experiments and Student t-test used for significance. Large data sets were analyzed using Storey and Tibshirani method [34] comparing non-target control vs. siRNA Prdx6 treated. The threshold for statistically significant differences was set at p -value adjust ≤ 0.05 ; q -values are also included as an additional reference.

3. Results and Discussion

3.1. Prdx6 down-Regulation Reduced Cell Proliferation

The peroxidatic Cys47 in Prdx6 is predominantly (> 60%) in a reversibly oxidized state in HepG2 cells (see data in Supplementary File S2) but its overoxidation would decrease the peroxidase activity and stimulate the PLA2 activity [13].

It was not possible to measure the Prdx6-specific peroxidase activity in cell lysates, but its phospholipase A2 activity (PLA2) was determined using a standard fluorimetric assay in the presence of MJ33, a Prdx6 specific PLA2 inhibitor, as described in Materials and Methods. The assay gives a high variability and, although the resulting data from five different experiments were not statistically significant, a trend was observed with lower activity in siRNA-Prdx6 treated cells (Figure 1A) in parallel with decreased levels of Prdx6 protein by $\approx 60\%$, as determined by Western blot and confirmed by mass spectrometry quantitative analysis (See data in Supplementary File 1).

The number of cells and incorporation of BrdU, indicative of the number of cells in the S phase or proliferation, both decreased after 72 h treatment with siRNA-Prdx6 (Figure 1B,C). Cell viability did not change in either condition (data not shown), but the size of the cells augmented as evidenced by a significant increase in nuclear size (Figure 1D). The nuclear size is an important parameter governing entry into the cell cycle. These results suggest cell cycle blockade induced by Prdx6 down-regulation.

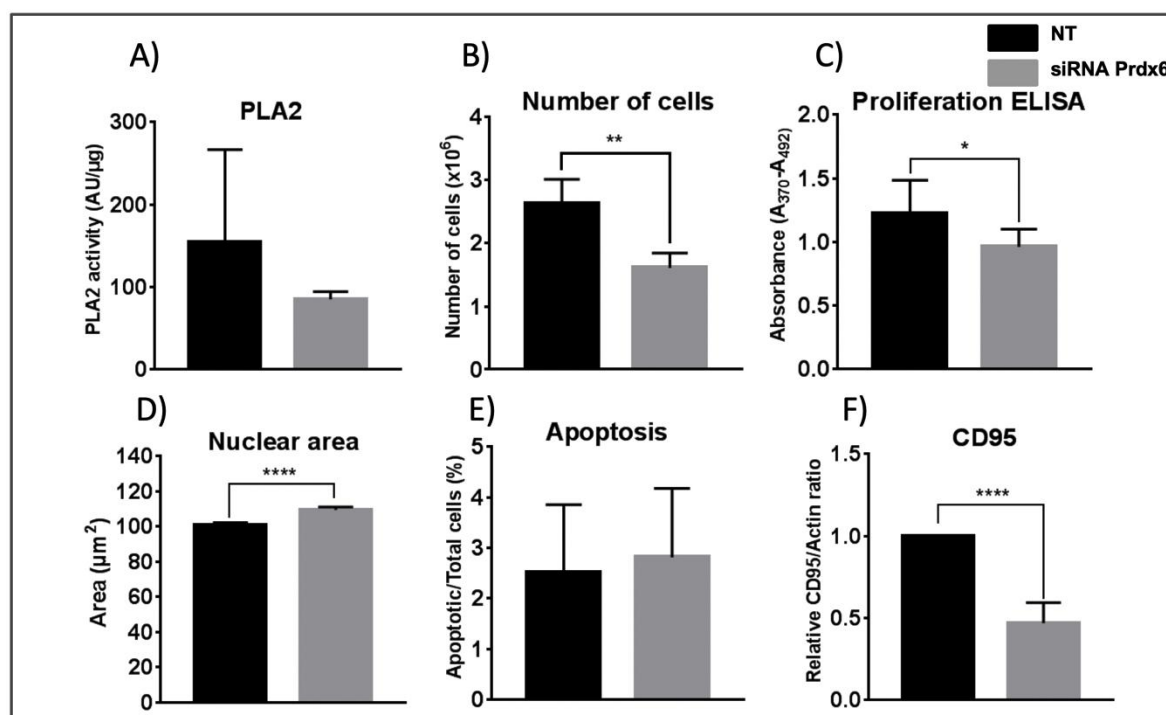


Figure 1. Effect of Prdx6 silencing on PLA2 activity, cell viability, nuclear area, apoptosis, and CD95 level. (A) Prdx6-dependent PLA2 activity was determined, as described in Materials and Methods, in cell lysates of HepG2 cells treated with siRNA-Prdx6 or with non-target siRNA (NT) as indicated. Activity is expressed as arbitrary fluorescence units normalized for protein content. Data are the mean of 5 independent biological replicates. (B) The number of cells determined as indicated in M&M. (C) Proliferation in terms of cells entering the S phase was determined by the degree of BrdU incorporation to replicating DNA and expressed in absorbance units. (D) The nuclear area of cells was determined as indicated in M&M. >500 cells were measured, from 6 different slides, in each sample. The area is given in arbitrary units. (E) Apoptosis was determined by the Annexin V fluorescence method; the number of positive cells relative to the total number of cells in percentage is represented. (F) CD95 levels were determined by western blotting with specific antibodies and band density was normalized to the signal for actin. Parameters in (B), (C), (E) and (F) were determined in three independent experiments; error bars show SD; statistical significance was assessed by Student's T-test and is shown with a number of asterisks inversely proportional to the p-value (**** < 0.0001, ** < 0.01, * < 0.05).

3.2. Prdx6 Silencing Interferes with Apoptotic Signaling from CD95 but does not Induce Apoptosis in HepG2 Cells

To check whether the anti-proliferative action of Prdx6 down-regulation could be due to activation of cell death mechanisms, we analyzed several apoptotic parameters. Prdx6 silencing did not affect apoptosis significantly in HepG2 cells as shown by Annexin V fluorescence (Figure 1 E), but did induce a marked decrease in CD95 protein levels (Figure 1F). This effect could not be associated to caspase modulation, since the levels and activities of caspases 3, 8 and 9 did not change significantly, although caspase 3 displayed unusually high variability (data not shown). It is well established that activation of CD95 receptor mediates the induction of apoptosis mostly in the context of immune response. CD95 is ubiquitously expressed in all types of cells, including cancer cells, but its expression in cancer cells implies that they are themselves resistant to CD95-mediated apoptosis [35]. It is now widely accepted that CD95 has multiple non-apoptotic functions and that stimulation of CD95 in cancer cells can turn this death receptor into tumor promoting receptor [35] through diverse tumorigenic signaling pathways. In lung cancer cells, activation of CD95 induced the production of proinflammatory factor PGE2 through the p38 pathway, and promoted cell growth that was reduced by administration of the cyclooxygenase-2 inhibitor [36]. Interestingly,

accelerated entry into the cell cycle S-phase by CD95 stimulation was demonstrated in pancreatic ductal adenocarcinoma cells in vitro in a process not dependent on the DISC (death-inducing signaling complex) formation but mediated by recruitment of the adapter protein Sck (SH2 domain protein C2) [37].

Altogether, these results show that the response of HepG2 cells to Prdx6 silencing is rather complex, with a mixture of apparently contradictory outcomes like CD95 down-regulation but no changes in caspases and cell swelling. It would be worth determining whether the antiproliferative action could be due to the blockade of entry into cell cycle S-phase by down-regulation of CD95 and the possible involvement of signaling events dependent on the PLA2 activity of Prdx6. These aspects will be discussed below in a wider context including changes at metabolomic, proteomic, and redox levels.

3.3. Metabolic Remodeling after Prdx6 Silencing

Metabolic remodeling and protein posttranslational modification (PTM) are the first levels of cellular response to a stimulus before a stable response is set up at the transcriptional level. We carried out a metabolomic analysis (Supplementary File S3) to determine the possible effect of Prdx6 down regulation in the metabolic profile of HepG2 cells.

3.3.1. Lipids

Lipid metabolism plays a critical role in cell survival and proliferation since these varied molecules are indispensable for the structural, signaling, and energy needs of every cell. Phospholipids are synthesized during entry in the cell cycle but the synthesis pauses for cell division, so that the G1 and S phases are characterized by doubling of phospholipid content [38].

Increased levels of all kinds of phospholipids, lysophospholipids, plasmalogens and ceramides, with the exception of lactosylceramide, was a marked trend in siRNA-Prdx6 treated cells. A parallel increase in UDP-glucose and UDP-galactose levels (Figure 2B) is consistent with the enhanced rate of glycolipids synthesis. CDP-ethanolamine, P-choline and P-ethanolamine of the Kennedy pathway were particularly elevated. Augmented levels of phosphocholine have been observed in a wide variety of human cancers, caused in part by the growth factor-activated Ras and phosphatidylinositol 3-kinase (PI3K) signaling cascades that stimulate the initial enzyme of the choline branch of the pathway [39]. It would be valuable to know if the elevated levels of these phospholipid precursors caused by Prdx6 silencing involve this signaling pathway. Increased phospholipid content could contribute to the observed increase in the cell volume described above (Figure 1D).

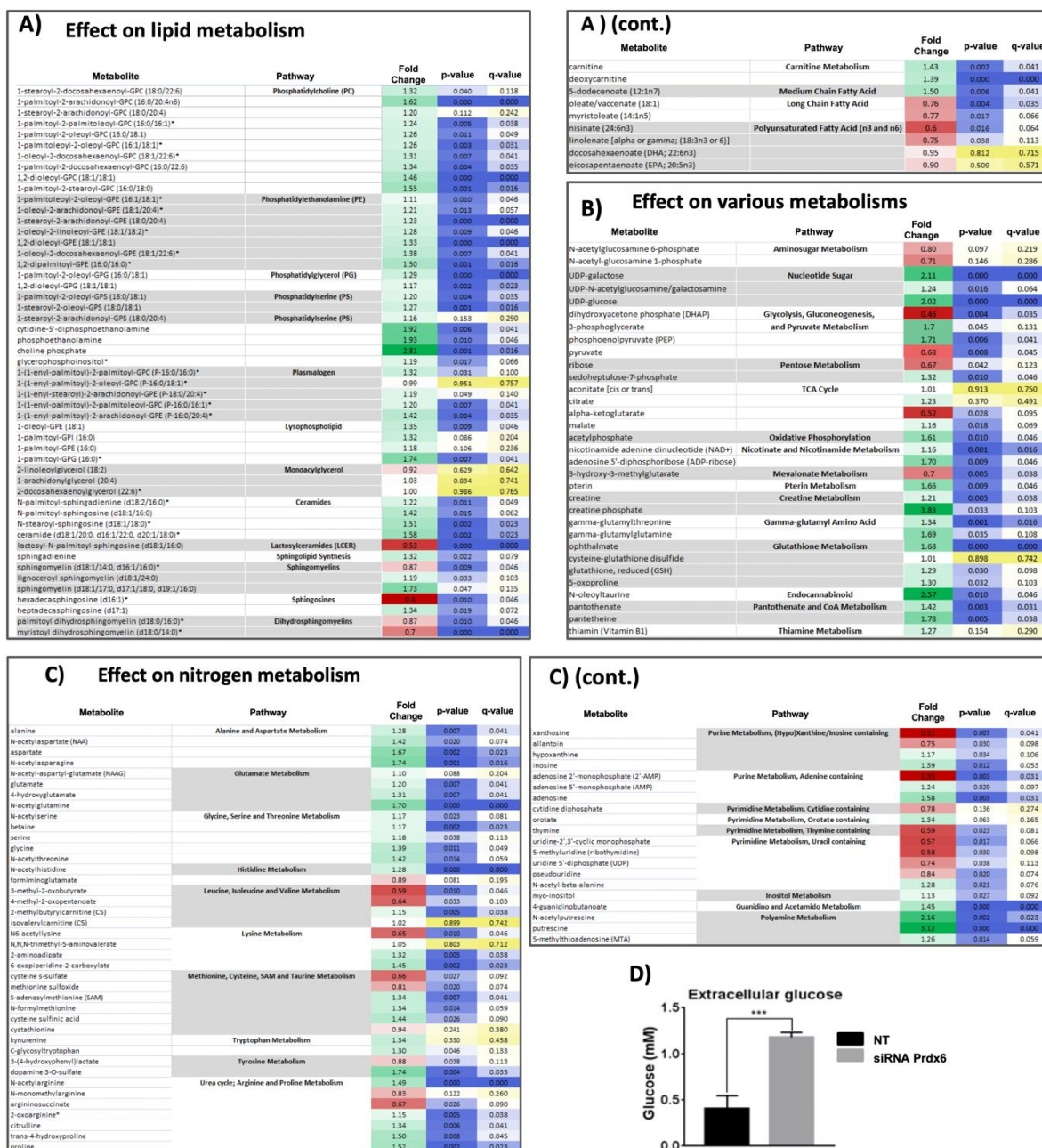


Figure 2. Summary of significant metabolomic changes. A metabolomic analysis was carried out as described in Materials and Methods. The fold change (up-regulation, green; down-regulation, red) of each metabolite level on Prdx6 silencing in HepG2 cells is shown in the first column; the second and third columns show the p-values and q-values, respectively, for statistical significance; p and q-values ≤ 0.05 are in blue with the color intensity inversely proportional to p- or q-value. The results have been clustered into three figures and into pathways therein: (A) Metabolites of lipid metabolism; (B) metabolites of other pathways and (C) metabolites of aminoacids and nucleotides metabolism. (D) The concentration fold change of extracellular glucose determined by standard colorimetric methods in three independent experiments (***) $p < 0.001$.

Long chain monoacylglycerols (MAG) were an exception to this trend of increased lipid content. Some MAG are known as endocannabinoids, like 2-arachidonyl-glycerol and it has been recognized that they have important signaling functions [40]. MAG can form through the action of PLA2 on phosphatidic acid (PA) while their degradation is carried out by membrane bound MAG hydrolases of which two types have been described, the ubiquitously expressed serine hydrolase α/β -hydrolase domain 6 (ABHD6) and classical MAG lipase, a housekeeping enzyme. ABHD6 is expressed at high

levels in certain tumors and its pharmacological or genetic suppression, which leads to an elevation in 1- and 2-MAG content in different tissues, appears to have multiple health benefits, likely mediated via MAG signaling [40]. Only three members of this family of lipases were detected in the proteomic analysis (ABHD10, ABHD12, and ABHD14B; see data in Supplementary File S1) and none of them showed significant quantitative changes on Prdx6 silencing, stressing the possible contribution of Prdx6 PLA2 activity down-regulation to unchanged MAG levels.

Long chain fatty acids decreased in siRNA-Prdx6 treated cells while the levels of carnitine followed a reciprocal trend (Figure 2A cont.). The accumulation of carnitine is indicative of reduced entry of long chain fatty acids into the mitochondria for β -oxidation. A natural variant C304→W (VAR_020548; dbSNP: rs80356776) of carnitine O-palmitoyltransferase 1 (CPT1A) with pathological consequences produces an unstable, inactive form of the enzyme [41] stressing the importance of Cys residues for optimal import of long chain fatty acids into the mitochondria. Redox changes observed in CPT1A (See Supplementary File S2) could be relevant to these trends in long chain fatty acid metabolism. Our results show that CPT1A-Cys96 was oxidized (0.3 red/ox ratio fold change; $p = 0.005$) on siRNA-Prdx6 silencing. Reversible oxidation of CPT1A-Cys96 would slow down fatty acid β -oxidation in favor of increased biosynthesis and incorporation into phospholipids in siRNA-Prdx6 treated cells.

There could also be a relationship between the levels of unsaturated long chain fatty acids and PLA2 activity of Prdx6. Early characterization of Prdx6 PLA2 activity showed high activity with arachidonic acid (AA) containing phospholipids [42,43]. A proapoptotic role of Prdx6 via induction of AA release by its PLA2 activity has been postulated in human bronchial epithelial cells [44] but another study found that AA production by PLA2 activity of Prdx6 induced cell proliferation through activation of Src family kinases in human melanoma cells [26]. These contradictory results reveal the complexity of Prdx6 action mechanisms and highlight the importance of lipid signaling in cancer.

3.3.2. Nitrogen Metabolism

A generalized increase in aminoacids, with few exceptions, was observed that could be a consequence of increased biosynthesis and/or protein degradation. A marked similar trend was observed for polyamines, a sign of the cells being prepared for proliferation since elevated polyamine levels, are necessary for transformation and tumor progression [45]. This increment could also contribute to the above-mentioned increase in cell volume (Figure 1D). It would be worth checking whether these changes are due to alteration in the PI3/Akt/mTOR pathway.

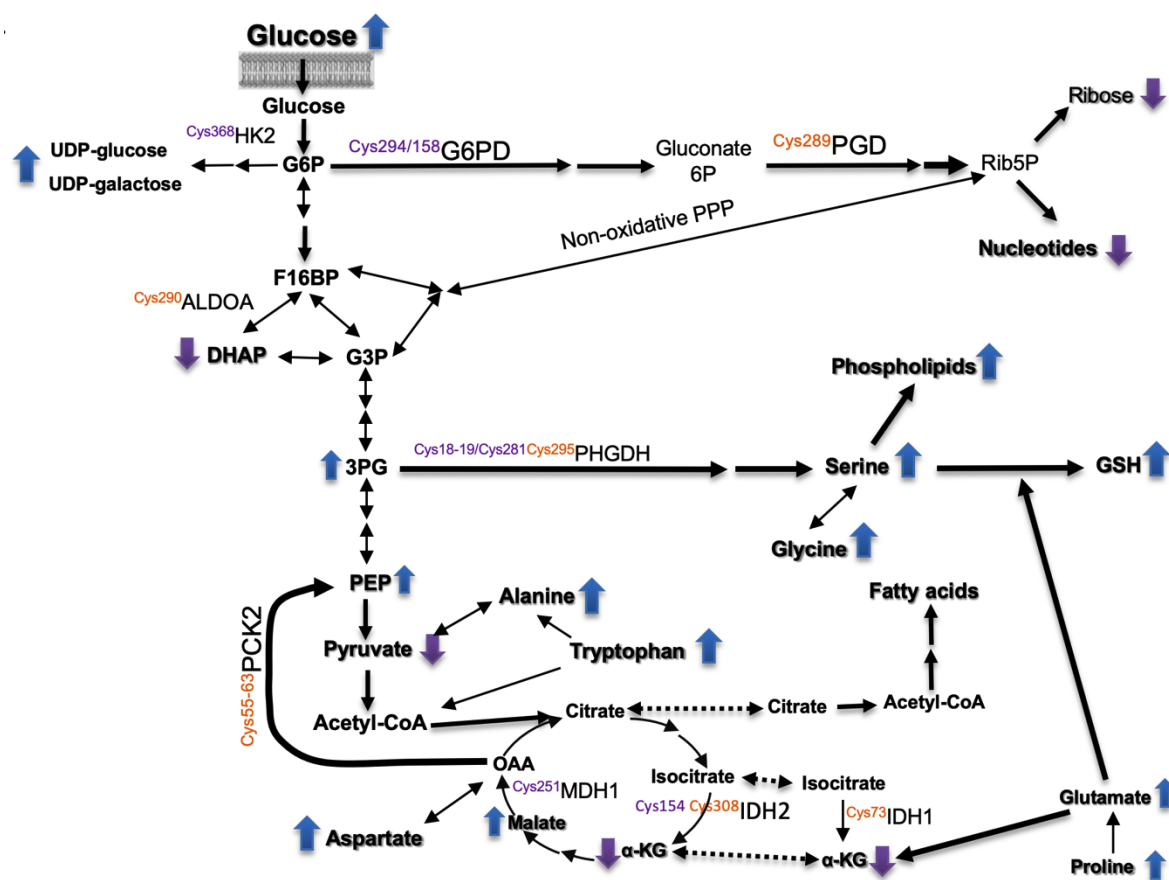
There was an overall decrease in metabolites of the purine and pyrimidine metabolism subfamilies, with the exception of adenosine, inosine, and hypoxanthine upon Prdx6 silencing. These results are indicative of diminished nucleotide biosynthetic activity and activation of adenine catabolism, although urate was not detected.

3.3.3. Other Metabolites

Several metabolites of the glutathione metabolism subfamily were elevated in siRNA-Prdx6 treated cells likely as a consequence of glutathione demand in the face of diminished antioxidant defenses. A conspicuous increase of the Glutamate and Serine, Threonine, and Glycine pathways was also detected at metabolome level reinforcing the idea of metabolic pathways converging on glutathione synthesis.

Regarding carbon metabolism (Figure 2B), treatment of HepG2 cells with siRNA-Prdx6 lowered dihydroxyacetone-phosphate (DHAP), pyruvate, ribose, and 2-oxoglutarate (α KG) levels whereas extracellular glucose (Figure 2D), phosphoenol-pyruvate (PEP), 3-phosphoglycerate (3-PG), sedoheptulose-7-phosphate (Shu7P), malate, aspartate, and serine increased. These changes are compatible with reduced import of glucose and diminished flow through the upper glycolytic pathway, the non-oxidative part of the Pentose-phosphate pathway (PPP) and the nucleotide biosynthetic pathway. In the lower part of the pathway a predominant gluconeogenic flow from

aminoacids with diversion at 3-PG toward serine and other biosynthetic pathways thereon would be taking place (Scheme 1).



Scheme 1. Overview of metabolic pathways affected by Prdx6 down-regulation. Relative levels of metabolites and thiol redox changes in enzymes in siRNA-Prdx6 treated HepG2 cells. Up and down arrows indicate increased or decreased levels, respectively. Mapped redox sensitive Cys showing a differential redox state (oxidative purple; reductive, orange). See main text for detailed explanation.

Changes detected in the redox proteome could be relevant to these metabolic set up, since glucose-6-phosphate and 6-phosphogluconate dehydrogenases (G6PD and PGD), aldolase (ALDOA), hexokinase (HK2), malate dehydrogenase (MDH1), PEP carboxykinase (PCK2), and 3-phosphoglycerate dehydrogenase (PHGDH) showed redox changes at specific Cys residues that could affect their catalytic performance (highlighted in Scheme 1 and commented below).

3.4. Changes at Proteome Level

The extent of down-regulation of Prdx6 under our experimental conditions was not incisive enough to provoke extensive changes at global proteome level through transcriptional regulation, but had a marked effect at posttranslational level as observed by changes in the redox proteome.

3.4.1. Global Proteome

As a proof of concept, the quantitative global proteomic analysis (Supplementary File S1) detected 0.5-fold Prdx6 down-regulation in silenced cells. The number of differentially expressed proteins after siRNA-Prdx6 treatment was rather low. However, a group of differential proteins on Prdx6 silencing were significantly enriched in endocytosis (GO:0030100 term and hsa04144 KEGG pathway): the ADP-ribosylating factor GTPase-activating protein (ARFGAP1) involved in membrane trafficking was up-regulated while vacuolar protein sorting-associated protein 4B

(VPS4P) and 4 members of Ras-related proteins (RAB5A, RAB5B, RAB7A and RAB11A) were down-regulated (Supplementary File S1).

These data run parallel to increased phospholipid content and demonstrate that Prdx6 is involved in membrane arrangement and vesicle trafficking, but it remains to be determined which activity of Prdx6, either the peroxidase, the PLA2, the LPAT, or a combination of these, is responsible for this role.

3.4.2. Redox Proteome

Down-regulation of Prdx6 should be expected to alter the redox homeostasis by diminution of its antioxidant capacity, so we analyzed the Redox Proteome, namely, the set of proteins undergoing redox changes at sensitive cysteines on siRNA-Prdx6 treatment in HepG2 cells. A large set of nearly one thousand cysteinyl peptides were detected (Supplementary File S2). We selected those differential Cys-peptides with statistical significance ($p < 0.05$) and > 1.5 -fold or < 0.6 -fold change in their Cys reduced/oxidized ratio. The main changes were detected in enzymes of carbon and glutathione metabolism, pentose phosphate pathway, citrate cycle, fatty acid metabolism, biosynthesis of aminoacids, and Glycolysis/Gluconeogenesis.

A significant redox target was Hexokinase-2 (HK2) at Cys368, that was half reduced in HepG2 cells but was reversibly oxidized after siRNA-Prdx6 treatment (Table 1). HK2 is known to play a critical role in the connection between metabolic and cell survival pathways and is upregulated in hepatocellular carcinoma and other tumors [46,47]. HK2 associates with the outer mitochondrial membrane via a binding motif at the N-terminal that interacts with voltage dependent anion channel (VDAC).

Table 1. Reversible thiol redox changes in specific sensitive Cys.

	siRNA Prdx6	HK2-Cys ³⁶⁸	Prdx6-Cys ⁹¹	PHGDH-Cys ¹⁸⁻¹⁹
	–	0.58	1.78	10.43
Ratio red/ox ± sd (n = 4)		± 0.04	± 0.33	± 2.75
	+	0.26	0.92	4.98
		± 0.03	± 0.06	± 1.98
Fold Change		0.45	0.52	0.48
<i>p</i> -value		1.6×10^{-5}	2.2×10^{-2}	2×10^{-4}

The reduced/oxidized ratio of specific cysteines in three proteins, specifically discussed in the main text, suffering reversible redox changes upon Prdx6 silencing as determined by the quantitative redox proteome protocol described in Materials and Methods. The ratio values (\pm s.d.; $n = 4$) are shown and the fold change provoked by Prdx6 silencing is also indicated together with the statistical significance index (*p*-value) for HepG2 cells.

This association provides a metabolic advantage by bringing HK2 closer to the ATP production site, and an apoptosis suppressive capacity by competing with proapoptotic factors for the binding to VDAC [48]. Cys368 occupies a central position in the VDAC-HK contact area [49] (Figure 3A) and it is conceivable that its oxidative modification on siRNA-Prdx6 treatment could have altered its interaction with VDAC, affecting its subcellular localization and inducing a decrease in the rate of glucose phosphorylation and entry into the cell.

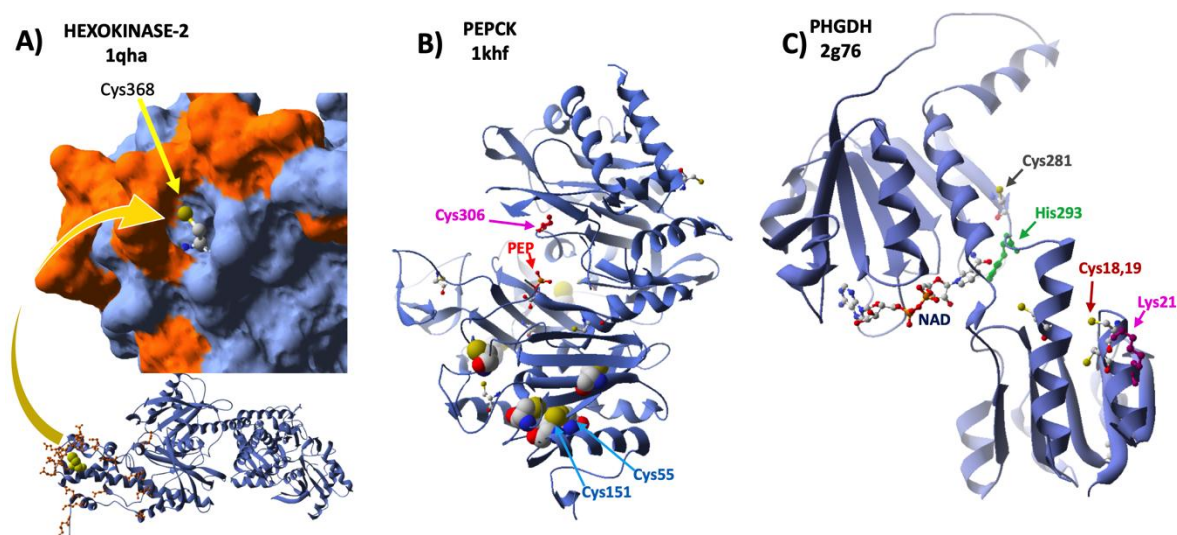


Figure 3. Structural mapping of redox sensitive Cys. The 3D structures of three enzymes of carbohydrate metabolism, HK2, PCK, and PHGDH, with the indicated PDB ID codes, were analyzed to map the Cys residues that showed significant redox changes upon Prdx6 silencing in HepG2 cells. (A) One subunit of HK2 is shown below in a ribbon model with Cys368 atoms as yellow Van der Waals spheres and sidechains of residues involved in interaction contacts with VDAC1 highlighted in orange; the C-terminus is enlarged in molecular surface mode, except for Cys368, with the same highlighting criterium as below. (B) PCK in ribbon mode and detected Cys residues with atoms as Van der Waals spheres, color CPK; one molecule of substrate PEP (red) is bound at the active site; the positions of Cys306, Cys55 and Cys151 are indicated with arrows. (C) PHGDH in ribbon cartoon with the coenzyme NAD bound at the active site cleft; sidechains of redox modified Cys residues upon Prdx6 silencing are shown in CPK color; acetylation and sumoylation sensitive Lys21 is shown in purple next to redox sensitive Cys18-Cys19; catalytic His283 is shown in green with the redox sensitive Cys281 in the neighborhood.

Prdx6 was abundant enough to be clearly detected (24 peptides) even in silenced cells (Supplementary Files S1 and S2). The peptide containing the “non-catalytic” Cys91 was prominent and showed sensitivity to reversible oxidation, as it was fairly reduced in HepG2 cells but was significantly more oxidized after siRNA-Prdx6 treatment (Table 1). The peptide containing its catalytic peroxidatic Cys47 did not show significant reversible redox changes (See data in Supplementary File S2). The “extra” Cys91 is not conserved among members of the 1-Cys subfamily of Prx and has been thoroughly neglected or routinely substituted by Ser in the recombinant protein and other experimental setups. However, we have found that Cys91 of human Prdx6 was specifically sensitive to reversible oxidation in glutaredoxin 1 (Grx1) down-regulated HepG2 cells and had shown that it is prone to glutathionylation in recombinant Prdx6 [28]. Experiments are under way to elucidate whether this “extra” Cys in human Prdx6 is relevant to its structure and function in the context of redox signaling.

Silencing of Prdx6 in HepG2 cells led to redox changes in Cys191 of the intracellular chloride ion channel-1 (CLIC1). This is a soluble globular protein that can undergo an extended conformational change to get embedded in intracellular membranes, mainly in the nucleus, and form a Cl⁻ ion channel that has been linked to apoptosis, pH, cell volume and cell cycle regulation [50,51]. The soluble form of CLIC1 consist of two domains, the N-terminal one with a thioredoxin fold similar to glutaredoxin and the C-terminal typical of the GST superfamily; it also contains a glutathione binding site [52]. These properties of CLIC1 suggested that it may be under some kind of redox control. Cys191, which is located in the GST domain of CLIC1, was more reduced in siRNA-Prdx6 treated cells (See data in Supplementary File S2). Coincidentally, Prdx6 interacts with GST- π during the peroxidase catalytic cycle [53]. It is tempting to hypothesize on a possible redox

relationship between Prdx6 and CLIC1 contributing to the effects of Prdx6 silencing on cell swelling and cell cycle arrest described above.

Redox changes in two enzymes of the Glycolysis/gluconeogenesis pathway are worth of mention. Eight cysteines were detected out of a total of 12 in the sequence of mitochondrial PEP-carboxykinase (PCK2), which is composed of two large domains, with the active site in between, that move relative to each other during the catalytic cycle. Of these Cys, seven are clustered in the C-terminal domain (Figure 3B), but only the peptide containing Cys55 and Cys63, conserved in eukaryotes, showed significant redox changes. Cys55 could form a disulfide bond with Cys151, which would be $\approx 3\text{\AA}$ apart. The enzyme is inactivated by glutathionylation of Cys306, which is close to the active site, in a way reversed by SH2 [54]. We have detected this cysteine in all the samples in a highly reduced state (red/ox >20) insensitive to Prdx6 silencing, allowing for full activity (Supplementary File S2).

3-phosphoglycerate dehydrogenase (PHGDH) plays a critical role in a relevant metabolic diversion of Glycolysis that leads to serine, a precursor of proteins, phospholipid head groups and glutathione and driving force for the folate and methionine cycles [55]. Its gene is overexpressed in several types of cancers, where it can catalyze the reduction of 2-oxo-glutarate to 2-hydroxyglutarate, a potent oncometabolite [56]. In the current study, we have found several redox sensitive Cys in PHDH all of which are in a highly reduced state (red/ox ratios ≈ 5 -30). However, Cys281 and the peptide containing contiguous Cys18Cys19, three Cys conserved in mammals, were significantly less reduced under conditions of Prdx6 silencing in HepG2 cells (Table 1 and Supplementary File S2). Cys281, which was identified as a target for S-nitrosation in a high-throughput study [57], is in the NAD-binding catalytic domain, close to the essential active site residue His293, while Cys18Cys19 are located in the so called allosteric regulatory domain in close proximity to Lys21 (Figure 3C), which is a target for acetylation and sumoylation [58]. Reversible redox changes in these sensitive Cys of the enzyme could affect its catalytic and regulatory properties [59].

4. Conclusions

The complex wide effects of moderate Prdx6 down-regulation should be a reflection of its moonlighting properties acting as peroxidase, phospholipase, and LPC-acyltransferase. The response of HepG2 cells to Prdx6 silencing spans from metabolic and signaling pathways remodeling to alterations in the redox proteome and membrane turnover with effects in cell cycle progression and proliferation. The role of Prdx6 in cancer cells has been studied previously with conflicting outcomes. Most reports point to a pro-proliferating and antiapoptotic action of Prdx6, but some studies have found the opposite effect, depending on the stage of tumor development. Moreover, these effects have not always been assigned to a particular activity of Prdx6, either peroxidase, PLA2, or LPCAT, neither a common mechanism has been provided.

In the study reported herein Prdx6 silencing down to $\approx 40\%$ would represent a situation mimicking a cellular response to endogenous or exogenous stimuli under normal or oxidative stress conditions.

It appears that the cell responds to Prdx6 down-regulation by initiating a biosynthetic program, leading to membrane and vesicle trafficking rearrangement with signs of entering a cell cycle G1 phase but an inability to proceed on to the S phase. The mechanisms behind these phenomena involve reversible thiol oxidative changes in key proteins. HK2-Cys368 and Prdx6 "extra" Cys91 stand out as relevant thiol switches. The former could affect association with the mitochondrial membrane with consequences on the rate of glucose catabolism and mitochondrial permeability; the latter is not conserved among the 1-Cys type Peroxiredoxins and has been given little attention so far, but could turn out to bear relevant functions in human cells.

Supplementary Materials: The following are available online at www.mdpi.com/xxx/s1; Supplementary File 1: Excel file showing results of global quantitative proteomic analysis in Prdx6 silenced HepG2 cells. The first sheet shows protein ID, protein name, gene name and number of unique peptides in the first columns. NT and siRNA-Prdx6 indicate treatment with unspecific "non-target" siRNA and with specific siRNA, respectively.

Columns M and N with blue colored headings show the calculated fold change induced by siRNA-Prdx6 treatment together with the statistical significance index (p value). Statistically significant data have been selected and disclosed into the second sheet with the fold change colored green and red for down- and up-regulated values, respectively. The sheets named “GOTERM_Enrichment” and “KEGG_Enrichment” show the results of “Biological Process GO-term” and “KEGG pathway” enrichment analysis of the set of differentially expressed proteins on siRNA-Prdx6 treatment; Supplementary File 2: Excel file showing results of cysteinyl peptides proteomic quantitative analysis of in Prdx6 silenced HepG2 cells. The peptide sequence, accession ID and protein name are shown in the first columns. NT and siRNA-Prdx6 indicate treatment with unspecific “non-target” siRNA and with specific siRNA, respectively. The data in columns D to K are the reduced/oxidized ratio values for each of 4 replicas for every Cys-peptide; NA, data not available. Columns L and M, colored orange show the fold change of the red/ox ratio induced by siRNA-Prdx6 treatment together with the statistical p value for significance. The second sheet with the fold change colored green and red for down- and up-regulated values, respectively shows the selected significant fold change values (column E) induced by Prdx6 silencing ordered by increasing p-values (column F); the position of the Cys residue in the sequence of the protein is given in column D and a horizontal double red line marks the statistical threshold for significance; Supplementary File 3: Excel file showing results of metabolomic analysis in Prdx6 silenced HepG2 cells. Columns A and B show the metabolite family and the name of the metabolite, respectively. The data show the normalized quantitative values for each metabolite in each of 4 replicas for the treatment with unspecific siRNA (NT) and siRNA-Prdx6. NA, missing or outlier value. The fold change induced by Prdx6 silencing is shown in column K, together with the statistical p-value for significance, with values <0.05 highlighted in yellow.

Author Contributions: Formal analysis, M.J.L.-G., D.J.L., J.P., B.M. and R.R.-A.; Funding acquisition, C.A.P.; Investigation, M.J.L.-G., R.M.T. and B.C.-H.; Methodology, M.J.L.-G., R.M.T., B.C.-H., D.J.L. and J.P.; Resources, B.M.; Supervision, J.A.B., C.A.P., B.M. and R.R.-A; Writing – review & editing, J.A.B. and C.A.P..

Funding: This research has been financed by grants from the Spanish Ministry of Economy and Competitiveness (BFU2016-80006-P) and the Andalusian Government (Consejería de Economía, Innovación, Ciencia y Empleo, BIO-0216). BC-H and RMT have been financed by Programa de Empleo Joven, FEDER/Junta de Andalucía, EJI17-BIO216 and EJI-17-BIO216, respectively. D.J.L. is recipient of a predoctoral fellowship Mod. 6.2-2018 from the University of Córdoba.

Acknowledgments: Technical support by the staff of the Proteomics facility, Central Service for Research Support (SCAI) at the University of Cordoba, is acknowledged.

Conflicts of Interest: “The authors declare no conflict of interest”.

References

1. Soito, L.; Williamson, C.; Knutson, S.T.; Fetrow, J.S.; Poole, L.B.; Nelson, K.J. PREX: PeroxiRedoxin classification indEX, a database of subfamily assignments across the diverse peroxiredoxin family. *Nucleic Acids Res* **2010**, *39*, D332–D337.
2. Chen, J.W.; Dodia, C.; Feinstein, S.I.; Jain, M.K.; Fisher, A.B. 1-Cys peroxiredoxin, a bifunctional enzyme with glutathione peroxidase and phospholipase A2 activities. *J. Biol. Chem.* **2000**, *275*, 28421–28427.
3. Manevich, Y.; Sweitzer, T.; Pak, J.H.; Feinstein, S.I.; Muzykantov, V.; Fisher, A.B. 1-Cys peroxiredoxin overexpression protects cells against phospholipid peroxidation-mediated membrane damage. *Proc. Natl. Acad. Sci. USA* **2002**, *99*, 11599–11604.
4. Pedrajas, J.R.; McDonagh, B.; Hernández-Torres, F.; Miranda-Vizueté, A.; González-Ojeda, R.; Martínez-Galisteo, E.; Padilla, C.A.; Bárcena, J.A. Glutathione Is the Resolving Thiol for Thioredoxin Peroxidase Activity of 1-Cys Peroxiredoxin Without Being Consumed During the Catalytic Cycle. *Antioxid. Redox Signal.* **2016**, *24*, 115–128.
5. Pedrajas, J.R.; Padilla, C.A.; McDonagh, B.; Bárcena, J.A. Glutaredoxin participates in the reduction of peroxides by the mitochondrial 1-CYS peroxiredoxin in *Saccharomyces cerevisiae*. *Antioxid. Redox Signal.* **2010**, *13*, 249–258.
6. Hall, A.; Karplus, P.A.; Poole, L.B. Typical 2-Cys peroxiredoxins—Structures, mechanisms and functions. *FEBS J.* **2009**, *276*, 2469–2477.
7. Stöcker, S.; Maurer, M.; Ruppert, T.; Dick, T.P. A role for 2-Cys peroxiredoxins in facilitating cytosolic protein thiol oxidation. *Nat. Chem. Biol.* **2018**, *14*, 148–155.
8. Fisher, A.B. Peroxiredoxin 6: A bifunctional enzyme with glutathione peroxidase and phospholipase A2

- activities. *Antioxid. Redox Signal.* **2011**, *15*, 831–844.
9. Fisher, A.B.; Dodia, C.; Sorokina, E.M.; Li, H.; Zhou, S.; Raabe, T.; Feinstein, S.I. A novel lysophosphatidylcholine acyl transferase activity is expressed by peroxiredoxin 6. *J. Lipid Res.* **2016**, *57*, 587–596.
 10. Fisher, A.B. Peroxiredoxin 6 in the repair of peroxidized cell membranes and cell signaling. *Arch. Biochem Biophys.* **2017**, *617*, 68–83.
 11. Chatterjee, S.; Feinstein, S.I.; Dodia, C.; Sorokina, E.; Lien, Y.-C.; Nguyen, S.; Debolt, K.; Speicher, D.; Fisher, A.B. Peroxiredoxin 6 phosphorylation and subsequent phospholipase A2 activity are required for agonist-mediated activation of NADPH oxidase in mouse pulmonary microvascular endothelium and alveolar macrophages. *J. Biol. Chem.* **2011**, *286*, 11696–11706.
 12. Kim, S.Y.; Jo, H.-Y.; Kim, M.H.; Cha, Y.-Y.; Choi, S.W.; Shim, J.-H.; Kim, T.J.; Lee, K.-Y. H₂O₂-dependent hyperoxidation of peroxiredoxin 6 (Prdx6) plays a role in cellular toxicity via up-regulation of iPLA2 activity. *J. Biol. Chem.* **2008**, *283*, 33563–33568.
 13. Zhou, S.; Dodia, C.; Feinstein, S.; Harper, S.; Forman, H.; Speicher, D.; Fisher, A. Oxidation of Peroxiredoxin 6 in the Presence of GSH Increases its Phospholipase A2 Activity at Cytoplasmic pH. *Antioxidants* **2019**, *8*, 4–14.
 14. Sorokina, E.M.; Feinstein, S.I.; Zhou, S.; Fisher, A.B. Intracellular targeting of peroxiredoxin 6 to lysosomal organelles requires MAPK activity and binding to 14-3-3 ϵ . *Am. J. Physiol. Cell Physiol.* **2011**, *300*, 1430–1441.
 15. Ma, S.; Zhang, X.; Zheng, L.; Li, Z.; Zhao, X.; Lai, W.; Shen, H.; Lv, J.; Yang, G.; Wang, Q., et al. Peroxiredoxin 6 Is a Crucial Factor in the Initial Step of Mitochondrial Clearance and Is Upstream of the PINK1-Parkin Pathway. *Antioxid. Redox Signal.* **2016**, *24*, 486–501.
 16. Ambruso, D.R.; Ellison, M.A.; Thurman, G.W.; Leto, T.L. Peroxiredoxin 6 translocates to the plasma membrane during neutrophil activation and is required for optimal NADPH oxidase activity. *BBA Mol. Cell Res.* **2012**, *1823*, 306–315.
 17. Pacifici, F.; Della-Morte, D.; Capuani, B.; Pastore, D.; Bellia, A.; Sbraccia, P.; Di Daniele, N.; Lauro, R.; Lauro, D. Peroxiredoxin6, a Multitask Antioxidant Enzyme Involved in the Pathophysiology of Chronic Noncommunicable Diseases. *Antioxid. Redox Signal.* **2019**, *30*, 399–414.
 18. Arevalo, J.; Vázquez-Medina, J. The Role of Peroxiredoxin 6 in Cell Signaling. *Antioxidants* **2018**, *7*, 172–212.
 19. Yun, H.-M.; Park, K.-R.; Lee, H.P.; Lee, D.H.; Jo, M.; Shin, D.H.; Yoon, D.Y.; Han, S.B.; Hong, J.T. PRDX6 promotes lung tumor progression via its GPx and iPLA2 activities. *Free Radic. Biol. Med.* **2014**, *69*, 367–376.
 20. Yun, H.-M.; Choi, D.Y.; Oh, K.-W.; Hong, J.T. PRDX6 Exacerbates Dopaminergic Neurodegeneration in a MPTP Mouse Model of Parkinson's Disease. *Mol. Neurobiol.* **2015**, *52*, 422–431.
 21. Anwar, S.; Yanai, T.; Sakai, H. Overexpression of Peroxiredoxin 6 Protects Neoplastic Cells against Apoptosis in Canine Haemangiosarcoma. *J. Comp. Pathol.* **2016**, *155*, 29–39.
 22. Pak, J.H.; Choi, W.H.; Lee, H.M.; Joo, W.-D.; Kim, J.-H.; Kim, Y.-T.; Kim, Y.-M.; Nam, J.-H. Peroxiredoxin 6 Overexpression Attenuates Cisplatin-Induced Apoptosis in Human Ovarian Cancer Cells. *Cancer Investig.* **2010**, *29*, 21–28.
 23. Yun, H.-M.; Park, K.-R.; Park, M.H.; Kim, D.H.; Jo, M.R.; Kim, J.Y.; Kim, E.-C.; Do Young Yoon Han, S.B.; Hong, J.T. PRDX6 promotes tumor development via the JAK2/STAT3 pathway in a urethane-induced lung tumor model. *Free Radic. Biol. Med.* **2015**, *80*, 136–144.
 24. Rolfs, F.; Huber, M.; Gruber, F.; Böhm, F.; Pfister, H.J.; Bochkov, V.N.; Tschachler, E.; Dummer, R.; Hohl, D.; Schäfer, M.; et al. Dual role of the antioxidant enzyme peroxiredoxin 6 in skin carcinogenesis. *Cancer Res.* **2013**, *73*, 3460–3469.
 25. Ho, J.-N.; Lee, S.B.; Lee, S.-S.; Yoon, S.H.; Kang, G.Y.; Hwang, S.-G.; Um, H.-D. Phospholipase A2 activity of peroxiredoxin 6 promotes invasion and metastasis of lung cancer cells. *Mol. Cancer Ther.* **2010**, *9*, 825–832.
 26. Schmitt, A.; Schmitz, W.; Hufnagel, A.; Scharl, M.; Meierjohann, S. Peroxiredoxin 6 triggers melanoma cell growth by increasing arachidonic acid-dependent lipid signalling. *Biochem. J.* **2015**, *471*, 267–279.
 27. Vázquez-Medina, J.P.; Dodia, C.; Weng, L.; Mesaros, C.; Blair, I.A.; Feinstein, S.I.; Chatterjee, S.; Fisher, A.B. The phospholipase A2 activity of peroxiredoxin 6 modulates NADPH oxidase 2 activation via lysophosphatidic acid receptor signaling in the pulmonary endothelium and alveolar macrophages.

- FASEB J.* **2016**, *30*, 2885–2898.
28. López-Grueso, M.J.; González-Ojeda, R.; Requejo-Aguilar, R.; McDonagh, B.; Fuentes-Almagro, C.A.; Muntané, J.; Bárcena, J.A.; Padilla, C.A. Thioredoxin and glutaredoxin regulate metabolism through different multiplex thiol switches. *Redox Biol.* **2019**, *21*, 101049.
 29. Rueden, C.T.; Schindelin, J.; Hiner, M.C.; DeZonia, B.E.; Walter, A.E.; Arena, E.T.; Eliceiri, K.W. ImageJ2: ImageJ for the next generation of scientific image data. *BMC Bioinform.* **2017**, *18*, 529.
 30. Schattauer, S.S.; Land, B.B.; Reichard, K.L.; Abraham, A.D.; Burgeno, L.M.; Kuhar, J.R.; Phillips, P.E.M.; Ong, S.E.; Chavkin, C. Peroxiredoxin 6 mediates Gai protein-coupled receptor inactivation by cJN kinase. *Nat. Commun.* **2017**, *8*, 743, doi:10.1038/s41467-017-00791-2.
 31. Wu, Y.; Feinstein, S.I.; Manevich, Y.; Chowdhury, I.; Pak, J.H.; Kazi, A.; Dodia, C.; Speicher, D.W.; Fisher, A.B. Mitogen-activated protein kinase-mediated phosphorylation of peroxiredoxin 6 regulates its phospholipase A2 activity. *Biochem. J.* **2009**, *419*, 669–679.
 32. Cox, J.; Mann, M. MaxQuant enables high peptide identification rates, individualized p.p.b.-range mass accuracies and proteome-wide protein quantification. *Nat. Biotechnol.* **2008**, *26*, 1367–1372.
 33. MacLean, B.; Tomazela, D.M.; Shulman, N.; Chambers, M.; Finney, G.L.; Frewen, B.; Kern, R.; Tabb, D.L.; Liebler, D.C.; MacCoss, M.J. Skyline: An open source document editor for creating and analyzing targeted proteomics experiments. *Bioinformatics* **2010**, *26*, 966–968.
 34. Storey, J.D.; Tibshirani, R. Statistical significance for genomewide studies. *Proc. Natl. Acad. Sci. USA* **2003**, *100*, 9440–9445.
 35. Peter, M.E.; Hadji, A.; Murmann, A.E.; Brockway, S.; Putzbach, W.; Pattanayak, A.; Ceppi, P. The role of CD95 and CD95 ligand in cancer. *Cell Death Differ.* **2015**, *22*, 549–559.
 36. Zhang, Y.; Liu, Q.; Zhang, M.; Yu, Y.; Liu, X.; Cao, X. Fas signal promotes lung cancer growth by recruiting myeloid-derived suppressor cells via cancer cell-derived PGE2. *J. Immunol.* **2009**, *182*, 3801–3808.
 37. Teodorczyk, M.; Kleber, S.; Wollny, D.; Sefrin, J.P.; Aykut, B.; Mateos, A.; Herhaus, P.; Sancho-Martinez, I.; Hill, O.; Gieffers, C.; et al. CD95 promotes metastatic spread via Sck in pancreatic ductal adenocarcinoma. *Cell Death Differ.* **2015**, *22*, 1192–1202.
 38. Jackowski, S. Cell cycle regulation of membrane phospholipid metabolism. *J. Biol. Chem.* **1996**, *271*, 20219–20222.
 39. Ridgway, N.D. The role of phosphatidylcholine and choline metabolites to cell proliferation and survival. *Crit. Rev. Biochem. Mol. Biol.* **2013**, *48*, 20–38.
 40. Poursharifi, P.; Madiraju, S.R.M.; Prentki, M. Monoacylglycerol signalling and ABHD6 in health and disease. *Diabetes Obes. Metab.* **2017**, *19*, 76–89.
 41. Brown, N.F.; Mullur, R.S.; Subramanian, I.; Esser, V.; Bennett, M.J.; Saudubray, J.M.; Feigenbaum, A.S.; Kobari, J.A.; Macleod, P.M.; McGarry, J.D.; et al. Molecular characterization of L-CPT I deficiency in six patients: Insights into function of the native enzyme. *J. Lipid Res.* **2001**, *42*, 1134–1142.
 42. Kim, T.S.; Sundaresh, C.S.; Feinstein, S.I.; Dodia, C.; Skach, W.R.; Jain, M.K.; Nagase, T.; Seki, N.; Ishikawa, K.; Nomura, N.; et al. Identification of a human cDNA clone for lysosomal type Ca²⁺-independent phospholipase A2 and properties of the expressed protein. *J. Biol. Chem.* **1997**, *272*, 2542–2550.
 43. Akiba, S.; Dodia, C.; Chen, X.; Fisher, A.B. Characterization of acidic Ca²⁺-independent phospholipase A2 of bovine lung. *Comp. Biochem. Physiol. B Biochem. Mol. Biol.* **1998**, *120*, 393–404.
 44. Kim, S.Y.; Chun, E.; Lee, K.Y. Phospholipase A2 of peroxiredoxin 6 has a critical role in tumor necrosis factor-induced apoptosis. *Cell Death Differ.* **2011**, *18*, 1573–1583.
 45. Casero, R.A.; Murray Stewart, T.; Pegg, A.E. Polyamine metabolism and cancer: Treatments, challenges and opportunities. *Nat. Rev. Cancer* **2018**, *18*, 681–695.
 46. Kwee, S.A.; Hernandez, B.; Chan, O.; Wong, L. Choline Kinase Alpha and Hexokinase-2 Protein Expression in Hepatocellular Carcinoma: Association with Survival. *PLoS ONE* **2012**, *7*, e46591-8.
 47. Roberts, D.J.; Miyamoto, S. Hexokinase II integrates energy metabolism and cellular protection: Acting on mitochondria and TORCing to autophagy. *Cell Death Differ.* **2014**, *22*, 248–257.
 48. Abu-Hamad, S.; Zaid, H.; Israelson, A.; Nahon, E.; Shoshan-Barmatz, V. Hexokinase-I protection against apoptotic cell death is mediated via interaction with the voltage-dependent anion channel-1: Mapping the site of binding. *J. Biol. Chem.* **2008**, *283*, 13482–13490.
 49. Rosano, C. Molecular model of hexokinase binding to the outer mitochondrial membrane porin

- (VDAC1): Implication for the design of new cancer therapies. *Mitochondrion* **2011**, *11*, 513–519.
50. Valenzuela, S.M.; Martin, D.K.; Por, S.B.; Robbins, J.M.; Warton, K.; Bootcov, M.R.; Schofield, P.R.; Campbell, T.J.; Breit, S.N. Molecular cloning and expression of a chloride ion channel of cell nuclei. *J. Biol. Chem.* **1997**, *272*, 12575–12582.
 51. Valenzuela, S.M.; Mazzanti, M.; Tonini, R.; Qiu, M.R.; Warton, K.; Musgrove, E.A.; Campbell, T.J.; Breit, S.N. The nuclear chloride ion channel NCC27 is involved in regulation of the cell cycle. *J. Physiol. (Lond.)* **2000**, *529*, 541–552.
 52. Littler, D.R.; Harrop, S.J.; Fairlie, W.D.; Brown, L.J.; Pankhurst, G.J.; Pankhurst, S.; DeMaere, M.Z.; Campbell, T.J.; Bauskin, A.R.; Tonini, R.; et al. The Intracellular Chloride Ion Channel Protein CLIC1 Undergoes a Redox-controlled Structural Transition. *J. Biol. Chem.* **2004**, *279*, 9298–9305.
 53. Manevich, Y.; Feinstein, S.I.; Fisher, A.B. Activation of the antioxidant enzyme 1-CYS peroxiredoxin requires glutathionylation mediated by heterodimerization with pi GST. *Proc. Natl. Acad. Sci. USA* **2004**, *101*, 3780–3785.
 54. Gao, X.-H.; Li, L.; Parisien, M.; Mcleod, M.; Wu, J.; Bederman, I.; Gao, Z.; Krokowski, D.; Chirieleison, S.M.; Diatchenko, L.; et al. Discovery of a redox-thiol switch regulating cellular energy metabolism. *bioRxiv* **2019**, bioRxiv:520411, doi:10.1101/520411.
 55. Locasale, J.W. Serine, glycine and one-carbon units: Cancer metabolism in full circle. *Nat. Rev. Cancer* **2013**, *13*, 572–583.
 56. Fan, J.; Teng, X.; Liu, L.; Mattaini, K.R.; Looper, R.E.; Vander Heiden, M.G.; Rabinowitz, J.D. Human phosphoglycerate dehydrogenase produces the oncometabolite D-2-hydroxyglutarate. *ACS Chem. Biol.* **2015**, *10*, 510–516.
 57. Doulias, P.-T.; Tenopoulou, M.; Greene, J.L.; Raju, K.; Ischiropoulos, H. Nitric oxide regulates mitochondrial fatty acid metabolism through reversible protein S-nitrosylation. *Sci. Signal.* **2013**, *6*, rs1.
 58. Impens, F.; Radoshevich, L.; Cossart, P.; Ribet, D. Mapping of SUMO sites and analysis of SUMOylation changes induced by external stimuli. *Proc. Natl. Acad. Sci. USA* **2014**, *111*, 12432–12437.
 59. Grant, G.A. Contrasting catalytic and allosteric mechanisms for phosphoglycerate dehydrogenases. *Arch. Biochem. Biophys.* **2012**, *519*, 175–185.



© 2019 by the authors. Submitted for possible open access publication under the terms and conditions of the Creative Commons Attribution (CC BY) license (<http://creativecommons.org/licenses/by/4.0/>).

ARTICLE 3

Thioredoxin Downregulation enhances Sorafenib Effects in Hepatocarcinoma Cells. **María José López-Grueso**, *Raúl González, Jordi Muntané, José Antonio Bárcena**, and *C. Alicia Padilla*. **Antioxidants** 8 (2019) 501

DOI: 10.3390/antiox8100501



Article

Thioredoxin Downregulation Enhances Sorafenib Effects in Hepatocarcinoma Cells

María José López-Grueso ¹, Raúl González ², Jordi Muntané ^{2,3,4}, José Antonio Bárcena ^{1,5,*} and C. Alicia Padilla ^{1,5}

¹ Department of Biochemistry and Molecular Biology, University of Córdoba, 14071 Córdoba, Spain; q02logrm@uco.es (M.J.L.-G.); bb1papec@uco.es (C.A.P.)

² Institute of Biomedicine of Seville (IBiS), Hospital University “Virgen del Rocío”/CSIC/University of Seville, 41013 Sevilla, Spain; b62goojr@uco.es (R.G.); jmuntane-ibis@us.es (J.M.)

³ Departamento de Cirugía General, Hospital Universitario Virgen del Rocío/Instituto de Biomedicina de Sevilla (IBiS)/CSIC/Universidad de Sevilla, 41013 Sevilla, Spain

⁴ Centro de Investigación Biomédica en Red de Enfermedades Hepáticas y Digestivas (CIBERehd), 41013 Sevilla, Spain

⁵ Instituto Maimónides de Investigación Biomédica de Córdoba (IMIBIC), 14004 Córdoba, Spain

* Correspondence: bb1barua@uco.es

Received: 11 September 2019; Accepted: 21 October 2019; Published: 22 October 2019



Abstract: Sorafenib is the first-line recommended therapy for patients with advanced hepatocarcinoma (HCC) in de-differentiation stage (presenting epithelial–mesenchymal transition, EMT). We studied the role of the thioredoxin system (Trx1/TrxR1) in the sensitivity or resistance of HCC cells to the treatment with Sorafenib. As a model, we used a set of three established HCC cell lines with different degrees of de-differentiation as occurs in metastasis. By quantitative proteomics, we found that the expression levels of Trx1 and TrxR1 followed the same trend as canonical EMT markers in these cell lines. Treatment with Sorafenib induced thiol redox reductive changes in critical elements of oncogenic pathways in all three cell lines but induced drastic proteome reprogramming only in HCC cell lines of intermediate stage. Trx1 downregulation counteracted the thiol reductive effect of Sorafenib on Signal Transducer and Activator of Transcription 3 (STAT3) but not on Mitogen-Activated Protein Kinase (MAPK) or Protein Kinase B (Akt) and transformed advanced HCC cells into Sorafenib-sensitive cells. Ten targets of the combined Sorafenib–siRNA^{Trx1} treatment were identified that showed a gradually changing expression trend in parallel to changes in the expression of canonical EMT markers, likely as a result of the activation of Hippo signaling. These findings support the idea that a combination of Sorafenib with thioredoxin inhibitors should be taken into account in the design of therapies against advanced HCC.

Keywords: hepatocarcinoma; thioredoxin; sorafenib; redox signaling; EMT

1. Introduction

Hepatocarcinoma (HCC) represents 80% of the primary hepatic neoplasms that appear mainly in a context of chronic liver cirrhosis. It is the sixth most frequent neoplasm, the third cause of cancer death, and accounts for 7% of registered malignancies [1]. Sorafenib is the standard of care for advanced-stage HCC, as demonstrated in two large-scale trials [2] and the Asia-Pacific trial [3].

Epithelial–mesenchymal transition (EMT) is an important process that happens in normal development in which epithelial cells lose many of their properties to become mesenchymal cells by means of drastic changes in architecture and behavior. A similar transition also occurs during tumor progression and malignant transformation, leading to increased cell motility and invasiveness.

Transforming Growth Factor- β (TGFB) is known as the main, although not exclusive, inducer of EMT, which takes place through various signaling pathways [4]. A critical molecular event of EMT is the downregulation of the cell adhesion molecule E-cadherin and its replacement by N-cadherin [5]. Activation of Akt leads to a significant reduction in E-cadherin expression and to nuclear localization of SNAI1, suggesting a role for the PI3K/Akt signaling pathway in the shift from E-cadherin to N-cadherin expression and in EMT progression in cancer [6,7]. The serine/threonine kinase Akt is thought to be responsible for mediating the acquired resistance to Sorafenib in HCC cells [8]. Akt can be activated by insulin and survival and growth factors through phosphorylation mediated by mTOR2 and PDK1 at specific threonine residues. The process can be reverted by protein phosphatase 2 (PP2A) when Akt is oxidized, suggesting that Akt is subjected to redox regulation [9]. Moreover, it was shown that the interaction between Akt and PP2A under conditions of oxidative stress could be impaired by the reduction of a specific disulfide bond in Akt catalyzed by glutaredoxin (Grx). Activation of Akt after stimulation with insulin and various growth and survival factors, leading to the phosphorylation at Thr308 and Ser473 by PDK1 and mTOR2, respectively. Akt in its oxidized form can also be inactivated by protein phosphatase 2 (PP2A) dephosphorylation, which suggests that Akt is a redox-regulated protein [9]. It has been shown that Grx prevented Akt from forming a specific disulfide bond between Cys-297 and Cys-311 and suppressed its association with PP2A under oxidative stress, [9–11].

STAT3 is a pro-survival transcription factor which is constitutively activated in human cancer cell lines. Constitutive phosphorylation of STAT3 causes important changes in apoptosis, angiogenesis, invasion, migration, and proliferation, resulting in cell malignant transformation [12]. It has been observed that STAT3 activation is involved in EMT, invasion, and generation of metastasis in HCC [13]. Tyrosine phosphorylation of STAT3 is dependent on the thiol redox state modulated by H_2O_2 and Prx2 levels and the thioredoxin system activity [14]. Trx1–STAT3 disulfide exchange intermediates were detected, suggesting that Trx1 may be a direct mediator of STAT3 disulfide reduction.

Overexpression of Trx1 has been detected in human cervical neoplastic squamous epithelial cells, lung, colon, and HCC tumors [15–18]. Targeting Trx1 for cancer therapy and as prognostic marker of HCC has been considered because of the observed relationship between Trx1 expression and tumor aggressiveness, although the mechanisms underlying this association are still not well known [19]. Overexpression of Trx1 is one of the mechanisms for drug resistance in HCC treatment. A possible strategy that is gathering strength is to combine Trx1 gene therapy with chemotherapy to increase the effectiveness of treatments in HCC [20]. Thioredoxin-interacting protein (TXNIP) is a member of the alpha-arrestin protein family that binds to the active site and counteracts the action of Trx1 functioning as tumor suppressor [21]. Downregulation of TXNIP exacerbates cancer progression, and its expression is actually reduced in various human cancer cells [22]. TXNIP deficiency enhances the induction of the Zinc finger proteins SNAI1 and SNAI2 by TGF- β and promotes TGF- β -induced EMT [23].

A comparative genomic characterization of 19 cell lines derived from HCC allowed clustering them into two groups (I and II) according to their gene expression patterns [24].

In this study, we selected three hepatocarcinoma cell lines, i.e., HepG2 belonging to group I and SNU423 and SNU475 belonging to group II, to carry out a comparative study of their basal proteome and of how it responds to Sorafenib treatment and/or thioredoxin downregulation. We also analyzed redox modifications and phosphorylation of Akt, MAPK, and STAT3. The results obtained support the use of a combination of Sorafenib with Trx1 inactivation in HCC therapy.

2. Materials and Methods

2.1. Materials

HepG2 (HB-8065TM, ATCC/LGC Standards, SLU, Barcelona, Spain), SNU423 (CRL-2238, ATCC/LGC Standards) and SNU475 (CRL-2236, ATCC/LGC Standards) cell lines were obtained from American Type Culture Collection (ATCC; LGC Standards, S.L.U., Barcelona, Spain). Anti-Trx1 was obtained in-house from rabbit immunization with Trx1. Antibodies against STAT3 (#4904S),

MAPK (#9102), Thr²⁰²/Tyr²⁰⁴pMAPK (#4370P), Ser⁴⁷³pAkt (#4060S) were obtained from Cell Signaling Technology. Antibodies against Tyr⁷⁰⁵pSTAT3 (#sc-7993), TXNIP (#sc-271237), Akt1 (#sc-5298), and β -actin (#sc-47778) were from Santa Cruz Biotechnology, Inc. (Dallas, TX, USA). Anti-TrxR1 (#ab124954) was provided by Abcam, Inc. Secondary antibodies were from Sigma. ECL reagent was from GE Healthcare (Chicago, Illinois, USA); siRNA for Trx1 was from Dharmacon, Inc. (#L-006340-00; Lafayette, Colorado, USA).

2.2. Cell Growth Conditions

Cell cultures were negative for mycoplasma contamination. Cells were maintained in Eagle's minimum essential medium (EMEM), pH 7.4, supplemented with 10% FBS (#S181G-500, Biowest), sodium pyruvate (1mM) (#L0642-100, Biowest), and a penicillin–streptomycin–amphotericin solution (100U/mL–100 μ g/mL–0.25 μ g/mL) (#L0010-100, Biowest) at 37 °C in a humidified incubator with 5% CO₂. The cells were seeded at a density of 10⁵ cells/cm² in 2D culture. When applied, Sorafenib was added to the cell culture at a concentration of 10 μ M, as set up in a previous study [25] and the cells were incubated for 24 h before cell lysis to measure cell proliferation and protein activities and expression and to perform proteomic analysis. Cells lysis was carried out using 50 mM HEPES pH 7.5, 5 mM EDTA, 150 mM NaCl, 1% NP-40, a proteases inhibitor cocktail (#P8340, Sigma-Aldrich), 1 mM phenylmethylsulfonyl fluoride (PMSF), 1 mM NaF, and 1mM Na₃VO₄. The lysates were incubated on ice and vortexed for 15 s in four intervals of 5 min each. The samples were centrifuged at 13,000 rpm at 4 °C. The supernatants were collected for protein quantification and analysis.

2.3. Determination of Proliferation and Caspase-3 Activity Measurement

Cell proliferation was analyzed using a colorimetric ELISA (Roche Applied Science, Penzberg, Germany). In total, 2 \times 10⁴ cells/cm² were cultured in 96-well plates at 37 °C and 5% CO₂. At the end of the experiment, the cells were incubated with a 10 μ M BrdU labelling solution for 6h at 37 °C following the protocol recommended by the manufacturer. Caspase-3-associated activity was determined using the peptide-based substrate Ac-DEVD-AFC (100 μ M), as described elsewhere [10].

2.4. SDS-PAGE and Western Blotting

The protein expression levels of Trx1, TrxR1, TXNIP, STAT3, pSTAT3, Akt1, pAkt, MAPK, and pMAPK were determined by SDS-PAGE coupled to Western blotting analysis, following the same procedure and using the same antibody dilutions as described before [10].

2.5. Silencing of Trx1

Human Trx1 was knocked down in HepG2, SNU423, and SNU475 cells using a pool of four specific siRNA in 6-well plates (20,000 cells/cm²), according to the manufacturer's recommendations (Dharmacon, GE Healthcare Life Sciences) and as described before for HepG2 cells [10]. Non-targeting negative controls were run. Silencing of Trx1 was always checked by Western blotting and activity assay to confirm that its levels were reduced by \approx 80%.

2.6. Redox Mobility Shift Assay

Detection of thiol redox changes in Akt, MAPK, and STAT3 proteins was performed by differentially labeling reduced cysteines with 5 mM N-ethylmaleimide (NEM) and reversibly oxidized cysteines by reduction with 5 mM tris (2-carboxyethyl) phosphine (TCEP), followed by labeling with 10 mM 4-acetamido-4'-maleimidylstilbene-2,2'-disulfonic acid (AMS) (Thermo Scientific Pierce), which increases the molecular weight of the native protein by 536.44 Da. The protocol was the same as described before [10].

2.7. LC–MS/MS, Label-Free MS Protein Quantification, and Systems Analysis

Proteomic analyses were performed at the Proteomics Facility, University of Córdoba (SCAI). The procedure started with a culture of 2×10^4 cells/cm², and the protocol was the same as described previously [26]. Peptides were scanned and fragmented with the Thermo Orbitrap Fusion (Q-OT-qIT, Thermo Scientific) equipped with a nano-UHLC Ultimate 3000 (Dionex-Thermo Scientific). The analysis of MS raw data was performed using the MaxQuant (v1.5.7.0) software [27] and the label-free quantification configuration described before [26]. Three RAW data files per sample from three separate experiments were analyzed. Human UniProtKB/Swiss-Prot protein database (February 2018 version) was searched for protein identification as described before [26]. The method used for the imputation of missing values was the mean imputation. Finally, only the conditions with 3 values per identification were considered and analyzed through ANOVA and Tukey's post-hoc tests. A protein was considered differentially expressed if identified and quantified with at least 2 unique peptides and had a fold change of at least 1.50 and *p* value ≤ 0.05 .

The differentially expressed proteins together with the fold change values were analyzed with the online IPA software package (Qiagen, version 48207413) and the open software DAVID [28]. For IPA, each protein was mapped to its corresponding gene object in the Ingenuity Pathways Knowledge. The "core analysis" function was carried out considering direct and indirect relationships experimentally observed in all mammalian tissues and species, as well as all node types, data sources, and mutations. The list of significantly enriched canonical pathways, biological functions, and upstream factors is presented together with the activation or inhibition z-score values in a scale of colors.

2.8. Statistical Analysis

Results are expressed as mean \pm SD of data from ≥ 3 independent experiments. One-way ANOVA with the least significant difference Tukey's test as post-hoc multiple comparison analysis with a single pooled variance was used for comparisons; output *p* value ranges were handled in GP style: 0.0332 (*), 0.0021 (**), 0.0002 (***), < 0.0001 (****). The threshold for statistically significant differences was set at *p* adjust ≤ 0.05 value.

3. Results

3.1. Tracing the Proteomic Signature of EMT in Human Hepatocarcinoma Cell Lines

A "label-free" quantitative proteomics analysis detected 1170 proteins with significant differences between HepG2, SNU423, and SNU475 cell lines (Supplementary File S1). This is the first comparative proteomic analysis carried out with these cell lines, and the results obtained for canonical markers of EMT showed increasing and decreasing gradients, in agreement with the classification of these human HCC cells as epithelial or mesenchymal [29,30]. These results strongly correlate with previous microarray and Western blotting analyses of human HCC cell types [29,30] and constitute a definitive proof of concept for our experimental approach. E-cadherin was not detected, likely because our proteomic protocol was not optimized for membrane proteins. The members of the Trx system Trx1 and TrxR1 were also present in increasing levels from HepG2 to SNU475 cells (Figure 1), which agrees with the role described for Trx1 as a pro-metastasis factor [31].

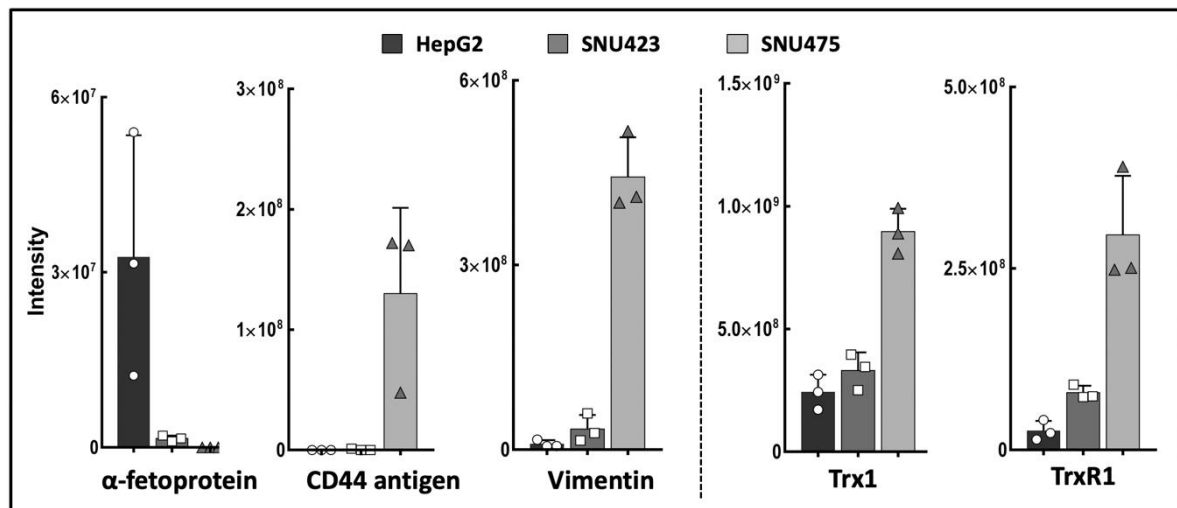


Figure 1. Epithelial–mesenchymal transition (EMT) markers and thioredoxin system in three hepatocarcinoma (HCC) cells lines. Data for vimentin, alpha-fetoprotein, CD44 antigen, Trx1, and TrxR1 were retrieved from the quantitative proteomic analysis of HepG2, SNU423, and SNU475 cells (Supplementary File S1). The scale in the vertical axis is the relative intensity from the LC–MS/MS quantitative analysis and varies between proteins; the maximum value for each protein ranges from $3.25e + 007$ for alpha-fetoprotein in HepG2 cells to $8.97e + 008$ for Trx1 in SNU475 cells. ($N = 3$, individual values are shown).

A system analysis of these 1170 differential proteins yielded significant enrichments in several canonical pathways (Figure 2A; the identities of the proteins are shown in Supplementary File S1). Integrin and actin cytoskeleton signaling, remodeling of epithelial adherent junction, and PI3K/Akt signaling, which have been described as being involved in EMT, were activated. On the reverse side, there was an overall inactivation of amino acid metabolism, fatty acid beta-oxidation, neurotransmitter catabolism, glutathione metabolism, and oxido-reduction processes. SNU423 and SNU275 cells showed similar activation and inactivation trends in many processes, although these processes were affected to a lesser extent in SNU423 cells, in parallel to their degree of mesenchymal properties. System analysis of 100 upregulated and 156 downregulated proteins common to the first two cell lines by Kyoto Encyclopedia of Genes and Genomes (KEGG) pathways and Gene Ontology (GO) biological processes using DAVID software confirmed and stressed these similarities (Figure S1). A search for upstream regulators brought to light differences and commonalities (Figure 2B). To name a few, MYCN and MITF transcription factors appeared to be activated in SNU423 but inactivated in SNU475 cells, whereas HIF1A and the KDM5A histone H3 demethylase behaved in the opposite way.

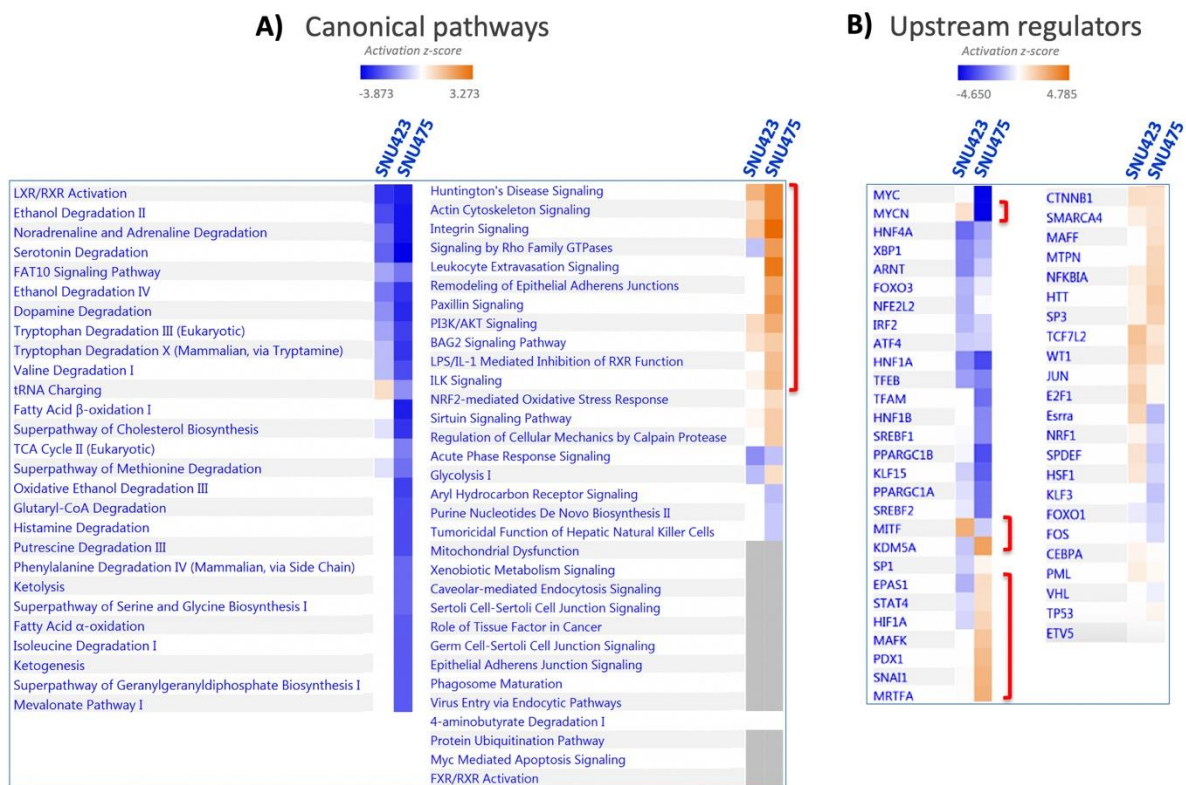


Figure 2. Systems Biology analysis of differential proteomic data from three HCC cell lines. Quantitative data on protein levels in SNU423 and SNU475 cells relative to the levels in HepG2, the more differentiated cell line, were analyzed. Up- and down-regulated proteins were analyzed using the IPA software in terms of (A) canonical pathways based on the content of the Ingenuity Knowledge Base, and (B) Upstream Regulator Analysis to identify the cascade of upstream transcriptional regulators (see M&M Section 2.7 for more details). The degree of activation is represented in a color scale as indicated. Red brackets have been added to highlight significant data commented on in the main text.

Altogether, these results identified a number of proteins and regulatory elements related to de-differentiation of HCC cells that could be an interesting focus for further research.

3.2. The Trx/TrxR/TXNIP System is Highly Sensitive to Sorafenib Treatment in HCC Cell Lines

The basal levels of Trx1 and TrxR1 in control cells were markedly higher in mesenchymal SNU475 cells (Figure 1), but Sorafenib induced a significant decrease in their levels in all HCC cell lines (Figure 3A,B). TXNIP behaved in a reciprocal manner relative to Trx1 and TrxR1. It was upregulated both by Sorafenib and by siRNATrx1, either independently or jointly, in all three cell lines (Figure 3C). These results indicate that the downregulation of the Trx system is part of the antitumoral action mechanism of Sorafenib and support our hypothesis that co-treatment with Trx1 inactivation adjuvants would potentiate Sorafenib-based antitumoral therapy.

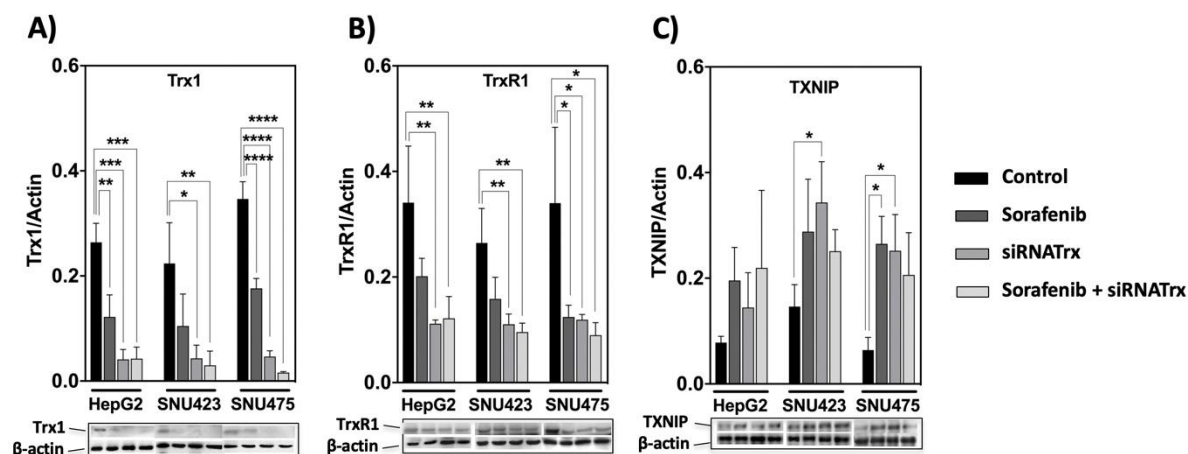


Figure 3. Response of the thioredoxin system to Sorafenib and siRNATrx1 treatments. Changes in the levels of three components of the thioredoxin system, (A) Trx1, (B) TrxR1 and (C) TXNIP were determined in HepG2, SNU423 and SNU475 cells by Western blotting with their specific antibodies on treatment with Sorafenib or siRNATrx1 independently or combined under the conditions described in M&M. Densitometric data normalized for β -actin are shown; samples from 3 different experiments ($N = 3$) for each cell line were run in the same gel; protein levels between cells cannot be compared since each set of 3 replicas for each cell line was developed on a different WB membrane; for a comparison of Trx1, TrxR1 between cell lines, refer to quantitative proteomic data in Figure 1; a composition of representative blots is shown below each graph. p values 0.0332 (*), 0.0021 (**), 0.0002 (***), <0.0001 (****), see Materials & Methods for statistical details.

3.3. The Effect of Sorafenib on the Global Proteome Depends on the Cell De-Differentiation Stage

Sorafenib alone was very effective in SNU423 cells, inducing significant changes in 465 proteins, whereas in HepG2 and SNU475 cells, the number of proteins affected was restricted to only 23 and 83, respectively (Figure 4A). The effect of siRNATrx1 alone was rather low in all three cell types, as should be expected since the effects of this antioxidant protein at the transcriptional regulatory level are limited. The cellular environment determined which proteins were affected by Trx1 downregulation, since there were no common siRNATrx1 targets among the three cell lines, although most of the proteins affected did also change when siRNATrx1 treatment was combined with Sorafenib (Supplementary File S1). Interestingly, a very strong synergistic effect was observed when Sorafenib was applied to Trx1-downregulated SNU475 cells (Figure 4A). This synergistic effect was also observed in HepG2 cells, although to a lesser extent, but was absent in SNU423 cells.

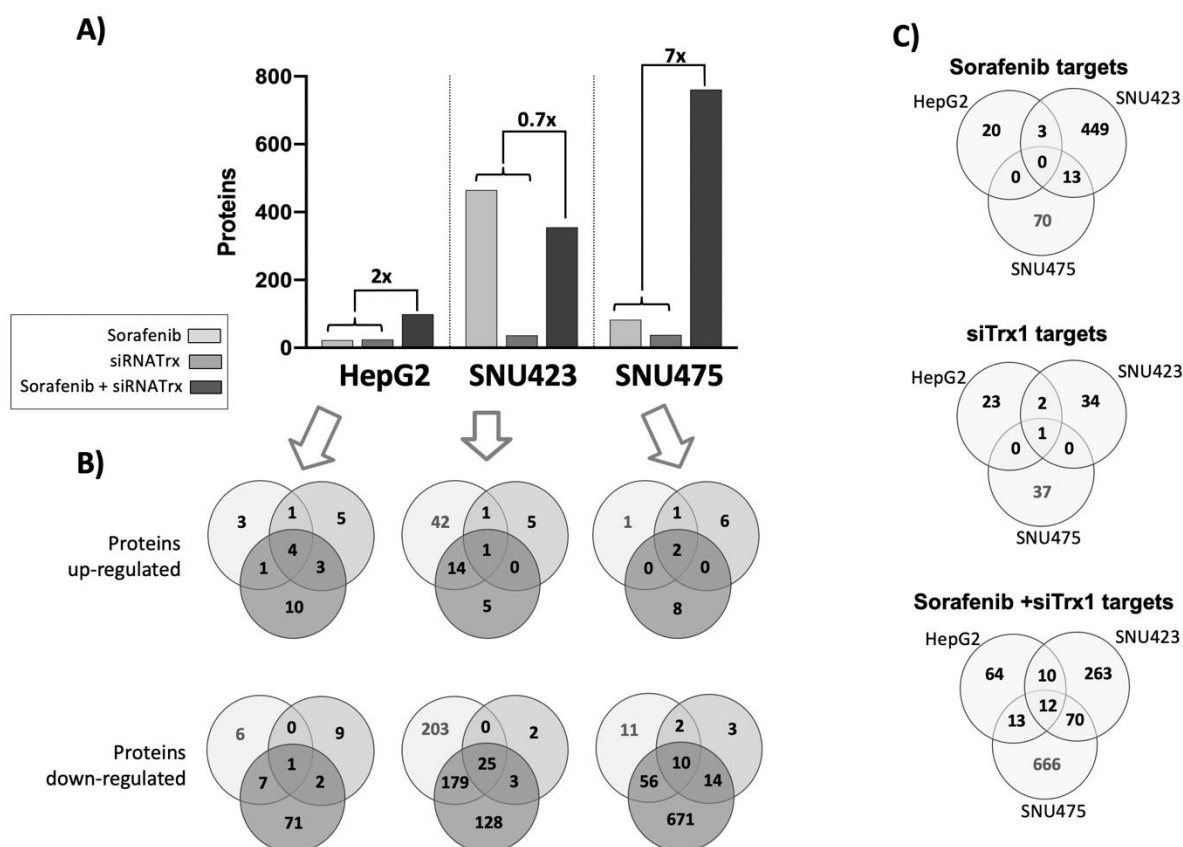


Figure 4. Summary of the quantitative proteomic analysis of HCC cell lines subjected to Sorafenib and/or siRNATrx1 treatments. (A) The total number of significantly (adjusted $p \leq 0.05$) different proteins (fold change ≥ 1.5 and ≤ 0.6) quantified upon each treatment relative to their controls; the numbers above the brackets and thin lines are the “synergy factor” reached by siRNATrx1 and Sorafenib calculated by the ratio between the number of proteins affected by the combined treatment and the number of proteins affected by individual Sorafenib and siRNATrx1 treatments. (B) Venn diagrams of upregulated and downregulated proteins by each treatment, by cell line; the color code indicated in the legend applies to (A) and (B). (C) Venn diagrams of proteins affected in each cell line by treatment.

Altogether, these proteomic data indicate that Sorafenib is highly active in moderately differentiated tumor cells but it has a limited effect in Trx1-rich and poorly differentiated cells, unless the antioxidant thioredoxin-related signaling is weakened. Its action is minor in epithelial HepG2 cells even in combination with Trx1 downregulation.

A comparison of the Sorafenib and Trx1 silencing targets of each cell line (Figure 4C) highlighted the fact that there were no common targets between the se cell lines, suggesting that the effects of each treatment are dependent on the de-differentiation stage of HCC cell lines. However, there were 12 common targets of the combined treatment in the three cell lines (Figures 4C and 5). These common proteins are related to lipids biosynthesis, protein nuclear transport, and actin organization. The increasing degree of downregulation of most of these common proteins runs parallel to their degree of de-differentiation.

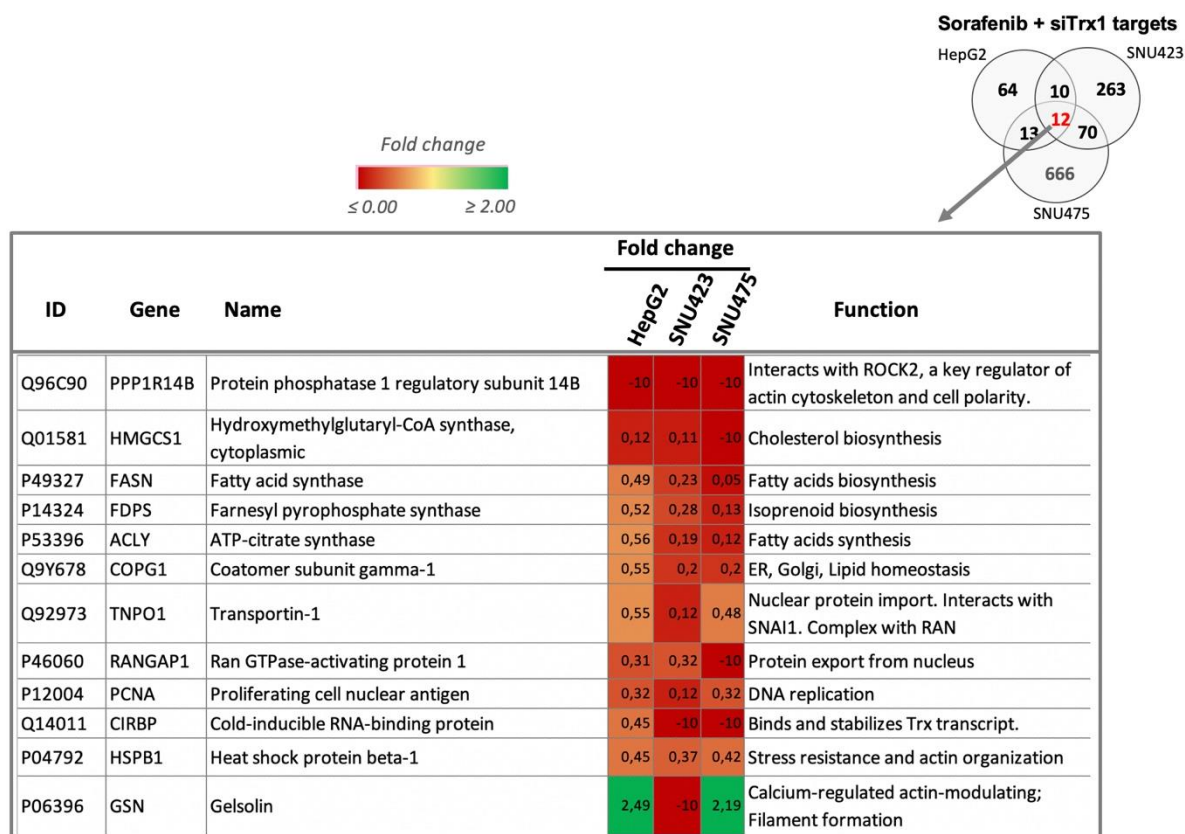


Figure 5. Common target proteins of the Sorafenib + siRNATrx1 treatment. Twelve proteins that changed significantly in HepG2, SNU423, and SNU475 cells are shown. A brief description of their function was extracted from UniProt; fold changes relative to their respective controls treated with solvent + Non-target siRNA are indicated in a color scale. Quantitative proteomic analysis as described in Materials and Methods (*N* = 3). Tenfold-change values correspond to proteins that were present in the controls but were not detected in the treated samples.

System analysis of the proteomic data provided some clues about the differential effect of Sorafenib in each cell type (Figure 6). The only pathways altered by Sorafenib in SNU475 cells were those of IGF-1 and renin–angiotensin signaling, which appeared inactivated with the concomitant differential inactivation of several upstream regulators, i.e., NFE2L2, PDGF-B, a potent mitogen for cells of mesenchymal origin, XBP1, involved in the unfolded protein response (UPR), and Ige (Figure 6). None of these pathways and upstream regulators were affected in SNU423 cells.

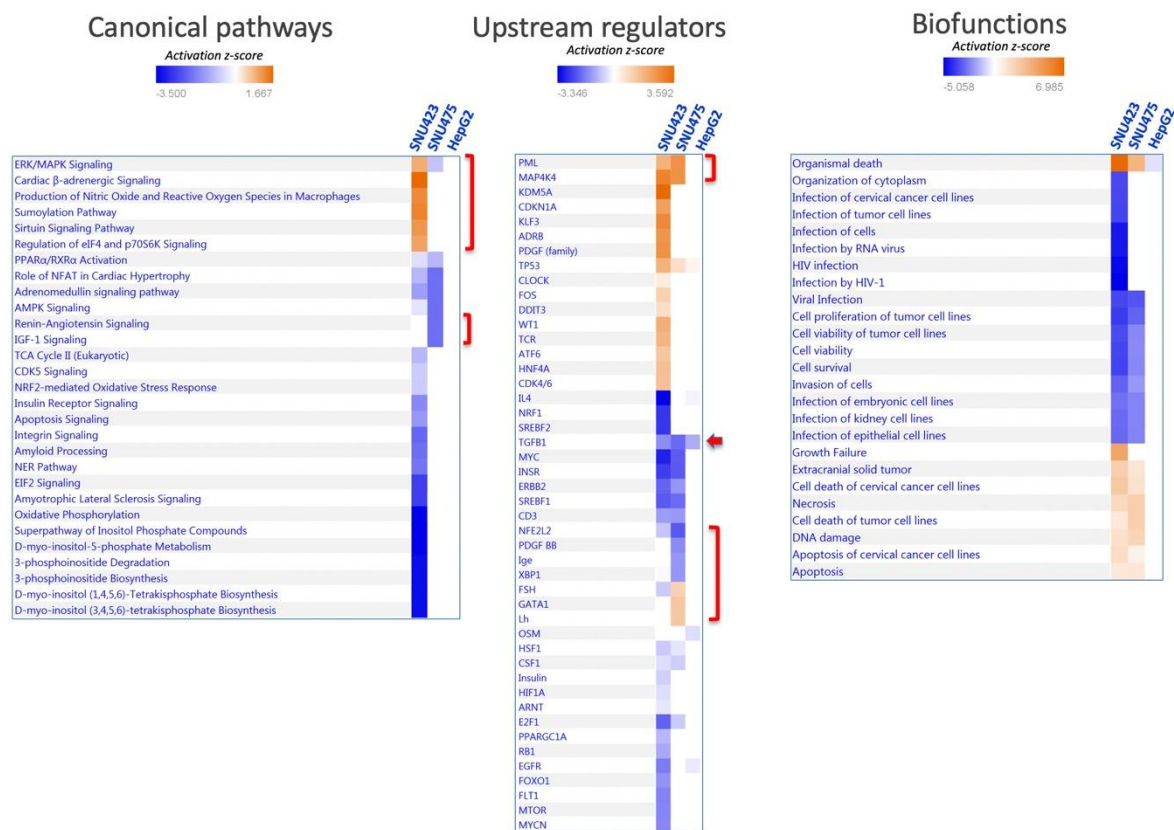


Figure 6. Enrichment analysis of proteins affected by Sorafenib treatment in each cell line. Proteins affected by Sorafenib treatment alone were analyzed using the IPA software in terms of canonical pathways, upstream regulators, and biofunctions as indicated, in the three cell lines studied. Brackets and arrow highlight elements that are commented on in the main text.

Pathways affected by Sorafenib solely in SNU423 cells were those related to integrin and EIF2 signaling, oxidative phosphorylation, and phosphoinositol metabolism, which were inactivated, and to sumoylation and sirtuin, which were activated (Figure 6). In parallel with these changes, a set of upstream regulators were uniquely either inactivated—IL4, SREBF2, NRF1, FOXO1, EGFR, MTOR, MYCN—or activated—KDM5A histone H3 demethylase, KLF3, and PDGF, to name the most relevant.

Despite the striking differential outcomes of Sorafenib treatment between SNU423 and SNU475 cells in terms of pathways and number of proteins affected, several upstream regulators responded equally to Sorafenib in both cell types. Briefly, MAP4K4 and the protein PML, which is regulated by sumoylation, were activated, whereas MYC, E2F1, the growth enhancer and cysteine-rich receptor tyrosine-protein kinase ERBB2, which interacts with STAT3, the steroid regulatory element-binding factor 1 SREBF1, and the insulin receptor tyrosine kinase INSR were inactivated. TGFB1, the main inducer of EMT [4], was the only regulator affected in all the cells and was inactivated even in HepG2.

3.4. The Alteration of the Global Proteome by Sorafenib in Human HCC Cell Lines at Different De-Differentiation Stages is Conditioned by Trx1 Downregulation

The number of new proteins affected by Sorafenib under conditions of Trx1 downregulation was 81, 133, and 679 in HepG2, SNU423, and SNU475 cells, respectively (Figure 4B). GO terms enrichment analysis of these newly affected sets of proteins with DAVID software revealed some common biological processes affected in the three cell lines: cholesterol and isoprenoid metabolism, cell–cell adhesion, and proteostasis.

Analysis of the set of proteins affected in SNU475 cells under the combined treatment revealed the target pathways (Figure 7). The general trend was inactivation of most pathways (actin, integrin,

14-3-3-mediated signaling, PI3K/Akt, sirtuin, mTOR, ILK, EIF2 signaling pathways, glycolysis, gluconeogenesis, and pentose phosphate pathway), except for two pathways that were activated: HIPPO and RhoGDI signaling (Figure 7). Despite the profound effect of the Sorafenib+siRNATrx1 treatment on the proteome and pathways of SNU475 cells, only a small number of transcriptional regulators was markedly affected, with TGFβ1 inactivation standing out. These changes were paralleled at the level of diseases and biofunctions by the inactivation of cytoskeleton organization, tumoral cell movement, migration, invasion, viability, and survival, and by the activation of cell death (Figure 7)

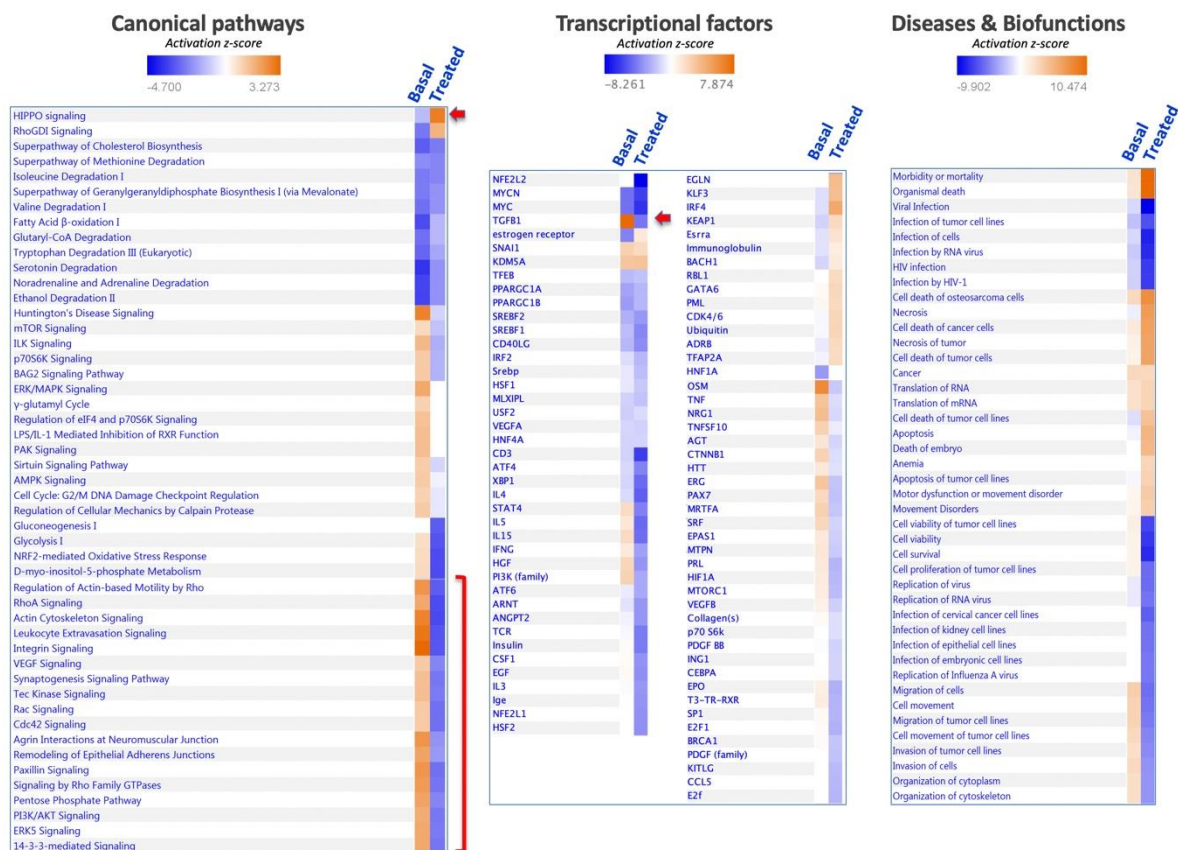


Figure 7. Enrichment analysis of proteins affected by combined treatment of Sorafenib and siRNATrx1 in SNU475 cells. In total, 761 proteins differentially quantified in SNU475 cells upon the combined treatment of Sorafenib and siRNATrx1 were analyzed using the IPA software by canonical pathways, transcriptional factors, and biofunctions. The enrichment results are indicated in colored scale in the right column (“Treated”) in each panel; the left column, headed “Basal”, shows the proteomic signature of SNU475 cells obtained by reference to HepG2 cells in the absence of treatment.

Activation of the HIPPO signaling pathway by the combined treatment of Sorafenib and siRNATrx1 would restrict cell proliferation and promote differentiation to cell death [32].

3.5. Effect of Sorafenib and Trx1-Silencing on Proliferation and Apoptosis in Three HCC Cell Lines

Proliferation under basal conditions was higher in HepG2 cells. Sorafenib and siRNATrx1, either individually or combined, had a significant, non-additive, negative effect on cell proliferation, as determined by BrdU incorporation (Figure 8A). The effect of Sorafenib was lower in SNU423 cells, despite the thorough change induced on the proteome (Figure 4).

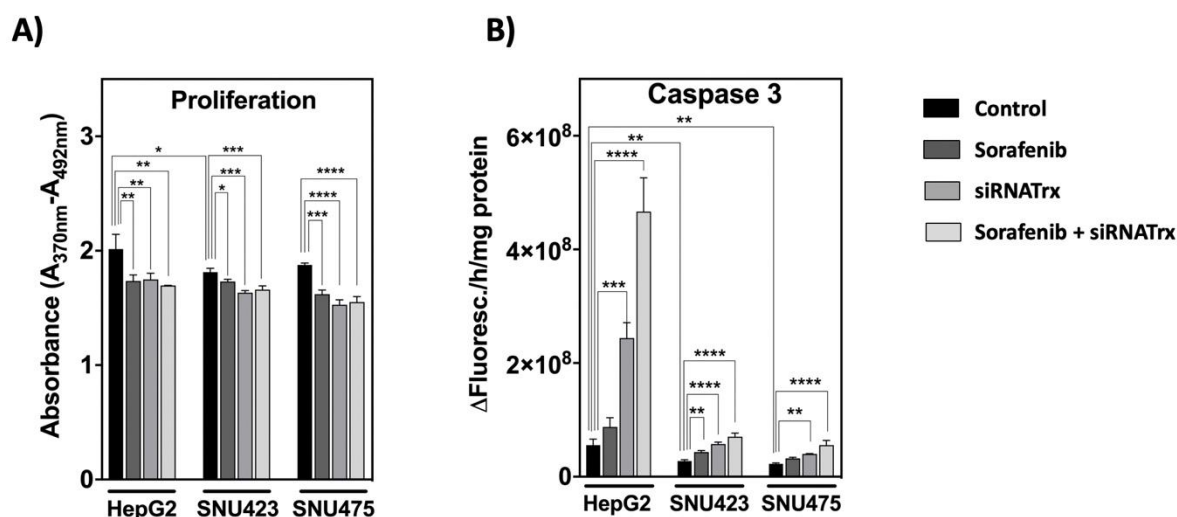


Figure 8. Proliferation and apoptosis of HCC cell lines subjected to Sorafenib and/or siRNATrx1 treatments. (A) Proliferation as determined by BrdU incorporation into DNA and (B) caspase-3 activity determined by fluorescence using a specific peptide substrate. Three different experiments ($N = 3$) for each cell line. p values 0.0332 (*), 0.0021 (**), 0.0002 (***), <0.0001 (****), see Materials & Methods for statistical details.

Regarding apoptosis (Figure 8B), Trx1 downregulation induced a significant increase in caspase-3 activity in all three cell types, which was inversely proportional to the basal levels of Trx1: prominent in HepG2 cells, as described previously [10], but subtle in SNU423 and SNU475. The effect of Sorafenib alone was slightly significant in SNU423 cells but was markedly enhanced by Trx1 silencing. Again, the enhancing effect was especially prominent in HepG2 cells (Figure 8B).

It seems that the more epithelial HepG2 cells have a programmed cell death response to Sorafenib under Trx1 down-regulation aimed at tissue survival, but this response mechanism seems to be impaired in the more mesenchymal cells. The proteomic data showed a decrease in proteins involved in cell proliferation, survival, invasiveness and migration but an increase in proteins involved in cell death in SNU423 and SNU475 cells (Figure 6). Regulated cell death can proceed by mechanisms different from apoptosis and it has been described that Sorafenib induces cell death by ferroptosis in hepatocarcinoma cell lines [33].

3.6. Sorafenib Reductive Effect on the Thiol Redox State of Akt, MAPK, and STAT3 Is General but the Counteracting Action of Trx1 Knock-Down is Specific for STAT3

Systems biology analysis of our proteomic data indicated activation of PI3K/Akt signaling in SNU423 and SNU475 cells (Figure 2), but, surprisingly, no significant changes were observed in the ratio between phosphorylated and dephosphorylated Akt, MAPK, and STAT3 in all three cell lines (Figure 9A,D,F). However, Sorafenib treatment provoked a prominent thiol reductive change in Akt, Ser^{473} Akt, MAPK, and STAT3 in all three cell types that was higher for Akt and Ser^{473} Akt in SNU475 cells (Figure 9B,C,E,G). This may be indicative of predominance of redox changes over phosphorylation changes regarding the action of Sorafenib on these signaling pathways. This reductive thiol redox change was insensitive to siRNATrx1, except for STAT3 for which it was totally blunted by Trx1 downregulation (Figure 9G). The involvement of Trx1 in thiol redox changes of STAT3 agrees with the report of the formation of Trx1–STAT3 disulfide exchange intermediates [14], suggesting that Trx1 may be a direct mediator of STAT3 disulfide reduction.

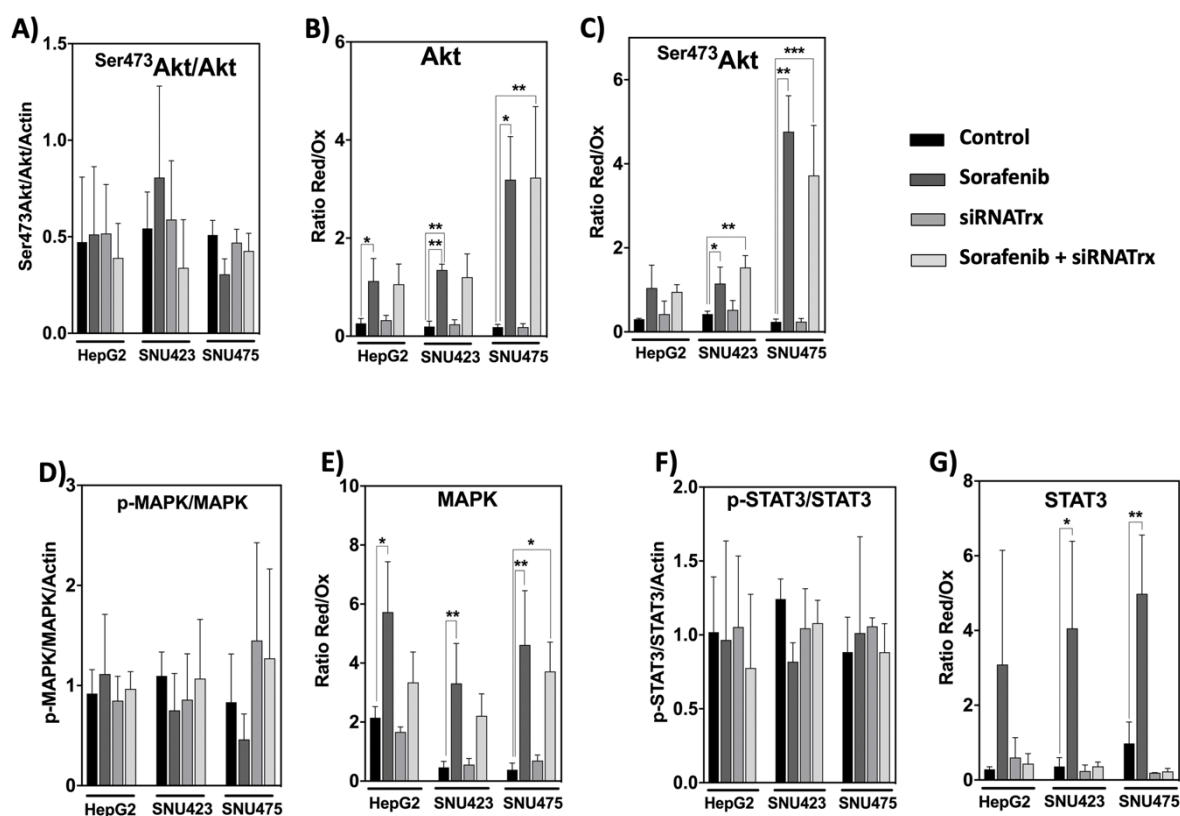


Figure 9. Phosphorylation and thiol redox state of key signaling elements in HCC cell lines treated with Sorafenib and/or siRNATrx1. The phosphorylated/unphosphorylated ratios of the indicated proteins were calculated from the densitometric quantitation data of each form normalized for β -actin. The ratio Red/Ox reflects the thiol redox state and was calculated from the densitometric data of the bands obtained by the “thiol redox electrophoretic mobility shift assay” as described in Materials and Methods; samples from three different experiments ($N = 3$) for each cell line were run in the same gel; protein levels cannot be compared between cells. p values 0.0332 (*), 0.0021 (**), 0.0002 (***), see Materials & Methods for statistical details. (A) Ratio of $\text{Ser}^{473}\text{pAkt}/\text{Akt}$; (B,C) thiol redox changes of $\text{Ser}^{473}\text{pAkt}$ and Akt; (D,E) phosphorylation and redox changes, respectively, of MAPK; the same is shown for STAT3 in (F,G).

4. Discussion

4.1. Proteomic Changes during EMT

The current curative treatments of HCC are indicated during the early stages of the disease [34]. Nowadays, however, two-thirds of patients are diagnosed in more advanced stages of the disease [35], urgently requiring new effective and safe drugs. The transition from well-differentiated carcinoma to poorly differentiated invasive carcinoma is a predominant event in the aggressive tumor progression of human HCC. Actually, EMT has been linked to tumor cell invasion and metastasis [36].

We made the first comparative characterization of EMT at the level of expressed proteins in three hepatocarcinoma cell lines, HepG2, SNU423, and SNU475, that present markers indicative of a gradual transition from epithelial to mesenchymal characteristics. A global proteome analysis of these cell lines revealed a thorough change in metabolic processes, consistent with the fact that mesenchymal cells have different metabolic needs compared to epithelial cells, in part because of their motility and invasiveness. Metabolic reprogramming upon EMT in different types of cancer cells is complex and controversial [37], but mitochondrial dysfunction has been widely linked to aggressiveness of cancer and activation of EMT. The finding of a significant decrease in succinate dehydrogenase (SDH) and isocitrate dehydrogenase (IDH) in the Tricarboxylic Acid Cycle (TCA) cycle

in the most de-differentiated SNU475 cells (Supplementary File S1), together with a specific activation of a few upstream regulators, including SNAI1 (Figure 2B), agrees with the report that silencing or mutation of both enzymes promoted cell migration and invasion in different types of cancer cells mediated by TGF- β /SNAI1 [38,39].

Altogether, this first characterization of EMT at a proteome level should help to focus research on events that occur when cancer cells acquire their metastatic and invasive potential and would help in the design of therapies for advanced HCC.

4.2. Effect of Trx1 Downregulation on Sorafenib Antitumoral Treatment

Our data show that Sorafenib downregulates specific EMT-related pathways like integrin signaling. However, we found that its proteomic reprogramming capacity is prominent in moderately differentiated SNU423 cells but limited in poorly differentiated SNU475 cells, which represent the most advanced stage of the disease.

Interestingly enough, weakening cell antioxidant defenses by Trx1 downregulation exerted a marked synergistic effect on proteomic rearrangement in Sorafenib-treated SNU475 cells (Figure 4). Sorafenib itself had a down-regulatory effect on the Trx/TrxR1 system and an up-regulatory effect on TXNIP in all three cell types (Figure 3) but only triggered an extensive proteomic reprogramming in SNU423, where the basal levels of Trx1/TrxR1 are lower and those of TXNIP might be higher (Figures 1 and 3). However, additional Trx1 downregulation exerted an adjuvant effect that dramatically expanded the action of Sorafenib in SNU475 cells where the basal Trx1/TrxR1 levels are higher and those of TXNIP might be lower. The effect was minor in HepG2 cells.

Although the general significance of these *in vitro* data in the context of cancer treatment is limited, they strongly support the importance of an anticancer therapy based on a combined treatment of Sorafenib with inhibitors of the Trx system or other prooxidant agents for advanced HCC and encourage the undertaking of further research on this ground.

Few common target proteins were identified in the three cell lines (Figure 4C), likely as a consequence of differences in their cell de-differentiation staging, though several commonalities were obvious at the level of upstream regulators that were affected. A careful characterization of these few common targets may lead to the discovery of true markers for diagnostic and therapeutic purposes. At this point, it is worth mentioning that Protein Phosphatase 1 Regulatory Subunit 14B (PPP1R14B) disappeared from the three cell lines after the Sorafenib + siRNA_{Trx1} combined treatment. PPP1R14B interacts with ROCK2 (“IntAct” EBI-7009696), which is a key regulator of the actin cytoskeleton and cell polarity and is one of the most highly overexpressed phosphatase-related proteins in triple-negative breast cancer (TNBC), which has the worst prognosis among all breast cancers [40].

The only pathway clearly activated by co-treatment was HIPPO signaling, which promotes cell differentiation and contact inhibition of cell proliferation and plays a central role in regulating organ growth and regeneration [32]. It is a critical regulator of liver growth and a potent suppressor of liver tumor formation [41]. Activation of HIPPO signaling by Sorafenib treatment under Trx1 downregulation in poorly differentiated SNU475 HCC cells might impact on the alleviation of EMT and cancer malignancy. To dig deeper into the mechanism, it would be worth checking for possible thiol redox changes in members of the HIPPO signaling pathway that have been reported to be sensitive to the redox environment [42,43].

4.3. Involvement of the Trx1-Dependent Thiol Redox State of Key Signaling Pathways

Sorafenib and Trx1 downregulation had a significant negative effect on the proliferation in HCC cell lines independently of their degree of de-differentiation, although their effects were not additive (Figure 8A). Regarding cell death, Trx1 knock-down induced apoptosis in all three cell lines, but the effect was prominent only in differentiated HepG2 cells. The effect of Sorafenib alone was negligible in either cell type, but Sorafenib combined with Trx1 downregulation had a marked pro-apoptotic effect, particularly in HepG2 cells (Figure 8B) and also appreciable in SNU475 cells (Figures 7 and 8B,

biofunctions). It seems that the ability of HCC cells to trigger a pro-apoptotic response to Trx1 downregulation and to Sorafenib treatment declines as their basal Trx1 levels and their degree of de-differentiation increase.

The phosphorylation states of Akt, MAPK, and STAT3 were not altered by Sorafenib and/or siRNATrx1 treatments. However, Sorafenib induced a thiol reductive burst that was independent of Trx1 in the case of Akt and MAPK but was totally abolished by Trx1 downregulation in the case of STAT3. These results provide further insight into the importance of redox homeostasis in the mechanism of Sorafenib action and suggest that Sorafenib might protect Akt from PPA2 inactivation by inducing a thiol reductive change, particularly in SNU475 cells. The lack of sensitivity of the thiol redox state of Akt to Trx1 downregulation indicates that this redox change could be mediated by the glutathione system, as had also been previously pointed out in HepG2 cells [10].

Thiol reductive changes in MAPK were also independent of Trx1 silencing but were coincident with the activation of MAP4K4 detected in SNU423 and SNU475 cells treated with Sorafenib alone (Figure 6). The strong enhancing effect of Trx1 silencing on the action of Sorafenib at the proteome level in the poorly differentiated SNU475 cells did not seem to be mediated by phosphorylation or redox changes of Akt and MAPK in the studied cell lines.

Reactive Oxygen Species (ROS) induce tyrosine phosphorylation by inactivation of tyrosine phosphatases and upregulate the DNA binding activity of STAT3 [44]; however, ROS could also induce oxidation of conserved cysteines, impeding STAT3 transcriptional activity [45]. The mechanism of this redox regulation in HepG2 cells involves glutathionylation of STAT3 at Cys328 or Cys542, which are within the DNA-binding domain and the linker domain, respectively, and would affect STAT3 activity under oxidative stress, even when it is phosphorylated at Tyr705 [46,47]. The formation of Trx1-STAT3 disulfide exchange intermediates has been reported, suggesting that Trx1 may be a direct mediator of STAT3 disulfide reduction [14]. The activity of STAT3 must have been affected by the observed redox changes, despite the lack of differences in the degree of phosphorylation, and could have played a role in the response of SNU475 cells to the combined Sorafenib+siRNATrx1 treatment.

Combined treatments of Sorafenib with other agents have been reported. For instance, its combination with metformin downregulated the expression of Trx1 and improved the efficacy of Sorafenib in the treatment of HCC, decreasing tumor invasiveness and cell motility [31], while its combination with tetrandrine was described to induce apoptosis through ROS/Akt signaling in human HCC [48].

5. Conclusions

The proteomes of the three HCC cell lines studied reveal differences in proteins involved in motility and invasiveness, coherent with their EMT markers outfit. The present study shows that Sorafenib treatment induces the highest proteomic reprogramming in SNU423 cells whose Trx1/TrxR1 levels are lower and TXNIP levels are higher. However, its effect was limited in poorly-differentiated HCC SNU475 cells, which are expected to be present at high proportion in the advanced stage of the disease and whose basal Trx1/TrxR1 levels are high. However, application of Sorafenib combined with Trx1 knock-down, dramatically enhances proteomic rearrangement, including inactivation of TGF β and activation of HIPPO signaling, accompanied by thiol oxidative changes in STAT3. Combination of Sorafenib with thioredoxin inhibitors should be taken into account in the design of anticancer therapies

Supplementary Materials: The following are available online at <http://www.mdpi.com/2076-3921/8/10/501/s1>, Figure S1: System analysis of differential proteins common to SNU423 and SNU475 cells. (A) Proteins upregulated or downregulated in both cell lines relative to HepG2 cells; (B) common proteins from each set were analyzed for enrichment by KEGG pathways and GO biological processes using DAVID software; number of proteins on the right side of the bars refers to the number of proteins clustered in each term; adjusted *p* value is shown on the horizontal axis in a logarithmic scale for statistical significance; Supplementary File S1. Excel file showing the results of quantitative proteomic analysis of HepG2, SNU423, and SNU475 cells. The 1st, 2nd, and 3rd sheets, ("HepG2 treatments", "SNU4232 treatments", and "SNU475 treatments") show protein ID, number of unique peptides, and protein name in columns A–C. Columns D–O show the normalized abundance for each of three replicates of untreated ("control"), Sorafenib-treated ("Sorab"), siRNATrx1-treated ("Trx1"), and Sorafenib +

siRNATrx1 combined treatment (“ST”); columns P–U show the abundance fold change (“FC”) relative to the control and their respective statistical significance (*p*-values, a value of “1” means not significant FC). In the 4th sheet, (“Cell lines”), columns A–D show protein ID, protein name, gene name, and number of unique peptides; columns E–M show the normalized abundance for each of three replicates of untreated HepG2 cells (“HepG2”), SNU423 cells (“S3”), and SNU475 cells (“S5”); columns N–Q show the protein abundance fold change of SNU423 and SNU475 cells (“FCS3_HepG2” and “FCS5_HepG2”) relative to HepG2 together with the statistical significance index (*p* value). A value of “1” means not significant FC.

Author Contributions: Conceptualization, J.M., J.A.B., and C.A.P.; Formal analysis, M.J.L.-G. and R.G.; Funding acquisition, J.M., J.A.B., and C.A.P.; Investigation, M.J.L.-G. and R.G.; Methodology, M.J.L.-G. and R.G.; Software, M.J.L.-G.; Writing—original draft, J.A.B., and C.A.P.; Writing—review & editing, J.M.

Funding: This research has been financed by grants from the Spanish Ministry of Economy and Competitiveness (BFU2016-80006-P), the Institute of Health Carlos III (ISCIII) (PI13/00021 and PI16/00090), and the Andalusian Government (Consejería de Economía, Innovación, Ciencia y Empleo, BIO-0216 and CTS-6264; Consejería de Igualdad, Salud y Políticas Sociales, PI-00025-2013, and PI-0198-2016). We thank the Biomedical Research Network Center for Liver and Digestive Diseases (CIBERehd) founded by the ISCIII and co-financed by European Development Regional Fund “A way to achieve Europe” ERDF for their financial support.

Acknowledgments: Technical support by the staff of the Proteomics facility, Central Service for Research Support (SCAI) at the University of Cordoba, and the computer resources, technical expertise and assistance provided by the PAB (Andalusian Bioinformatics Platform) center located at the University of Málaga are acknowledged.

Conflicts of Interest: The authors declare no conflict of interest.

References

1. Galle, P.R.; Forner, A.; Llovet, J.M.; Mazzaferro, V.; Piscaglia, F.; Raoul, J.L.; Schirmacher, P.; Vilgrain, V. EASL Clinical Practice Guidelines: Management of hepatocellular carcinoma. *J. Hepatol.* **2018**, *69*, 182–236. [[CrossRef](#)] [[PubMed](#)]
2. Llovet, J.M.; Ricci, S.; Mazzaferro, V.; Hilgard, P.; Gane, E.; Blanc, J.F.; De Oliveira, A.C.; Santoro, A.; Raoul, J.L.; Forner, A.; et al. Sorafenib in Advanced Hepatocellular Carcinoma. *N. Engl. J. Med.* **2008**, *359*, 378–390. [[CrossRef](#)] [[PubMed](#)]
3. Cheng, A.L.; Kang, Y.K.; Chen, Z.; Tsao, C.J.; Qin, S.; Kim, J.S.; Luo, R.; Feng, J.; Ye, S.; Yang, T.S.; et al. Efficacy and safety of sorafenib in patients in the Asia-Pacific region with advanced hepatocellular carcinoma: A phase III randomised, double-blind, placebo-controlled trial. *Lancet Oncol.* **2009**, *10*, 25–34. [[CrossRef](#)]
4. Lamouille, S.; Xu, J.; Derynck, R. Molecular mechanisms of epithelial-mesenchymal transition. *Nat. Biotechnol.* **2014**, *15*, 178–196. [[CrossRef](#)] [[PubMed](#)]
5. Thiery, J.; Sleeman, J. Complex networks orchestrate epithelial–mesenchymal transitions. *Nat. Rev. Mol. Cell Biol.* **2006**, *7*, 131–142. [[CrossRef](#)] [[PubMed](#)]
6. Barber, A.G.; Castillo-Martin, M.; Bonal, D.M.; Jia, A.J.; Rybicki, B.A.; Christiano, A.M.; Cordon-Cardo, C. PI3K/AKT pathway regulates E-cadherin and Desmoglein 2 in aggressive prostate cancer. *Cancer Med.* **2015**, *8*, 1258–1271. [[CrossRef](#)]
7. Larue, L.; Bellacosa, A. Epithelial-mesenchymal transition in development and cancer: Role of phosphatidylinositol 3^okinase/AKT pathways. *Oncogene* **2005**, *24*, 7443–7454. [[CrossRef](#)]
8. Dong, J.; Zhai, B.; Sun, W.; Hu, F.; Cheng, H.; Xu, J. Activation of phosphatidylinositol 3-kinase/AKT/snail signaling pathway contributes to epithelial-mesenchymal transition-induced multi-drug resistance to sorafenib in hepatocellular carcinoma cells. *PLoS ONE* **2017**, *12*, e0185088. [[CrossRef](#)]
9. Murata, H.; Ihara, Y.; Nakamura, H.; Yodoi, J.; Sumikawa, K.; Kondo, T. Glutaredoxin exerts an antiapoptotic effect by regulating the redox state of Akt. *J. Biol. Chem.* **2003**, *278*, 50226–50233. [[CrossRef](#)]
10. González, R.; López-Grueso, M.J.; Muntané, J.; Bárcena, J.A.; Padilla, C.A. Redox regulation of metabolic and signaling pathways by thioredoxin and glutaredoxin in NOS-3 overexpressing hepatoblastoma cells. *Redox Biol.* **2015**, *6*, 122–134.
11. Huang, X.; Begley, M.; Morgenstern, K.A.; Gu, Y.; Rose, P.; Zhao, H.; Zhu, X. Crystal Structure of an InactiveAkt2 Kinase Domain. *Structure* **2003**, *11*, 21–30. [[CrossRef](#)]
12. Linher-Melville, K.; Singh, G. The complex roles of STAT3 and STAT5 in maintaining redox balance: Lessons from STAT-mediated xCT expression in cancer cells. *Mol. Cell. Endocrinol.* **2017**, *451*, 40–52. [[CrossRef](#)] [[PubMed](#)]

13. Zhang, C.H.; Guo, F.L.; Xu, G.L.; Jia, W.D.; Ge, Y.S. STAT3 activation mediates epithelial-to-mesenchymal transition in human hepatocellular carcinoma cells. *Hepatogastroenterology* **2014**, *61*, 1082–1089. [[PubMed](#)]
14. Sobotta, M.C.; Liou, W.; Stöcker, S.; Talwar, D.; Oehler, M.; Ruppert, T.; Scharf, A.N.; Dick, T.P. Peroxiredoxin-2 and STAT3 form a redox relay for H₂O₂ signaling. *Nat. Chem. Biol.* **2015**, *11*, 64–71. [[CrossRef](#)]
15. Gasdaska, P.Y.; Oblong, J.E.; Cotgreave, I.A.; Powis, G. The predicted amino acid sequence of human thioredoxin is identical to that of the autocrine growth factor human adult T-cell derived factor (ADF): Thioredoxin mRNA is elevated in some human tumors. *Biochim. Biophys. Acta* **1994**, *1218*, 292–296. [[CrossRef](#)]
16. Berggren, M.; Gallegos, A.; Gasdaska, J.R.; Gasdaska, P.Y.; Warneke, J.; Powis, G. Thioredoxin and thioredoxin reductase gene expression in human tumors and cell lines, and the effects of serum stimulation and hypoxia. *Anticancer Res.* **1996**, *16*, 3459–3466.
17. Fujii, S.; Nanbu, Y.; Nonogaki, H.; Konishi, I.; Mori, T.; Masutani, H.; Yodoi, J. Coexpression of adult T-cell leukemia-derived factor, a human thioredoxin homologue, and human papillomavirus DNA in neoplastic cervical squamous epithelium. *Cancer* **1991**, *68*, 1583–1591. [[CrossRef](#)]
18. Nakamura, H.; Masutani, H.; Tagaya, Y.; Yamauchi, A.; Inamoto, T.; Nanbu, Y.; Fujii, S.; Ozawa, K.; Yodoi, J. Expression and growth-promoting effect of adult T-cell leukemia-derived factor. A human thioredoxin homologue in hepatocellular carcinoma. *Cancer* **1992**, *69*, 2091–2097. [[CrossRef](#)]
19. Reichl, P.; Mikulits, W. Accuracy of novel diagnostic biomarkers for hepatocellular carcinoma: An update for clinicians (Review). *Oncol. Rep.* **2016**, *36*, 613–625. [[CrossRef](#)]
20. Li, W.; Shi, J.; Zhang, C.; Li, M.; Gan, L.; Xu, H.; Yang, X. Co-delivery of thioredoxin 1 shRNA and doxorubicin by folate-targeted gemini surfactant-based cationic liposomes to sensitize hepatocellular carcinoma cells. *J. Mater. Chem. B* **2014**, *2*, 4901–4910. [[CrossRef](#)]
21. Nishiyama, A.; Matsui, M.; Iwata, S.; Hirota, K.; Masutani, H.; Nakamura, H.; Takagi, Y.; Sono, H.; Gon, Y.; Yodoi, J. Identification of thioredoxin-binding protein-2/vitamin D(3) up-regulated protein 1 as a negative regulator of thioredoxin function and expression. *J. Biol. Chem.* **1999**, *274*, 21645–21650. [[CrossRef](#)] [[PubMed](#)]
22. Zhou, J.; Chng, W.J. Roles of thioredoxin binding protein (TXNIP) in oxidative stress, apoptosis and cancer. *Mitochondrion* **2013**, *13*, 163–169. [[CrossRef](#)] [[PubMed](#)]
23. Masaki, S.; Masutani, H.; Yoshihara, E.; Yodoi, J. Deficiency of Thioredoxin Binding Protein-2 (TBP-2) Enhances TGF- β Signaling and Promotes Epithelial to Mesenchymal Transition. *PLoS ONE* **2012**, *7*, e39900. [[CrossRef](#)] [[PubMed](#)]
24. Zimonjic, D.B.; Keck, C.L.; Thorgeirsson, S.S.; Popescu, N.C. Novel recurrent genetic imbalances in human hepatocellular carcinoma cell lines identified by comparative genomic hybridization. *Hepatology* **1999**, *29*, 1208–1214. [[CrossRef](#)] [[PubMed](#)]
25. Rodríguez-Hernández, M.A.; González, R.; de la Rosa, Á.J.; Gallego, P.; Ordóñez, R.; Navarro-Villarán, E.; Contreras, L.; Rodríguez-Arribas, M.; González-Gallego, J.; Álamo-Martínez, J.M.; et al. Molecular characterization of autophagic and apoptotic signaling induced by sorafenib in liver cancer cells. *J. Cell Physiol.* **2018**, *234*, 692–708. [[CrossRef](#)] [[PubMed](#)]
26. López-Grueso, M.J.; González-Ojeda, R.; Requejo-Aguilar, R.; McDonagh, B.; Fuentes-Almagro, C.A.; Muntané, J.; Bárcena, J.A.; Padilla, C.A. Thioredoxin and glutaredoxin regulate metabolism through different T multiplex thiol switches. *Redox Biol.* **2019**, *21*, 101049.
27. Cox, J.; Mann, M. MaxQuant enables high peptide identification rates, individualized p.p.b.-range mass accuracies and proteome-wide protein quantification. *Nat. Biotechnol.* **2008**, *26*, 1367–1372. [[CrossRef](#)]
28. Huang, D.; Sherman, B.; Lempicki, R. Systematic and integrative analysis of large gene lists using DAVID Bioinformatics Resources. *Nat. Protoc.* **2009**, *4*, 44–57. [[CrossRef](#)]
29. Lee, J.; Thorgeirsson, S. Functional and genomic implications of global gene expression profiles in cell lines from human hepatocellular cancer. *Hepatology* **2002**, *35*, 1134–1143. [[CrossRef](#)]
30. Fuchs, B.C.; Fujii, T.; Dorfman, J.D.; Goodwin, J.M.; Zhu, A.X.; Lanuti, M.; Tanabe, K.K. Epithelial-to-Mesenchymal Transition and Integrin-Linked Kinase Mediate Sensitivity to Epidermal Growth Factor Receptor Inhibition in Human Hepatoma Cells. *Cancer Res.* **2008**, *68*, 2391–2399. [[CrossRef](#)]
31. Guo, Z.; Cao, M.; You, A.; Gao, J.; Zhou, H.; Li, H.; Cui, Y.; Fang, F.; Zhang, W.; Song, T.; et al. Metformin inhibits the prometastatic effect of sorafenib in hepatocellular carcinoma by upregulating the expression of TIP30. *Cancer Sci.* **2016**, *107*, 507–513. [[CrossRef](#)] [[PubMed](#)]
32. Misra, J.R.; Irvine, K.D. The Hippo Signaling Network and Its Biological Functions. *Ann. Rev. Genet.* **2018**, *52*, 65–87. [[CrossRef](#)] [[PubMed](#)]

33. Lachaier, E.; Louandre, C.; Godin, C.; Saidak, Z.; Baert, M.; Diouf, M.; Chauffert, B.; Galmiche, A. Sorafenib Induces Ferroptosis in Human Cancer Cell Lines Originating from Different Solid Tumors. *Anticancer Res.* **2014**, *34*, 6417–6422. [[PubMed](#)]
34. Bruix, J.; Reig, M.; Sherman, M. Evidence-Based Diagnosis, Staging, and Treatment of Patients with Hepatocellular Carcinoma. *Gastroenterology* **2016**, *150*, 835–853. [[CrossRef](#)]
35. Stravitz, R.T.; Heuman, D.M.; Chand, N.; Sterling, R.K.; Shiffman, M.L.; Luketic, V.A.; Sanyal, A.J.; Habib, A.; Mihas, A.A.; Giles, H.C.S.; et al. Surveillance for hepatocellular carcinoma in patients with cirrhosis improves outcome. *Am. J. Med.* **2008**, *121*, 119–126. [[CrossRef](#)]
36. Mikulits, W. Epithelial to mesenchymal transition in hepatocellular carcinoma. *Future Oncol.* **2009**, *5*, 1169–1179.
37. Sciacovelli, M.; Frezza, C. Metabolic reprogramming and epithelial-to-mesenchymal transition in cancer. *FEBS J.* **2017**, *284*, 3132–3144. [[CrossRef](#)]
38. Wang, H.; Chen, Y.; Wu, G. SDHB deficiency promotes TGF β -mediated invasion and metastasis of colorectal cancer through transcriptional repression complex SNAIL1-SMAD3/4. *Transl. Oncol.* **2016**, *9*, 512–520. [[CrossRef](#)]
39. Aspúria, P.J.P.; Lunt, S.Y.; Våremo, L.; Vergnes, L.; Gozo, M.; Beach, J.A.; Salumbides, B.; Reue, K.; Wiedemeyer, W.R.; Nielsen, J.; et al. Succinate dehydrogenase inhibition leads to epithelial-mesenchymal transition and reprogrammed carbon metabolism. *Cancer Metab.* **2014**, *2*, 21. [[CrossRef](#)]
40. Den Hollander, P.; Rawls, K.; Tsimelzon, A.; Shepherd, J.; Mazumdar, A.; Hill, J.; Fuqua, S.A.; Chang, J.C.; Osborne, C.K.; Hilsenbeck, S.G.; et al. Phosphatase PTP4A3 Promotes Triple-Negative Breast Cancer Growth and Predicts Poor Patient Survival. *Cancer Res.* **2016**, *76*, 1942–1953. [[CrossRef](#)]
41. Lu, L.; Li, Y.; Kim, S.M.; Bossuyt, W.; Liu, P.; Qiu, Q.; Wang, Y.; Halder, G.; Finegold, M.J.; Lee, J.S.; et al. Hippo signaling is a potent in vivo growth and tumorsuppressor pathway in the mammalian liver. *Proc. Natl. Acad. Sci. USA* **2010**, *107*, 1437–1442. [[CrossRef](#)] [[PubMed](#)]
42. Khanal, P.; Jia, Z.; Yang, X. Cysteine residues are essential for dimerization of Hippo pathway components YAP2L and TAZ. *Sci. Rep.* **2018**, *8*, 3485. [[CrossRef](#)] [[PubMed](#)]
43. Gandhirajan, R.K.; Jain, M.; Walla, B.; Johnsen, M.; Bartram, M.P.; Anh, M.H.; Rinschen, M.M.; Benzing, T.; Schermer, B. Cysteine S-Glutathionylation Promotes Stability and Activation of the Hippo Downstream Effector Transcriptional Co-activator with PDZ-binding Motif (TAZ). *J. Biol. Chem.* **2016**, *291*, 11596–11607. [[CrossRef](#)] [[PubMed](#)]
44. Carballo, M.; Conde, M.; El Bekay, R.; Martín-Nieto, J.; Camacho, M.J.; Monteseirín, J.; Conde, J.; Bedoya, F.J.; Sobrino, F. Oxidative stress triggers STAT3 tyrosine phosphorylation and nuclear translocation in human lymphocytes. *J. Biol. Chem.* **1999**, *274*, 17580–17586. [[CrossRef](#)] [[PubMed](#)]
45. Li, L.; Cheung, S.H.; Evans, E.L.; Shaw, P.E. Modulation of Gene Expression and Tumor Cell Growth by Redox Modification of STAT3. *Cancer Res.* **2010**, *70*, 8222–8232. [[CrossRef](#)]
46. Xie, Y.; Kole, S.; Precht, P.; Pazin, M.J.; Bernier, M. S-Glutathionylation impairs signal transducer and activator of transcription 3 activation and signaling. *Endocrinology* **2009**, *150*, 1122–1131. [[CrossRef](#)]
47. Butturini, E.; Darra, E.; Chiavegato, G.; Cellini, B.; Cozzolino, F.; Monti, M.; Pucci, P.; Dell’Orco, D.; Mariotto, S. S-Glutathionylation at Cys328 and Cys542 Impairs STAT3 Phosphorylation. *ACS Chem. Biol.* **2014**, *9*, 1885–1893. [[CrossRef](#)]
48. Wan, J.; Liu, T.; Mei, L.; Li, J.; Gong, K.; Yu, C.; Li, W. Synergistic antitumour activity of sorafenib in combination with tetrandrine is mediated by reactive oxygen species (ROS)/Akt signaling. *Br. J. Cancer* **2013**, *109*, 342–350. [[CrossRef](#)]



OTHER SCIENTIFIC CONTRIBUTIONS

Redox regulation of metabolic and signaling pathways by thioredoxin and glutaredoxin in NOS-3 overexpressing hepatoblastoma cells. *Raúl González, M. José López-Grueso, Jordi Muntané, J. Antonio Bárcena*, C. Alicia Padilla.* **Redox Biology** 6 (2015) 122–134.

DOI: 10.1016/j.redox.2015.07.007



ELSEVIER

Contents lists available at ScienceDirect

Redox Biology

journal homepage: www.elsevier.com/locate/redox

Research Paper

Redox regulation of metabolic and signaling pathways by thioredoxin and glutaredoxin in NOS-3 overexpressing hepatoblastoma cells

Raúl González^{a,b,*}, M. José López-Grueso^a, Jordi Muntané^{c,d}, J. Antonio Bárcena^{a,b}, C. Alicia Padilla^{a,b}^a Departamento de Bioquímica y Biología Molecular, Universidad de Córdoba, Córdoba, Spain^b Instituto Maimónides de Investigación Biomédica de Córdoba (IMIBIC), Córdoba, Spain^c Departamento de Cirugía General, Hospital Universitario Virgen del Rocío/Instituto de Biomedicina de Sevilla (IBIS)/CSIC/Universidad de Sevilla, Sevilla, Spain^d Centro de Investigación Biomédica en Red de Enfermedades Hepáticas y Digestivas (CIBERehd), Spain

ARTICLE INFO

Article history:

Received 22 May 2015

Received in revised form

9 July 2015

Accepted 14 July 2015

Available online 17 July 2015

Keywords:

Thioredoxin

Glutaredoxin

Oxidative/nitrosative stress

Apoptosis

Cancer

ABSTRACT

Nitric oxide (NO) plays relevant roles in signal transduction in physiopathology and its effects are dependent on several environmental factors. NO has both pro-apoptotic and anti-apoptotic functions but the molecular mechanisms responsible for these opposite effects are not fully understood. The action of NO occurs mainly through redox changes in target proteins, particularly by S-nitrosylation of reactive cysteine residues. Thioredoxin (Trx) and glutaredoxin (Grx) systems are the main cellular controllers of the thiolic redox state of proteins exerting controversial effects on apoptosis with consequences for the resistance to or the development of cancer.

The aim of this study was to ascertain whether Trx and/or Grx systems mediate the antiproliferative effect of NO on hepatoblastoma cells by modulating the redox-state of key proteins.

Proliferation decreased and apoptosis increased in HepG2 cells overexpressing Nitric Oxide Synthase-3 (NOS-3) as a result of multilevel cellular responses to the oxidative environment generated by NO. Enzyme levels and cysteine redox state at several metabolic checkpoints were consistent with prominence of the pentose phosphate pathway to direct the metabolic flux toward NADPH for antioxidant defense and lowering of nucleotide biosynthesis and hence proliferation. Proteins involved in cell survival pathways, proteins of the redoxin systems and phosphorylation of MAPK were all significantly increased accompanied by a shift of the thiolic redox state of Akt1, Trx1 and Grx1 to more oxidized.

Silencing of Trx1 and Grx1 neutralized the increases in CD95, Akt1 and pAkt levels induced by NO and produced a marked increase in caspase-3 and -8 activities in both control and NOS-3 overexpressing cells concomitant with a decrease in the number of cells.

These results demonstrate that the antiproliferative effect of NO is actually hampered by Trx1 and Grx1 and support the strategy of weakening the thiolic antioxidant defenses when designing new antitumoral therapies.

© 2015 The Authors. Published by Elsevier B.V. This is an open access article under the CC BY-NC-ND license (<http://creativecommons.org/licenses/by-nc-nd/4.0/>).

Abbreviations: ACO, aconitase; ASK1, apoptosis signal-regulating kinase 1; Bcl-2, B-cell lymphoma 2; CaM, calmodulin; CD95, cluster of differentiation 95; DTNB, 5,5-dithio-bis-2-nitrobenzoic acid; ELISA, enzyme-linked immunosorbent assay; GAPDH, glyceraldehyde-3-phosphate dehydrogenase; Grx, glutaredoxin; HED, 2-hydroxyethyl disulfide; JAKs, Janus protein tyrosine kinases; JNK, c-Jun N-terminal kinase; MAPK, mitogen-activated protein kinase; MATII, methionine adenosyltransferase II; MM(PEG) 24, Methyl-PEG₂₄-Maleimide; mTOR, mammalian target of rapamycin; NEM, N-ethylmaleimide; NO, nitric oxide; NOS, nitric oxide synthase; PBS, phosphate buffered saline; PDK, phosphoinositide-dependent kinase; PKB, protein kinase B; PKM2, pyruvate kinase isozyme M2; PMSF, phenylmethylsulfonyl fluoride; PP2A, protein phosphatase 2A; PrSSG, mixed disulfide between protein and glutathione or glutathionylated protein; PrSSPr, inter- or intra-molecular protein disulfide; RNS, reactive nitrogen species; ROS, reactive oxygen species; SDS-PAGE, sodium dodecyl sulfate-polyacrylamide gel electrophoresis; STAT3, signal transducer and activator of transcription 3; TCEP, tris(2-carboxyethyl)phosphine; TKT, transketolase; Trx, thioredoxin; TrxR, thioredoxin reductase; TUNEL, terminal deoxynucleotidyl transferase (TdT)-mediated dUTP nick end labeling; TXNIP, thioredoxin-interacting protein; ROD, uroporphyrin decarboxylase

* Corresponding author at: Departamento de Bioquímica y Biología Molecular, Universidad de Córdoba, Córdoba, Spain.

E-mail address: raulangel@hotmail.com (R. González).

<http://dx.doi.org/10.1016/j.redox.2015.07.007>

2213-2317/© 2015 The Authors. Published by Elsevier B.V. This is an open access article under the CC BY-NC-ND license (<http://creativecommons.org/licenses/by-nc-nd/4.0/>).

1. Introduction

Nitric oxide (NO) is a very small, lipophilic, readily diffusible, chemically unstable molecule with a very short half-life (seconds) that plays a relevant role in signal transduction in physiopathology such as vasodilation, respiration, cell migration, immune response and apoptosis [1]. NO is known to be synthesized in a large number of different tissues by the NO synthases (NOS) using L-arginine as substrate. Three different isoforms of NOS have been identified, products of different genes, with different localization, regulation, catalytic properties and inhibitor sensitivity [2]. Their expression and activity are cellular and tissue specific with differential regulation at transcriptional, translational and post-translational levels [3,4]. These isoforms in mammals are: neuronal NOS (nNOS or NOS-1), inducible NOS (iNOS or NOS-2) and endothelial NOS (eNOS or NOS-3) [5–8]. The NOS-1 and NOS-3 isoforms are constitutively expressed and can be activated as a result of calmodulin (CaM) binding following a rise in intracellular calcium, and also by phosphorylation/dephosphorylation modifications. The expression of NOS-2 isoform is induced by inflammatory stimuli and is maximally activated by Ca^{2+} /CaM even at basal levels of intracellular Ca^{2+} [1,2,9]. The intracellular localization is relevant for the activity of NOS and accumulating evidence indicates that NOSs are subject to specific targeting to subcellular compartments (plasma membrane, Golgi, cytosol, nucleus and mitochondria) and that this trafficking is crucial for NO production and specific posttranslational modifications of target proteins [10–12].

NO can have opposite biological effects, depending on their local concentration, the target cell type involved and the levels of reactive oxygen species (ROS). The role of NO as a bioregulator of apoptosis is well established, having both antiapoptotic and proapoptotic functions [13]. The molecular mechanisms responsible for its opposite effect are not fully understood but there is strong evidence indicating the involvement of redox changes in key proteins [14].

The cellular redox state plays a critical role in regulating many signaling pathways including activation, differentiation, proliferation, and apoptosis [15–17]. ROS and reactive nitrogen species (RNS), cause irreversible damage when their amounts exceed the cellular antioxidant defense capacity, and are harmful to biomolecules, including genomic and mitochondrial DNA, membrane lipids and proteins. But they can also lead to reversible oxidations that play regulatory roles of protein function. Within proteins, the thiol group (–SH) of cysteine (Cys) can be oxidized in several ways: two thiols can form a disulfide bond as in some proteins (PSSP), or mixed disulfide in glutathionylated proteins (PSSG). Additionally, cysteine can be reversibly oxidized by ROS or RNS to sulfenic acid (–SOH) and nitrosothiol (–SNO). The nitrosylation of reactive cysteine residues in proteins takes part in NO signaling processes and can affect a multitude of intracellular events, beneficial or harmful, depending upon biological context [18–22].

The redox states of Cys residues are controlled by two major cellular systems, the Trx/thioredoxin reductase system and the glutathione (GSH)/Grx system [15,23,24]. The Trx system consists of redox active Trx, thioredoxin reductase (TrxR) and NADPH, which are critical for maintaining DNA synthesis and the cellular redox balance. Human Trx1 and TrxR1 are located in cell cytosol/nucleus. The Grx system consists of Grx, GSH and NADPH-dependent glutathione reductase. Human Grx1 is located in the cytosol [25] and is involved in redox-regulation through the reduction of protein disulfides and mixed disulfides, e.g. deglutathionylation of proteins [24,26].

A relationship exists between redoxins levels and apoptosis with consequences for the resistance or the development of cancer. As an antioxidant system Trx/TrxR catalyzes the

denitrosylation of SNO-caspase-3 [27] and some experimental data suggested that it also participates in the denitrosylation of SNO-caspase-9 and the reductive reactivation of caspase-8 [28]. But as a pro-oxidant Trx has been described trans-nitrosylating and inactivating caspase-3 thus showing an anti-apoptotic action [29].

It has been shown that Trx1 and TrxR1 are often overexpressed in tumor cells and that high Trx could be linked to drug resistance during cancer treatment [30]. Other studies suggest that high Trx and TrxR may induce apoptosis and reduce the mitotic index of certain tumors linked to p53 dependent cell death [31]. Reduced Trx is a negative regulator of ASK1 (apoptotic-inducing kinase), which relates the Trx system to evasion of apoptosis [32]. Another apoptosis-regulatory enzyme whose nitrosylation status is reversibly regulated by Trx1 is glyceraldehyde-3-phosphate dehydrogenase (GAPDH) [33]. Because reduced Trx1 plays a critical role in cellular proliferation and viability, excessive oxidation of Trx will lead to cell death [30,34].

On the other hand, Grx1 plays an important role in protecting cells from apoptosis by regulating the redox state of Akt1, also called protein kinase B (PKB), that has consequences for cell survival and also affect the multiple roles played by Akt1, as in the Akt-mTOR signaling cascade [35]. Mitochondrial Grx2 also exerts a protective effect on mitochondrial mediated apoptosis, preventing cardiolipin oxidation and cytochrome c release [36].

The intracellular mechanism regulating cell death and cell proliferation are intimately connected and different studies have shown that NO production has an important role in the regulation of the carcinogenic process. For instance, S-nitrosylation of some proteins, such as GAPDH and CD95, stimulates apoptosis whereas S-nitrosylation of other proteins, such as caspases and Bcl-2, inhibits apoptosis [33]. NO exerts an antineoplastic effect in tumoral cells by increasing cell death [37] and a specific pattern of S-nitrosylation has been observed during induction of apoptosis in hepatocytes [38].

The role of antioxidants in cancer has been controversial for decades. On one hand, ROS could mediate the activation of multiple signaling cascades that promote cell proliferation and on the other hand, the consequent increase in oxidative stress could cause senescence or apoptosis and became a tumor suppressor. Recent evidence indicates that antioxidants such as GSH and Trx can actually contribute to tumorigenesis by preventing ROS accumulation in cancer cells. The cellular response will depend on the levels of ROS and antioxidant status in the cell [31,39,40].

The main objective of this study was to ascertain whether Trx and/or Grx systems mediate the antiproliferative effect of NO on hepatoblastoma cells by modulating the redox-state of key proteins. We demonstrate that Trx1 and Grx1 behave differentially depending on the intracellular oxidative/nitrosative stress in HepG2 cells. They are required for proliferation but they also contribute to the antiproliferative effect of NO, associated with Akt1 redox changes.

2. Material and methods

2.1. Materials

All reagents were of analytical grade and were purchased from Sigma, unless otherwise specified.

HepG2 cell line used in this work was obtained from ATCC LGC Standards Company (Teddington, UK). Cell culture dish and flasks were from TPP (Switzerland). Anti-Trx1 and anti-Grx1 were obtained from rabbit in our laboratory. Antibodies against STAT3, MAPK, Thr²⁰²/Tyr²⁰⁴p-MAPK (p-MAPK) and Ser⁴⁷³p-Akt (p-Akt) were from Cell Signaling Technology. Antibodies against ACO1 and

UROD were from Aviva Systems Biology (San Diego, CA, USA). Antibodies against ACO2, TKT, TXNIP, Akt1, MATII, Bcl2, PKM2, caspase-3, CD95, NOS-3 and β -actin were from Santa Cruz Biotechnology, Inc. (Dallas, TX, USA). Anti-TrxR1 was from Abcam, Inc. Secondary antibodies were from Sigma. ECL was from GE Healthcare (Wauwatosa, Wisconsin, USA). Caspase substrates Ac-DEVD-AFC, Ac-LETD-AFC and Ac-LEHD-AFC were from Alexis Biochemicals (Enzo Life Sciences, Farmingdale, NY, USA). DNase I was from Ambion Life Technologies, Inc. (Foster City, California). siRNA for Grx1 and Trx1, and DharmaFECT 1 were from GE Healthcare Dharmacon, Inc. (Wauwatosa, Wisconsin, USA).

2.2. Cell growth conditions

HepG2 cells were transfected with the pcDNA/4TO (5100 bp; Invitrogen, Molecular Probes, Inc.) expression vector containing NOS-3 cDNA sequence (3462 bp; NCBI, Imagenes, full length cDNA clone sequence BC063294) under the control of the cytomegalovirus promoter (4TO-NOS). Cell lineages 4TO and 4TO-NOS were selected with zeocin (15 mg/L; Invitrogen) as described by González et al. [37]. Cells were maintained in EMEM Medium (Minimum Essential Medium Eagle), pH 7.4, supplemented with 10% fetal bovine serum, 2.2 g/L HCO_3Na , 1 mM sodium pyruvate, 100 U/L penicillin, 100 $\mu\text{g}/\text{mL}$ streptomycin, 0.25 $\mu\text{g}/\text{mL}$ amphotericin, and the corresponding selective zeocin antibiotic in 5% CO_2 atmosphere at 37 °C. The experiments were routinely carried out at 100,000 cells/cm². Cell extracts were obtained using lysis solution containing 50 mM HEPES (pH 7.5), 2 mM EDTA, 100 mM NaCl, 0.6% Nonidet NP-40, 1 mM phenylmethylsulfonyl fluoride (PMSF), 5 $\mu\text{g}/\text{mL}$ aprotinin, 10 $\mu\text{g}/\text{mL}$ leupeptin. Afterward, samples were homogenized and centrifuged at 15,000 g for 5 min at 4 °C and the supernatant was stored at –80 °C until use.

2.3. Assay of enzymatic activities

Grx activity was determined spectrophotometrically by measuring the reduction of 0.5 mM 2-hydroxyethyl disulfide (HED) by 0.5 mM GSH in the presence of NADPH and 0.5 units of yeast glutathione reductase, at 25 °C. The disappearance of NADPH was monitored at 340 nm [41]. Trx activity was determined spectrophotometrically by measuring its ability to reduce insulin disulfides in the presence of NADPH and rat thioredoxin reductase [42]. An assay mixture was prepared by mixing 200 μL 1 M HEPES pH 7.6, 40 μL 0.2 M EDTA, 40 μL 40 mM NADPH and 500 μL insulin (10 mg/mL). 40 μL of this mixture was added to test tubes containing 20 μL mammalian TrxR (1 μg) and the sample of protein and the assay volume was completed up to 120 μL with water. The tubes were incubated at 37 °C for 20 min and the reaction was stopped by the addition of 500 μL of a solution containing 0.4 mg/mL DTNB in 6 M guanidine-HCl, 50 mM Tris-HCl, pH 7.5. The absorbance at 412 nm was determined.

2.4. SDS-PAGE and Western blotting

The protein expression of Trx1, TrxR1, TXNIP, Grx1, Bcl-2, STAT3, Akt1, p-Akt, MAPK, p-MAPK, MATII, UROD, ACO, PKM2, TKL, caspase-3, CD95, NOS-3 and TKT were determined by SDS-PAGE coupled to Western blotting analysis. SDS-PAGE was performed with homogeneous 6% (NOS-3) 8% (STAT3, MAPK, ACO1, and TKT), 10% (Trx1, TXNIP, Akt, MATII, UROD, and ACO2), 12% (CD95) and 14% (Trx1, Grx1, Bcl-2, PKM2, and caspase-3) acrylamide gels. After electrophoresis, proteins were transferred to nitrocellulose membrane with a semi-dry electrophoretic transfer system (Bio-Rad). The membranes were incubated overnight at 4 °C with the corresponding primary antibodies against Thr²⁰²/Tyr²⁰⁴p-MAPK, 1:2000 dilution; or against ACO1 and UROD, 1:500 dilution; or

against Trx1, Grx1, STAT3, MAPK, ACO2, TKT, TXNIP, TrxR1, Akt1, Ser⁴⁷³p-Akt, MATII, Bcl-2, PKM2, caspase-3, CD95 and NOS-3, 1:1000 dilution. Then washed and incubated with the corresponding secondary antibodies conjugated to peroxidase (anti-rabbit, anti-goat or anti-mouse) used at 1:8000 dilution and the chemiluminescent signal was induced by ECL reagent. β -actin detected with the corresponding antibody at 1:5000 dilution, was used as cell protein-loading control.

2.5. Measurement of cell death

Caspase-8, caspase-9 and caspase-3-associated activities were determined using the corresponding peptide-based substrates (100 μM) in the reaction mixture (50 mM HEPES, pH 7.5, 100 mM NaCl, 10% sucrose, 0.1% Chaps, 1 mM EDTA and 5 mM DTT). The substrates used were Ac-DEVD-AFC, Ac-LETD-AFC and Ac-LEHD-AFC for caspase-3, -8, and -9, respectively. The fluorescence due to the reaction product was recorded with a GENios Microplate Reader (TECAN) set at 400 nm excitation and 505 nm emission [37].

The level of protein caspase-3-active fragment (p17) and cell death receptor, CD95, were also determined by SDS-PAGE coupled to Western blotting analysis as described in the previous section.

Apoptosis in HepG2 cells was also analyzed through DNA fragmentation detected by terminal deoxynucleotidyl transferase (TdT)-mediated dUTP nick end labeling (TUNEL) (Biotool). HepG2 cells 72 h after siRNA interference were fixed in 4% paraformaldehyde solution in PBS (pH 7.4) and later these cells were permeabilized with 0.2% Triton X-100 solution in PBS. Processing the cells was performed according to the recommendations of the manufacturer (Biotool) using DAPI (Molecular Probes) to stain the cell nuclei. Fluorescence provided by the cells was analyzed with fluorescence microscope (Olympus BX43) using standard fluorescein filter set to view the Apo-green fluorescence at 520+20 nm and view blue DAPI at 460 nm.

2.6. Cell viability and total number of cells

Total number of cells and cell viability in a HepG2 cell suspension were determined using the trypan blue dye exclusion method. The cells attached to the plate were washed with PBS and trypsinized for 7 min at 37 °C followed by incubation with complemented culture medium to halt the effect of trypsin. The cell suspension was centrifuged at 238g for 5 min at room temperature and the pellet was resuspended in 0.5 mL complemented culture medium. Cell viability and total number of cells were measured by mixing equal volumes of cell suspension and trypan blue. A viable cell will have a clear cytoplasm whereas a non-viable cell will have a blue cytoplasm. Cell viability was obtained by referring the number of living cells to the total number of cells in the initial cell suspension.

2.7. Cell proliferation

This parameter was analyzed using a cell proliferation colorimetric ELISA (Roche Applied Science) based on the measurement of BrdU incorporation during DNA synthesis in proliferating cells. Cells were cultured (20,000 cells/cm²) in flat-bottomed 96-well multiplates at 37 °C and 5% CO_2 . 72 h after siRNA Trx1 and Grx1 downregulation HepG2 cells were incubated with 10 μM BrdU labeling solution for 6 h at 37 °C. Later on were followed the steps according to the recommendations of the manufacturer (Roche) and detected the absorbance of the samples at 370 nm (reference wavelength 492 nm).

2.8. Determination of nitrotyrosine

The levels of nitrotyrosine were determined by Western blotting after 12% non-reducing SDS-PAGE as described before. The primary antibody was anti-3-nitrotyrosine (1:1000) from Sigma.

2.9. Silencing of *Grx1* and *Trx1*

Human *Grx1* and *Trx1* were knocked-down in wild type, 4TO and 4TO-NOS cells using specific siRNA in 6-well plate (20,000 cells/cm²) according to the manufacturer's recommendations (Dharmacon, GE Healthcare Life Sciences). *Grx* and *Trx* siRNA (25 nmol) were mixed with the transfection reagent DharmaFECT 1, previously pre-incubated with culture medium (antibiotic/antimycotic and serum free), and incubated for 20 min at room temperature. These interference solutions were added to cells in 2% of culture medium without antibiotic/antimycotic solution and kept for 72 h [43].

2.10. Redox mobility shift assay

Cells were treated with lysis buffer consisting of 50 mM HEPES pH 7.5, 2 mM EDTA, 100 mM NaCl, 1% Nonidet NP-40, 8 M urea, 1 mM PMSF and containing 5 mM *N*-ethylmaleimide (NEM) to block all free cysteine thiols. The lysates were centrifuged at 15,000 g for 5 min at 4 °C and the supernatant was desalted with Zeba spin desalting columns (Thermo Scientific Pierce) to eliminate the remaining NEM reagent, and then treated with 5 mM Tris (2-carboxyethyl)phosphine (TCEP) at room temperature for 30 min to reduce all cysteine disulfides. Recovered cysteine thiols were reacted at room temperature for 4 h with 6.25 mM Methyl-PEG₂₄-Maleimide (MM(PEG)₂₄, Thermo Scientific Pierce), which adds a 1239.44 Da label to any free thiol present, and desalted again on Zeba spin desalting columns. Labeled proteins in the

samples processed this way would show an increase of 1.2 kDa in their apparent Mw per each reversibly oxidized cysteine, compared to the same protein with their cysteines originally in the free thiol form, which had been initially blocked with the non-PEG maleimide reagent present in the lysis buffer. Protein concentration was determined and the samples were processed for SDS-PAGE and Western blotting as described above.

2.11. Statistical analysis

Results are expressed as mean \pm SEM of three independent experiments. Data were compared using ANOVA with the least significant difference test a *post hoc* multiple comparison analysis. The threshold for statistically significant differences was set at $p \leq 0.05$. The values labeled with "a" were significantly different versus the corresponding internal control in the same cell lineage. The values labeled with "b" were significantly different versus the corresponding control cell lineage.

3. Results

3.1. Characterization of NOS-3 overexpressing HepG2 cells

NOS-3 overexpression was performed as described before and was confirmed by measurement of mRNA and protein levels by Western blotting (supplementary Fig. S1A and B) CD95 protein levels and caspase-3, -8 and -9 activities were also determined and confirmed that their levels increased significantly in NOS-3 overexpressing HepG2 cells (supplementary Fig. S1C–F). The concentrations of NO and ROS were \approx 40% higher and the levels of nitrite and nitrate in the culture medium also increased significantly in NOS-3 overexpressing cells compared to the cells carrying the empty plasmid, as described before [37]. These results

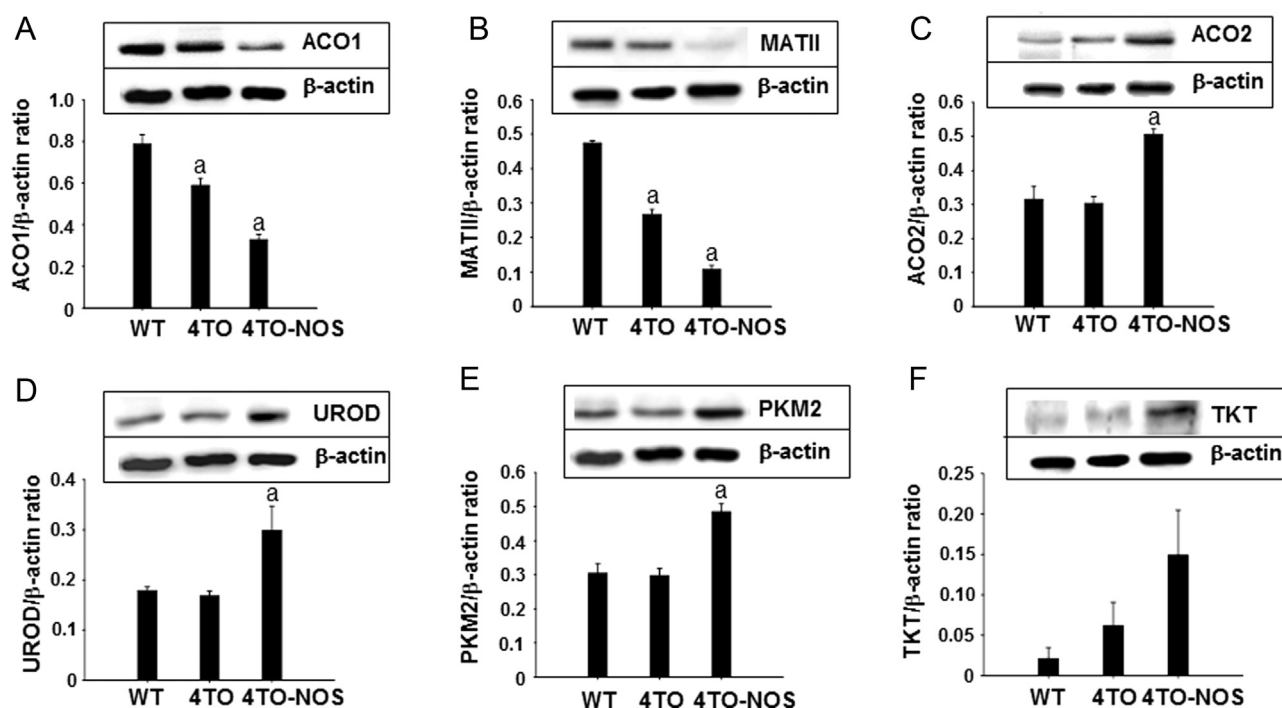


Fig. 1. Effect of high levels of NO on different metabolic pathways. Western blot analysis of the expression of different metabolism proteins and their relative quantitation in the HepG2 wild type cells (WT) and control cells (4TO), as well as in NOS-3 overexpressing cells (4TO-NOS). The levels of two key cytosolic proteins involved in iron metabolism, ACO1 (A), and one carbon metabolism, MATII (B), were significantly lower in NOS-3 overexpressing cells compared to control cells. However, mitochondrial ACO2 from energy metabolism and cytosolic UROD (heme biosynthesis), PKM2 (glycolysis) and TKT (pentose phosphate pathway) were up-regulated in NOS-3 overexpressing cells (C–F). Data are presented as mean \pm SEM ($n=3$ independent experiments). The values labeled with "a" were significantly different ($p \leq 0.05$) versus the corresponding control cell lineage. The images are representative of three different experiments.

indicate that NOS3 overexpressing cells are subject to oxidative stress and that the apoptotic pathways are activated.

3.2. Effect of high levels of NO produced by overexpression of NOS-3 on different metabolic pathways

Metabolic impairment is a characteristic feature of tumor cells due to the demand of biomass for cellular division, so we analyzed several checkpoints of biosynthetic, energetic and iron metabolic pathways. ACO1, a marker of cytosolic iron homeostasis and MATII involved in one carbon metabolism were diminished in NOS-3 overexpressing cells (Fig. 1A and B). By contrast, mitochondrial ACO2 from energy metabolism and cytosolic UROD (heme biosynthesis), PKM2 (glycolysis) and TKT (pentose phosphate pathway) increased significantly under NOS-3 overexpression conditions (Fig. 1C–F). These results confirm that NOS3 overexpression induces a marked metabolic rearrangement in HepG2 cells.

3.3. Effect of high levels of NO produced by overexpression of NOS-3 on different signaling pathways

Growing evidence shows that some transcription factors and proteins involved in signaling pathways could be modulated by

both oxidation/reduction and phosphorylation [44]. We chose several well-established representative proteins involved in cell survival pathways to study their response to the oxidative conditions prevailing in NOS-3 overexpressing cells. MAPK, p-MAPK, Bcl-2, STAT3, Akt1 and p-Akt, were all significantly increased in NOS-3 overexpressing cells compared to the control cells (Fig. 2A–F). The ratio of p-MAPK/MAPK increased markedly as a consequence of empty vector introduction but was further increased in NOS3 overexpressing cells (Fig. 2G). However, the ratio p-Akt/Akt1 did not change significantly despite the increase in both forms (Fig. 2H). These results demonstrate that the cell signaling pathways are thoroughly affected by overexpression of NOS3.

3.4. Effect of overexpression of NOS-3 on the redoxin levels

Proteins related to the thioredoxin and glutaredoxin systems are prominent players in thiol redox homeostasis in cells and were studied. Protein levels and activity of Trx1, Grx1 and levels of TrxR1 and TXNIP, increased significantly in NOS-3 overexpressing HepG2 cells (Fig. 3A–F). The simultaneous increase of both Trx1 and its opposing protein TXNIP is a conflicting situation likely a reflection of the cellular response to redox changes under the prevailing nitrosative conditions where Trx1 and TXNIP may not

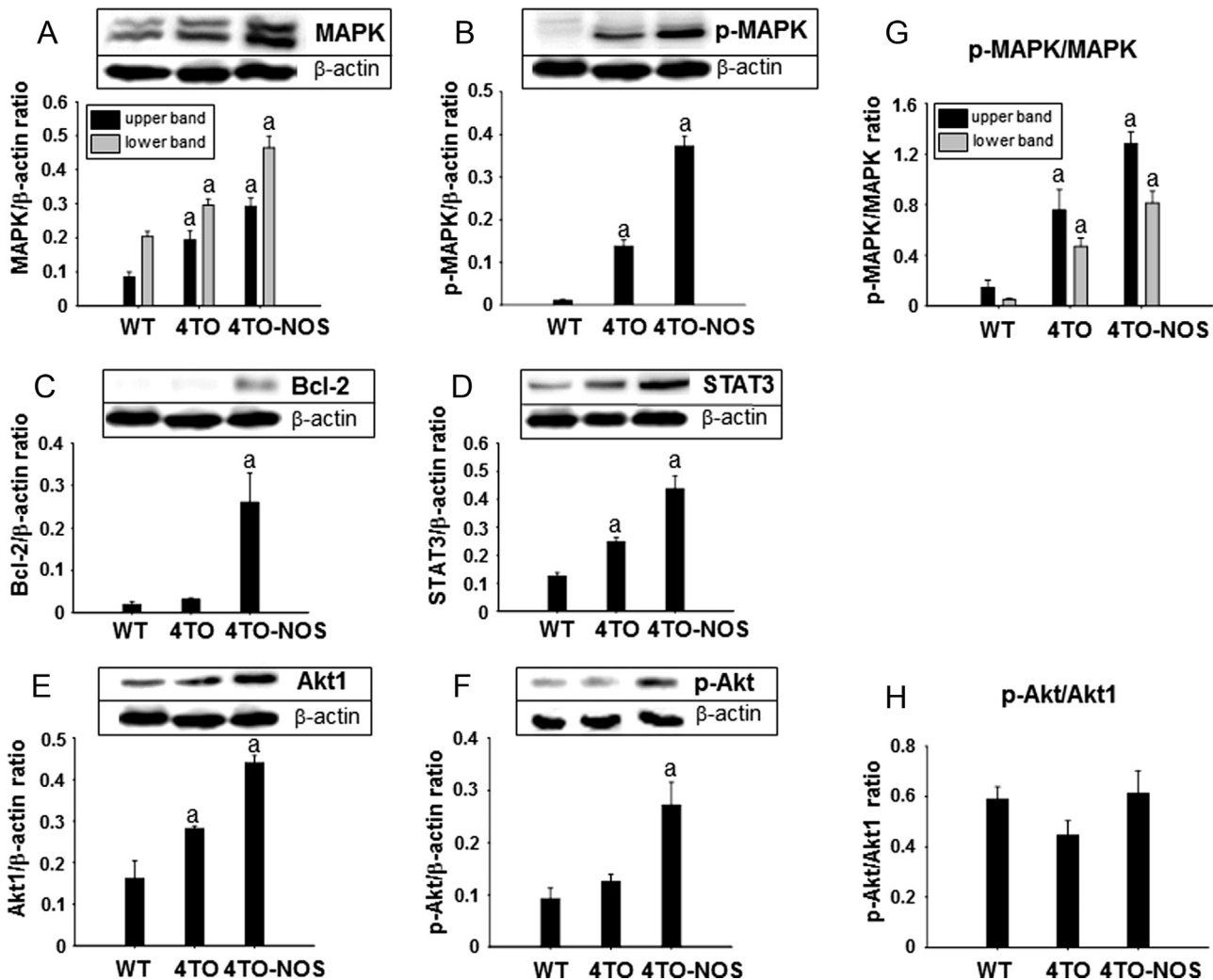


Fig. 2. Effect of NOS-3 overexpression on different signaling pathways. Western blot analysis of the expression of different signaling proteins and their relative quantitation in the HepG2 wild type cells (WT) and control cells (4TO), as well as in NOS-3 overexpressing cells (4TO-NOS). The levels of MAPK (A), p-MAPK (B), Bcl-2 (C), STAT3 (D), Akt1 (E) and p-Akt (F) were all significantly increased in NOS-3 overexpressing cells compared to cells transfected with the empty vector. The proportion of p-MAPK/MAPK ratio increased markedly (G) whereas the p-Akt relative to total Akt1 did not change (H). Data are presented as mean ± SEM ($n=3$ independent experiments). The values labeled with "a" were significantly different *versus* the corresponding control cell lineage. The images are representative of three different experiments.

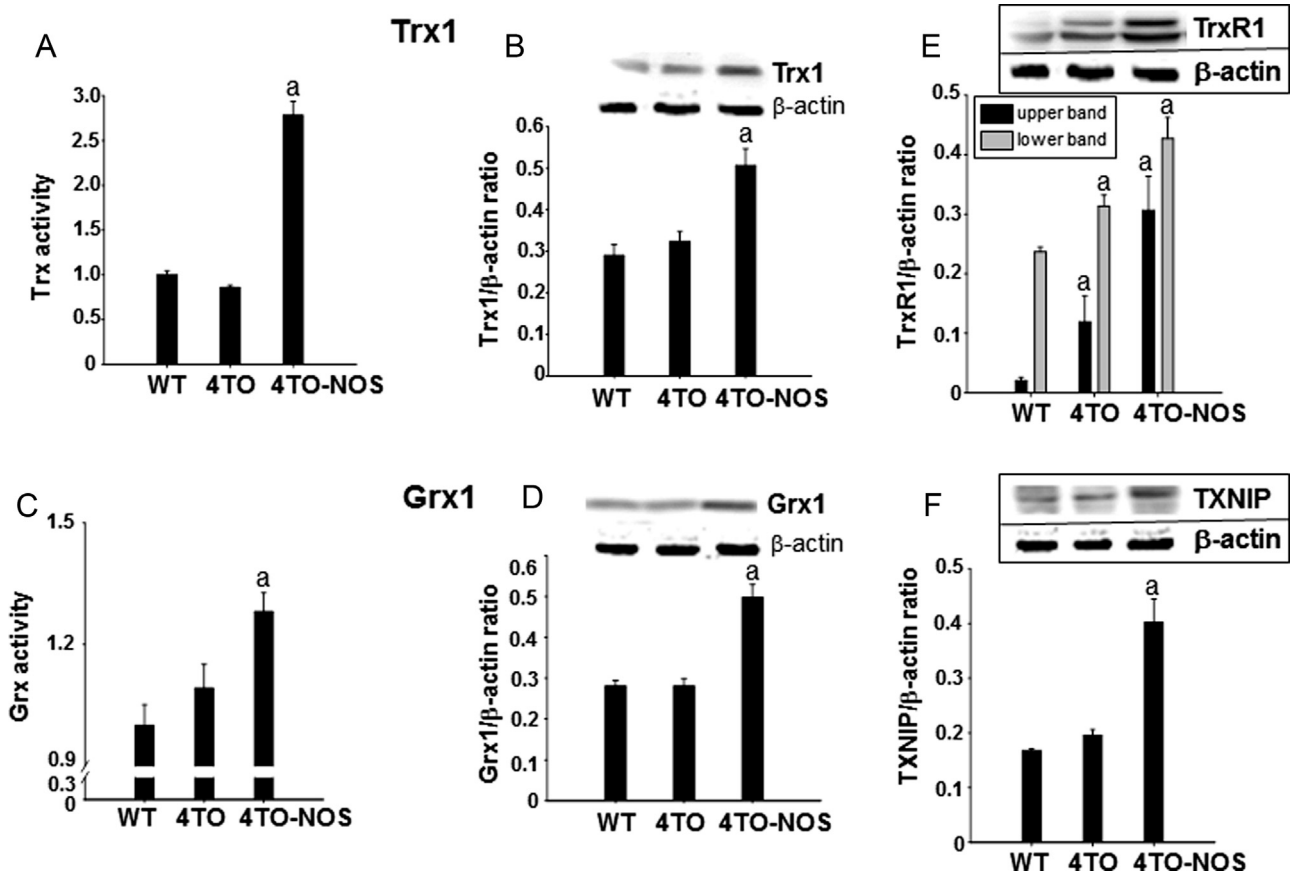


Fig. 3. High levels of nitric oxide induced activity and expression of redox proteins. Trx activity (A) and Trx1 protein expression (B), Grx activity (C) and Grx1 protein expression (D), TrxR (E) and TXNIP (F) protein expression increased in NOS-3 overexpressing cells compared to cells transfected with the empty vector. Data are presented as mean ± SEM ($n=3$ independent experiments) and the groups labeled with "a" were significantly statistical ($p \leq 0.05$) versus the corresponding control group. Representative Western blotting images are shown.

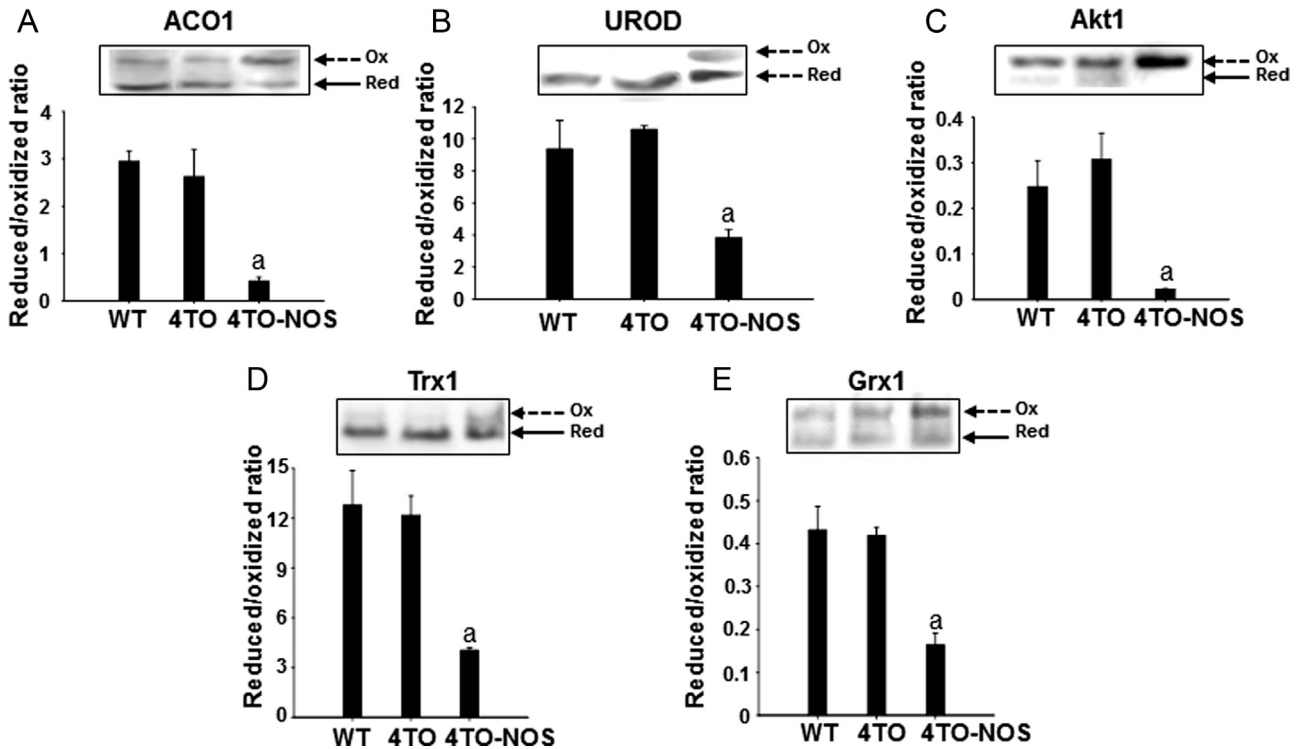


Fig. 4. Effect of overexpression of NOS-3 on thiolic redox state of different proteins. Electrophoretic redox mobility shift to detect the oxidized and reduced forms (arrows) are showed. The high levels of NO known to prevail in these cells caused a redox shift to more oxidized in ACO1 (A), UROD (B), Akt1 (C) and in both studied redoxins, Trx (D) and Grx (E).

be interacting (see below).

3.5. Effect of overexpression of NOS-3 on thiolic redox state of several proteins

Thiol redox changes may be part of regulatory mechanisms of proteins, so we analyzed the thiolic redox state of several proteins to check whether this type of mechanism could be potentially operative in NOS3 overexpressing cells. We have detected a redox shift of ACO1 and UROD towards more oxidized states (Fig. 4A and B), which could result in iron metabolism perturbation. Signaling pathways could also be affected by redox changes since Akt1 shifted to more oxidized state under nitrosative pressure (Fig. 4C). Changes in the redox state of MAPK, STAT3 and Bcl-2 could not be detected under our experimental conditions and with our redox electrophoretic mobility shift assay. However, the thiolic redox state of Trx1 and Grx1 shifted to more oxidized in the NOS-3 overexpressing cells (Fig. 4D and E) a likely consequence of the nitrosative and oxidative stress [37].

3.6. Specific silencing of Trx1 and Grx1

As shown above, Trx1 and Grx1 levels increased upon NOS3 overexpression in HepG2 cells. To go deep into the role of these

proteins in the adaptation to high NO levels, we studied the effect of down-regulation of both proteins. Treatment of WT, 4TO and NOS-3 overexpressing HepG2 cells with vectors harboring siRNA specifically directed to Trx1 and Grx1 mRNA produced a $\approx 75\%$ decrease in Trx1 and Grx1 protein levels in the three cell lineages (Fig. 5A and C). These changes in protein levels were accompanied by equivalent functional fall off, as indicated by their canonical enzymatic activities (Fig. 5B and D).

3.7. Effect of Trx1 and Grx1 silencing on the levels of tyrosine nitration in normal and NOS-3 overexpressing HepG2 cells

Tyrosine nitration is mediated by reactive nitrogen species such as peroxynitrite (ONOO^-) anion and nitrogen dioxide, formed as secondary products of NO metabolism in the presence of oxidants including superoxide radicals ($\text{O}_2^{\cdot-}$) and hydrogen peroxide (H_2O_2) [45]. For this reason, the level of Tyr nitration is indicative of the degree of nitrosative and oxidative stress and we measured it to check the effect of Trx1 and Grx1. Overexpression of NOS-3 in HepG2 cells induced protein Tyr nitration (Fig. 6, black bars). Silencing of Trx1 and Grx1 also increased protein tyrosine nitration in wild type and 4TO cells, but, interestingly, had the opposite effect on NOS-3 overexpressing cells (Fig. 6). These results uncover an apparent conflict, e.g., a decrease in antioxidant defenses, Trx1

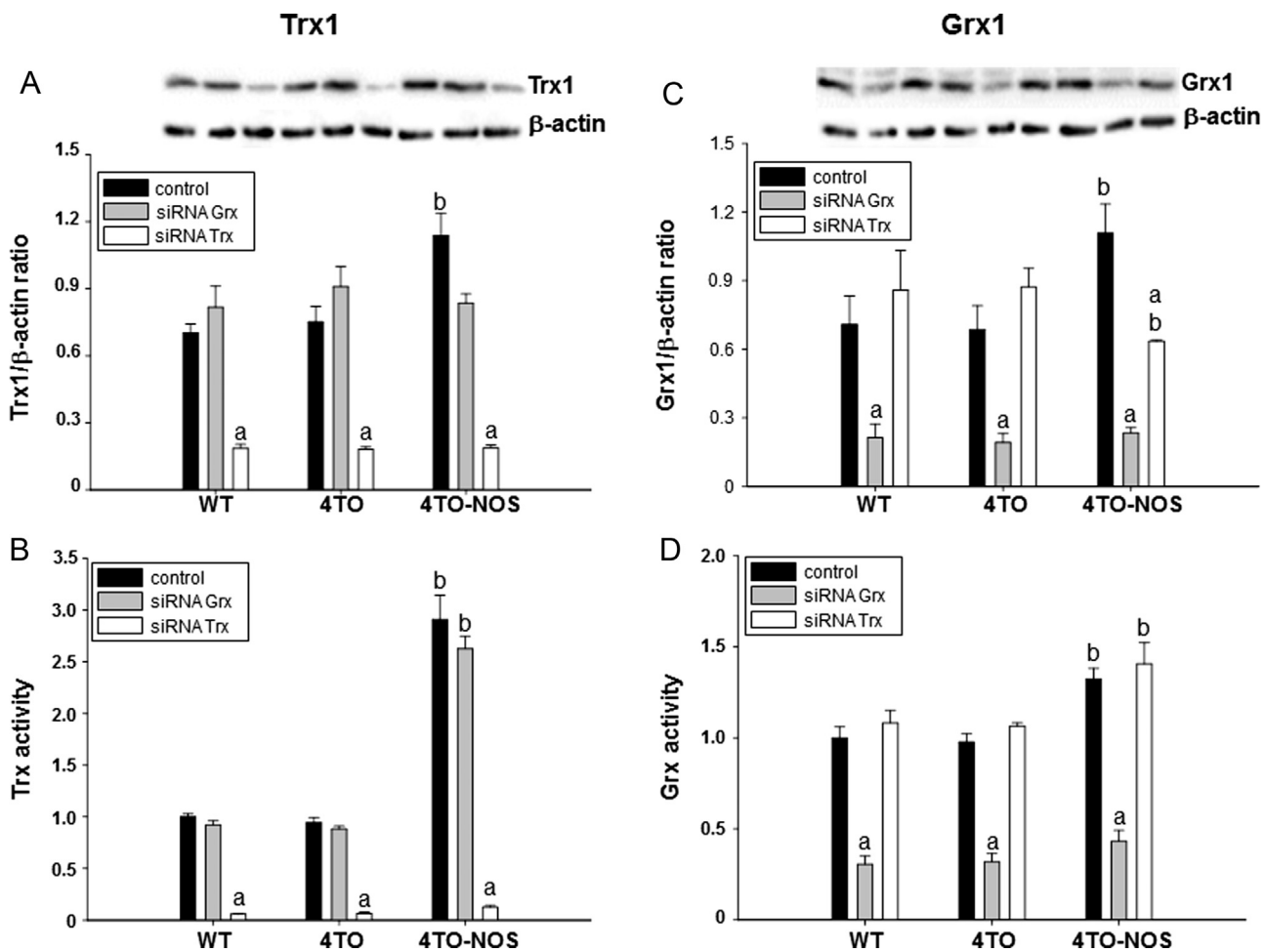


Fig. 5. Down regulation of Trx1 and Grx1 in HepG2 cells by treatment with specific siRNAs. Protein levels and activity of Trx1 (A, B) and Grx1 (C, D) were determined in HepG2 cells with and without NOS-3 overexpression and treated or not with siRNATrx and siRNAGrx. Representative images of Western blot membranes used to quantify protein levels are shown in A and C. The protein levels and activities of both redoxins were significantly higher in NOS-3 overexpressing cells (4TO-NOS, black bars). Treatment with the specific siRNA produced a $\approx 75\%$ decrease in protein levels and activities of both redoxins in control and NOS-3 overexpressing cells, confirming the efficacy of the treatments. Data are presented as mean \pm SEM ($n=3$ independent experiments). The values labeled with "a" were significantly different versus the corresponding internal control in the same cell lineage. The values labeled with "b" were significantly different versus the corresponding control cell lineage. The images are representative of three different experiments.

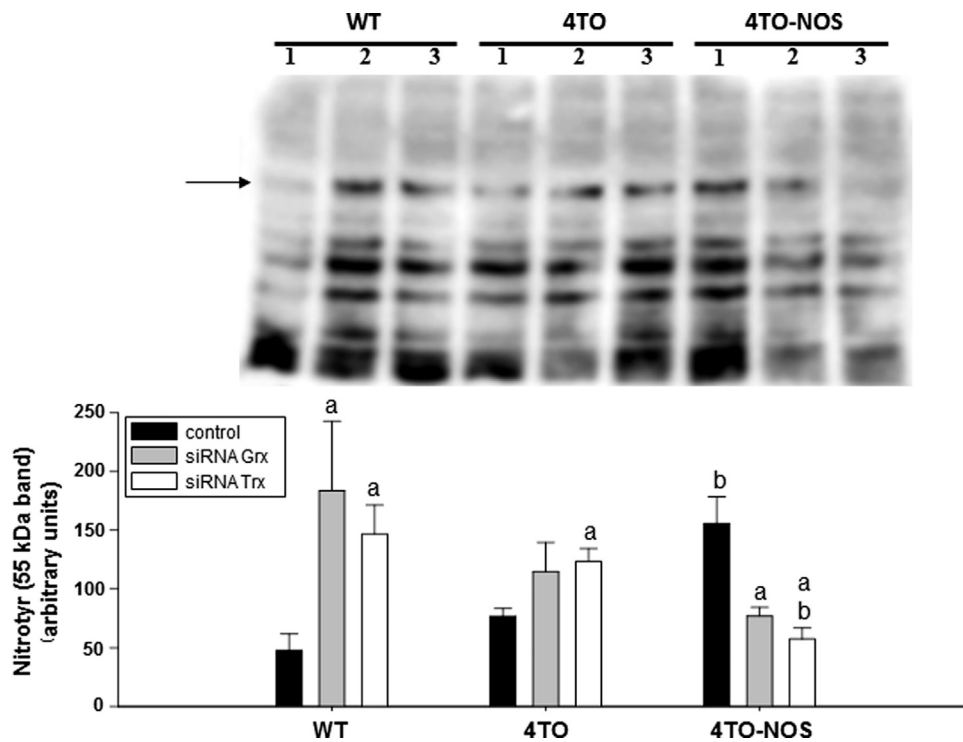


Fig. 6. Detection of nitrotyrosine levels in NOS-3 overexpressing HepG2 cells with Grx and Trx down regulation. The detection of this postranslational modification was performed by Western blot with the analysis focused on a representative 55 kDa band (arrow). The image is representative of three different experiments and densitometric data of $n=3$ independent experiments are presented in the histogram below as mean \pm SEM. The numbers 1, 2 and 3 indicate the cell treatments control, siRNA Grx and siRNA Trx respectively. NOS-3 overexpression induced Tyr nitration of proteins in HepG2 cells (black bars). This effect was offset by treatment with siRNA Grx and siRNA Trx as shown in the 4TO-NOS group. However, in WT and 4TO HepG2 cells siRNA Grx and siRNA Trx treatment had the opposite effect, inducing Tyr nitration of proteins. Statistical significance was assessed by ($p \leq 0.05$). The values labeled with "a" were significantly different versus the corresponding internal control in the same cell lineage. The values labeled with "b" were significantly different versus the corresponding control cell lineage.

and Grx1, results in alleviation of oxidative stress.

3.8. Cellular proliferation and apoptosis in NOS-3 overexpressing cells: effect of Trx1 and Grx1

Nitrosative stress in HepG2 cells as a consequence of NOS3 overexpression results in reduction of cell number and proliferation (Fig. 7A and C) in agreement with a previous report [37]. In the current study we show that silencing Trx1 or Grx1 further decreased the number of cells and proliferation in all cell lineages and siRNA Trx further reduced cell viability (Fig. 7A–C). siRNA Grx or siRNA Trx treatments also provoked a striking increase in caspase-3 and caspase-8 activities in all cells (Fig. 7D and E), but lowered the levels of CD95 in NOS-3 overexpressing cells (Fig. 7F). Increase in caspases activities was actually accompanied by signs of increased apoptosis like DNA fragmentation as determined by TUNEL assay (Fig. 8). These results are worthy of consideration as they point to a moonlighting role of the redoxins depending on the prevailing cellular redox conditions as will be discussed in the next section (Fig. 9).

3.9. Effect of Trx1 and Grx1 silencing on the levels and redox state of Akt1 in normal and NOS-3 overexpressing HepG2 cells

Akt1 is known to be affected by thiol redox changes and is a major agent in the control of apoptosis, so it was pertinent to study its response to redoxins down-regulation. Trx1 or Grx1 specific siRNA counteracted the effect of the NOS-3 overexpression, regarding both, total levels (Fig. 8A–C) and redox state (Fig. 8D) of Akt. Grx1 and Trx1 down-regulation shifted Akt towards a more reduced state but at the same time, there was a parallel marked decrease in total Akt protein.

4. Discussion

NOS3 overexpression in HepG2 cells induces oxidative stress and slight but significant activation of apoptosis. In these conditions the cells undergo a pronounced metabolic remodeling as deduced from the changes observed in the levels of checkpoint enzymes from key metabolic pathways.

In mammals, there are two genes encoding pyruvate kinase that produce two isoforms. Whereas PKM1 is a constitutively active enzyme, PKM2 is expressed in all cancers and cancer cell lines studied to date. PKM2 is highly regulated at both the activity and expression levels allowing this isoform to act as floodgate keeper to change the metabolic flux from lactate production to NADPH and anabolic pathways. This metabolic change is particularly relevant under conditions of oxidative stress [46], thus explaining the induction of PKM2 in NOS3 overexpressing cells and in coherent with the observed concomitant induction of TKT.

UROD has been considered a target for head and neck cancer treatment [47]. It plays a key role in the biosynthesis of heme group and its down-regulation has been shown to increase oxidative stress and affect the cellular iron homeostasis. Its up-regulation in NOS3 overexpressing cells (Fig. 1D) could be counterbalanced by inactivation through thiol oxidation [48] as shown in Fig. 4B. These results, together with the observed down-regulation of ACO1, indicate that cytosolic iron metabolism is perturbed.

MATs (methionine adenosyltransferases) are regulated by oxidative stress and are associated to different pathologies such as hepatocellular carcinoma and diabetes [49]. The decrease in MATII levels we have observed in NOS-3 overexpressing cells mean that AdoMet levels were reduced in those cells, with negative consequences for nucleotide biosynthesis and hence for proliferation, which would agree with the results on cell proliferation shown in

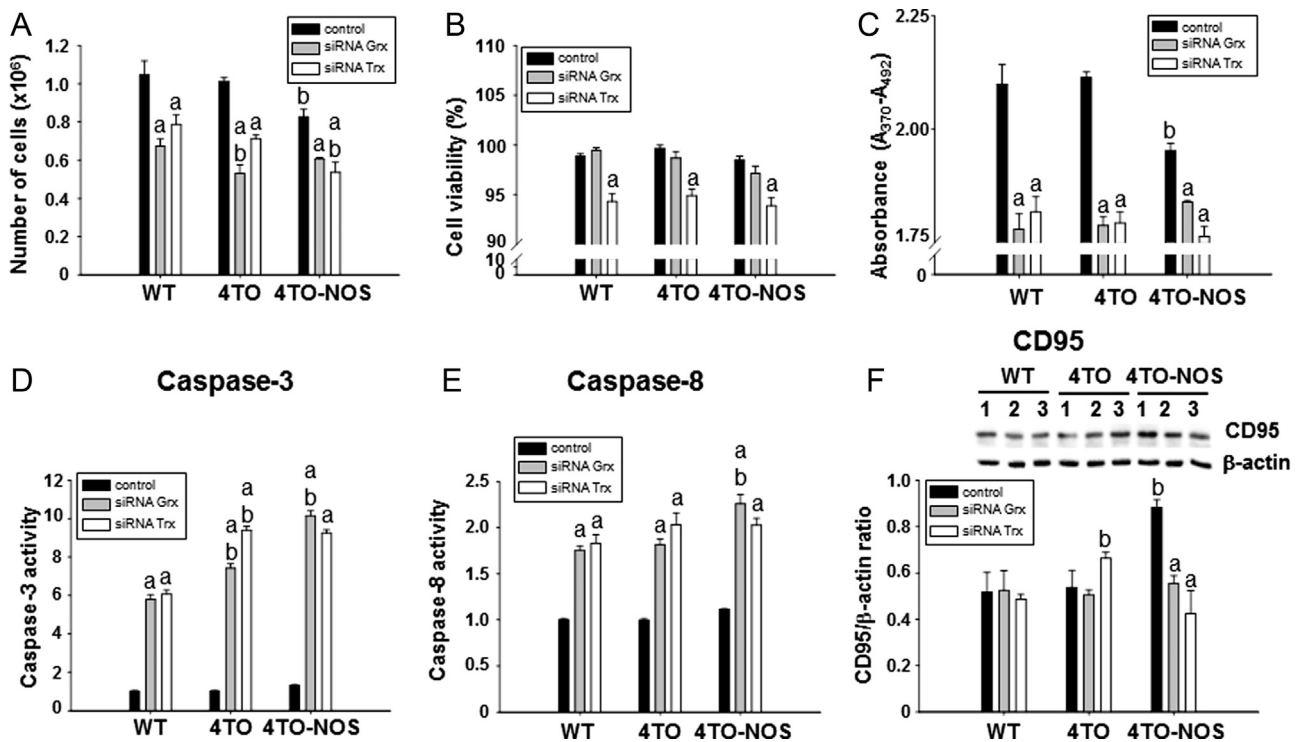


Fig. 7. Effect of down-regulation Grx and Trx on cell proliferation and cell death induced by NOS-3. Number of total cells (A), cell viability (B) and incorporation of BrdU (C) in WT, 4TO and 4TO-NOS cells. Treatment with siRNA Grx and siRNA Trx significantly diminished the number of cells (gray and white bars) and siRNA Trx further reduced cell viability in all cell lineages (white bars). Caspase-3 (D) and caspase-8 (E) activities, known markers of apoptosis, were also markedly increased in all cell types by treatment with either siRNA Grx or siRNA Trx, whereas the same treatments offset the increase in CD95 receptor levels induced by NOS-3 overexpression (F). The numbers 1, 2 and 3 refer to control, siRNA Grx and siRNA Trx treatments, respectively. Data are presented as mean \pm SEM ($n=3$ independent experiments). The values labeled with "a" were significantly different versus the corresponding internal control in the same cell lineage. The values labeled with "b" were significantly different versus the corresponding control cell lineage. The images are representative of three different experiments.

Fig. 7. This situation would make sense under the oxidative conditions prevailing in those cells, since the metabolic flux would be compensated by diversion towards pentose phosphate pathway for NADPH production and antioxidant defense.

The serine/threonine kinase Akt is a critical component of an intracellular signaling pathway that exerts effects on cell survival and apoptosis. Akt is activated by insulin and various growth and survival factors. The unphosphorylated form of Akt is inactive and it is activated by phosphorylation at Thr308 by PDK1 and at Ser473 by mTOR2. It can also be inactivated by protein phosphatase 2A (PP2A) dephosphorylation when Akt is in its oxidized form [50]. It has been shown that Grx prevented Akt from forming a specific disulfide bond and suppressed its association with PP2A under oxidative stress, resulting in phosphorylation of Akt and inhibition of apoptosis. In Fig. 2E–H, we show that nitrosative stress caused the increase of both Akt forms (Akt1 and p-Akt), accompanied by a shift towards a more oxidized state (Fig. 4C). This would mean that Akt is prone to inactivation by dephosphorylation under NOS-3 overexpression conditions, which indicates that apoptosis is being favored.

The redox state and total protein levels of Akt are both under the influence of Trx1 and Grx1 as will be detailed in another section below.

The mitogen-activated protein kinase (MAPK) cascades are multifunctional signaling pathways involved in cell growth, differentiation, apoptosis and cellular response to stress. Two different MAP kinase cascades that converge to c-Jun N-terminal kinases (JNK) and p38 MAP Kinases are mainly activated by cytotoxic stresses, oxidative/nitrosative stress and proinflammatory cytokines such as tumor necrosis factor (TNF)- α [32].

Our results show that MAPK is more phosphorylated in NOS3 overexpressing cells and hence less active. At first sight, this result

would conflict with the fact that Trx1 and Grx1 had shifted to more oxidized state in these cells (Fig. 4D and E) because oxidation of both redoxins would suppress their inhibiting interaction with apoptosis signal-regulating kinase 1 (ASK1) [50]. ASK1 would then be free to initiate the MAPK cascade leading to activation of JNK or p38 [51]. The explanation of this apparently contradictory result could be that downstream p38MAPK, which is prone to tyrosine nitration as opposed to phosphorylation, could not be activated under the nitrosative pressure with elevated levels of nitrotyrosine (see Fig. 6).

Human Bcl-2 is an anti-apoptotic, membrane-associated oncoprotein that can be directly affected by oxidative stress induced by NO [44] and could play an important role in NO-induced apoptosis. In Fig. 2C, we show a significant increase in Bcl-2 in HepG2 cells under nitrosative stress. STAT3, the key cell growth regulator signal transducer and activator of transcription, is subject to redox regulation by glutathionylation and ROS trigger tyrosine phosphorylation and nuclear translocation of STAT3. Glutathionylated STAT3 was a poor Janus protein tyrosine kinase 2 substrate, and it exhibited low DNA-binding activity [52]. Furthermore, the effect of inactivation of STAT3 has resulted in inhibition of growth and metastasis of human hepatocellular carcinoma cells, and increase in their chemo-sensitivity.

The observed increases in Bcl-2 and STAT3 in NOS3 overexpressing cells may be part of a counteracting cellular response to induction of cell death, although the activation state of Bcl-2 and the glutathionylation state of STAT3 should have to be determined to support this reasoning. So far, we could not detect redox changes in both proteins by the electrophoretic redox mobility shift assay, but ongoing redox proteomic studies could throw light to this question.

Trx1 was detected in a more oxidized state in NOS3

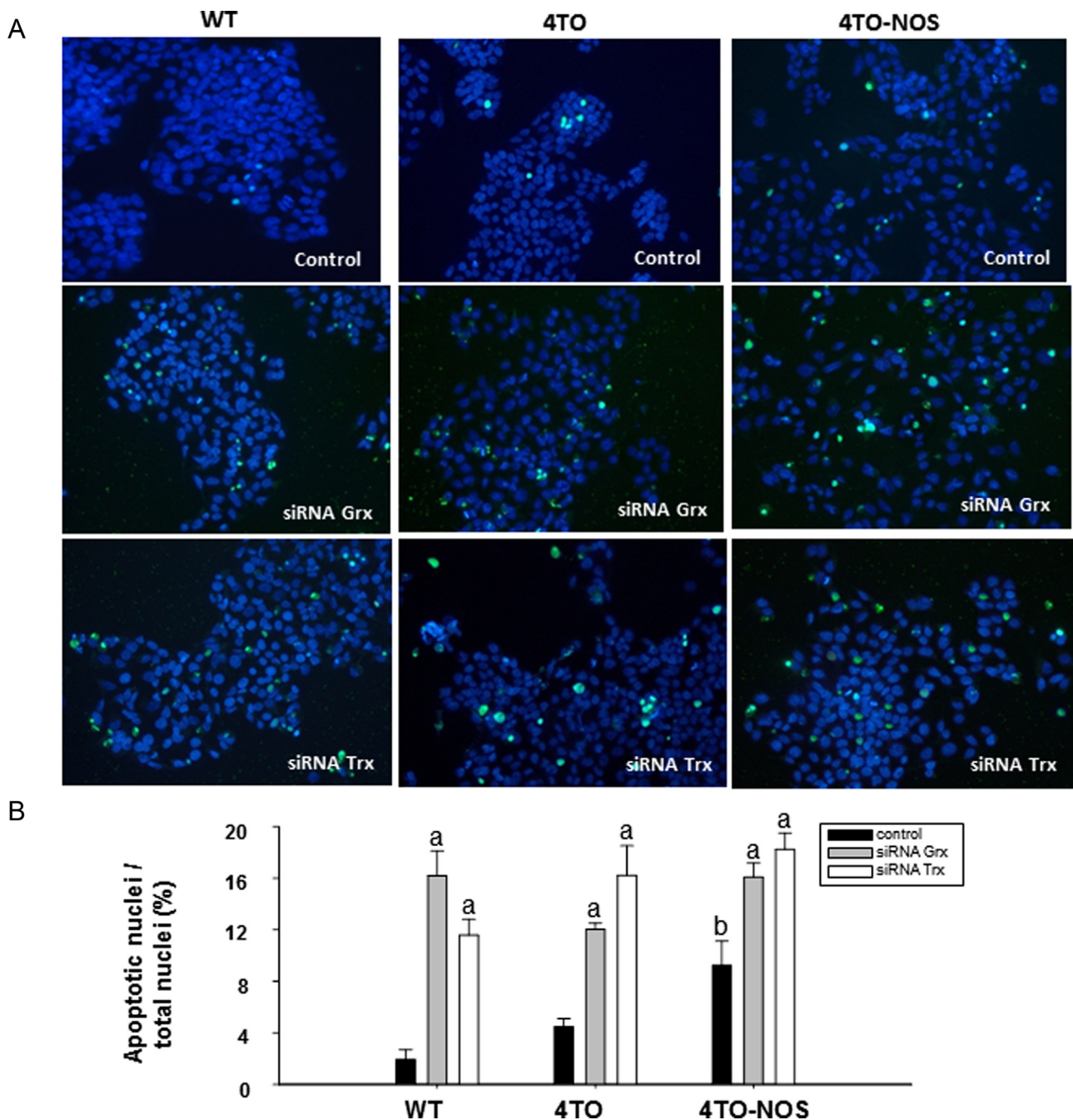


Fig. 8. Effect of down-regulation of Grx and Trx on apoptosis. DNA fragmentation in cells detected by terminal deoxynucleotidyl transferase (TdT)-mediated dUTP nick end labeling (TUNEL). We have selected representing merged images of FITC and DAPI fluorescence of these treatments in the cell lineages studied (A). Apoptotic nuclei vs. total nuclei in percentage detected in different fluorescence images of control, siRNA Grx and siRNA Trx treated cells in 3 independent experiments (B). The values labeled with "a" were significantly different ($p \leq 0.05$) versus the corresponding internal control in the same cell lineage. The values labeled with "b" were significantly different versus the corresponding control cell lineage.

overexpressing cells than in normal HepG2 cells (Fig. 4D). Trx1 is mostly found in the cytoplasm; however, it moves to the nucleus as a response to nitrosative/oxidative stress and this Trx1 nuclear migration has been described as part of a survival signaling pathway, associated with intracellular compartmentalization and activation of ERK1/2 MAP Kinases. TXNIP prevents Trx1 nuclear migration and its expression was down-regulated in different human carcinomas [53], however, it binds to reduced Trx1 but not to oxidized Trx1. Hence, in the oxidative environment of NOS-3 overexpressing cells, inhibition of Trx1 by TXNIP might not be fully operative despite the increase in TXNIP levels.

The increase in protein Tyr nitration occurring in WT cells upon

Trx1 and Grx1 down-regulation was an indication of oxidative stress [54], the expected consequence of a drop in thiol antioxidant defenses. However, in NOS-3 overexpressing cells, whose redoxins levels are markedly higher (Fig. 3), silencing of Trx1 and Grx1 provokes a decrease in nitro-Tyr levels (Fig. 6). It has been noted that nitration processes are promoted over other oxidative modifications in specific protein targets [55] and it has also been suggested that nitration is a reversible process [56]. Whether the observed parallel drop in protein nitration and Trx1 and Grx1 levels in NOS-3 overexpressing cells is an indication of specificity of the nitration process, its reversibility or the degradation of nitrated proteins, is an interesting matter for further research and adds up

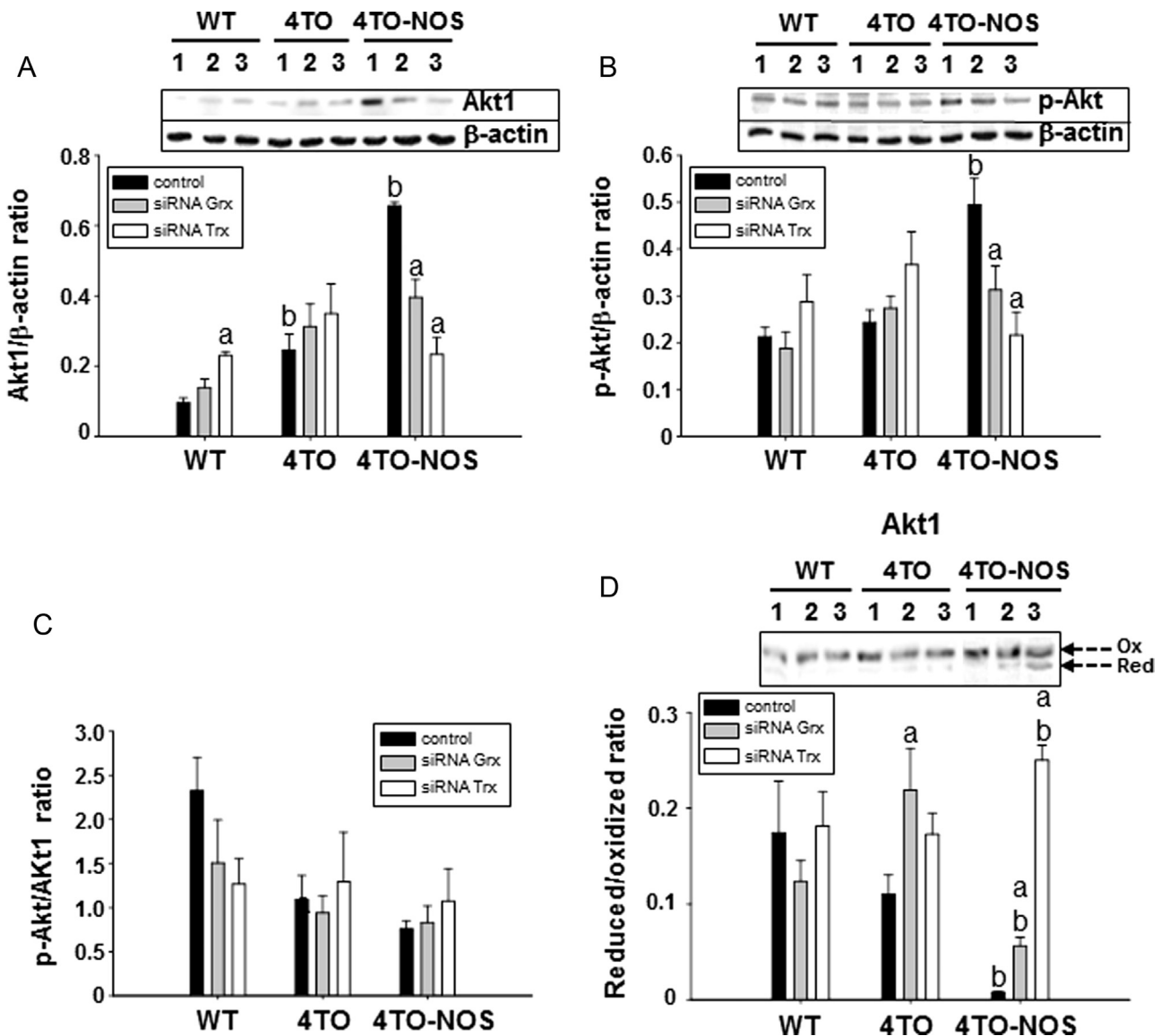


Fig. 9. Effect of down-regulation of Grx and Trx on Akt phosphorylation and redox state. Western blot analysis of the expression of Akt1 (A) and p-Akt (B) proteins and their relative quantitation in the HepG2 wild type cells (WT) and control cells (4TO), as well as in NOS-3 overexpressing cells (4TO-NOS). The numbers 1, 2 and 3 refer to control, siRNA Grx and siRNA Trx treatments, respectively. The enhancing effect of NOS-3 overexpression on Akt1 (A) and p-Akt (B) protein levels was offset by siRNA Grx (gray bars, 2) and even more by siRNA Trx (white bars, 3). None of these siRNA treatments had effect on the p-Akt/Akt1 ratio (C). However, silencing Grx1 and more prominently Trx1, shifted the redox state of Akt1 to the reduced form (arrows) in NOS-3 overexpressing cells (D). Data are presented as mean \pm SEM ($n=3$ independent experiments). The values labeled with "a" were significantly different ($p \leq 0.05$) versus the corresponding internal control in the same cell lineage. The values labeled with "b" were significantly different versus the corresponding control cell lineage. The images are representative of three different experiments.

to the debate [57].

The observed neutralization of CD95 induction in NOS-3 overexpressing cells by Trx1 or Grx1 down regulation (Fig. 7F) suggest that the high levels of both thiol-disulfide oxidoreductases prevailing in these cells (Fig. 3) are required to induce the expression of CD95. Activation of the extrinsic apoptotic pathway, indicated by the increase in caspase-8 activity (Fig. 7E), despite the drop in dead receptor CD95 levels, points to the operation of other proapoptotic mechanism involving thiol redox changes.

Many reports have documented the influence of redox changes on the apoptotic signaling pathways in a variety of cell types through glutathionylation and S-nitrosylation of cysteines in various proteins along the signaling cascade, from receptors to caspases, with the involvement of Grx and Trx in most cases [58]. Trx1 acting as denitrosylating enzyme counteracted inactivation of caspase-3 and -8 by S-nitrosylation in HepG2 cells [28]. But on the other hand, Trx1 can be S-nitrosylated itself [59] and this oxidized

Trx1 can impede apoptosis by S-transnitrosylation of caspase-3 [29,60]. Thus, depending on the redox state of the cell, Trx1 can catalyze either trans-S-nitrosylation or S-denitrosylation reactions [29,61]. Total levels of Trx1 increase in NOS-3 overexpressing cells but a measurable proportion of the protein is in the oxidized state (Fig. 4D) and could be acting on caspase-3 to inhibit it. This inhibitory effect would be alleviated in siRNA Trx treated cells in which the total amount of Trx1 drops down to $\approx 25\%$.

Most of the effects of siRNA Trx treatment were also attained by treatment with siRNA Grx, reflecting a degree of similarity of both redoxins in the control of redox homeostasis, although differences also exist. Both proteins have been related to apoptosis regulation through redox modulation of stress activated and ASK1 [32] although the role of Grx1 has been documented to more extent [50].

This increase of thiolic form of Akt when the levels of thiol antioxidant redoxins decrease would favor activation by phosphorylation and apoptosis inhibition, whereas the parallel

decrease in total Akt protein would attenuate the antiapoptotic potential of Akt. This increase of thiolic form of Akt when the levels of thiol antioxidant redoxins decrease may sound contradictory, but could be caused by the proteasome differentially degrading the oxidized form, thus unbalancing the redox equilibrium towards the reduced form. Inactivation and proteasomal degradation of Akt upon Grx1 down-regulation had been observed before [35]. The effect of down-regulation of Grx1 and Trx1 on Akt redox state followed the same trend but the changes were more pronounced when Trx1 was silenced, which could be correlated with fading of its denitrosylase activity.

5. Conclusions

Overexpression of NOS-3 has antiproliferative effect on HepG2 cells. Activation of apoptosis, as demonstrated by increases in caspases activity, is the final outcome resulting from the balance of multilevel and conflicting cellular responses to the oxidative stress generated by the elevated level of NO. Among these, metabolic remodeling potentiates the pentose phosphate pathway to increase the metabolic flux towards NADPH production for antioxidant defense at the expenses of lowering nucleotide biosynthesis and therefore proliferation. Proteins of the antioxidant redoxin systems and proteins involved in cell survival pathways and phosphorylation of MAPK increase significantly. At the same time, the thiolic redox state of Akt1, Trx1 and Grx1 shifts to more oxidized.

The important finding of our study is that Trx1 and Grx1, principal actors of the antioxidant response induced by increased NO levels, are actually a hindrance to the antiproliferative action of NO. Down regulation of either redoxin by specific siRNAs activates caspases dramatically and reduces cell proliferation. These results support the contention that weakening the thiolic antioxidant defenses enhances the antiproliferative effects on tumoral cells.

Acknowledgments

This research was supported by grants from the Spanish Ministry of Economy and Competitiveness (BFU2012-32056) and from the Andalusian Government (BIO-0216 and CTS-6264). We thank Biomedical Research Network Center for Liver and Digestive Diseases (CIBERehd) founded by "Instituto de Salud Carlos III".

Appendix A. Supplementary material

Supplementary data associated with this article can be found in the online version at <http://dx.doi.org/10.1016/j.redox.2015.07.007>.

References

- [1] J. Muntané, M. la Mata, Nitric oxide and cancer, *World J. Hepatol.* 2 (2010) 337–344.
- [2] W. Alderton, C. Cooper, R. Knowles, Nitric oxide synthases: structure, function and inhibition, *Biochem. J.* 357 (2001) 593–615.
- [3] D.A. Geller, T.R. Billiar, Molecular biology of nitric oxide synthases, *Cancer Metastasis Rev.* 17 (1998) 7–23.
- [4] U. Forstermann, J.P. Boissel, H. Kleinert, Expressional control of the 'constitutive' isoforms of nitric oxide synthase (NOS I and NOS III), *FASEB J.* 12 (1998) 773–790.
- [5] D. Bredt, P. Hwang, G. CE., C. Lowenstein, R. Reed, S. Snyder, Cloned and expressed nitric oxide synthase structurally resembles cytochrome P-450 reductase, *Nature* 351 (1991) 714–718.
- [6] S. Lamas, P. Marsden, G. Li, P. Tempst, T. Michel, Endothelial nitric oxide synthase: molecular cloning and characterization of a distinct constitutive enzyme isoform, *Proc. Natl. Acad. Sci. USA* 89 (1992) 6348–6352.
- [7] C. Lyons, G. Orloff, J. Cunningham, Molecular cloning and functional expression of an inducible nitric oxide synthase from a murine macrophage cell line, *J. Biol. Chem.* 267 (1992) 6370–6374.
- [8] Q. Xie, H. Cho, J. Calaycay, R. Mumford, K. Swiderek, T. Lee, A. Ding, T. Troso, C. Nathan, Cloning and characterization of inducible nitric oxide synthase from mouse macrophages, *Science* 256 (1992) 225–228.
- [9] W. Xu, L. Liu, M. Loizidou, M. Ahmed, I. Charles, The role of nitric oxide in cancer, *Cell Res.* 12 (2002) 311–320.
- [10] Y. Boo, H. Kim, H. Song, D. Fulton, W. Sessa, H. Jo, Coordinated regulation of endothelial nitric oxide synthase activity by phosphorylation and subcellular localization, *Free Radic. Biol. Med.* 41 (2006) 144–153.
- [11] S. Oess, A. Icking, D. Fulton, R. Govers, W. Müller-Esterl, Subcellular targeting and trafficking of nitric oxide synthases, *Biochem. J.* 396 (2006) 401–409.
- [12] Y. Iwakiri, A. Satoh, S. Chatterjee, D. Toomre, C. Chalouni, D. Fulton, R. Groszmann, V. Shah, W. Sessa, Nitric oxide synthase generates nitric oxide locally to regulate compartmentalized protein S-nitrosylation and protein trafficking, *Proc. Natl. Acad. Sci. USA* 103 (2006) 19777–19782.
- [13] C. Li, G. Woga, Nitric oxide as a modulator of apoptosis, *Cancer Lett.* 226 (2005) 1–15.
- [14] H. Li, A. Wan, Apoptosis of rheumatoid arthritis fibroblast-like synoviocytes: possible roles of nitric oxide and the thioredoxin 1, *Mediat. Inflamm.* 2013 (2013) 1–8.
- [15] B. Buchanan, Y. Balmer, Redox regulation: a broadening horizon, *Annu. Rev. Plant Biol.* 56 (2005) 187–220.
- [16] J. Burgoyne, M. Madhani, F. Cuello, R. Charles, J. Brennan, E. Schröder, D. Browning, P. Eaton, Cysteine redox sensor in PKG(α) enables oxidant-induced activation, *Science* 317 (2007) 1393–1397.
- [17] P. Ghezzi, V. Bonetto, M. Fratelli, Thiol-disulfide balance: from the concept of oxidative stress to that of redox regulation, *Antioxid. Redox Signal.* 7 (2005) 964–972.
- [18] A. Martínez-Ruiz, S. Cadenas, S. Lamas, Nitric oxide signaling: classical, less classical, and nonclassical mechanisms, *Free Radic. Biol. Med.* 51 (2011) 17–29.
- [19] D. Hess, A. Matsumoto, S. Kim, H. Marshall, J. Stamler, Protein S-nitrosylation: purview and parameter, *Nat. Rev. Mol. Cell. Biol.* 6 (2005) 150–166.
- [20] B. Derakhshan, G. Hao, S. Gross, Balancing reactivity against selectivity: the evolution of protein S-nitrosylation as an effector of cell signaling by nitric oxide, *Cardiovasc. Res.* 75 (2007) 210–219.
- [21] M. Foster, T. McMahon, J. Stamler, S-nitrosylation in health and disease, *Trends Mol. Med.* 9 (2003) 160–168.
- [22] H. Nakamura, K. Nakamura, J. Yodoi, Redox regulation of cellular activation, *Annu. Rev. Immunol.* 15 (1997) 351–369.
- [23] A. Holmgren, Thioredoxin and glutaredoxin systems, *J. Biol. Chem.* 264 (1989) 13963–13966.
- [24] A. Holmgren, C. Johansson, C. Berndt, M. Lönn, C. Lillig, Thiol redox control via thioredoxin and glutaredoxin systems, *Biochem. Soc. Trans.* 33 (2005) 1375–1377.
- [25] C. Padilla, E. Martínez-Galisteo, J. Bárcena, G. Spyrou, A. Holmgren, Purification from placenta, amino acid sequence, structure comparisons and cDNA cloning of human glutaredoxin, *Eur. J. Biochem.* 227 (1995) 27–34.
- [26] M. Gallogly, J. Mieyal, Mechanisms of reversible protein glutathionylation in redox signaling and oxidative stress, *Curr. Opin. Pharmacol.* 7 (2007) 381–391.
- [27] M. Benhar, M. Forrester, J. Stamler, Regulated protein denitrosylation by cytosolic and mitochondrial thioredoxins, *Science* 320 (2008) 1050–1054.
- [28] R. Sengupta, T. Billiar, V. Kagan, D. Stoyanovsky, Nitric oxide and thioredoxin type 1 modulate the activity of caspase 8 in HepG2 cells, *Biochem. Biophys. Res. Commun.* 391 (2010) 1127–1130.
- [29] D. Mitchell, M. Marletta, Thioredoxin catalyzes the S-nitrosylation of the caspase-3 active site cysteine, *Nat. Chem. Biol.* 1 (2005) 154–158.
- [30] Y. Du, H. Zhang, J. Lu, A. Holmgren, Glutathione and glutaredoxin act as a backup of human thioredoxin reductase 1 to reduce thioredoxin 1 preventing cell death by aurothioglucose, *J. Biol. Chem.* 287 (2012) 38210–38219.
- [31] E. Arner, A. Holmgren, The thioredoxin system in cancer, *Semin. Cancer Biol.* 16 (2006) 420–426.
- [32] M. Saitoh, H. Nishitoh, M. Fujii, K. Takeda, K. Tobiume, Y. Sawada, M. Kawabata, K. Miyazono, H. Ichijo, Mammalian thioredoxin is a direct inhibitor of apoptosis signal-regulating kinase (ASK) 1, *EMBO J.* 17 (1998) 2596–2606.
- [33] H. Li, A. Wan, G. Xu, D. Ye, Small changes huge impact: the role of thioredoxin 1 in the regulation of apoptosis by S-nitrosylation, *Acta Biochim. Biophys. Sin.* 45 (2013) 153–161.
- [34] D. Greetham, P. Kritsiligkou, R. Watkins, Z. Carter, J. Parkin, C. Grant, Oxidation of the yeast mitochondrial thioredoxin promotes cell death, *Antioxid. Redox Signal.* 18 (2013) 376–385.
- [35] F. Ahmad, P. Nidadavolu, L. Durgados, V. Ravindranath, Critical cysteines in Akt1 regulate its activity and proteasomal degradation: implications for neurodegenerative diseases, *Free Radic. Biol. Med.* 74 (2014) 118–128.
- [36] M. Enoksson, A. Fernandes, S. Prast, C. Lillig, A. Holmgren, S. Orrenius, Overexpression of glutaredoxin 2 attenuates apoptosis by preventing cytochrome c release, *Biochem. Biophys. Res. Commun.* 327 (2005) 774–779.
- [37] R. González, G. Ferrín, P. Aguilar-Melero, I. Ranchor, C. Linares, R. Bello, M. De la Mata, V. Gogvadze, J. Bárcena, J. Álamo, S. Orrenius, F. Padillo, B. Zhivotovskiy, J. Muntané, Targeting hepatoma using nitric oxide donor strategies, *Antioxid. Redox Signal.* 18 (2013) 491–506.
- [38] L. López-Sánchez, F. Corrales, M. De la Mata, J. Muntané, A. Rodríguez-Ariza, Detection and proteomic identification of S-nitrosated proteins in human hepatocytes, *Methods Enzymol.* 440 (2008) 273–281.

- [39] I. Harris, A. Treloar, S. Inoue, M. Sasaki, C. Gorrini, K. Lee, K. Yung, D. Brenner, C. Knobbe-Thomsen, M. Cox, A. Elia, T. Berger, D. Cescon, A. Adeoye, A. Brüstle, S. Molyneux, J. Mason, W. Li, K. Yamamoto, A. Wakeham, H. Berman, R. Khokha, S. Done, T. Kavanagh, C. Lam, T. Mak, Glutathione and thioredoxin antioxidant pathways synergize to drive cancer initiation and progression, *Cancer Cell* 27 (2015) 211–222.
- [40] J. Watson, Oxidants, antioxidants and the current incurability of metastatic cancers, *Open Biol.* 3 (2013) 1–9.
- [41] M. Luthman, A. Holmgren, Glutaredoxin from calf thymus. Purification to homogeneity, *J. Biol. Chem.* 257 (1982) 6686–6690.
- [42] A. Holmgren, Thioredoxin catalyzes the reduction of insulin disulfides by dithiothreitol and dihydroliipoamide, *J. Biol. Chem.* 254 (1979) 9627–9632.
- [43] L. Yang, D. Wu, X. Wang, A. Cederbaum, Depletion of cytosolic or mitochondrial thioredoxin increases CYP2E1-induced oxidative stress via an ASK1–JNK1 pathway in HepG2 cells, *Free Radic. Biol. Med.* 51 (2011) 185–196.
- [44] D. Trachootham, W. Lu, M. Ogasawara, N. Rivera-Del Valle, P. Huang, Redox regulation of cell survival, *Antioxid. Redox Signal.* 10 (2008) 1343–1374.
- [45] R. Radi, Nitric oxide, oxidants, and protein tyrosine nitration, *Proc. Natl. Acad. Sci. USA* 101 (2004) 4003–4008.
- [46] D. Anastasiou, G. Poulogiannis, J. Asara, M. Boxer, J. Jiang, M. Shen, G. Bellinger, A. Sasaki, J. Locasale, D. Auld, C. Thomas, M. Vander Heiden, L. Cantley, Inhibition of pyruvate kinase M2 by reactive oxygen species contributes to cellular antioxidant responses, *Science* 334 (2011) 1278–1283.
- [47] E. Ito, S. Yue, E. Moriyama, A. Hui, I. Kim, W. Shi, N. Alajez, N. Bhogal, G. Li, A. Datti, A. Schimmer, B. Wilson, P. Liu, D. Durocher, B. Neel, B. O'Sullivan, B. Cummings, R. Bristow, J. Wrana, F.-F. Liu, Uroporphyrinogen decarboxylase is a radiosensitizing target for head and neck cancer, *Sci. Transl. Med.* 3 (2011) 1–7.
- [48] B. McDonagh, J. Pedrajas, C. Padilla, J. Barcena, Thiol redox sensitivity of two key enzymes of heme biosynthesis and pentose phosphate pathways: uroporphyrinogen decarboxylase and transketolase, *Oxid. Med. Cell. Longev.* (2013) 1–13 (ID 932472).
- [49] M. Pajares, G. Markham, Methionine adenosyltransferase (s-adenosylmethionine synthetase), *Adv. Enzymol. Relat. Areas Mol. Biol.* 78 (2011) 449–521.
- [50] H. Murata, Y. Ihara, H. Nakamura, J. Yodoi, K. Sumikawa, T. Kondo, Glutaredoxin exerts an antiapoptotic effect by regulating the redox state of Akt, *J. Biol. Chem.* 278 (2003) 50226–50233.
- [51] J. Song, Y. Lee, Differential role of glutaredoxin and thioredoxin in metabolic oxidative stress-induced activation of apoptosis signal-regulating kinase 1, *Biochem. J.* 373 (2003) 845–853.
- [52] Y. Xie, S. Kole, P. Precht, M. Pazin, M. Bernier, S-glutathionylation impairs signal transducer and activator of transcription 3 activation and signaling, *Endocrinology* 150 (2009) 1122–1131.
- [53] F. Ogata, W. Batista, A. Sartori, T. Gesteira, H. Masutani, R. Arai, J. Yodoi, A. Stern, H. Monteiro, Nitrosative/oxidative stress conditions regulate thioredoxin-interacting protein (TXNIP) expression and thioredoxin-1 (TRX-1) nuclear localization, *PLoS One* 8 (2013) e84588.
- [54] H. Ischiropoulos, Biological selectivity and functional aspects of protein tyrosine nitration, *Biochem. Biophys. Res. Commun.* 305 (2003) 776–783.
- [55] A. Haqqani, J. Kelly, H. Birnboim, Selective nitration of histone tyrosine residues in vivo in mutator tumors, *J. Biol. Chem.* 277 (2002) 3614–3621.
- [56] Y. Kamisaki, K. Wada, K. Bian, B. Balabanli, K. Davis, E. Martin, F. Behbod, Y.-C. Lee, F. Murad, An activity in rat tissues that modifies nitrotyrosine-containing proteins, *Proc. Natl. Acad. Sci. USA* 95 (1998) 11584–11589.
- [57] R. Radi, Protein tyrosine nitration: biochemical mechanisms and structural basis of its functional effects, *Acc. Chem. Res.* 46 (2013) 550–559.
- [58] R. Sengupta, A. Holmgren, The role of thioredoxin in the regulation of cellular processes by S-nitrosylation, *Biochim. Biophys. Acta* 1820 (2012) 689–700.
- [59] S. Hashemy, A. Holmgren, Regulation of the catalytic activity and structure of human thioredoxin 1 via oxidation and S-nitrosylation of cysteine residues, *J. Biol. Chem.* 283 (2008) 21890–21898.
- [60] J. Haendeler, J. Hoffmann, V. Tischler, B. Berk, A. Zeiher, S. Dimmeler, Redox regulatory and anti-apoptotic functions of thioredoxin depend on S-nitrosylation at cysteine 69, *Nat. Cell Biol.* 4 (2002) 743–749.
- [61] K. Barglowa, C. Knutsonb, J. Wishnokb, S. Tannenbaum, M. Marletta, Site-specific and redox-controlled S-nitrosation of thioredoxin, *Proc. Natl. Acad. Sci. USA* 108 (2011) 600–606.

UNPUBLISHED DATA

Unpublished data

Quantification of the activity and expression levels of Trx1, Grx1 and Prdx6 in HepG2 cells subject or not to high levels of NO as well as low levels of Prdx6

According to the objective 4, quantification of the activity and expression levels of Trx1, Grx1 and Prdx6 in HepG2 cells that express high levels of NO or normal as well as low levels of Prdx6 was done but these results are not included in the thesis articles.

Methodology

Human Prdx6 was down-regulated in control cells (4TO) and cells that overexpressed NOS3 (4TO_NOS) using specific siRNA according to the manufacturer's recommendations (Dharmacon, GE Healthcare Life Sciences). The cells were incubated with the interference solution for 72h in 2% culture medium in the absence of antibiotic/antimycotic solution.

The protein expression of Trx1, Grx1 or Prdx6 were determined by Western blotting analysis using specific primary antibodies against Trx1 and Grx1, 1:500 dilution; or Prdx6, 1:2000 dilution(dilution...). The secondary antibodies were conjugated to peroxidase and the chemiluminescent signal was induced by ECL reagent (Thermo-Fisher). β -actin protein was used as cell protein-loading control.

Trx activity was determined spectrophotometrically at 412 nm, as described by Holmgren in 1979, through its ability to reduce insulin disulfides in the presence of NADPH and rat thioredoxin reductase. Grx activity was also determined spectrophotometrically, as described by Luthman and Holmgren in 1982, by measuring the reduction of 2-hydroxyethyl disulfide (HED) in the presence of NADPH and yeast glutathione reductase. The consumption of NADPH was monitored at 340 nm. By the other hand, it was not possible to measure the Prdx6-specific peroxidase activity in cell lysates, but its phospholipase A2 activity (PLA2) was assayed using the Red/Green BODIPY based EnzChek Phospholipase A2 Assay (Invitrogen) in the presence or absence of MJ33. The samples were measured at excitation 460 nm and emission 515 nm.

Results and Discussion

As proof of concept, it has always been checked by Western Blot the Prdx6 silencing and in all cases, the Prdx6 levels went down ~ 60%. The level of Prdx6 does

not change in cells that overexpressed NOS3 with respect to control cells. The PLA2 assay gives a high variability and, although the resulting data from four different experiments were not statistically significant, a trend was observed with higher activity in NOS3 overexpressing cells. Prdx6 is S-nitrositated in NOS3 overexpressing HepG2 cells as shown in Article 1.

Regarding Trx1 and Grx1, the results obtained showed that Prdx6 silencing did not significantly affect the activity and expression of Trx1 and Grx1 in both normal cells and those that overexpressed NOS3. However, proteins levels and activity of Trx1 and Grx1 show a tendency to increase in NOS3 overexpressing HepG2 cells as it is published (González R., et al. 2015) (Other scientific contributions).

Conclusion

There is a cross-relationship between the signaling function of NO and the activity of Prdx6 that may be due to its regulation by S-nitrositation.

Generation of a stable HepG2 cell line Knockout for Prdx6 (HepG2prdx6^{-/-}) by CRISPR/Cas9

According to the objective 7, the HepG2 Knockout cell line for Prdx6 through CRISPR/Cas9 technology was obtained.

Methodology

The CRISPR-Cas9 technique was used into the human hepatocarcinoma cell line HepG2, transfected using lipofectamine (LipofectamineTM CRISPRMAX Cas9 Transfection Reagent, Thermo Fisher) with a specific gRNA directed to the peroxiredoxin 6 gene and with the Cas9 nuclease (TrueCutTM Cas9 Protein v2, Thermo Fisher), responsible for the double chain cut in DNA. This gRNA was designed using the website of "Thermo Fisher TrueGuide Synthetic gRNA" so that the double-stranded cut was directed towards the third coding region of human prdx6 gene. To optimize the transfection method, different proportions of Cas9 nuclease and gRNA were used following the instructions of the manufacturer and then the efficiency of the CRISPR-Cas9 technique was calculated using a kit (GeneArtTM Genomic Cleavage Detection Kit, Thermo Fisher).

The cells, preserved after transfection, were used to carry out a limit dilution in 96-well plates. Due to the difficulty of HepG2 cells to grow isolated, the medium was supplemented with the 50% of filtered medium used to grow the HepG2 cells (approximately at 50% confluence) to provide the growth and survival factors necessary for a greater number of isolated cells to grow in the different wells of the 96-well plate. The selected clones were transfected to 24-well plates for later analysis by Western blotting (WB) with specific antibodies against Prdx6 (Abcam). Moreover, the sequence analysis of peroxiredoxin 6 gene of the positive clone was carried out through Sanger sequencing methods using primers which encoding the peroxiredoxin 6 gene area that would be susceptible for cutting by Cas9.

Results and Discussion

The best efficiency of transformation was obtained with 1:2 proportions of Cas9 nuclease and gRNA, getting an efficiency of 0.153, which meant a probability of yield a knockout clone of 3.3%. A number of 157 clones grew and them, they were transfected to 24-well plates for later analysis by WB. All of them were analyzed and only clone 39

did not express Prdx6. This knockout for Prdx6 was characterized and sequence analysis allowed to know that both alleles were mutated by deletion: one allele had a deletion of one nucleotide and the other had elimination of 11 nucleotides.

Conclusion

A stable HepG2 cell line knockout for human Prdx6 has been successfully obtained by CRISPR/Cas9 technology. The mutation has been characterized and has been shown to be a biallelic and heterozygotic deletion.